UNIVERSITY OF LEICESTER

Investigation into novel gut-microbiome mediated pathways in cardiovascular disease

Thesis submitted for the degree of

Doctor of Philosophy at the

University of Leicester

by

Simona Esposito (Mpharm)

Department of Cardiovascular Sciences University

of Leicester

July 2021

Abstract

Dietary metabolism is increasingly implicated in the regulation of cardiovascular disease and there is intense focus on understanding this relationship. The bacterial flora, which shows heterogeneity between individuals with seasonal and dietary influences, generates metabolites from dietary nutrients. One pathway involves carnitine, a large nutritional component of red meat, which is digested by bacteria into the downstream metabolite, trimethylamine N-oxide (TMAO).

TMAO has been the primary focus of recent investigations as being both causative and predictive of heart disease which has included studies on the latter in heart failure and in myocardial infarction cohorts. Mechanistic actions of TMAO on heart disease, however, are still not well understood.

The aim of the present study is to investigate mechanistic actions of TMAO by conducting metabolic pathway analysis of TMAO through a strategic series of experimental studies. These studies include investigations on the molecular and cellular basis of excitability, conduction and electrical remodelling in heart failure.

Initial experiments using calcium fluorescence imaging suggested that the calcium transients of cardiomyocytes were larger in the presence of high levels of TMAO. It was hypothesised that TMAO altered ion channels response by potentiation of calcium currents. These changes in ionic currents would lead to pronounced changes in the cardiac action potential and so have effects on excitation contraction coupling.

Furthermore, experiments were completed to demonstrate the molecular and cellular effects of TMAO, and its relationships with energy substrate uptake and utilisation. To investigate this, this work used a combination of evaluation of ATP, evaluation of LDH and a metabolic flux analyser to assess rates of oxygen consumption on rat and human cardiac cells. Once again, this experimental approach showed that high concentrations of TMAO negatively impacted cardiac cells function by altering cells bioenergetics.

In summary, this work was able to provide insight on the mechanistic actions of TMAO and to find evidence of alterations of normal cardiac function by high levels of TMAO.

Acknowledgments

I remember always being sceptical when hearing people refer to their PhD as a discovery journey, and if I ever was painfully wrong about something, this is most definitely one of such occasions.

My first thanks go to my supervisor, Dr Richard Rainbow, without whom none of this would have been possible. Thanks for being the Dumbledore to my Harry Potter, helping me defeat my very own dementors and constantly reminding me of my own worth. Thanks to my supervisory team, Dr Karl Herbert and Prof Dave Lambert, for all the advice, help and care that was provided to me over these four years.

Special thanks go to the post-doc in the lab group, Dr Sean Brennan, who showed me that it was possible to have an incredible amount of fun while doing this work. Thanks for always being "honest to the point of brutality". Go Liverpool!

A thank you must be extended to both the University of Leicester and University of Liverpool teams. Thanks to Dr Lory Francescut, Dr Amy Chadwick, Dr Parveen Sharma and Dr Sophie Penman for sharing your extensive cell culture wisdom and lab knowledge with me. Thanks to Alina, Abrar, Muhammad, Fada and Lauren, sharing an office with you over the years has been so much fun and you made coming into work an enjoyable experience.

Thank you to all of my wonderful friends in Leicester, Liverpool and Napoli for your support during my PhD. Serena, Sara, Roberta, Mary, Vanessa, Andrea and Aayushi, thank you for all of the fun times over the last 4 years. Thank you for being by my side throughout.

It would be impossible to thank my family enough. To my mom and my brother, for being my absolute rocks and reminding me that home is always there to welcome you in the toughest of times. To Antonino, the best supporter. Thank you for your constant patience, love and support.

Most importantly, I'd like to dedicate this thesis to my late Father, Carlo Esposito. All of the good that I am and that I could ever dream of achieving is possible because I had the immense privilege of being your daughter. I hope I am making you proud.

Grazie di tutto, dal profondo del mio cuore.

Table of Contents

List of Figures

List of Tables

List of Abbreviations

$[Ca^{2+}]_i$	Intracellular Ca^{2+} concentration
°C	Degrees centigrade
0CaT	Ca^{2+} free Tyrode's
ADP	Adenosine diphosphate
AF	Atrial fibrillation
Ag	Silver
AgCl	Silver chloride
AM	Acetoxymethyl
ANOVA	Analysis of variance
ANS	Autonomous nervous system
AP	Action potential
APD	Action potential duration
ApoE-null	Apolipoprotein E-null
ATP	Adenosine-5'-triphosphate
AUC	Area under the curve
AV	Atrioventricular
BSA	Bovine serim albumin
BA	Bile acid
BCA	Bicinchonic acid
BMI	Body mass index
Ca^{2+}	Calcium
$CaCl_2$	Calcium chloride
CA	Cholic acid
CAD	Coronary artery disease
CASQ2	Calsequestrin

CDCA	Chenodeoxycholic acid
cGMP	Cyclic guanosine monophosphate
CICR	Calcium-induced calcium release
Cl^-	Chloride
CKD	Chronic kidney disease
CNS	Central nervous system
CO_2	Carbon dioxide
$COOH^-$	Carboxy-
CoA	Coenzyme A
CVD	Cardiovascular disease
Cu^{2+}	Copper
Da	Dalton
DAD	Delayed afterdepolarization
DMEM	Dulbecco's Modified Eagle's Medium
DMSO	Dimetylsulfoxide
DNA	Deoxyribonucleic acid
EAD	Early afterdepolarization
ECAR	Extracellular acidification rate
ECC	Excitation contraction coupling
ECG	Electrocardiogram
EDTA	Ethylenediaminetetraacetic acid
EFS	Electric field stimulation
EGTA	Ethylene glycol-bis(β-aminoethyl ether)-N,N,N',N'-tetraacetic acid
E_K	K^+ equilibrium potential
E_{Na}	Na^+ equilibrium potential
ENS	Enteric nervous system
EM	Electron microscopy
ETC	Electron transport chain
$FADH_2$	Flavin adenine dinucleotide
FBS	Fetal bovine serum

FCCP	Carbonyl cyanide-4-trifluoromethoxyphenylhydrazone
FFAR	Free fatty acid receptor
FMO_S	Flavin monooxygenases
FMN	Flavin mononucleotide
FMT	Faecal microbiota transplantation
FXR	Farnesoid X receptor
g	Gram
GAPDH	Glyceraldehyde-3-phosphate dehydrogenase
GBA	Gut-brain axis
GPCR	G protein-coupled receptor
GTP	Guanosine triphosphate
h	Hour
H^+	Hydrogen proton
H_2O_2	Hydrogen peroxide
HDL	High density lipoprotein
HEPES	(4-(2-hydroxyethyl)-1-piperazineethanesulfonic acid
hERG	Human ether-a-go-go related gene
HF	Heart failure
HFpEF	Heart failure with preserved ejection fraction
HFrEF	Heart failure with reserved ejection fraction
Hz	Hertz
IBD	Inflammatory bowel disease
IBS	Irritable bowel syndrome
I_{K1}	Inward rectifier K^+ channel
I_{Kr}	Cardiac rapid relayed rectifier K^+ current
I_{KS}	Cardiac slow delayed rectifier K^+ current
IPC	Ischaemic preconditioning
I_{to}	Cardiac transient outward K^+ current

IMM	Inner mitochondrial membrane
JCN	Junction
k	Kilo
K^+	Potassium
K_{ATP}	K^+ channel ATP-sensitive
KCl	Potassium chloride
K_{ir}	Inward rectifier K^+ channel
K_v	Voltage-dependent K^+ channel
KOH	Potassium hydroxide
L	Litres
LAD	Left anterior descending
LC	Liquid chromatography
LDL	Low density lipoprotein
LDH	Lactate dehydrogenase
LPS	Lypopolisaccharides
LQTS	Long QT syndrome
LTCC	L-type Ca^{2+} channel
LVEF	Left ventricular ejection fraction
m	Milli
M	Molar
MALDI	Matrix-assisted laser desorption/ionization
MAPK	Mitogen activated protein kinase
Mg^{2+}	Magnesium
$MgCl_2$	Magnesium chloride
MI	Myocardial infarction or Metabolic inhibition
MI/R	Metabolic inhibition/reperfusion

min	Minutes
ms	Milliseconds
MS	Mass spectometry
mRNA	Messenger ribonucleic acid
mtDNA	Mitochondrial DNA
mtPTP	Mitochondrial permeability transition pore
mV	Millivolts
Na^+	Sodium
Na_2HPO_4	Sodium phosphate dibasic
NADH	Reduced nicotinamide adenine dinucleotide
NAD(P)H	Nicotinamide adenine dinucleotide phosphate
NAFLD	Non-alcoholic fatty-liver disease
NCX	Na^+-Ca^{2+} exchanger
NF	Nuclear factor
NGS	Next generation sequencing
NH_2^-	Ammino
NMR	Nuclear magnetic resonance
nm	Nanometres
NSTEMI	Non-ST-segment elevation myocardial infarction
NT	Normal Tyrode
NO	Nitric oxide
O_2	Oxygen
O_2^-	Superoxide
OCR	Oxygen consumption rate
OMM	Outer mitochondrial membrane
OXPHOS	Oxidative phosphorylation
PBS	Phosphate-buffered saline
PCR	Polymerase chain reaction

PLB	Phospholamban
PMCA	Plasma membrane Ca^{2+} ATPase
P_O	Open probability
RMP	Resting membrane potential
RyR	Ryanodine receptor
ROS	Reactive oxygen species
rpm	Revolutions per minute
rRNA	Ribosomial ribonucleic acid
s	Seconds
S.E.M.	Standard error of the mean
SA	Sinoatrial
SCFA	Short chain fatty acid
SD	Standard deviation
$SERCA_2$	Sarco/endoplasmic reticulum Ca^{2+}-ATPase type-2
SFT	Substrate-free Tyrode's
SR	Sarcoplasmic reticulum
STEMI	ST-segment elevation myocardial infarction
TCA	Tricarboxylic acid cycle
TOF	Time-of-flight
Tn	Troponin
TNF	Tumor necrosis factor
TRD	Triadin
TTC	2-3-5-triphenyltetrazoline chloride
TTCC	T-type Ca^{2+} channel
T2DM	Type 2 diabetes
XF	Extracellular flux

XO	Xanthine oxidase
α	Alpha
β	Beta
$\Delta\Psi_M$	Mitochondrial membrane potential
µg	Microgram
µL	Microliter
µM	Micromolar

Chapter 1

Introduction

1 Introduction

1.1 The heart: structure and function

The heart is a critical organ responsible for the circulation of blood in the healthy body. Structurally, the heart is separated into the left and right side, each responsible for different components of the regular circulation. Each side comprises of a thin walled chamber, the atria, functioning as a reservoir of blood, and a thicker walled chamber, the ventricle, responsible for pumping blood into the circulatory systems. The flow of blood proceeds from the atria into the muscular ventricles and is then forcefully ejected to either the lungs (pulmonary circulation) or the rest of the body (systemic circulation) whilst strategically positioned valves impede bidirectional flow in the healthy heart (Figure 1.1).

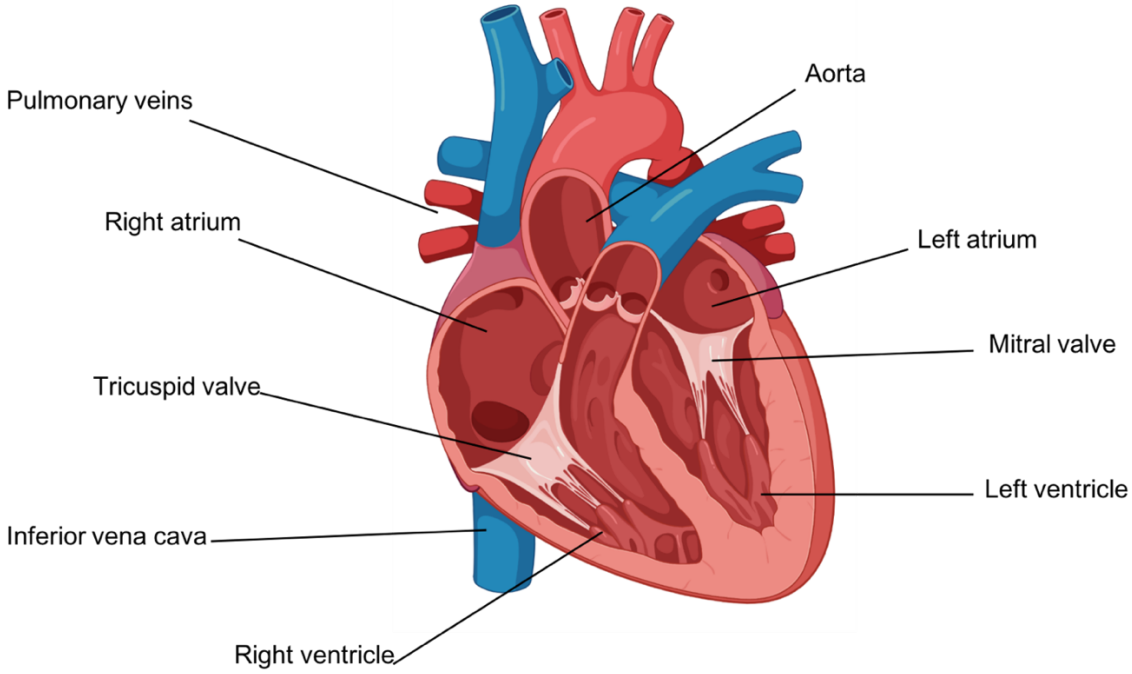

Figure 1.1. Structure of the heart. The heart is organised into four chambers: two atria and two ventricles, one atrium and one ventricle on the right side and one atrium and one ventricle on the left side. One-way valves separate the four chambers. The bicuspid or mitral valve separating the chambers on the left side, while the tricuspid valve separates the right side's chambers. Closure of the valves prevents blood from flowing backwards against the physiological flow. Created with BioRender.com.

With the heart as the central pump through which the blood passes, the circulation can be divided into two different functional components: the systemic circulation and the pulmonary circulation. Four main blood vessels take blood into and out of the heart. The vena cava, the largest vein in the body, carries deoxygenated blood from the body back to the heart through the systemic circulation. The deoxygenated blood is then pumped away from the right ventricle to the lungs through the pulmonary artery system for exchange of carbon dioxide and oxygen. The pulmonary vein returns oxygenated blood from lungs to the heart and finally the aorta, the largest artery in the body, propels oxygenated blood around the body from the left ventricle.

1.2 Electrophysiological properties of the heart

A coordinated spread of electrical excitability is essential to the correct mechanical contraction of the heart. At the basis of the physiological electrical activity of the heart is the ability to correctly generate an electrical stimulus, the action potential, at the sinoatrial node pacemaker cells and the coordinated propagation and termination of this stimulus throughout the myocardium. Once the action potential is generated, the electrical signal is translated into a mechanical process: excitation-contraction coupling (ECC).

In the adult human body in normal physiological conditions at rest, cardiac cells undergo the depolarisation and repolarisation events that form the cardiac action potential approximately once a second. The shape and duration of each action potential is determined by the activity of protein complexes that allow the permeation of ions across the otherwise impermeable membrane. Ion channels, carriers and membrane pumps allow the flux of ions across the membrane of the cells. Pumps use the energy from the hydrolysis of adenosine-5’-triphosphate (ATP) to actively move ions across the membrane against their concentration gradient whilst carriers often use potential energy from the gradient of sodium ions to allow movement of ions and molecules across the membrane barrier. Finally, ion channels allow the facilitated diffusion of ions down their concentration gradients to generate ionic currents; the coordinated

selective permeability and kinetics of these ion channels in cardiac ventricular cells giving rise to a characteristic cardiac action potential.

1.2.1 The cardiac action potential

The general description of the cardiac action potential, and of the ionic currents that generate it, is different for some of the cardiac cells that form the myocardium, due to different expression profiles of ion channels and of ion transport pumps specific to their role (Nerbonne et al., 2005).

Sino-atrial (SA) node cells have a slowly depolarising resting potential compared to other conduction cells, which underlies their role as pacemaker in the heart. SA node cells and atrio-ventricular (AV) node cells lack significant voltage-gated sodium (Na^+) currents that underlie rapid depolarisation in other myocardial cells. Instead these cells have a slow influx of sodium (Na^+) ions at rest that show steady depolarization that enables them to spontaneously reach the threshold for opening L-type calcium channels (LTCC) to fire an action potential. SA node cells lack potassium (K^+) *inward rectifier*, I_{K1}, the main current responsible for myocardium protection from spontaneous depolarization, making easier for these cells to fire action potential (Figure 1.2). The rate at which Na^+ enters the cell to cause depolarisation determines the heart rate. The T- and LTCC are therefore responsible for depolarization in the SA node and as such the depolarisation is less rapid in SA node cells compared with the Na^+-dependent depolarisation seen in ventricular and atrial tissue.

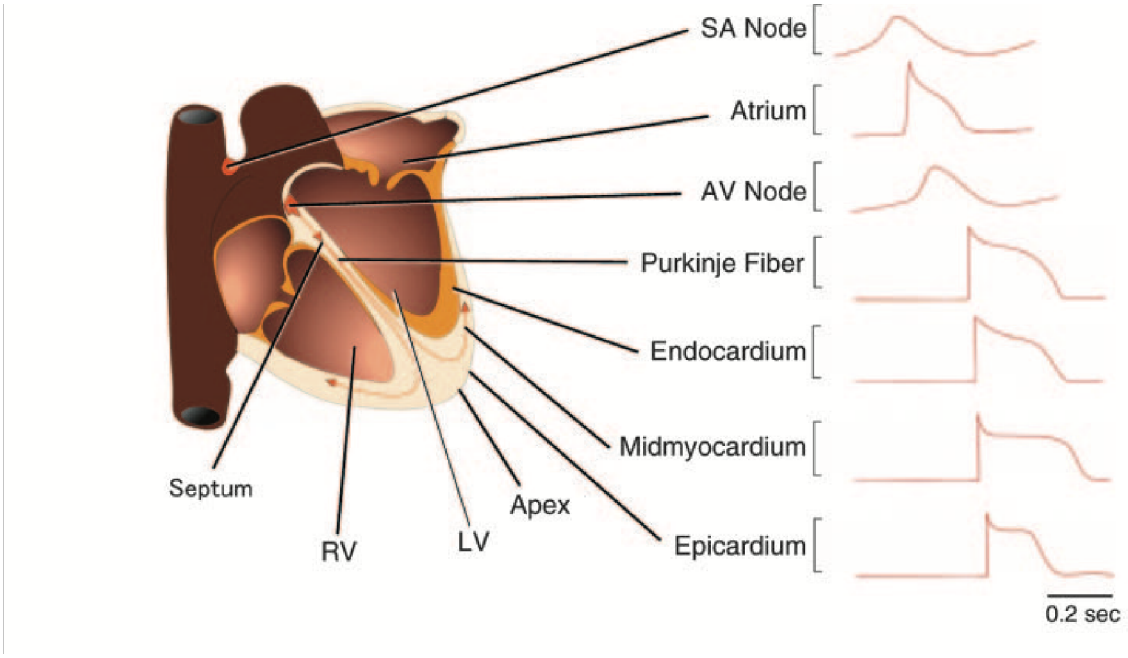

Figure 1.2. Shape of the cardiac action potential bases on different areas of the heart. Action potentials have different shapes and duration based on the region of the heart to which the cells belong to. Image modified from Nerbonne and Kass (2005).

The ventricular action potential has unique characteristics including a long duration of the action potential with a sustained plateau phase. This unique feature allows significant calcium (Ca^{2+}) ion influx to trigger contraction. In the ventricle, the duration and shape of the action potential differs throughout the chamber wall.

1.2.2 Ionic currents underlying the cardiac action potential

As previously described, the ventricular action potential is uniquely shaped and is characterised by a longer duration compared to the action potential in other regions of the heart (Figure 1.2). The longer action potential duration is due to a prominent plateau phase, which delays the repolarization of the cell and prevents the cells from being stimulated prior to the end of the ventricular contraction.

The excitation is passed through the conduction system via changes in excitability of the cells that are electrically coupled to one another via gap junctions, and the consequent changes in the permeability of the cell membrane to ions; mainly Na^{+}, potassium (K^{+}) and Ca^{2+} allow the spread of excitation into the adjoining cells.

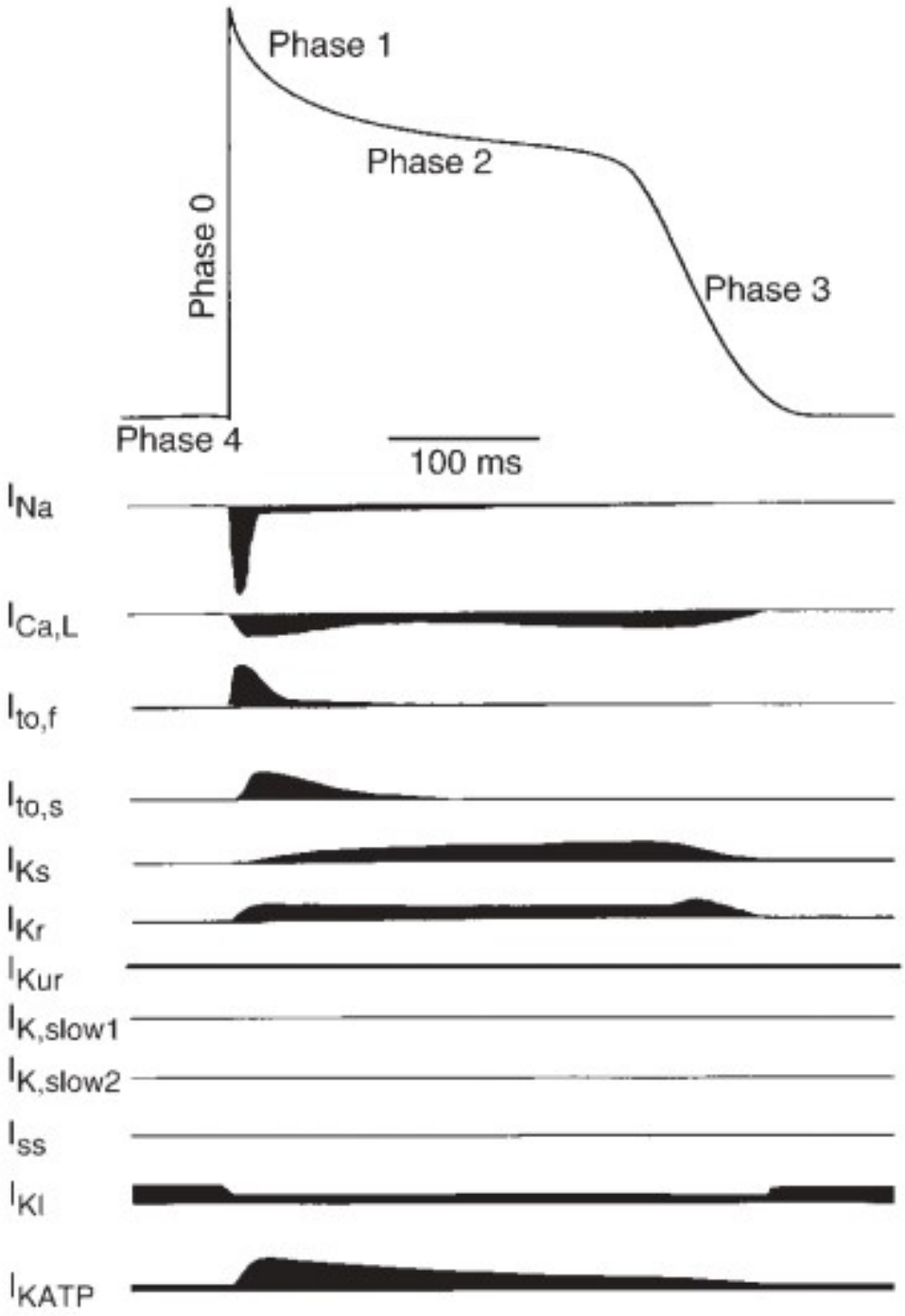

Figure 1.3. Profile of the active currents during the cardiac action potential. Action potential waveforms and underlying ionic currents in adult human ventricular cardiomyocytes. Image modified from Nerbonne and Kass (2005).

The cardiac cell has a resting membrane potential of approximately -80 to -90 millivolt (mV) in diastolic conditions, meaning that the sum of all ion flux at rest gives a potential difference across the membrane of ~-80 to -90 mV. This gradient of electrical potential

is established by pumps, in particular the Na^+-K^+- ATPase and the plasma membrane Ca^{2+} ATPase (PMCA). Normally the electro-chemical gradient between the intra and extracellular compartments would favour Na^+ entering the cells. However, the voltage-gated Na^+ channels that allow ions to move down the electro-chemical gradient into the cells are closed when the membrane potential is negative, blocking Na^+ from entering the cells at rest. In contrast, inwardly rectifying K^+ channels are open at negative membrane potentials and allow K^+ to freely move through the membrane.

Inwardly rectifying K^+ (K_{ir}) are formed from tetramers of a subunits assembled around a central pore. Each a subunit is composed of two putative transmembrane domains (TM1 and TM2) linked by an extracellular pore-forming region (H5) loop and cytoplasmic amino (NH_2)- and carboxy (COOH)- terminal domains. This structure constitutes the basic building blocks for all types of K_{ir} channels. The K_{ir} family is categorized into seven subfamilies ($K_{ir}1$-$K_{ir}7$). The cardiac inward rectifier current I_{K1} is carried by $K_{ir}2$ subunits and exhibits strong inward rectification. The $K_{ir}2$ subfamily consists of six members ($K_{ir}2.1$-$K_{ir}2.6$), of which three are expressed in human cardiac myocytes ($K_{ir}2.1$, $K_{ir}2.2$, and $K_{ir}2.3$, encoded by genes *KCNJ2*, *KCNJ12*, and *KCNJ4*, respectively) (M. N. Foster et al., 2016).

In experimental conditions, K_{ir} channels are able to pass inward currents at potentials more negative than the equilibrium potential for K^+ (E_K). *In vivo*, they pass outward current at potentials close to E_K to maintain a relatively hyperpolarised membrane potential, but as the membrane potential gets more positive, they are blocked by a combination of magnesium (Mg^{2+}) ions and intracellular polyamines (such as spermine) (Dhamoon et al., 2005). These characteristics make I_{K1} crucial in shaping the ventricular action potential. The limited outward current through I_{K1} prevents the efflux of K^+ during the plateau phase and is, therefore, essential to maintaining a prolonged plateau phase (Hibino et al., 2010). Finally, during the last phase of the action potential, the repolarization of the cell to more negative potentials, caused by influx of K^+ via voltage-gated channels, allows for relief of the polyamine block so allowing I_{K1} to pass a relatively large outward current, resulting in a faster final repolarization (Hibino et al., 2010). The I_{K1} current is, therefore, of crucial importance for maintaining the resting membrane potential and for the final stages of repolarization (Hibino et al., 2010).

Despite the activity of the K_{ir} family being voltage-independent, the inward rectification of I_{K1} channels is a result of the intrinsic high affinity of the channels for K^+ and of the strong voltage-dependent block of the inner channel pore by cytosolic Mg^{2+}, Ca^{2+} and positively charged polyamines, mainly spermine and spermidine. At increasingly more positive potential, polyamines physically block the channel pore, binding to specific charged amino acids in the lining of the pore, such as aspartate, resulting in a loss of inward current. As such, I_{K1} is voltage regulated despite the structural lack of a voltage-sensing pore (Skibsbye et al., 2016).

The resting phase of the cardiac action potential is also described as phase 4 (Figure 1.3) and it refers to the phase prior to the initiation of the action potential.

In order to fire an action potential, a resting cardiac myocyte needs to be depolarized above the threshold for activation of voltage-gated currents, usually through the gap junctions from an adjacent myocyte. Following an excitation trigger, voltage-gated Na^+ channels, Na_V 1.5 (encoded by the *SCN5A* gene), are opened, allowing the passage of approximately 10^7 Na^+ ions per second (s) inside cell. This movement causes a shift in the membrane potential towards E_{Na} (+65mV) and results in the upward stroke of the action potential. This rapid influx of Na^+ ions usually lasts no longer than a millisecond (ms), thereafter Na^+ channels inactivate and cannot allow current to pass. The upstroke phase of the action potential is also referred to as phase 0 (Figure 1.3).

The alteration of the membrane potential caused by Na^+ currents produces a series of openings of other channels. As Na^+ channels inactivate as fast as they activated, the K^+ current regains a dominant role. The depolarization caused by Na^+ triggers the opening of *transient outward* K^+ channels, I_{TO}; since at the end of the phase 0 of the action potential the membrane potential is positive, the opening of I_{TO} allows the flow of a repolarizing current. The repolarization of the action potential caused by the opening of I_{TO} is short-lived; I_{TO} channels close rapidly resulting in a short repolarization phase, referred to as phase 1 of the cardiac action potential (Figure 1.3).

After inactivation of I_{TO}, the membrane potential stabilizes itself in a plateau phase in which inward depolarizing currents are balanced by outward repolarizing currents, resulting in little change in the membrane potential. This plateau phase is referred to as phase 2 of the cardiac action potential (Figure 1.3). During phase 2, the main

depolarizing current occurs via the influx of Ca^{2+} ions through voltage-gated Ca^{2+} channels.

In the cardiac muscle, the influx of Ca^{2+} occurs via two types of Ca^{2+} channels, the L-type and the T-type. The "L" in LTCC stands for long-lasting, hinting at the slow inactivation of this channel when compared to Na^{+} channels, while the "T" in T-type Ca^{2+} channel (TTCC) stands for transient. While LTCCs are found in all cardiac cell types, TTCCs are primarily present in pacemaker, atrial and Purkinje cells.

LTCCs are composed of four polypeptide subunits (α1, β, α2, δ) and form a heterotetrameric complex (Y. Wang et al., 2014). The pore forming subunits of the LTCC are the Ca_v1 subfamily and includes four isoforms: $Ca_v1.1$ (α1S), $Ca_v1.2$ (α1C), $Ca_v1.3$ (α1D), and $Ca_v1.4$ (α1F), encoded by *CACNA1S*, *-C*, *-D*, and *-F*, respectively with $Ca_v1.2$ being the main isoform in cardiac muscle (Dolphin, 2016). LTCCs are characterized by a large single channel conductance. While they are closed at resting membrane potential, they activate as the membrane depolarises to more positive potentials (−40 mV). The maximal activity of I_{CaL} is at 0 to + 10 mV, and tends to reverse at +60 to +70 mV, following a bell-shaped current-voltage relationship. Despite I_{CaL} being activated during phase 0 of the action potential by the fast opening of Na^{+} channels, its contribution is substantially smaller than Na^{+}.

Influx of Ca^{2+} during the action potential plateau triggers Ca^{2+} release from the sarcoplasmic reticulum (SR) into the cytosol via activation of Ca^{2+}-release channels. This process causes a rapid increase in intracellular Ca^{2+} concentration (from ~100 nM to ~1 µM) to a level required for induction of contraction (Rios, 2018). The ECC process will be further discussed in paragraph 1.2.3.

Ca^{2+} influx through I_{CaL} is the regulatory point to maintain homeostasis of intracellular Ca^{2+}. The time-dependent inactivation of I_{CaL} is very slow and depends on both voltage dependent inactivation of LTCCs and Ca^{2+}-dependent inactivation. The voltage dependent inactivation, caused by membrane depolarization, prevents an increase in I_{CaL}. The Ca^{2+}-dependent inactivation creates a negative feedback that limits and regulates Ca^{2+} entry into the cell preventing Ca^{2+} overload, detrimental to the health of the cell. Ca^{2+}-dependant inactivation is also responsible for regulating the action potential duration, thus ensuring that contraction and relaxation of the heart is finely

controlled (Shaw et al., 2013). Although the Ca^{2+}-dependant inactivation regulates I_{CaL}, the inactivation mechanism depends principally on Ca^{2+} released from the SR. When cytoplasmic Ca^{2+} concentration increases, Ca^{2+} ions bind to calmodulin, a protein sensitive to variations of Ca^{2+} concentrations that presents four Ca^{2+}- binding sites. Upon saturation of the binding sites with Ca^{2+}, calmodulin undergoes a conformational change that ultimately results in block of the LTCC pore (Swulius et al., 2008).

As I_{CaL} decreases due to its inactivation, the repolarizing forces present during phase 2 lead the action potential into to final rapid repolarization phase, referred to as phase 3 of the action potential (Figure 1.3). The repolarizing phase constitutes in an increase in K^+ conductance and the K^+ currents are carried out by three different components, distinguished by their different kinetics: the *slow delayed rectifier* potassium current, I_{Ks}, the *rapid delayed rectifier* potassium current, I_{Kr}, and the *ultra-rapid delayed rectifier* potassium current, I_{Kur}, which lead to the late/rapid depolarization phase.

I_{Ks} is a current that activates extremely slowly when membrane depolarizes to potentials greater than -30 mV and reaches half-maximum activation close to +20 mV. Structurally, I_{Ks} is formed by coassembly of four pore-forming α subunits (K_v7.1, from the *KCNQ1* gene also formerly known as K_vLQT1) and β subunits (from the *KCNE1* gene, also formerly known as MinK) and is expressed in all cardiac cell types. The incorporation of KCNE1 subunits causes important changes in channel kinetics when compared to homomeric KCNQ1 voltage-gated K^+ channels. While homomeric KCNQ1 channels activate and deactivate rapidly, the KCNQ1/KCNE1 heteromultimer underlying I_{KS} has a very slow activation and deactivation kinetics to the point where it barely has any inactivation (Thompson et al., 2017). I_{Ks} current slowly increases during the plateau phase of the action potential therefore it contributes to the repolarizing current in the later stages of the action potential. I_{Ks} plays a key role in determining the shortening of the action potential during physiological increases in heart rate; during rapid heart rates the time of inactivation of I_{Ks} reduces causing the current to more rapidly accumulate and to contribute to a faster repolarization (Jeevaratnam et al., 2018).

I_{Kr} is formed by coassembly of four pore-forming α subunits (K_v11.1, encoded by *KCNH2*) and β subunits (MiRP1, encoded by *KCNE2*). KCNH2 is also known as the human-ethera-go-go-related gene (hERG). hERG channels have a unique voltage dependence; they

activate rapidly upon membrane depolarization, but the inactivation rate is faster than its activation rate (Jeevaratnam et al., 2018). Thanks to this unique feature, hERG is nonconsequential during phases 1 and 2 of the cardiac action potential but makes it the principal repolarizing current at the end of the plateau phase in most cardiac cells and plays an important role in governing the cardiac action potential duration and refractoriness. I_{Kr} is highly expressed in left atrial and in ventricular endocardium (L. Chen et al., 2016; Roden, 2016).

Finally, I_{Kur} activates rapidly and inactivates slowly during the course of the action potential. I_{Kur} is only present in human atria and not in the ventricles, therefore it can be said that this current is responsible for the shorter action potential in the atria compared to the ventricular action potential (Jeevaratnam et al., 2018).

As repolarisation progresses, there is a further increase in I_{K1} as the depolarisation induced block is released, leading to the restoration of the resting membrane potential.

1.2.2.1 ATP-sensitive potassium (K_{ATP}) channels

Amongst the K_{ir} channel family, there is a subgroup of channels, ATP-sensitive potassium (K_{ATP}) channels, that are characterized by being finely regulated by intracellular ATP and adenosine diphosphate (ADP) level. Since these channels are sensitive to the energy level of the cell, it is hypothesized that they are important in coupling electrical activity and membrane potential to the energetic pathways and cellular metabolism (Ortiz et al., 2013; H. S. Sun et al., 2013). Structurally, K_{ATP} channels are different from the other K_{ir} channels. They are hetero-octamers consisting of four pore-forming subunits ($K_{ir}6.x$) with four sulfonylurea receptors (SURx) (N. Li et al., 2017). Out of the four isoforms of K_{ATP} channels, $K_{ir}6.2$/SUR2A has been suggested as the principal isoform expressed in ventricular cardiomyocytes. However, there is evidence that suggest that other isoforms of K_{ATP} channels are also present (Morrissey et al., 2005; Singh et al., 2003). At physiological concentrations of ATP, K_{ATP} channels are normally blocked, and only open in cases of depletion of intracellular ATP thus meaning that they are sensitive to metabolic stress. Since K_{ATP} channels are generally considered to only open in response to metabolic stress, their opening would hyperpolarise the

membrane potential causing shortening of the action potential and reduction of Ca^{2+} entry, essential to preserve the intracellular ATP. However, as more evidence start to point at the existence of different isoforms of K_{ATP} in ventricular cardiomyocytes, it is possible that other roles for this channel subfamily are likely still to be revealed.

1.2.3 Excitation-contraction coupling

The process of ECC involves the mechanical conversion of the electrical impulses generated by propagation of the action potential. This process is finely regulated, and it requires the involvement of contractile proteins.

The region of the cardiomyocyte where ECC occurs is the sarcomere; each sarcomere responsible for contraction is composed of a thick myofilament, myosin, and a thinner myofilament, actin. Cardiac muscle contraction stems from an interaction between the actin and myosin filaments that generates their movement relative to one another. Myosin heads bind to actin filaments forming bridges that allow sliding of the filaments. Regulation of the ECC occurs thanks to the troponin complex, consisting of 3 proteins, troponin I (TnI), troponin C (TnC) and troponin T (TnT) that interacts with tropomyosin, a contractile protein coupled to the actin myofilament. Of the 3 proteins, TnI is of key importance in that inhibits the interaction between actin and myosin filaments, blocking the final contraction.

T-tubules, structures specific to striated muscle cells, are invaginations of the sarcolemma rich in ion channels that penetrate into the intracellular space of the cardiomyocytes. The t-tubules from a complex network connected inside the cytoplasm and contains regions that compartmentalize transmembrane ion handling proteins and signalling molecules, functioning as point of regulation for contractile function and electrophysiology (Hong et al., 2017).

At a cellular level, the contraction of a cardiomyocyte is mainly determined by intracellular Ca^{2+} concentration $[Ca^{2+}]_i$. Ca^{2+} enters the cell during the plateau phase of the action potential through LTCCs. However, the influx of Ca^{2+} ions is small and insufficient to induce contraction. The amount of Ca^{2+} entering the cell via I_{CaL}, however, acts as the trigger for the rapid release of Ca^{2+} from the SR into the cytosol by opening

the ryanodine-receptor 2 (RyR2) in a process known as calcium induced calcium release (CICR) (Lederer et al., 1990). Most of the LTCCs in the adult myocyte are localized in the transverse tubules (T tubules) facing the SR junction and the RyR2, organized as a complex that ensures coordinated Ca^{2+} release during ECC. During contraction, greater than 75% of Ca^{2+} in the cytoplasm comes from release by the SR (Ferreri-Jacobia et al., 2005) (Figure 1.4).

The Ca^{2+} release channel in the SR is a macromolecular complex composed of the RyR2 homotetramer, which represents the largest part of the complex which interacts with other proteins and operates as a Ca^{2+}-conducting channel. RyR2 channels are roughly 10 times larger than voltage-gated Ca^{2+} channels and they open upon binding with Ca^{2+}. Due to their size, structural analysis of this complex is particularly difficult (Lanner et al., 2010). Technological advances in single-particle cryo-electron microscopy (EM) techniques have allowed the determination of high-resolution structure of RyRs (Santulli et al., 2018). An important structural feature of the RyRs is that they contain multiple domains that allow binding for several functional ligands: ions such as Ca^{2+} and Mg^{2+}, proteins including calstabin, calmodulin, the voltage-gated Ca^{2+} channel and small molecules such as adenine nucleotides and caffeine (Santulli et al., 2018; Santulli, Lewis, et al., 2017).

Submicromolar $[Ca^{2+}]_i$ is sufficient to let Ca^{2+} ions bind the high affinity sites on RyR2, thus opening the channel and allowing Ca^{2+} release from the SR into the cytosol. The RyR2 channel activity reaches its peak when $[Ca^{2+}]_I$ is approximately 10 micromolar (µM), whereas higher concentrations lead to a reduction in the open probability of the channel, possibly caused by Ca^{2+} binding to inhibitory binding sites on the RyR channel (Santulli, Nakashima, et al., 2017). CICR lasts approximately 10 ms following RyR2 opening. CICR termination is a finely regulated process. Following Ca^{2+} release, the SR remains depleted of its Ca^{2+} content. This decline of Ca^{2+} triggers the inactivation of the RyR2, causing the termination of CICR (Gyorke et al., 2008). Luminal Ca^{2+} is not solely responsible for the termination of CICR but it interacts with a complex of proteins, namely the SR luminal proteins cardiac calsequestrin (CASQ2), junctin (JCN), and triadin 1 (TRD), to cause inactivation of RyR2 in a positive feedback mechanism (Gyorke & Terentyev, 2008). CASQ2 is a protein with low affinity Ca^{2+} that is able to bind luminal

Ca^{2+}. It acts as a sensor by modulating how the RyR2 reacts to fluctuation of luminal Ca^{2+}. As the concentration of luminal Ca^{2+} decreases, CASQ2 binds JCN and TRD resulting in the inhibition of the RyR2. Instead, higher concentration of SR Ca2+ results in the majority of luminal Ca^{2+} bound to CASQ2, which no longer interacts with JCN and TRD. JCN and TRD also modulate RyR2 function by themselves by increasing the activity of the RyR2 channel (Gyorke & Terentyev, 2008; Terentyev et al., 2008).

After the increase in $[Ca^{2+}]_i$, Ca^{2+} released by the SR binds the TnC protein causes a conformational change in the troponin-tropomyosin complex that strengthens the interaction with TnI and allows myosin to bind to a previously hidden site on the actin filament, permitting the formation of cross-bridges and ultimately contraction. The process of relaxation is also regulated by Ca^{2+}. During the repolarization phase of the action potential, $[Ca^{2+}]_i$ decreases causing the dissociation of Ca^{2+} from the binding site of TnC. Ca^{2+} is removed from the cytosol in two active processes; either by sequestration back into the SR by the SR Ca^{2+}-ATPase type-2 (SERCA2) or by exchange into the extracellular space by the PMCA. Alternatively, Na^{+}-Ca^{2+} exchanger (NCX) can move Ca^{2+} out of the cell exchanging it with Na^{+} ions, with all three mechanisms lowering the cytosolic Ca^{2+} concentration to baseline levels (Landstrom et al., 2017). SERCA sequesters Ca^{2+} back into the SR in an ATP-dependent manner and is regulated by phospholamban (PLB), which in its unphosphorylated state acts to inhibit Ca^{2+} transport and sequestration (WeisserThomas et al., 2005).

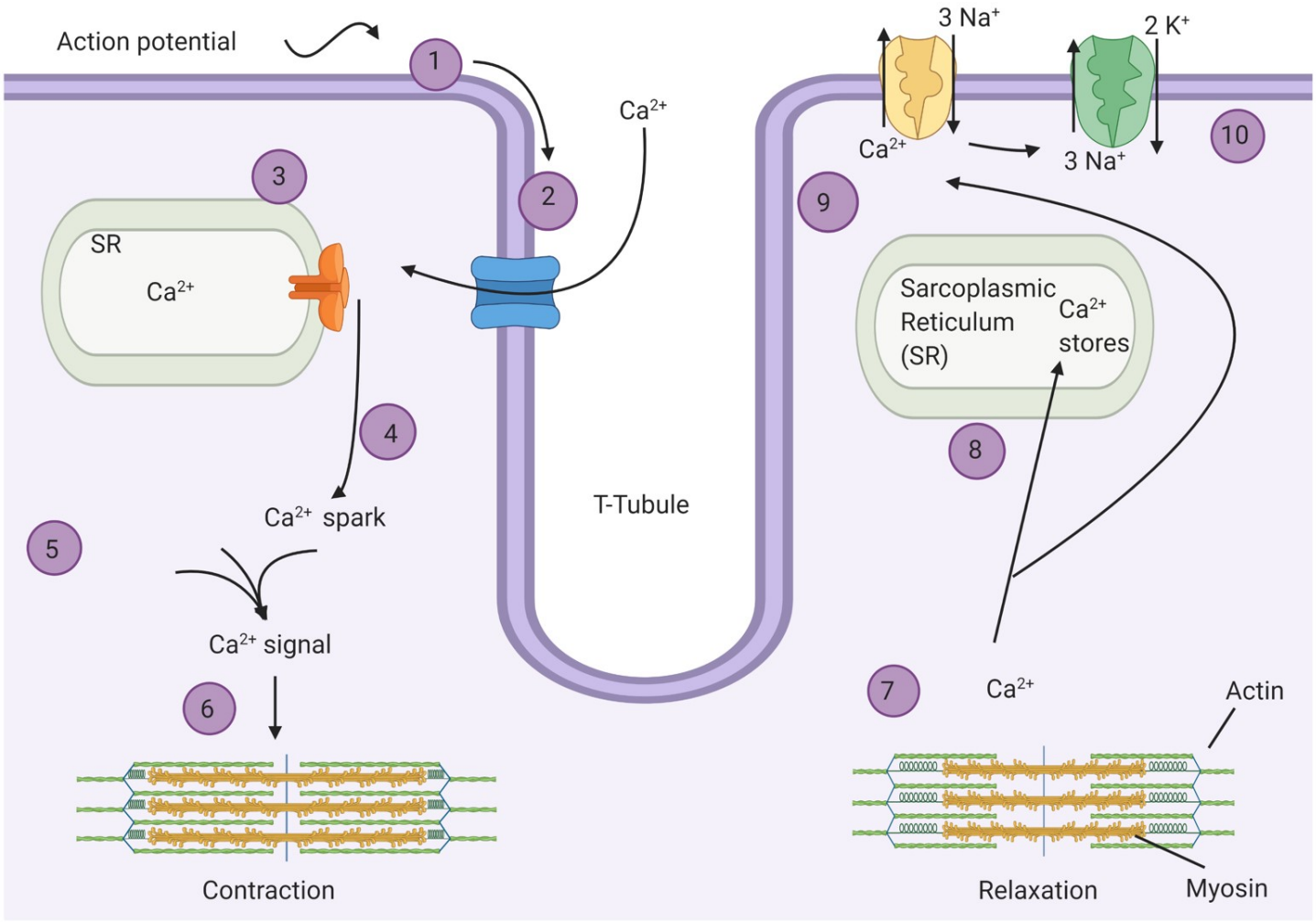

Figure 1.4. Schematic of Ca^{2+} handling during ECC. Action potential generated from adjacent cell (1) causes the opening of voltage-gated Ca^{2+} channels (2). Following the opening of the voltage-gated Ca^{2+} channels, Ca^{2+} enters the cell and triggers Ca^{2+} release from RyR2 (3). Local release of Ca^{2+} causes a Ca^{2+} spark and a Ca^{2+} signal in the cell (4-5). Ca^{2+} ions than bind to troponin to initiate contraction (6). Relaxation occurs when Ca^{2+} unbinds from troponin (7) and Ca^{2+} is pumped back into the sarcoplasmic reticulum for storage (8) or is exchanged with Na^{+} (9). At the end of the cycle, the Na^{+} gradient is maintained by the Na^{+}-K^{+}-ATPase (10). Created with BioRender.com.

1.2.4 Electric conduction system

The trigger for myocardial contraction originates by electrical signals produced at the SA node; a small group of cells located in the wall of the right atrium. The ability to spontaneously generate cardiac action potentials means that the SA node is referred to as the intrinsic cardiac peacemaker.

Once the impulse leaves the SA node, it rapidly propagates across the right, then the left atrium to initiate atrial contraction and reaches the AV node. The propagation of the impulse markedly slows down through the AV node, where the current directed inside the cells (through Ca^{2+} channels) is considerably less than the Na^{+} current in the atria and ventricles. The slowdown of the conduction allows the atrial contraction to pump the blood into the ventricles prior to ventricular contraction, so optimizing the cardiac output.

Following a short delay period, the wave leaves the AV node to enter the conduction system down the ventricles along the Bundle of His, further diverging along the Purkinje fibres, where the Na^{+} currents are more abundant than any other region of the heart and propagation of the impulse is faster.

Finally, the impulse reaches the ventricular endocardium from the His-Purkinje system and it spreads through the ventricular myocardium, stimulating a coordinated ventricular contraction.

1.3 Bioenergetics of the healthy heart

The human body produces and consumes roughly their body weight in ATP (about 65 kilograms, kg) on a daily basis (Tornroth-Horsefield et al., 2008) and despite accounting for only ~0.5% of the aforementioned body weight, the heart consumes almost 8% of all ATP produced.

The high rate of energetic consumption by the heart explains why the heart is the organ that has the largest number of mitochondria in our body (Sabbah, 2016). Mitochondria are essential for the cardiomyocytes that require energy derived from the synthesis of ATP for their contraction (Ikeda et al., 2015) and for their relaxation. In this constant

cycle of contraction-relaxation, almost 90% of the cellular ATP is consumed in the myocardium (Barth et al., 1992; Schaper et al., 1985).

The mitochondria and their associated phosphate-transfer couples are almost entirely responsible for keeping the balance of bioenergetics metabolism in the cardiomyocytes (D. A. Brown et al., 2016). Cardiac mitochondria work with elevated efficiency in order to maintain steady the oxygen flux for the heart and to adjust and satisfy the body's needs (D. A. Brown et al., 2016).

The mitochondria perform four central functions in the cell that are relevant to the pathophysiology of disease: they provide the majority of the cellular energy in the form of ATP, generate and regulate reactive oxygen species (ROS), buffer cytosolic Ca^{2+} and regulate apoptosis through the mitochondrial permeability transition pore (mtPTP).

1.3.1 Structure and function of mitochondria

Mitochondria are ubiquitous intracellular organelles that are bound by two lipid bilayer membranes. The outer mitochondrial membrane (OMM) is permeable to ions and solutes up to 14 kilodalton (kDa) while the inner mitochondrial membrane (IMM) encloses an aqueous compartment, the matrix, that contains both mitochondrial deoxyribonucleic acid (mtDNA) and various soluble enzymes (Figure 1.5), such as those of the tricarboxylic acid (TCA) cycle and the -oxidation pathway (Wallace et al., 2000). Since the IMM is not permeable to all ions and metabolites, special membrane bound transporters that allow for selective entry are responsible for the entry inside the matrix endogenous metabolite (e.g. ADP, pyruvate, fatty acids, glutathione) (Begriche et al., 2011). The lipid composition of IMM is unique in that it contains a large amount of cardiolipin and virtually no cholesterol (Wallace & Starkov, 2000). The importance of the IMM relays upon its content of proteins that participate in various metabolic activities, including ATP synthesis through oxidative phosphorylation (OXPHOS) (Cohen, 2010).

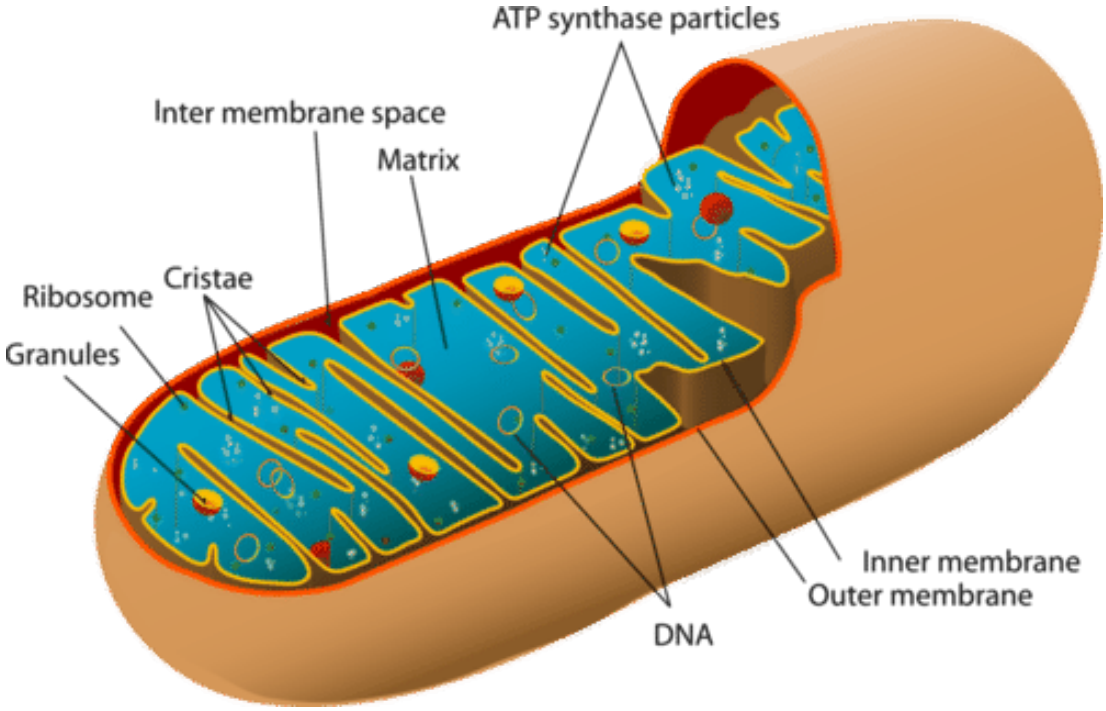

Figure 1.5. Structure of the mitochondria. Mitochondria are the cellular power unit. They have a characteristic bean-shape and consist of inner and outer membranes, separated by inter membrane space. The inner membrane has a very irregular surface, characterized by folds named cristae. It also encloses a dense solution called mitochondrial matrix, home of granules, enzymes and ribosomes. Along with chloroplasts, mitochondria are the only subcellular organelles that have their own DNA.

Mitochondria are responsible for the production of almost 90% of the cell's ATP through the OXPHOS, which couples the oxidation of reduced nicotinamide adenine dinucleotide (NADH) and flavin adenine dinucleotide ($FADH_2$) to the phosphorylation of ADP to form ATP, by utilization of the electron transpher chain (ETC) (a series of five enzyme complexes) in the IMM, acting as the energetic fuel of the cells (Cohen, 2010). Moreover, mitochondria are able to utilize different sources of energy, being able to oxidise many metabolites including fatty acids, pyruvate (generated from glycolysis) and several amino acids (such as glutamine, valine, leucine) to generate the reducing equivalents, NADH and $FADH_2$, via the TCA cycle and β-oxidation, for ATP production (Labbe et al., 2008).

Besides the production of ATP, mitochondria are also responsible for the generation and detoxification of ROS, involvement in some forms of apoptosis, regulation of cytoplasmatic and mitochondrial matrix Ca^{2+}, synthesis and catabolism of metabolites

(e.g. urea, haem and cholesterol) and the transport of the organelles themselves to correct locations within the cell (Brand et al., 2011; Chan et al., 2005; Dykens et al., 2007).

1.3.2 Energetic substrates and pathways

Cellular respiration is a process that occurs in different steps inside the cells (figure 1.6). The first step of this process, glycolysis, takes place in the cytosol of the cell. During this process, nutrients are broken down in a series of enzyme-catalysed reactions that allow glucose to be converted into pyruvate with the production of two molecules of ATP and two molecules of NADH, a reducing agent utilized by the cells in subsequent steps of the cellular respiration (Huttemann et al., 2007). Pyruvate is moved inside the mitochondria where the pyruvate dehydrogenase complex converts the molecule into acetyl-coenzimeA (CoA), used in the Krebs cycle (Patel et al., 2006).

The Krebs cycle takes place in the mitochondrial matrix (Figure 1.5) and consists into 8 enzyme-catalysed reactions in which one molecule of acetyl-coA is oxidised and molecules of NADH and $FADH_2$ are produced (together with carbon dioxide, CO_2), that serve as electron carriers in the final stage of the energetic pathway (H.A., 1937).

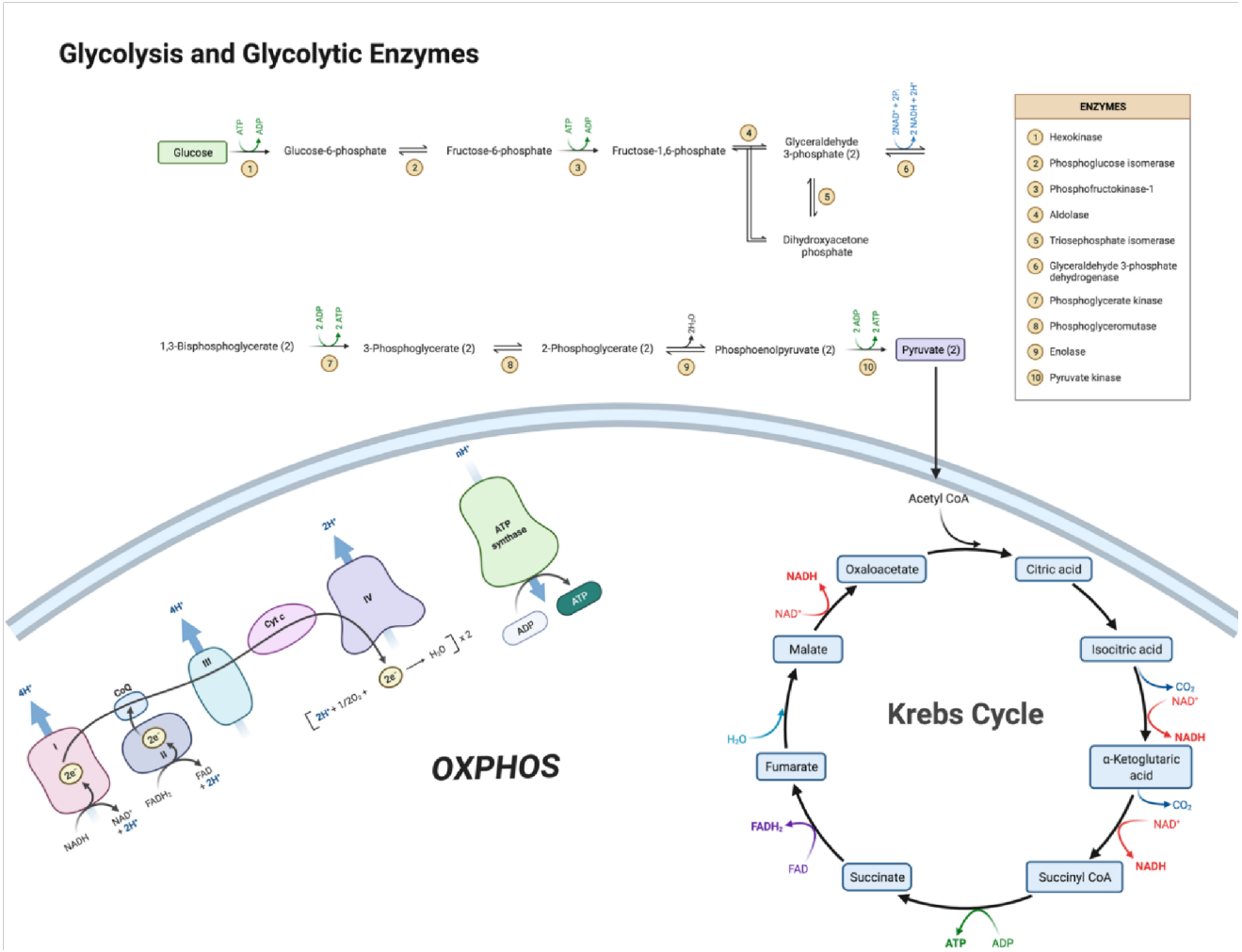

Figure 1.6. Energy production and cellular respiration. Cellular respiration stars into the cytosol with glycolysis, where glucose is converted into pyruvate. Pyruvate is then transported inside the mitochondria and converted into acetyl-coA. Acetyl-coA can, thus, participate to the Krebs cycle, where the electron carriers NADH and $FADH_2$ are generated. The electrons from NADH and $FADH_2$ are transferred to the ETC in order to generate ATP. Created with BioRender.com.

The final stage of cellular respiration is OXPHOS that occurs in the mitochondrial inner membrane (Huttemann et al., 2007). During this process, electrons carried by NADH and $FADH_2$ are transferred to molecular oxygen through the respiratory chain (Figure 1.6). The transfer of electrons in the respiratory chain is made possible by the activity of 85 different proteins that associate into four different complexes and, together with cytochrome c and ubiquinone, catalyse the transfer (Wojtczak et al., 2008).

Complex I is a large protein complex shaped as an "L" that extends into the mitochondrial matrix (Friedrich et al., 2004). Through complex I, NADH and 2 electrons get oxidized, and the electrons are transferred to flavin mononucleotide (FMN) (Mimaki et al., 2012). During this, 4 H^+ are transferred across the inner membrane into the intermembrane space, helping to create the proton motive force required for ATP production (Hirst, 2009).

Complex II is the link between the citric acid cycle and OXPHOS, as succinate is oxidised to fumarate and ubiquinone is reduced to ubiquinol. The release of energy is low so there is no proton force drive produced from complex II (Dudkina et al., 2008).

Electrons from complex I and complex II get transferred into complex III where they are passed from ubiquinol to cytochrome c. Complex III is a dimer unit containing cytochrome c and the cytochrome b1 complex (Solmaz et al., 2008). During electron transfer, 4 H^+ are transferred across the inner membrane into the intermembrane space (Schultz et al., 2001).

Finally, the electrons from the reduced cytochrome c produced by complex III are transferred to complex IV, which is the final oxidase of the ETC (Dudkina et al., 2008; Solmaz & Hunte, 2008).Through complex IV the transfer of electrons from cytochrome c to oxygen occurs, with the reduction of the latter to water (Dudkina et al., 2008). The actions of complex IV contribute to the electrochemical proton gradient as 4 H^+ are pumped into the intermembrane space (Dudkina et al., 2008).

In the end, the oxidation of the reduced electron carriers serves as the driving force for the phosphorylation of ADP and the final production of ATP. Essential in these two processes is the impermeability of the IMM; thanks to this, a proton motive force is generated, which promotes the translocation of protons from the intermembrane space

into the matrix through the ATP synthase resulting into the production of ATP (Wojtczak & Zablocki, 2008).

ATP synthase is a large protein complex made up of two different regions, the Fo region, situated within the IMM and the F1 region residing in the mitochondrial matrix (Jonckheere et al., 2012). During the OXPHOS, the protons present into the intermembrane space return into the mitochondrial matrix through the Fo region of ATP synthase. While the protons move into a negative charged space, the matrix, an electrochemical gradient is created. The energy generated by the electrochemical gradient promotes conformational changes into the catalytic site within the F1 region of ATP synthases, leading to the release of ATP into the mitochondrial matrix (Boyer, 1993; Capaldi et al., 2002).

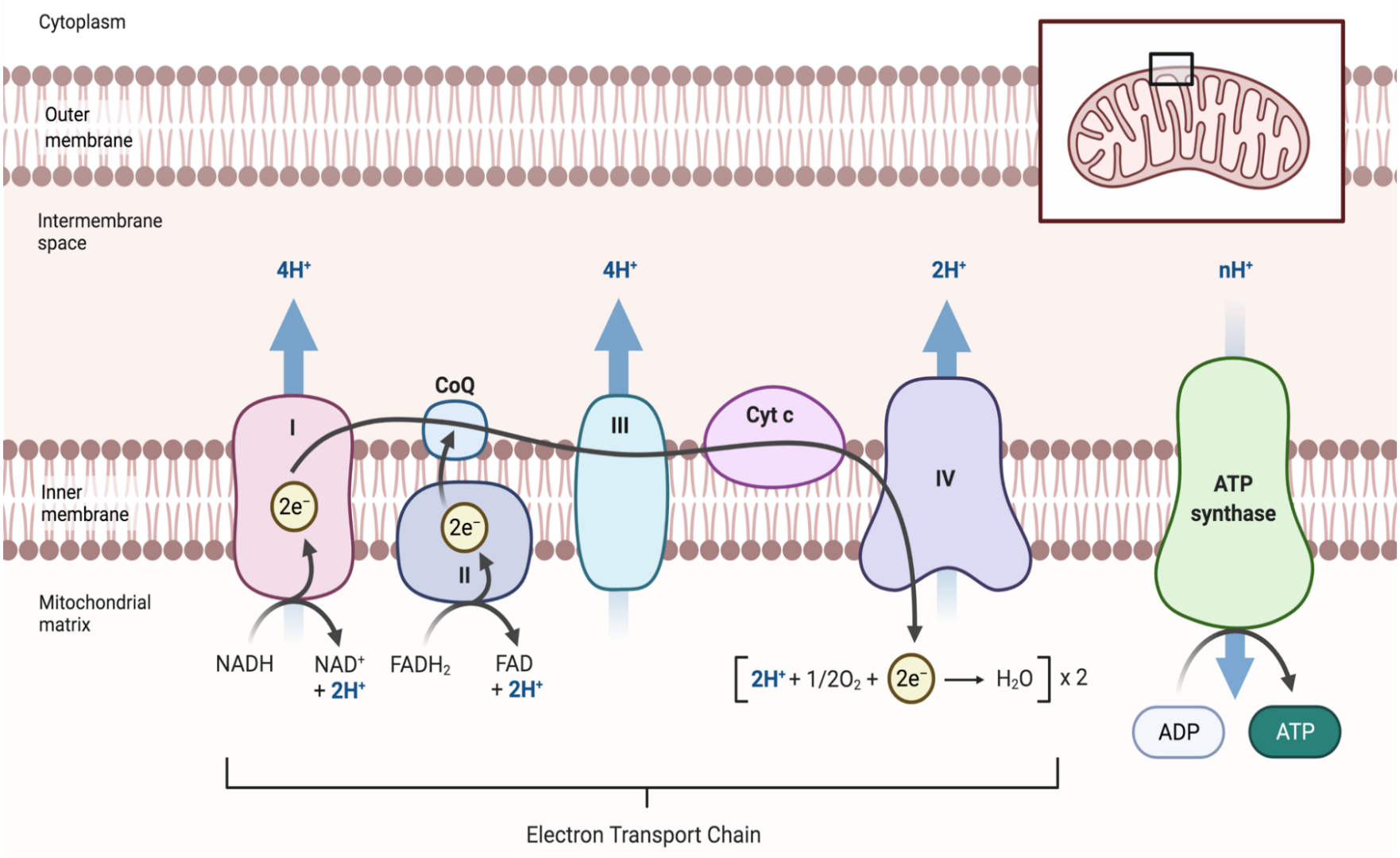

Figure 1.7. ATP synthesis. The ETC, situated in the inner membrane of the mitochondria, is a process that takes place thanks to coordination of four complexes and the ATP synthase to produce ATP. Electrons are transferred from the electron carriers (NADH and $FADH_2$) within the complexes through oxidative and reductive reactions. This generates an electrochemical proton gradient that drives the production of ATP through ATP synthase. Created with BioRender.com.

1.4 Mitochondrial dysregulation in cardiovascular diseases

Since the heart is extremely dependent on mitochondria for its energetic demands, every alteration of the production chain of energy can cause cardiac malfunction and failure of the regular contractility of the heart (Tanai et al., 2015).

In cardiovascular diseases (CVD) and in failing hearts, alterations of substrates and energetic resources can occur because of a reduction in the uptake by the cells of those substrates from the bloodstream, because of an alteration in the pathways that oxidize and/or reduce the substrates or because of a shift in the main metabolic resource. In the heart, the man metabolic source are usually fatty acids, that amount for 60-90% of the energy, compared to glucose, that amount for 10-40% of the energy. In CVD (especially in heart failure, HF), particularly in the earlier stages, there is an increase of metabolic energetic resources. Both fatty acid β-oxidation and glycolysis increase, initially, and in later stages of advanced HF they both decrease equally. Another energetic characteristic of failing heart is the increased production of glucose through hepatic gluconeogenesis and glycogenolysis and increased glucagon production due to the hyper-activation of the sympathetic system that causes a reduction of insulin release from the pancreatic β cells (Doenst et al., 2013; Nagoshi et al., 2011).

Alterations of the energetic production leads to a decrease in the normal distribution of ATP and other energetic substrates to cardiomyocytes and is the main cause for the limited cardiac function (van Empel et al., 2004; Ventura-Clapier et al., 2004). Reduction in the ATP production is mainly caused by a decrease in the oxygen supply to cardiomyocytes, generally due to a block or a reduction in the coronary blood flow. The reduction in the level of oxygen provided to the cardiomyocytes leads to the increased production of ROS, a cause of cardiac damage. ROS are responsible for damaging mitochondrial DNA and since this is almost incapable of self-repairing, it accumulates in the mitochondria and further damages the energetic chain production (O'Connell et al., 2014).

Lastly, alteration of the transfer of high-energy phosphates for final utilization can decrease contractile function. In the energy production chain, the main step that

regulates the number of energetic molecules produced in the heart is the final ADP-rephosphorylation and re-transport back into the mitochondria. This step is dependent on the function of an enzyme, creatine phosphokinase, that transfers ATP to cytosol of the cell and ADP to phosphocreatine. In the failing heart, the levels of creatine phosphokinase are low, leading to a slow re-phosphorylation of ADP and a slow retransport of it into the mitochondria.

Finally, mitochondrial dysfunction also affects the action potential. Impairment in the energetic production chain in the mitochondria affects the ability of cardiomyocytes to regulate calcium homeostasis, resulting in shortening of the action potential, slowed conduction velocities and delayed afterdepolarizations (DADs), ultimately resulting in arrythmias (Montaigne et al., 2015). In events of mitochondrial dysfunction, the increased ROS production and the increased NADH/NAD ratio alter both the RyR2 and SERCA function leading to Ca^{2+} leaking from the SR and accumulation of Ca^{2+} in the cytosol due to incomplete removal during diastole. The combination of the accumulation of Ca^{2+} in the cytosol during diastole and the low mitochondrial membrane potential ($\Delta\Psi_M$) due to alterations of the respiratory chain exacerbates the activity of the sarcolemmal NCX, a key component of the trigger for DADs.

1.4.1.1 Oxidative stress

Aerobic metabolism normally produces high levels of ROS. ROS are defined as oxygen-containing free radicals, such as superoxide anion (O_2^-), hydroxyl radicals, and compounds, such as hydrogen peroxide (H_2O_2), and are involved in mediating both normal and pathological reactions inside the cells (Tanai & Frantz, 2015).

O_2^- is produced inside the cells by either incomplete reduction of oxygen (O_2), from the activity of different enzymes like nicotinamide-adenine dinucleotide phosphate (NADPH) oxidase or xanthine oxidase (XO), uncoupling of nitric oxide (NO) synthase (NOS) or be a by-product of the electron transport from OXPHOS in the mitochondria. From O_2^-, H_2O_2 can be produced either spontaneously or enzymatically (Turrens, 2003).

H_2O_2 is able to generate highly reactive hydroxyl radicals under pathological conditions (Murphy, 2009). In addition, when metabolic cellular stress leads to higher levels of oxidative stress, O_2^- interacts with NO and forms peroxynitrite.

Peroxynitrite is an extremely powerful reactive oxygen derivate, capable of triggering several cytotoxic processes such as lipid-peroxidation or protein oxidation, leading to disruption of the normal cell function (Ferdinandy et al., 2000).

Alterations of protein by ROS results, in the disruption of EC coupling. Furthermore, it can also mediate fibroblast proliferation or collagen synthesis. Some potential sources of ROS include proinflammatory cells, mitochondria, XO, and NADPH oxidases. Under physiological conditions there is a precisely regulated balance between the production of ROS and the molecules, which are capable of "scavenging" ROS in order to limit the amount of ROS present into the cell and prevent their toxicity on the myocytes structure and function. ROS are able to activate transcription factors, hypertrophy and apoptosis signalling pathways (Zorov et al., 2014).

ROS also play an important role in G-protein-coupled receptor (GPCR) hypertrophic stimulation by angiotensin II or β-adrenergic stimulation. Reactive species can effectively modulate other physiological signalling pathways as well, for example, the induction of the expression of proteins involved in ECC (i.e. ion channels or SERCA) or myofilament proteins and protein kinases (Steinberg, 2013).

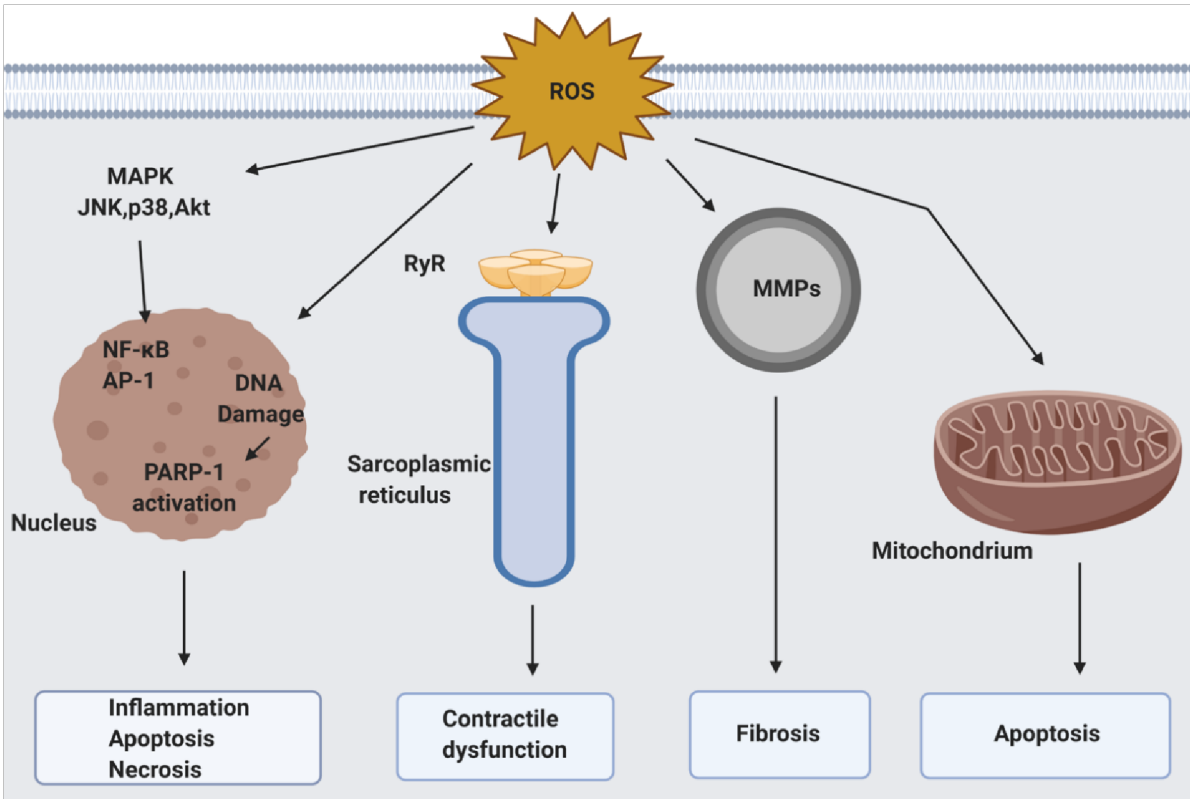

Figure 1.8. Activity of ROS on the heart. Several factors play a role in the detrimental effects of ROS on the heart. ROS are able to activate and modulate the inflammatory pathways mediated by mitogen-activated protein kinase (MAPK) and that, eventually, leads to apoptosis and necrosis of the tissue. Another effector affected by the presence of ROS is the sarcoplasmic reticulum, whose alteration leads to contractile dysfunction. Additionally, ROS are able to lead to the formation of fibrotic tissue through alteration of matrix metalloproteinases (MMPs). Lastly, ROS have a direct effect on the mitochondria, resulting in their own damage and consequent apoptosis. Created with BioRender.com.

A state of activated oxidative stress has been demonstrated in human HF; patients with both ischaemic and non-ischaemic HF showed a marked increase in malondialdehyde-like activity; a marker of lipid peroxidation. Other molecules and mechanisms that were reported to play a significant role in the development and progression of HF in humans are biopyrrins, oxidative metabolites of bilirubin, nitrotyrosins, intracellular marker of oxidative stress, and xanthine-oxidase activity.

Another important mechanism that mediates the damage due to the presence of ROS on normal cardiac function is the inflammatory pathway. ROS are able to activate severe proinflammatory mediators the activation of redox-sensitive signalling pathways and transcription factors is also implicated in the development of cardiomyocyte hypertrophy (Takimoto et al., 2007). Finally, the well-known risk factors for CVD, like

hypertension, diabetes, or obesity, are also associated with increased oxidative stress though increase of repetitive ischemic events and reperfusion periods, or auto-oxidation of catecholamines.

1.4.1.2 Energetic remodelling

Mitochondria were the first intracellular organelle to be investigated regarding Ca^{2+} flux homeostasis after numerous studies showed that Ca^{2+} is sequestered by the mitochondria into the cells (Deluca et al., 1961; Lehninger et al., 1963; Vasington et al., 1962).

Ca^{2+} stored in the mitochondria is responsible for intrinsic functions of the organelle and plays a key role in ATP production (Rizzuto et al., 2012). In particular, Ca^{2+} can activate three key mitochondrial matrix dehydrogenases: pyruvate dehydrogenase is regulated by a Ca^{2+}-dependent phosphatase, and α-ketoglutarate- and isocitrate- dehydrogenases are both regulated by direct binding of Ca^{2+} to these enzymes (Rizzuto et al., 2012).

The activation of these Ca^{2+}-sensitive dehydrogenases increases NADH availability, which in turn increases the flow of electrons down the respiratory chain, resulting in the end in activation of ATP synthesis from the mitochondria (Rizzuto et al., 2012). When oxidizable substrates are provided to mitochondria, electrons are fed into the respiratory chain, which couples electron flow to proton pumps across the IMM. An electrochemical proton gradient is established that drives ATP synthesis and provides the thermodynamic force for Ca^{2+} accumulation in mitochondria (Rizzuto et al., 2012).

In the cardiac myocyte, the two major consumers of ATP during the cardiac cycle are the Ca^{2+}-dependent myofilament ATPase and ion transport ATPases (SERCA, PMCA and Na^{+}-K^{+}-ATPase) (Bers, 2008).

In failing hearts, the homeostasis of Ca^{2+} flux is profoundly altered, translating in equally altered contractility and potential genesis of fatal cardiac arrhythmias (Marks, 2013).

1.5 Heart Failure

HF is a wide-spread cardiac disease in the modern world that puts a significant strain on public health system since hospitalization is extremely common in patients and mortality rates are high (Tanai & Frantz, 2015). In Europe and NorthAmerica the risk of developing HF is of one in five for an average 40-year old person (Mosterd et al., 2007). HF is described as the inability of the heart to meet the demand of peripheral tissue with the right amount of blood to satisfy the metabolic demands of the organs. This inability to provide blood and oxygen to the tissues leads to a clinical syndrome characterized by symptoms such as fatigue, dyspnoea, tachycardia, peripheral oedema and elevated jugular venous pressure (Tanai & Frantz, 2015). The principal risk factors of HF are coronary artery disease (CAD), hypertension, arrythmias, diabetes, hypercholesterolemia, hereditary history of CVDs, chronic pulmonary diseases, drug abuse, smoking and obesity. HF is usually caused by alteration of the myocardial function but alterations in the valves, endocardium and pericardium and conduction disorders may also contribute and/or cause cardiac dysfunction (Malik et al., 2020).

HF can be classified differently according to the criteria: the severity of the symptoms (Table 1.1), developmental stage of the myocardial remodelling, underlying pathophysiological factors (based on the symptoms, and whether these are pressure or volume-induced), area of the system affected (left or right) and cardiac function (systolic or diastolic).

Class	Severity of symptoms and physical activity
I.	No limitation of physical activity. Ordinary physical activity does not cause undue breathlessness, fatigue, or palpitations.
II.	Slight limitation of physical activity. Comfortable at rest, but ordinary physical activity results in undue breathlessness, fatigue, or palpitations.
III.	Marked limitation of physical activity. Comfortable at rest, but less than ordinary physical activity results in undue breathlessness, fatigue, or palpitations.
IV.	Unable to carry on any physical activity without discomfort. Symptoms at rest can be present. If any physical activity is undertaken, discomfort is increased.

Table 1.1. New York Heart Association (NYHA) classification of heart failure.

Another important parameter used to classify HF is the left ventricular ejection fraction (LVEF). HF with an EF ≤40% are defined as HF with reduced ejection fraction (HFrEF), while HF with and EF ≥50% are classified as HF with preserved ejection fraction (HFpEF) and they constitute the two major HF typed based on different etiology, pathophysiology and pharmacological treatment (Y. T. Chen et al., 2019). HFrEF and HFpEF are two distinct syndromes that differ not only in the impairment of the heart function, but also in macro and micromorphology of the heart (Tanai & Frantz, 2015). HFrEF is mostly caused by ischaemic disease, cardiomyopathies and heart valve diseases and is characterized by a major structural change in the morphology of the heart that include chamber dilation and a subsequent volume-overload. By contrast, HFpEF is mainly caused by chronic hypertension or ischemic heart diseases and is characterized by ventricle stiffness and ventricular hypertrophy caused by an alteration in ventricle relaxation and a subsequent pressure-overload. Because the EF is more similar to physiological levels, HFpEF is more difficult to diagnose and to follow-up (Borlaug, 2014; Ouzounian et al., 2008).

1.5.1.1 Biochemical changes in heart failure

Impairment in the regulation of cardiac contraction and relaxation are typically caused by detrimental changes in several different cellular processes, especially ion channels and pumps responsible for the ECC and all the related metabolic pathways. These alterations may be the factor responsible for the altered cardiac function or may be a consequence of other alterations that contribute to the further development of HF. Taken together, they slowly reduce myocardial function and contractility, leading to the problems that characterize HF (Tanai & Frantz, 2015).

One of the biggest biochemical modifications that occurs during HF is the alteration of the ECC (Gomez et al., 2001). In heart failure there's a decrease in the transport of Ca^{2+} into the cells through LTCCs, caused by a lower amount of LTCCs present on the membrane of the cells. This decrease in LTCCs activity leads to cardiac hypertrophy and consequently HF (Goonasekera et al., 2012). While the membrane density of I_{CaL} channels is reduced, channel phosphorylation is increased, which ultimately leads to an increase in single channel open probability that compensates for the lower number of channels (Eisner et al., 2017). Despite the fact that the amount of Ca^{2+} entering the cell remains roughly unchanged, Ca^{2+} transients in the cells by SR are smaller and slower in HF, impairing myocyte contractile properties (Eisner et al., 2017). Other alterations correlated to ECC in HF are the reduced sensitivity of Ca^{2+} to troponin C, leading to an attenuation of the ECC caused by the increase of Ca^{2+} surrounding the troponin complex and the impairment of the sarcoplasmic ATP-dependent Ca^{2+} pump, that leads to a delay in the rate of Ca^{2+} re-uptake by the SR and in turn causes a slower relaxation and diastolic dysfunction (Movsesian et al., 1994).

Dysfunction of RyR2 is a primary cause of arrhythmias leading to HF. Delayed DADs arrythmias are a great risk factor for the development of HF. At the basis of these, there's an hyperphosphorylation of RyR2 caused by chronic βadrenergic stimulation. The hyperactivation of RyR2 causes a diastolic Ca^{2+} leak from the SR and the generation on spontaneous Ca^{2+} waves (Kushnir et al., 2010).

While the principal alterations involved in HF revolve around alterations of Ca^{2+} homeostasis, biochemical changes regarding other currents are also important. In HF, peak I_{Na} is reduced, likely because of a reduction in *SCN5A* expression, whereas I_{NaL} is increased, likely because of increased phosphorylation of Na^+ channels (Amin, Tan, et al., 2010). The expression of $Na_v1.5$ is reduced in the non-damaged myocytes localized in the border zones of myocardial infarction (MI). Furthermore, $Na_v1.5$ expression is also reduced in the remodelling process of HF induced by atrial tachyarrhythmias, leading to a decrease in I_{Na} (Amin, Asghari-Roodsari, et al., 2010).

Regarding K^+ currents, HF is characterized by a downregulation of I_{to}, leading to a slower time course in the force of contraction and, therefore, to a worsened myocardial performance (Y. Wang et al., 2010). HF also reduces I_{Ks} in atrial, ventricular, and sinus node myocytes. The reduction in I_{Ks} may be regarded as the primary responsible for the prolongation of action potential in HF (Amin, Tan, et al., 2010). Lastly, I_{K1} is downregulated in patients with severe heart failure and cardiomyopathy. The downregulation of I_{K1} leads to membrane depolarization and prolongation of action potential, that in turns produces arrythmias (Ravens et al., 2008).

1.5.1.2 Role of the mitochondria in HF

The involvement of mitochondria in HF is complex. There is a decreased ability to generate ATP and satisfy the energetic needs of the heart, but also worsens cardiomyocyte injury and death, therefore speeds development of the disease (D. A. Brown et al., 2016). As mitochondria are the main organelle responsible for the production of ROS inside the cell, they play a role in the development of HF (Nojiri et al., 2006). Mitochondria are capable of generating high energy phosphates as byproducts of oxidation-reduction reactions following the activity of enzymatic respiratory complexes. As described in paragraph 1.3.3.1, superoxide and other ROS are generated when the oxidation-reduction processes are disrupted or incomplete. Physiologically, low levels of ROS are produced and maintained by the activity of endogenous antioxidant enzymes, such as super-oxide dismutase. In HF, the balance between the

production of ROS and the scavenger activity is imbalanced in favour of the production of ROS (Nojiri et al., 2006; Tanai & Frantz, 2015).

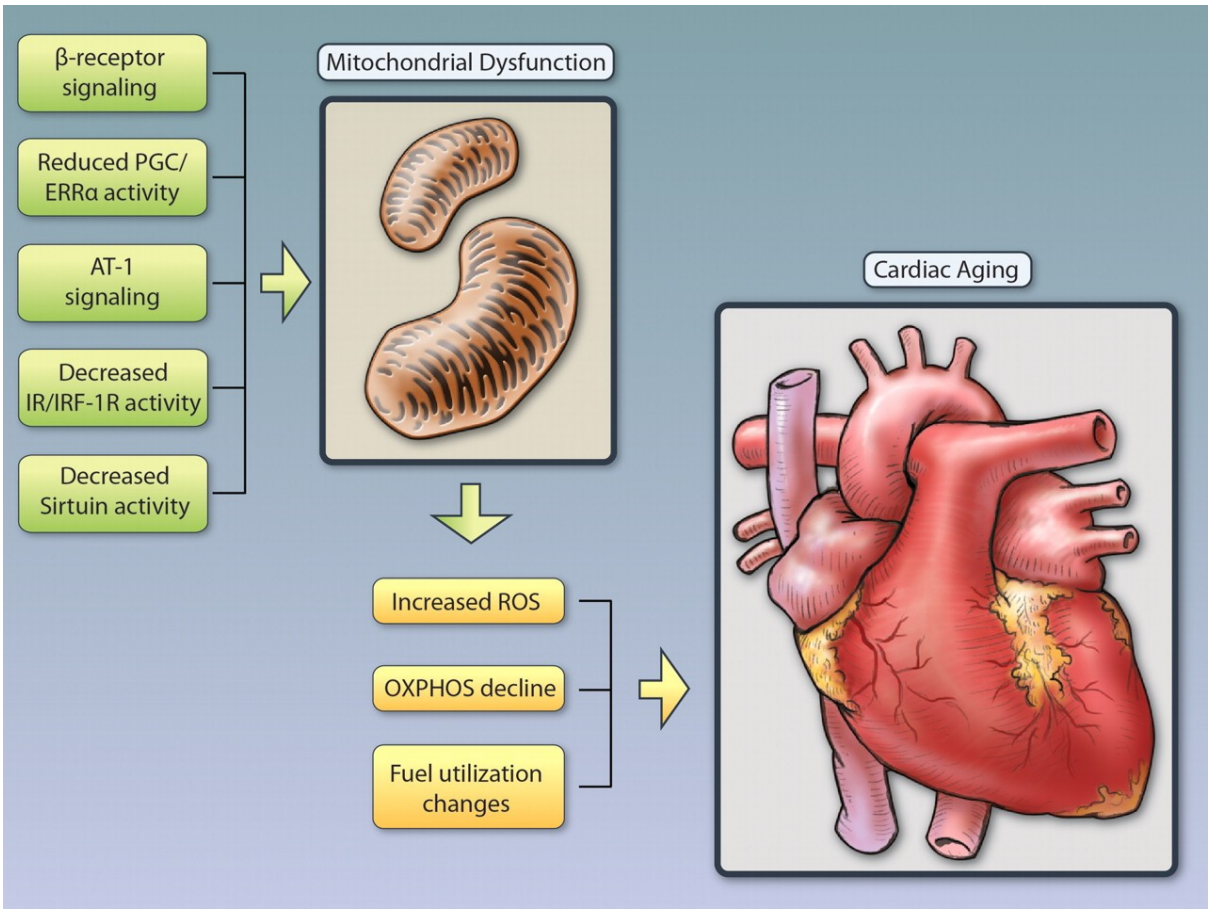

Figure 1.9. Correlation between mitochondrial dysfunction and cardiac aging. Several stimuli, such as β-receptor signalling or AT-1 receptor signalling, may lead to mitochondrial dysfunctions. Prolonged stimuli and dysfunctions may impair cardiac tissues, as non-efficient mitochondria are responsible for increased ROS levels, oxidative phosphorylation decline and changes in energy utilization.

Apart from the production of ROS, mitochondria are also involved in apoptotic processes by releasing cytochrome c, a signal for induction of the apoptosis mediator caspase family (Tanai & Frantz, 2015). Moreover, mitochondrial alterations are correlated to aberrant cellular Ca^{2+} homeostasis, vascular smooth muscle pathology, myofibrillar disruption, and altered cell differentiation, all important issues in CVD, including HF (D. A. Brown et al., 2016). Ultimately, because cardiomyocytes are dependent on the mitochondrial for metabolism and energy supply, pathological imbalances in the energy chain production are directly connected with myocyte

dysfunction, apoptosis and eventually HF (Nojiri et al., 2006; Oka et al., 2012; Tanai & Frantz, 2015).

1.6 Ischaemic damage

Ischaemia is defined as the reduction in the supply of oxygen and nutrients to tissues as a result of a lack of blood flow. Any stimuli that causes a significant reduction in the normal flow of blood to the myocardial tissue can, therefore, be considered a myocardial ischemic damage (Kalogeris et al., 2012). Damage to the myocardium can occur either during the ischaemic episode or during the following reperfusion phase, if the microvasculature connected to the local ischemic event still retains vasoconstriction and/or other type of blockage (Kalogeris et al., 2012).

Ischaemic episodes cause severe damage to cardiac cells, such as mishandling of intracellular energetic resources, alteration of metabolism, activation of inflammatory pathways and Ca^{2+} overload, which in turns disrupt the normal electrical flow of the cardiac cell. In particular, since during ischaemia oxygen levels are altered, the cells are forced to switch from the normal aerobic metabolism to anaerobic glycolysis to continue ATP synthesis. Furthermore, the depletion of ATP levels inside the cell reduces the activity of Na^{+}-K^{+} ATPase, SERCA, further increasing Ca^{2+} and proton (H^{+}) levels, through NCX and Na^{+}-H^{+} exchange (Gho et al., 1997). Also, as previously mentioned, is the role of inflammation in the damage to the cardiomyocytes during ischaemia. In particular, tumour necrosis factor TNF-α plays an important role in damage to the cardiac cells, by inducing mononuclear macrophage and T lymphocyte infiltration into the myocardium and leading to mortality and fibrosis of cardiomyocytes (Tian et al., 2015).

At the end of the ischaemic episode, when reperfusion of the damaged tissue occurs, part of the cardiomyocytes involved can regain normal contractile function while some can become increasingly damaged, enlarging the area involved in the infarct. A plausible explanation behind this phenomenon, generally referred to as ischaemia/reperfusion injury (Budas et al., 2007; Ovize et al., 2010; A. Rana et al., 2015; Yuan et al., 2014), is that the oxidative stress cardiac cells were subjected to, due to the release of ROS

following metabolic disruption, causes openings of mtPTP), resulting in swelling of the mitochondria themselves, uncoupling of the oxidative- phosphorylation chain and release of proteins. Other damages caused by the large production of ROS are damage to the membrane permeability via peroxidation, resulting in cellular oedema and damage ETC, so disruption of ATP synthesis and contribution to Ca^{2+} overload (Zorov et al., 2014).

1.7 Myocardial infarction

MI is the necrosis of a part of cardiac tissue caused by a rapid loss of coronary blood flow in the interested area of the myocardium. The interested area where necrosis occurs, the infarct area, results in permanent damage, as the cells present in this part of the tissue are dead, while the tissue that surrounds the infarcted area shows reversibility in the damage received (Sommer, 2017). While generally the main area affected by MI is the left ventricle, the damage can involve and extend to the right ventricle or atrium as well.

Based on the size of the area infarcted and on how badly the area is damaged during, the severity of MI can be classified in two main categories. The first, named ST- segment elevation myocardial infarction (STEMI), is characterized by elevation in the baseline between the S and T segment of the electrocardiogram (ECG) (Thygesen et al., 2018). This particular ECG is a signal of the unusual movement of electrical current around an area of infarct. The second, named non-ST-segment elevation myocardial infarction (NSTEMI), does not show any particular alteration of the ECG signal (Thygesen et al., 2018). Based on their relative severities, STEMI is usually described as being caused by a near complete occlusion, whereas NSTEMI is caused by a severe narrowing or incomplete block which is enough to cause ischaemia, but not to cause large areas of infarct.

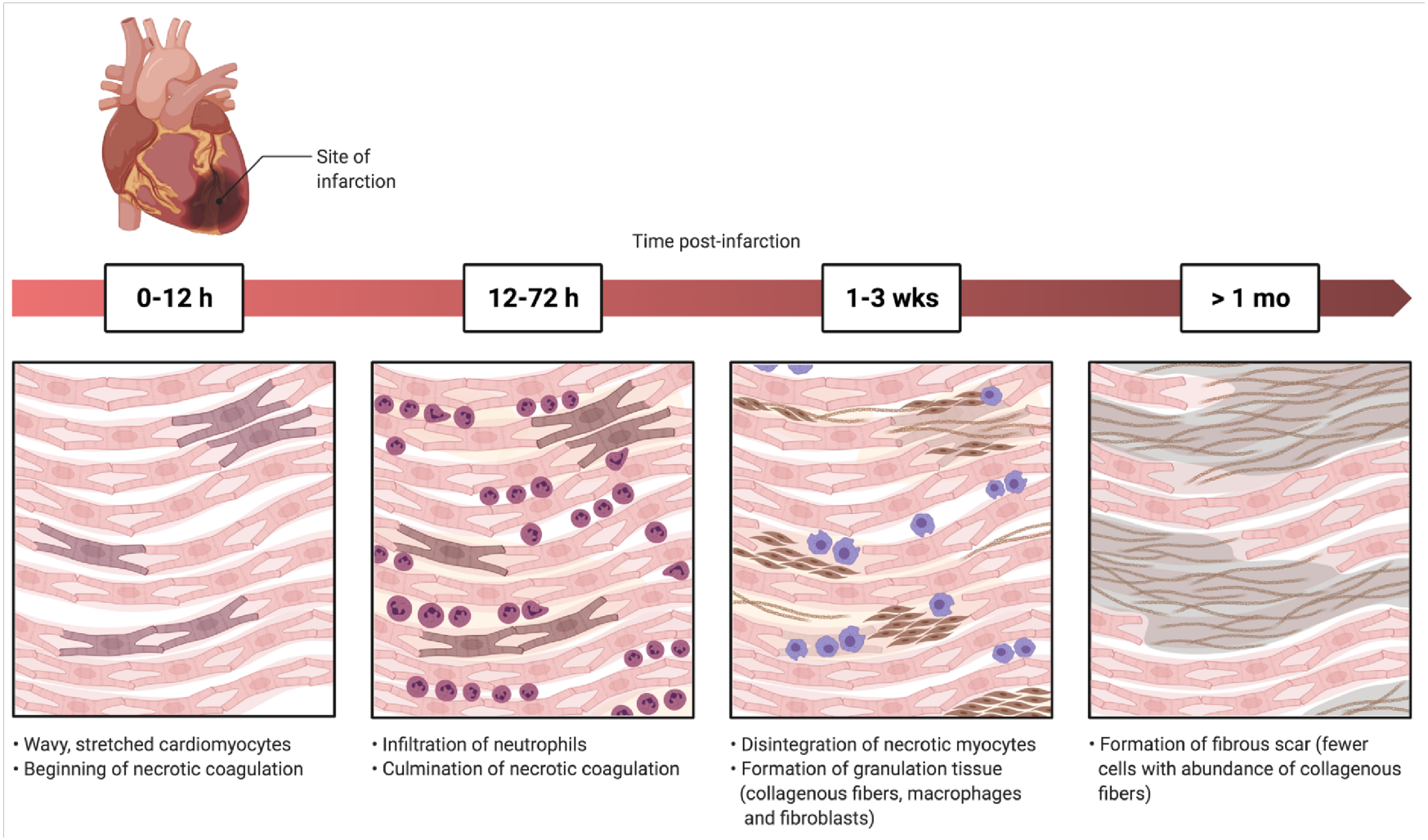

Figure 1.10. Evolution of myocardial infarction. In the first stage of MI, cardiomyocytes are affected by the necrotic tissue and coagulation generated from the infarcted are, causing the cells to stretch and elongate. In the following phase, there is infiltration of inflammatory cytokines and neutrophils that lead to the formation of granulation tissues, characterized by the presence of collagenous fibres, macrophages and fibroblasts. Lastly, dead cardiomyocytes are disintegrated, and the area is turned into a fibrous scar, characterized by a large abundance of collagenous fibres. Created with BioRender.com.

1.8 Conduction disorders

When the normal sequence of initiation and propagation of the cardiac impulse is altered, an arrythmia occurs. In the case of conduction disorders, the conduction system can be altered in different ways: the impulse can be slowed or altogether blocked, causing the normal rhythm of the heart to be disrupted. Causes of conduction disorders can be different, but generally these disorders are cause by underlying conditions such as ischemic heart disease or heart attack, drugs or genetics (Smits et al., 2005).

The principal abnormalities in the normal transmission of the impulse are cardiac arrythmias There are an enormous number of rhythm disturbances, most of them can occur in healthy individuals and many of them are entirely benign in their prognostic implications. There are different types of cardiac arrythmias and usually the symptoms of are complaints of dizziness, palpitations, fast heart beating, and feeling of weakness (D. G. Fu, 2015). Cardiac arrhythmias can be classified by their origin in the heart and by their speed or rhythm (Table 1.2).

Normal sinus impulse formation	• Normal sinus rhythm • Sinus arrhythmia
Disturbances from sinus	• Sinus bradycardia • Sinus tachycardia
Disturbances of ventricular impulse formation	• Ventricular premature complexes • Ventricular tachycardia • Ventricular asystole • Ventricular fibrillation
Disturbances of atrial impulse formations	• Atrial premature complexes • Atrial tachycardia • Atrial flutter • Atrial fibrillation
Disturbances of impulse conduction	• Sinus arrest • Atrial standstill • First degree AV block • Second degree AV block • Third degree AV block

Table 1.2 Classification of arrythmias.

The most common sustained arrhythmia is atrial fibrillation (AF). The prevalence in the general population varies somewhere between 0.15%-1%, with an overall prevalence rate of about 0.5%, which seems to be moderately consistent across international boundaries (Zoni-Berisso et al., 2014). AF is defined as any episode of abnormal electrical activity lasting 430s according to the ECG criteria (Fuster et al., 2006). Episodes of AF are generated when a train of ectopic beats at high frequency, from continuous ectopic activity (Jalife, 2011; Nattel, 2002; Ravens, 2015).

As all other tachyarrhythmias, AF depends on three major mechanisms: automaticity, triggered activity, and re-entry (Antzelevitch et al., 2011). Automaticity refers to the innate ability of an excitable tissue to spontaneously depolarize and is a key feature of the cardiac conduction system. Alterations in the automaticity happen when other areas apart from the conduction system began to show automatic activity faster than the peacemaker site or when the firing rate of the latter accelerates (Denham et al., 2018). Triggered activity refers to the addition of new impulses triggered by the original action potential that are known as afterdepolarizations. The majority of the alterations that lead to afterdepolarizations are related to abnormal Ca^{2+} handling. The afterdepolarizations are distinct in two types: early afterdepolarisations (EADs) and DADs. EADs are generally caused by an increase in I_{CaL} and occur during the phases 2-3 of the action potential (X. Qi et al., 2009; Weiss et al., 2010). DADs, on the other hand, are caused by spontaneous Ca^{2+} release from the SR in the form of an extra Ca^{2+} wave and occur during phase 4 of the action potential (Venetucci et al., 2008). Lastly, the re-entry mechanism refers to restimulation of the conduction system due to circling around an obstacle by the depolarizing waves. The obstruction to the conduction system may be of anatomical origin, such as scar tissue, or of functional nature, such as an area of tissue that is rendered unexcitable (refractory) by continuous depolarization (Denham et al., 2018).

AF is also promoted by the structural reorganization of the myocardium occurring because of aging and CVDs, that contribute to the initiation and progression of AF (Heijman et al., 2014).

1.8.1.1 Channelopathies

Imperfections in ion channel formation caused by genetics, external factors or a combination of both can lead to development of diseases defined as channelopathies. The major cause of channelopathies is the mutation in genes encoding for ion channels, which can cause impairment in the ion channel's function (J. B. Kim, 2014). Depending on the mutation, the consequence can be either a gain of channel function or a loss of it. Either way, a single mutation can cause different phenotypes or a combination of them. Cardiac channelopathies are likely responsible for approximately half the sudden arrhythmic death syndrome cases (Behr et al., 2008).

The first genetically identified cardiac disorder was congenital long QT syndrome (LQTS). LQTS takes its name from the typical shape of the ECG, with a prolonged Q-T interval, that patients with this disease have. It is characterized by a delayed ventricular repolarization, which leads to an increased risk of ventricular tachyarrhythmias and can, eventually, lead to sudden cardiac death. LQTS is not caused univocally by a single genetic mutation, but there are at least 13 types of LQTS linked to ion channels genetic mutations or mutations in proteins associated with them (Y. Yang et al., 2010).

The most common type of LQTS, LQT1, is present in almost 40-50% of patients and is caused by loss-of-function mutations on the *KCNQ1* gene ($K_v7.1$), encoding for an integral part of the I_{Ks} macromolecular complex (J. Wu et al., 2016). LQT1 is characterized by a decrease in the activity of I_{Ks}, which in turn causes a prolonged repolarization phase, action potential duration, and QT interval. Ventricular arrythmias caused by LQT1 are usually linked to stress, exercise and physical or emotional triggers and in general periods of increased sympathetic activity, where I_{Ks} has a more predominant role in the repolarization phase. Under physiological conditions, I_{KS} is promoted by sympathetic activity in order to shorten the longer action potential cause by an increase in Ca^{2+} activity. This physiological process is altered by LQT1, thus creating a pro-arrhythmogenic phenotype (J. Wu et al., 2016). Accordingly, βadrenergic blocking drugs suppress arrhythmic events in LQT1.

LQT2 is the second most prevalent type of LQTS. LQT2 is one of the two variants in which I_{Kr} is dysfunctional: LQT2, caused by *KCNH2* mutations, and LQT6, caused by *KCNE2*

mutations. LQT2 is caused by a loss of function in I_{Kr} that in turns causes a prolongation of action potential, especially near plateau voltages, favouring the development of EADs. Because of the relative distribution of K^+ channels, LQT2 leads to a more marked prolongations of the action potential duration in midmyocardial cells of the heart. The heterogeneity of the repolarization across the ventricular walls linked to LQT2 can trigger the formation of torsades de pointes type ventricular fibrillation (Adler et al., 2016).

LQT3, which accounts for approximately 5% to 10% of congenital LQTS cases, is caused by gain-of-function mutations in the *SCN5A* gene, which encodes the α subunit of the Na^+ channel ($Na_v1.5$). The majority of *SCN5A* mutations cause a gain of function by disrupting the fast inactivation typical of Na^+ channels and creating a small and non-physiological Na^+ current during the action potential plateau. The presence of a persistent inward I_{Na} during the plateau phase of the action potential causes a prolonged repolarization and a longer Q-T interval. Compared with other LQT subtypes, patients with LQT3 are less likely to suffer from adverse cardiac events but those cardiac events are more lethal; a 20% fatality rate is linked to LQT3 cardiac events compared to 4-5% rate of LQT1 and LQT2 (Perez-Riera et al., 2018). Other channelopathies that can be caused by loss of function in Na^+ channels are Brugada syndrome, familial atrial fibrillation, sick sinus syndrome, familial heart block, and atrial standstill (Wilde et al., 2011). Brugada syndrome is a channelopathy characterized by an elevated S-T segment and it can be caused by mutations in several different genes but principally a mutation in *SCN5A*.

A channelopathy related to an impairment in the Ca^{2+} homeostasis is catecholaminergic polymorphic ventricular tachycardia (CPVT). The predominant form of CPVT, CPVT1, is cause by a mutation in RyR2, in particular a gain of function mutation of this. The increase in function of RyR2 leads to an intracellular Ca^{2+} leakage from the SR, causing an increase in the likelihood of EADs and ventricular tachycardias (van der Werf et al., 2013). CPVT is characterized by development of ventricular tachycardia during adrenergic stimulation. Experiencing emotional or physical stress can induce dizziness, syncope, and/or sudden cardiac death in patients with CPVT (Postma et al., 2005).

1.9 The Gut Microbiome

The entire human microbiome is made up of ~10^{14} bacterial organisms belonging to >2,000 species within our bodies, the vast majority being in the gut (Neish, 2009). In this number are included commensal microorganisms that colonize the human gut and play crucial roles in protection from environmental exposure, digestion, and absorption of nutrients (Backhed et al., 2005; M. Li et al., 2008; Nicholson et al., 2005).

The composition of the gut microbiome is different for each human being and it differentiates mostly because of lifestyle factors and/or environmental exposure rather than by inherited genetic factors (Yatsunenko et al., 2012).

Noticeably, the human organism consists of 10-fold greater numbers of bacterial than animal cells that are metabolically and immunologically integrated (Gill et al., 2006; Xu et al., 2007), by including approximately 10^{14} prokaryotic organisms, with a biomass of >1 kg.

Anaerobes are several orders of magnitude more abundant that aerobes in the bacterial community, and a majority of the population (60%–90%) are representatives of 2 divisions: the *Bacteroidetes* and *Firmicutes* (Neish, 2009).

The strains of bacteria that lives in our bodies, particularly in our gut, have several different functions that benefits our body, such as: providing nutrient metabolism in the gut, calibrating metabolic function, educating the immune system, maintaining community integrity, and defending against pathogens (Flint et al., 2012; Maranduba et al., 2015). Amongst other functions that are very important to our systems, the gut microbiota is able to produce vitamins and the breakdown of oligo-/polysaccharides (Conly et al., 1994; Hill, 1997; Xu et al., 2003).

For this reason, our body needs to provide the correct habitat for these particular strains of bacteria that play a key role in our well-functioning and, at the same time, being able to defend from pathogenic species (Stinson et al., 2017). Crucial, in this scenario, is that human immune system is able to distinguish between beneficial and harmful bacteria (Stinson et al., 2017).

The work of the immune human system is simplified by the gut microbiota itself that participate in host defence (Salzman et al., 2007) by competing with the pathogenic

strains of bacteria for space and nutrients, by fermenting non-digestible nutrients, synthesizing vitamins and by producing anti-microbial compounds such as bacteriocins and lactic acid (O'Hara et al., 2006).

Numerous studies have started to take interests in the link between alterations of the gut microbiome and different metabolic syndromes such as non–insulin dependent diabetes, non-alcoholic hepato-steatosis, and atherosclerosis (Cani et al., 2007; Dumas et al., 2006), because it is now fully recognized that the gut microbiome play an important role in several different biochemical processes.

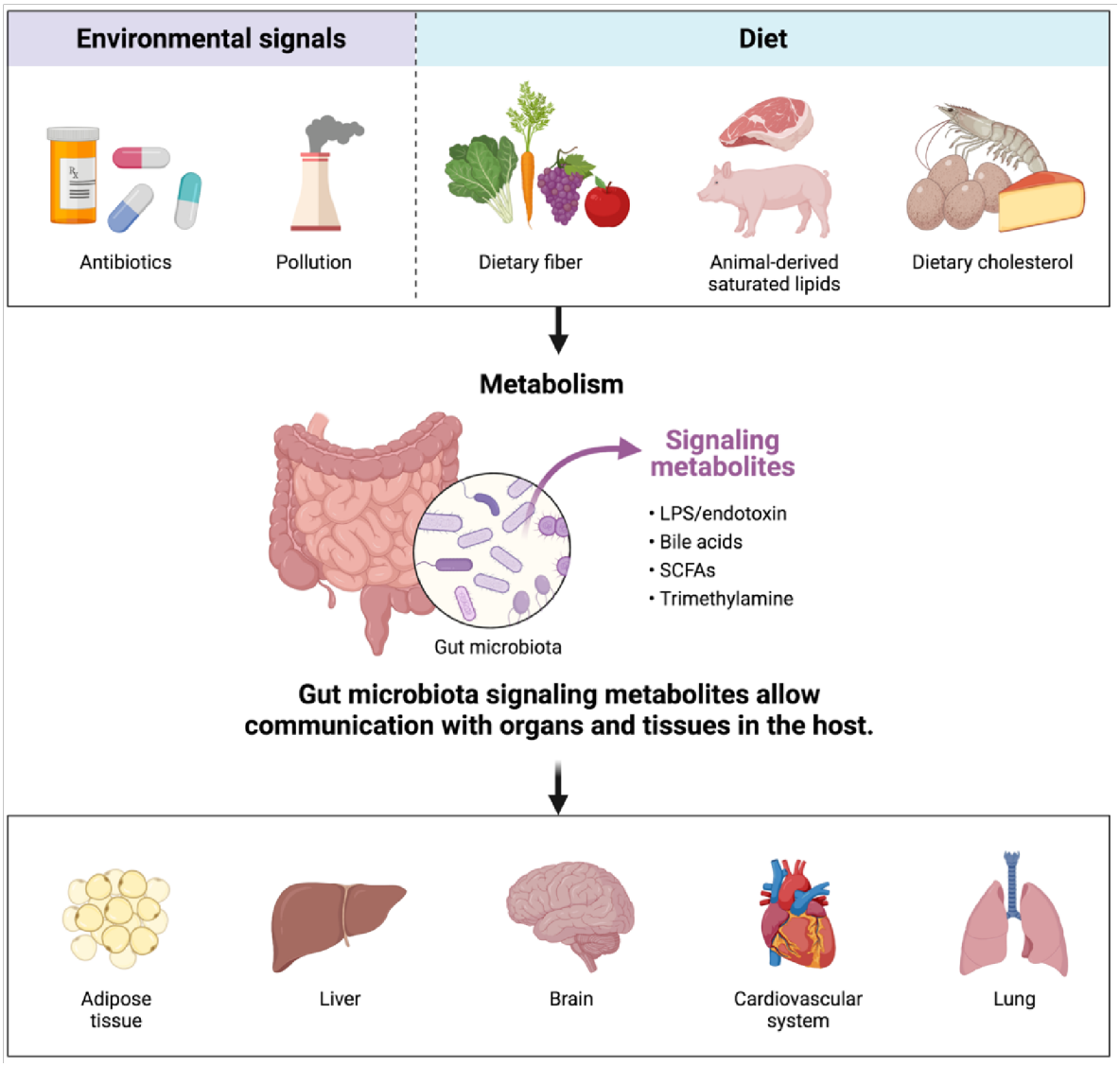

Figure 1.11. Schematic of production of metabolites and tissues they exert effects on. Molecules that enter our bodies, generally through diet, are broken down into our guts thanks to the help of the human gut microbiota. The human gut microbiota, thus, produces metabolites that are capable of interacting and entering pre-existing metabolic pathways and can be both extremely important to the normal physiological functions of our bodies or can have disrupting effects. Created with BioRender.com.

Increasingly, evidence is emerging to suggest that the disruption of this community (dysbiosis) may be responsible for a number of diseases, such as asthma, allergies, obesity, and autoimmune diseases (Debarry et al., 2007; Moreno-Indias et al., 2014; Thorburn et al., 2015).

1.9.1 Tools for the study of the gut microbiome: the –omics

As previously described, the human gut hosts trillions of microbial cells coming from thousands of different species with different phylogenetic backgrounds bacteria, archaea, and different microbial eukaryotes (Qin et al., 2010). Taken together, this plethora of cells hosted inside the human body that takes the name of gut microbiota has a number of cells almost similar to that of human cells and (Sender et al., 2016) and 450-fold more genes than the human genome (J. Li et al., 2014; X. Zhang et al., 2019). The determination of the nature of the organisms present in the human gut microbiome with standard microbiological techniques is impossible because each different organism may require special growth conditions that may be yet unknown. Generally, traditional studies of the human gut microbiome that are almost entirely dependent on cultivation techniques, only manage to cultivate successfully 10-30% of this microbial system (Tannock, 2001).

The discovery and introduction of DNA-based analysis that do not require cultivation of the microbial system has greatly improved the possibility to explore and understand the human gut microbiome. These DNA-based techniques have evolved during time from the use of polymerase chain reaction (PCR) using universal group-specific 16S ribosomial ribonucleic acid (rRNA) gene primers followed by electrophoresis to sequencing, to better comprehend the variety of the microbiome (Sirangelo, 2018). Currently, the most used techniques adopted in the study of the gut microbiome are referred to as the "meta-omics" approach, and include: 16S rRNA gene sequencing, metagenomics, metatranscriptomics, metaproteomics and metabolomics, that overall examine the phylogenetic markers, genes, transcripts, proteins, or metabolites from the samples (X. Zhang et al., 2019). The different "meta-omics" approaches take each into consideration different aspects of the microbial system and its interaction with the human body, each with their own advantages and disadvantages, discussed in the next sections (X. Zhang et al., 2019).

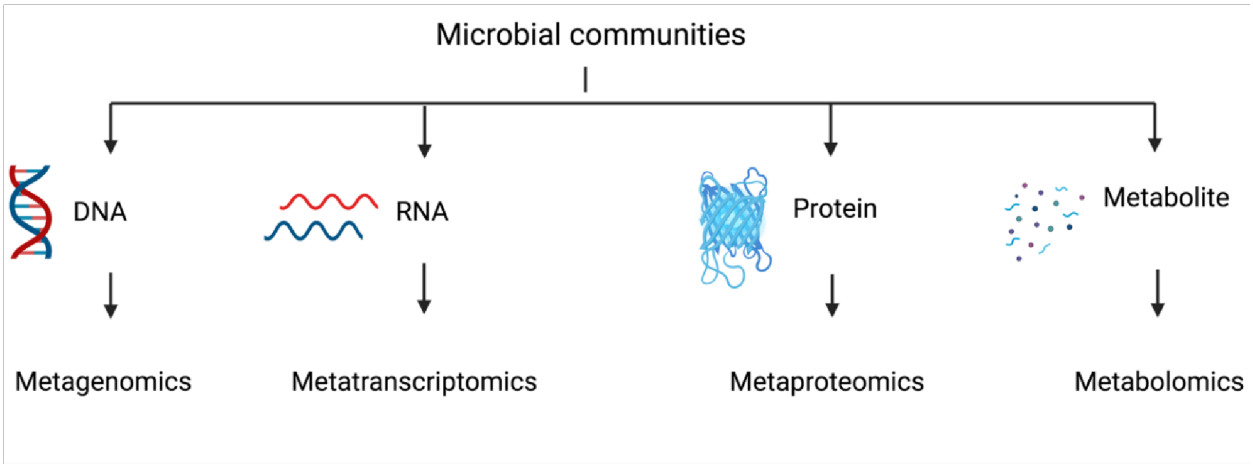

Figure 1.12. Schematic of the -omics and substrates utilised for the different techniques. Different experimental approaches and computational strategies are applied for the study of microbial communities. In metagenomics, genomic DNA sequences can be mapped to a reference database or used for assembly of genomes. In metatranscriptomics, mRNA is used to generate complementary DNA libraries that can be mapped to reference genomes. In metaproteomics, mass spectrometry and fragmentation is used to reveal the amino acid sequence of peptides. In metabolomics, metabolites are separated using chromatography techniques and identified and quantified using mass spectrometry. Created with BioRender.com.

1.9.1.1 Metagenomics

The first of the "meta-omics" to evolve out of the use of gene sequencing, metagenomics, focuses on the study of the entire genomes. While genomic is referred as the study of the genetic material of a specific organism, metagenomics allows the study of genetic material of an entire community of organisms (Aguiar-Pulido et al., 2016). This was made possible by the technological progress that have made high throughput microbial analysis easy and cost-effective, allowing for drastic improvements in the genomic field (Sirangelo, 2018).

Metagenomics gives us the opportunity to investigate the genetic composition of a microbial system. After the extraction of DNA from the samples, these studies usually utilize next generation sequencing (NGS) and are based on shotgun techniques that produce large volumes of short reads from DNA. NGS short reads are subsequently compared to reference genomes to identify variants and community population, from which is possible to piece together information on the microbial community investigated (Aguiar-Pulido et al., 2016). The data thus obtained can be compared to

pre-existing databases and abundance or analysed with appropriate software programs to cluster the reads into Operational Taxomonic Units (OTUs) (Weinstock, 2012).

Metagenomics is a powerful tool in the genetic analysis of the human gut microbiome; however, it has its downsides. First, metagenomics is only able to provide information on the gene sequences present in the microbiome but do not gives information about the actual physiological function of the gene or its protein expression level. Metagenomics is not capable to distinguish between microbiomes that are active, dormant or dead, therefore it does not provide any insight into the actual activity of the human gut microbiome (Mitra et al., 2013). Furthermore, in order to obtain high coverage required for metagenomic, high quality and quantity of DNA samples are of extreme importance (Wang et al., 2015). However, sampling is limited by absence of adequate methods that successfully cultivate indigenous microbial communities, biases introduced by preferential PCR amplification of 16S rDNA genes and limitations in individuating organismal function from these gene sequences (Gill et al., 2006), thus creating difficulties in achieving a full gut reading. Finally, metagenomic analysis is dependent on the use of computational algorithms and, most importantly, on a complete reference database, so it is essential to improve these methods in order to make the most out of the information obtained through metagenomics (Sirangelo, 2018).

The necessity to have more information at a functional through analysis of gene expression patterns brings us to the topic of our next section, metatranscriptomics (Aguiar-Pulido et al., 2016).

1.9.1.2 Metatranscriptomic

Metatranscriptomics focuses on providing information on the active functional profile of a microbiome based on the analysis of what genes are expressed in the entire microbiome (Aguiar-Pulido et al., 2016). Metatranscriptomics is based on the sampling and sequencing of environmental messenger ribonucleic acid (mRNAs) from a microbial system to give information on what genes may be present in that microbiome (Sirangelo, 2018).

Despite seemingly improving on the information obtained by metagenomics, metatranscriptomics have their own disadvantages. First, it is practically very difficult to obtain high-quality and sufficient amounts of RNA from environmental samples and it is also extremely difficult separating the mRNA of interest from the more abundant types of RNA such as rRNA. Lastly, the metatranscriptomics classification is restricted by the limited number of reference databases, a problem shared with metagenomics (Sirangelo, 2018).

1.9.1.3 Metaproteomics

Metaproteomics, the analysis of the protein content of a sample, is a very important tool to understand microbial functions of the human gut microbiome (Sirangelo, 2018). Metaproteomics is capable of giving important information on the functional aspect of the human gut microbiome, its physiological state and its interaction with the human body by analysis of the protein profile. Metaproteomics may be considered as an entire new research area, since it can be helpful by giving insight on pathologies relevant to the human gut microbiome (Sirangelo, 2018).

While all previous "meta-omics" required genetic material for its studies, metaproteomics has a different approach. Thanks to the technological advances of liquid chromatography (LC) enabling separation of highly complex peptide mixtures, high-resolution mass spectrometry (MS) enabling acquisition of large numbers of accurate mass spectra, and computational tools for data processing and analyses, metaproteomics now gives the ability to identify and quantify tens of thousands of peptides and 10,000 proteins per sample (Kleiner, 2019).

However, the great variety of species and variability of the human gut microbiome represent a big obstacle to the use of quantitative metaproteomics as a primary tool in the study of the microbiome. Furthermore, there are technical limitations and there are no standardized procedures as of yet (Sirangelo, 2018). Finally, similar to metagenomics and metatranscriptomics, pre-existing reference databases are necessary to assign functional classifications (Sirangelo, 2018).

1.9.1.4 Metabolomics

The term metabolomics refers to the study of the entire content of metabolites of a sample (metabolites are considered as small molecules released by a certain organism into its immediate surroundings), including their identification and quantification (Fiehn, 2002). Metabolomic profiling of a microbiome is considered as an important marker of the health of a certain system or, obviously, for its alteration (Bernini et al., 2009). Since variations in the productions of determined metabolites are important signals related to changes in the physiological metabolic pathways, metabolomics is an important tool for pathway analysis (Aguiar-Pulido et al., 2016; Krumsiek et al., 2015). While previous described techniques and analysis reveal information on gene products produced in the cell, metabolic profiling gives an insight into the actual physiology of the cell. Metabolomics, thus, defines the metabolic gut microbiome profile, by individuating and quantifying classes and metabolites of interest (Sirangelo, 2018). Tools used in this "omic approach" are completely different compared to the previously described analysis. Metabolomics uses MS and nuclear magnetic resonance spectroscopy (NMR) as the main technologies for the study. These methods are subsequently integrated with biostatistics and mathematical approaches in order to obtain biological information to compare with pre-existing datasets (Sirangelo, 2018). Metabolomic profiling can be strongly associated and influenced by different environmental factors, such as diet, environmental stress on the system and/or exposure to different substances, which means that that metabolomics can provide information that are not limited to the characteristic of the microbiome itself, but it can also provide insights into its interactions with the host environment (Manor et al., 2014; G. D. Wu et al., 2016). On these premises, metabolomics is a useful tool in the understanding of the role of the microbiome in the production and/or conversion of nutrients and other xenobiotics and how the microbiome can influence the homeostasis of the host environment (Aguiar-Pulido et al., 2016). Furthermore, metabolomics studies in the human gut microbiome have revealed the existence of different biomarkers, which could lead to new studies into the understanding of different pathologies and in the development of alternative therapies that have the gut

microbiome as a target for modulation (Vernocchi et al., 2016). Currently, metabolomics is increasingly used to study the gut microbiome (Heinken et al., 2014). Metabolomic studies into the human gut microbiome, however, face some limitations. Metabolites obtained from human samples are mixed and it is still difficult to discern information coming from the host and those obtained from the gut microbiome. In addition, before considering implementing metabolomics into general clinical practice, the establishment of a standardized protocols in analytical performance and data analysis would be of essential importance (Chau et al., 2008; Klupczynska et al., 2015), as differences in sample handling and acquisition can drastically impact outcomes in metabolomic studies, and sample stability and reproducibility of results are also strictly dependent on standardization of sample collecting, handling and storing (Chau et al., 2008). Standardization is of extreme importance especially in cases where large and fast changes of intracellular levels of metabolites occur during sampling collection, like in biopsy samples (Chau et al., 2008). Finally, metabolomics suffer of the same struggle that other omics thus mentioned encounter: databases are incomplete and there are multiple metabolites yet to be defined (Sirangelo, 2018).

It comes naturally that, since the aim of these studies is to determine which gene, enzymes, pathways are connected to specific metabolites, metabolomics is often integrated with other "omic" data to produce a comprehensive description of the microbiome (Aguiar-Pulido et al., 2016).

1.9.1.5 Integrative multi-omics approach

Integration of data obtained through different multi-omic approaches is the most powerful tool for understanding the physiology of microbiome functions. The different omics can be combined differently as to get different information. For example, by integrating data from metagenomics and metatranscriptomics, it is possible to obtain calculation of transcript/gene ratios, an insight into gene transcriptional activation of repression. Another example of integration of different omics is the combination of metaproteomics with metagenomics, that can be used for facilitating protein identification from MS spectra by taking advantage of a matched metagenomic

database or for information about the protein expression (Erickson et al., 2012; Tanca et al., 2015; X. Zhang et al., 2016). One of the most used multi-omic integration is the combination of metabolomics and metagenomics. Typical information obtained by this integration are identification of patterns between the composition of a microbiome and the metabolites identified and the characterization of a specific taxa and its contribution to metabolite production (Jansson et al., 2009; C. Zhang et al., 2015).

Another goal of data integration is the validation of pre-existing microbiome metabolic models. While this aspect of the multi-omic approach is still one of the most difficult, promising steps forward include the generation of >700 genome-scale metabolic reconstructions (Magnusdottir et al., 2017), the development of tools for microbiome metabolic modelling/prediction (Noecker et al., 2016; Shoaie et al., 2015), and the establishment of inter-species metabolic network databases (Sung et al., 2017). Applications of these offer the possibility to mark and differentiate between healthy or altered states or the possibility to flag and predict clinical outcomes, using integrated multi-omics and carefully built algorithms (Douglas et al., 2018).

However, even the integration of multi-omic data has limitations. In particular, the elaboration of multi-omic datasets is very demanding due to its complexity and the diversity of the data itself. Successful integration of data is strongly dependant on efficient bioinformatic tools and advanced statistical methods, such as multivariate statistics and machine-learning approaches (X. Zhang et al., 2019).

Future promising prospective are given by the application of advanced machine learning approaches (Chaudhary et al., 2018). It is expected that by integrating advance machine-learning it would be feasible the generation of microbiome-scale metabolic reconstruction, a tool that could potentially open way to a comprehensive analysis of new therapies that target the human gut microbiome. In summary, while multi-omic data integration still has several challenges to overcome, it is the most promising approach to finalize a complete analysis of composition, function and metabolic activity of microbiomes and its effect on the host environment (X. Zhang et al., 2019).

1.9.2 Variability in the Gut Microbiome

The human gut microbiome has a certain degree of flexibility when it concerns the composition of the microbiome. One of the most exemplary studies that highlights microbiome variation is the Human Microbiome Project, which recruited 242 healthy patients and characterized the microbiome by 16S sequencing at 18 distinct body sites (Human Microbiome Project, 2012a). Differences amongst this cohort were massive, at all the measured body sites, despite the cohort including only healthy patients (Human Microbiome Project, 2012b; Huse et al., 2012). While a certain degree of associations in the compositions of the microbiome was found amongst patients with the same ethnicity, other parameters evaluated, such as BMI, gender, temperature and blood pressure did not display the same degree of associations, and where therefore not considered reliable (Fodor, 2014; Huse et al., 2012).

The strongest factor that influences the composition of the gut microbiome is its physical architecture. Physical architecture of the gut microbiome is genetically dependent, thus gut microbiomes show more similarity amongst members of the same species as opposed to distantly related ones (Ley et al., 2008). Studies have shown that human gut microbiomes are more similar to each other that to the gut microbiomes of other species, despite differences in age, diet and geographic location (Ley et al., 2008). One of the factors that influence variability in the human gut microbiome is diet and lifestyle of the individual (Carmody et al., 2015; David et al., 2014; Goodrich et al., 2016; Goodrich et al., 2014). Factors correlated to diet and lifestyle that influence the composition of the human gut microbiome are usually linked to their ability of modifying the gut architecture; diet, body mass index (BMI) (Beaumont et al., 2016) and immune system activity (Goodrich et al., 2016; Goodrich et al., 2014). Another important aspect correlated to diet and lifestyle is antibiotic usage, a factor that can have marked effects on the composition of the human gut microbiome (Yassour et al., 2016).

Age is another important variable that has specific effects on the diversity and, most of all, in the richness of the human gut microbiome (Saraswati et al., 2014; Yassour et al., 2016). In particular, the gut microbiome of individuals before the age of 3 is

characterized by a less diverse composition that transitions into a more diverse configuration after the age of 3 (Hall et al., 2017; Rodriguez et al., 2015).

The variability of the human gut microbiome represents one of the most substantial challenge for the relevance of clinical studies that aim to link alterations of the human gut microbiome with diseases states. Consistent conclusions in cross-sectional studies can become quite challenging when the variability in the composition of the human gut microbiome changes the way healthy and dysbiotic states are differentiated. Thus, it is of extreme importance that variability in the human gut microbiome composition is considered when powering clinical studies (Fodor, 2014).

1.10 Gut derived metabolites

Metabolites produced by the human gut microbiome have important and diverse effects on the host normal physiology and can be detected in different biological tissues, including faeces, urine, serum, liver and cerebrospinal fluid (Holmes et al., 2011; Lavelle et al., 2020).

Several metabolite classes have become the scope of intense research, since it is increasingly evident that these metabolites are strictly linked to important pathways that regulate human physiology. Among these metabolite classes, the most discussed are bile acid derivatives (BAs), short chain fatty acids (SCFAs) and tryptophan metabolites.

These metabolite classes can affect the host through various mechanisms, and models of inflammation that incorporate diet, genetic risk and the microbiota have been developed that highlight the connections between the host, alterations of the human gut microbiome and an equally altered production of metabolites (Lavelle & Sokol, 2020).

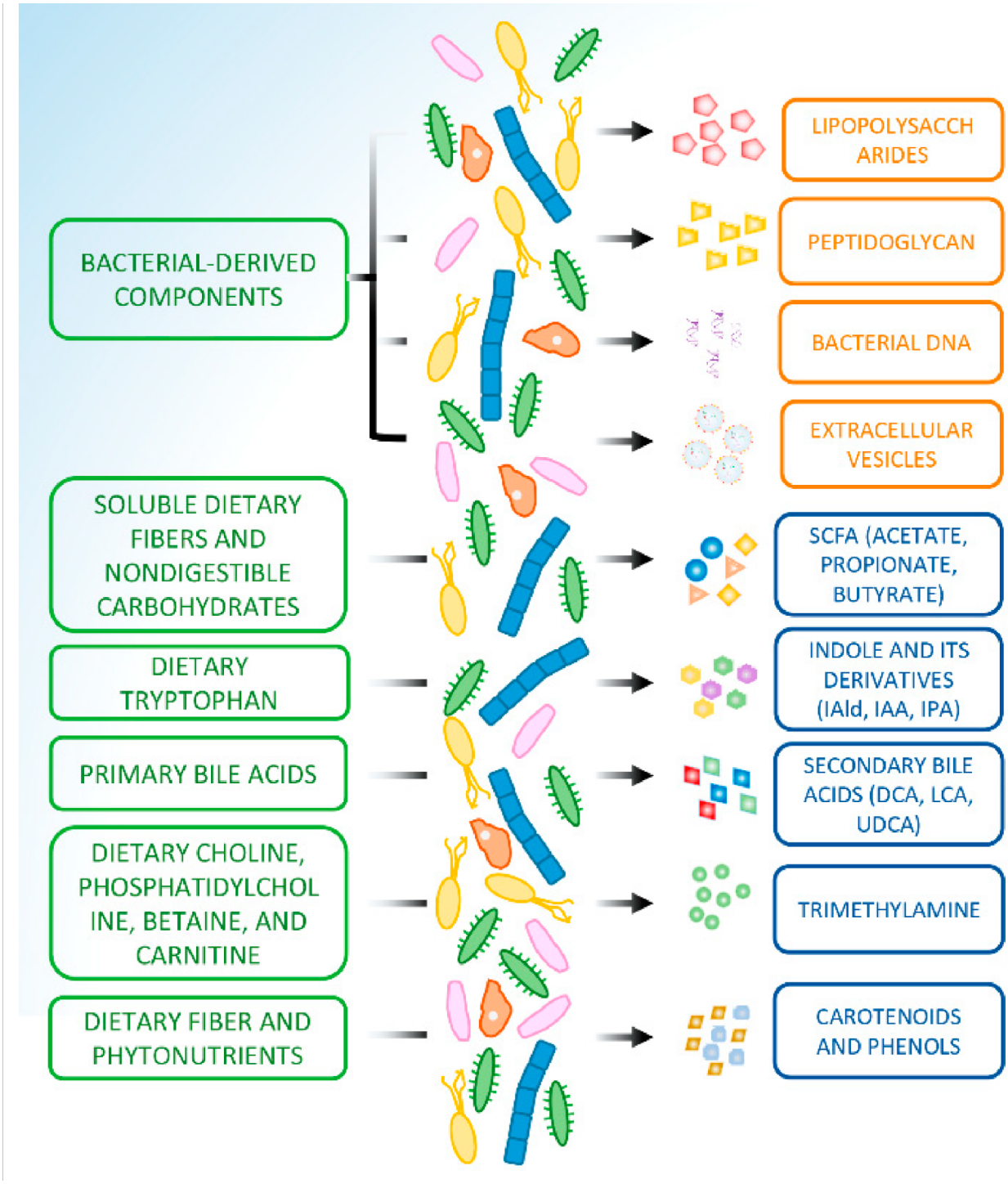

Figure 1.13. Schematic of dietary nutrients and the relative active metabolites in the human body. The gut microbiome can produce different metabolites from dietary components. Amongst them, some have been correlated to different pathologies. In particular, from dietary fibres and nondigestible carbohydrates fermentation are produced short chain fatty acids (SCFAs) such as acetate propionate and butyrate. Dietary tryptophan is metabolized to indole and its derivatives by the tryptophanase generated from specific species of the gut microbiome. Primary bile acids can be metabolized to secondary bile acids. Dietary components provide substrates for microbiota-derived carotenoids and phenols and, finally, choline is metabolized into trimethylamine, which is than oxidized to trimethylamine N-oxide (TMAO). Image modified from Ji et al. (2019).

1.10.1 Bile acids

BAs are small molecules produced by hepatocytes from cholesterol. Chenodeoxycholic acid (CDCA) and cholic acid (CA) are classified as primary BAs, conjugated to glycine or taurine, and are essential for lipid/vitamin digestion and absorption. 95% of primary BAs get reabsorbed actively from the terminal ileum and are introduced once again in the liver via the enterohepatic circulation. Primary BAs can also be transformed into secondary BAs and deconjugated by gut microbiota (Agus et al., 2020). After, they can be either passively reabsorbed to re-enter the circulating BA pool or excreted in the faeces.

BAs have different functions, both physiological and related to altered functionality. In particular, they can promotes glycogen synthesis and insulin sensitivity in the liver, can increase insulin secretion by the pancreas, facilitate energetic consumption, especially in the liver, brown adipose tissue and muscles, can impair lipid metabolism, especially by effecting triacylglycerol, can favours thermogenesis, resulting in a decrease in body weight and, finally, can mediate satiety in the brain (Ethanic et al., 2018).

Alterations of the BAs metabolism linked to the human gut microbiome is usually connected to the pathogenesis of metabolic disorders. In particular, metabolic disorders cause alterations in the human gut microbiome composition that, in turn, greatly affect BAs metabolism. In this altered state, primary BAs are not properly metabolized and accumulate at the liver level (Agus et al., 2020). Moreover, BAs have a significant effect on intestinal epithelium function, usually greatly impacted by diet (Agus et al., 2020).

1.10.2 Short chain fatty acids

SCFAs are among the most abundant class of metabolites produced by the human gut microbiome. SCFAs were found to be key factors in the control of different aspects of human immunity and metabolism (Morrison et al., 2016). SCFAs are the by-products of the fermentation of dietary fibres by the human gut microbiome. Soluble dietary fibres and nondigestible carbohydrates (such as cellulose), integral components of the human diet, that are not broken down by human metabolic pathways because humans lack the

enzymes to degrade such polysaccharides, are fermented in the cecum and large intestine by anaerobic commensal bacteria. Most common SCFAs thus generated include acetate, propionate, and butyrate (Levy et al., 2016).

SCFAs are implicated in numerous physiological functions (Morrison & Preston, 2016). They can regulate the maintenance of intestinal mucosa integrity (C. H. Kim, 2018), improve glucose and lipid metabolism (Chambers et al., 2015), control energy consumption (Hu et al., 2018) and regulate the immune system and inflammatory responses (Ratajczak et al., 2019). They exert their activity through specific GPCRs (Priyadarshini et al., 2018).

Obesity and diabetes can cause a reduction in the amount of SCFA-producing bacteria, resulting in reduction of SFCAs found in faecal samples of these patients (Makki et al., 2018). Studies conducted in rodents with diabetes and obesity, suggest that supplementation with SCFAs improves metabolic parameters by increasing glucose tolerance and homeostasis (Agus et al., 2020; Levy et al., 2016)

In humans, SCFAs administration leads to a reduction in weight gain (Agus et al., 2020; Chambers et al., 2015; Freeland et al., 2010). SCFAs administration also has important effects on haematopoiesis, resulting in an increase of the immune response to infections and a faster resolving of these (Balmer et al., 2014; Khosravi et al., 2014) and faster resolution of allergic reactions (Trompette et al., 2014).

1.10.3 Uremic toxins and lipopolysaccharides (LPS)

Substances that accumulate in the bloodstream in case of kidney excretory function impairment are generally referred to as “uremic retention solutes”. Amongst these compounds, some can result toxic (at high concentrations) and are thus referred to as “uremic toxins”.

Uremic toxins are known to have cumulative detrimental effect on the renal system, that can even lead to mortality during acute or chronic uremia, especially in the final development stages of chronic kidney disease (CKD)(Popkov et al., 2022) and are considered as an underlying factor responsible for the systemic inflammation accompanying uremia (Anders et al., 2013). Furthermore, uremic toxins are capable to

affect the gut microbiome system, via the introduction of urea into the intestine that causes the alteration of the biochemical environment of the gut during uremia and CKD (Vaziri et al., 2013). During CKD, alterations of the intestinal lumen of patients, like a decrease in pH and an increase of oxygen conditions, render this space inhospitable for the normal intestinal microbiota that mainly consists of obligate anaerobes and that are sensitive to changes. The result of these alterations is the disruption of the normal symbiotic relationship between the microbiota and the host and, eventually, dysbiosis of the gut microbiome(Nigam et al., 2019; Popkov et al., 2022). Uremic retention solutes and uremic toxins are all known to have detrimental effects on biological function, especially in patients with altered renal function, causing symptoms similar to those observed in patients with CKD (Falconi et al., 2021). Amongst these, especially uremic toxins with low molecular weight, after their absorption in the blood stream, bind to proteins and in this bound-state are difficult to excrete effectively from the system of CKD patients (Falconi et al., 2021). Protein-bound uremic toxins can promote deleterious effects, especially on the cardiovascular system. Likewise, the accumulation of uremic toxins such as p-cresyl sulfate, indoxyl sulfate and inorganic phosphate leads to numerous negative effects on the cardiovascular system (Falconi et al., 2021). Studies have shown that indoxyl sulfate can cause hypertrophy of cardiomyocytes in cultured cells, through activations of mitogen activated protein kinase (MAPK) and necrosis factor NFκB pathways (Kim et al., 2019). On a similar note, p-cresyl sulfate has been linked to different deleterious effects on the cardiovascular system (Gryp et al., 2017), such as the release of microparticles determining endothelial damage in the vascular endothelium, induction of oxidative stress, internal vascular remodelling and production of ROS in cardiac myocytes (Gross et al., 2015).

Finally, lipopolysaccharides (LPS, also known as endotoxins) constitute the major outer membrane component of gram-negative bacteria and is well known to be implicated in the activation of the host innate immune system (Pappo et al., 1992). While the role of LPS in stimulating inflammation has been acknowledged since the early 20th century, detrimental effects of LPS are not limited to septic shock and endotoxemia, but it can determine a variety of complications, especially when it is chronically present at low levels (Candelli et al., 2021). The presence of chronic low levels of LPS is caused by

alterations of the gut epithelial barrier that allow LPS produced by the gut microbiota itself to enter the bloodstream. Low-grade inflammation has been linked with many different diseases, such as diabetes, obesity, NAFLD, CKD, and cardiovascular disease (Mohammad et al., 2020).

1.11 Relationship between the gut microbiome and diseases

1.11.1 Immune system and autoimmunity

An immune response is usually initiated by the recognition of microbial patterns by the innate immune system that triggers a cascade of signals resulting into an anti-microbial immune response (Levy et al., 2016). Alterations in the innate immune pathways can cause variations in the composition of the microbiome, that can result in the pathogenesis of some diseases (Levy et al., 2016; Rakoff-Nahoum et al., 2004; Thaiss et al., 2014). A piece of important evidence that highlights the vital importance of the microbiome for the correct development of the immune system, is the fact that germfree mice have a strikingly less developed immune system, compared to normal (K. Smith et al., 2007). These germ-free mice can later be successfully colonized with accurately selected bacteria typical for the species, greatly improving the situation (Chung et al., 2012).

1.11.2 The gut-brain axis and modulation of behaviour

The gut-brain axis (GBA) is a term that refers to the communication between the central and the enteric nervous system, working in both directions, that connects emotional and cognitive centres of the brain with intestinal functions and finely regulates them (Carabotti et al., 2015).

Investigations on the connection between brain and the intestine enlightened the complexity of their communication system, which is deputed to maintain the gastrointestinal homeostasis but also influences affection, motivation, and complex

cognitive functions. For those reasons, this intricated system of connection has been named " GBA" (S. H. Rhee et al., 2009). GBA plays an important role in supervising and harmonizing intestinal functionalities alongside being interconnected with the cognitive and the emotional centres of the brain that regulates pivotal gut mechanisms such as immunoactivity, gut permeability, enteric reflexes, and the gut endocrine signalling. Neuro-immuno-endocrine mediators play a key role in GBA link. The interplay between gut and brain is carried out by the central nervous system (CNS, both brain and spinal cord), the autonomous nervous system (ANS), the hypothalamic pituitary adrenal axis, and the enteric nervous system (ENS) (Carabotti et al., 2015).

Clinical and experimental indications imply that gut microbiota plays a central role in GBA interactions with ENS and intestinal cells and furthermore affects CNS through neuroendocrine and metabolic pathways.

Clear evidence of GBA were discovered more than 20 years ago by observing the surprisingly great improvement of patients affected by hepatic encephalopathy when antibiotics were administered (Morgan, 1991). Meanwhile, further data suggested that microbiota played an important role in determining depression and anxiety, depressive like behaviours (J. A. Foster et al., 2013; Naseribafrouei et al., 2014) and dysbiosis in autism. Interestingly, autistic patients exhibit microbiota impairment in correlation with the severity of their condition (Mayer et al., 2014).

Functional gastrointestinal disorders are also associated with dysbiosis and are also responsible of mood disorders due to impairment in GBA (Berrill et al., 2013; Simren et al., 2013). Investigations showed that disrupted functionality in the brain-gut connection is majorly responsible for irritable bowel syndrome (IBS) (Koloski et al., 2012), while disfunction of the gut-brain communications is linked with alterations of the entero-endocrine and inflammation pathways, as long as causing visceral hypersensitivity and cellular alterations (Carabotti et al., 2015).

1.11.3 Metabolic syndrome, obesity and diabetes

Obesity is spiking around the world and its causes have been linked to a reduced level of activity, reducing energy utilised, whilst the level of energy intake has been increasing. Furthermore, obesity is the one of the leading causes of multifactorial diseases, such as type 2 diabetes mellitus (T2DM). Early studies in animal and human subjects linked obesity to an impaired ratio between Firmicutes and Bacteroidetes, with the first one having the advantage of the Bacteroidetes (Ley et al., 2005; Ley et al., 2006). During a restricted calories diet, weight loss correlated with decreased Firmicutes to Bacteroidetes ratio in both low carb and low-fat diets (Ley et al., 2006). Metagenomic analysis uncovered murine microbiota related upregulated energy intake derived from non-digestible carbohydrates, promoting the concept of a key role of microbiota composition in obesity and T2DM (Karlsson et al., 2013; Qin et al., 2012; Turnbaugh et al., 2009).

T2DM has been associated with a decrease in butyrate-producing bacteria abundance and increase of *Lactobacillus bulgaricus* (Karlsson et al., 2013; Qin et al., 2012). Among SCFAs, butyrate has an important role as energy substrate for gut epithelium (Donohoe et al., 2011; Donohoe et al., 2012). SCFAs generating bacteria pathways were found in abundance, in a faecal samples taken from obese subjects metagenomic studies, which showed increased concentrations of SCFAs in obese and overweight human and animal samples, that is in line with the observation that SCFAs are products of microbial fermentation and represent a surplus of calorie intake (T. W. Meyer et al., 2012; Tang et al., 2017). Moreover, gut metagenome-based models have been able to associate disrupted glucose tolerance with subject's phenotype (Karlsson et al., 2013). SCFAs activate GPCRs, which are also called free fatty acid receptors (FFARs), including GPR41 (FFAR3), GPR43 (FFAR2) and GPR109 (hydroxycarboxylic acid receptor 2 or HCA2)(M. Sun et al., 2017), that impact several important processes like inflammation and enteroendocrine regulation (Maslowski et al., 2009; Samuel et al., 2008). SCFAs also trigger secretion of GLP-1 by intestinal L-cells, which affects pancreatic function and insulin release, as well regulating appetite (Tolhurst et al., 2012).

BAs are further group of metabolites with a deep effect on human health, as they simplify the intake of dietary fat and fat-soluble molecules. Also, BAs are known regulators of energy metabolism via the activation of nuclear receptors such as farnesoid X receptor (FXR) (Lefebvre et al., 2009; Thomas et al., 2008). Activation of intestinal FXR activates fibroblast growth factor 15 (FGF15), a suppressor of hepatic cholesterol 7α-hydroxylase and a key enzyme that modulates Bas size and composition (Jiang et al., 2015; Tang et al., 2017).

1.11.4 Cardiovascular diseases

Patients with CVD gut microbiome can modulate inflammation by producing proinflammatory molecules. In recent years, rat experiments have discovered mechanistic connection between the severity of the myocardial infarction and the intestinal flora (Lam et al., 2016; Lam et al., 2012). Broad spectrum antibiotic use influences the concentrations of leptin, which is associated with the size of the infarct in the myocardium (Lam et al., 2016; Lam et al., 2012). Moreover, animal studies have shown that administration of Lactobacillus plantarum may reduce infarct size and ameliorates MI and left ventricle functionality (Lam et al., 2012). Additional animal studies of myocardial infarction demonstrated how administration of *Lactobacillus Rhamnosus* GR-1 improved left ventricular hypertrophy and HF (Gan et al., 2014). These findings suggest a beneficial effect of probiotics (see section 1.13.2 for a comprehensive description of probiotics and their beneficial effects),in combination with standard medications, in ameliorating the impact of HF after an episode of MI (Tang et al., 2017).

1.11.4.1 Hypertension

Hypertension is the most common altered risk factor for CVD. Despite the fact that not many studies have linked gut microbiota features with hypertension in humans, some early studies in animal models have proven that germ-free rats present high blood pressure, suggesting the potential for a role of gut microbiota in modulating blood pressure regulation (Honour, 1982).

Studies have shown a direct link between gut microbiota and blood pressure control in animal models (Adnan et al., 2017; Y. Qi et al., 2015; T. Yang et al., 2015).

In a study on germ-free mice in which angiotensin II, a potent vasoconstrictor agent, was administered, the involvement of the gut microbiota in enhancing angiotensin II-mediated vascular dysfunction and hypertension was demonstrated (Karbach et al., 2016). Furthermore, another study showed that patients with treatment-resistant hypertension showed a blood pressure-lowering effect when treated with a combination of antibiotics, suggesting that dysbiosis of the gut microbiota may play a role in the development and progression of hypertension (Y. Qi et al., 2015).

Other studies have focused on the role of SCFAs, which have been proved to have a role in modulating blood pressure (Pluznick et al., 2013). As previously described, SCFAs are one of the main products from the intestinal microbial activity and are likely responsible of many effects on different aspects of host physiology, as well as an impact disease susceptibility (Evans et al., 2013). SCFAs seem to be able to stimulate host GPCR pathways that affect renin secretion and blood pressure regulation (Pluznick et al., 2013). Communication between the gut enteric nervous system and the central nervous system has similarly emerged as a potential link to blood pressure (Santisteban et al., 2017).

Metabolites and molecules produced by gut microbiota have been proven to be involved in both sympathetic activation and in helping to maintain a regular influx of lymphocytes to intestinal tissue (Palsson et al., 1988). The combinations of these findings suggest that the gut microbiota could be considered as involved in the control of blood pressure, and that alteration of this modulation could be involved in hypertension. On this premise, a study was able to identify a positive connection between *Lactobacillus* probiotics and the regulation of blood pressure (Gomez-Guzman et al., 2015; Kawase et al., 2000). Additionally, a meta-analysis demonstrated that treatment with probiotics caused a significant decrease in blood pressure in patients (Khalesi et al., 2014; Tang et al., 2017).

1.12 Trimethylamine (TMA) and Trimethylamine N-Oxide (TMAO)

Trimethylamine N-Oxide (TMAO) is produced from trimethylamine (TMA), when bacteria residing in the human gut flora metabolize choline and other choline containing compounds, such as betaine and L-carnitine, ingested thought the diet. Gut microbiota was found to be required for the conversion of these nutrients into TMA in studies where germ-free mice were found to not be able to produce TMA (al-Waiz et al., 1992; Romano et al., 2015) and that treatments with antibiotics were responsible for a decrease in TMA levels in standard mice (al-Waiz et al., 1992). Furthermore, germfree mice that were colonized with strains of bacteria showed both an increase in TMA production and a lower levels of serum choline (Romano et al., 2015).

The anaerobic conversion of choline to TMA is mediated by different enzymes, and a key role in this is played by to cluster of genes named “Cut”, that were identified in the *Desulfovibrio desulfuricans* strain of bacteria (Craciun et al., 2012; Thibodeaux et al., 2012). In this cluster, of particular importance are CutC and CutD, genes encoding for TMA-lyase and its activating protein, respectively. These choline-TMA lyases belong to a large family of proteins that are able to attack the carbon-nitrogen bond in choline using a radical species generated from a conserved glycine residue, in order to produce TMA and acetaldehyde (Craciun et al., 2012). Experiments involved in the deletion of CutC gene in *Desulfovibrio alaskensis* and heterologous expression of the CutC and CutD genes in *Escherichia coli* were used to prove that these genes are fundamental for the conversion of choline into TMA (Craciun & Balskus, 2012). Another microbial pathway important for the production of TMA, is the hydroxylation of L-carnitine from the strains of bacteria belonging to Acinetobacter and Serratia, that reside in the human colon and produce malic semialdehyde as a by-product of the conversion (Falony et al., 2015). In this pathway, the genes CntA, encoding for a carnitine oxidase and CntB, encoding for a carnitine reductase, are responsible for the conversion of L-carnitine into TMA, as evidenced by experiments performed with knockout and heterologous expression animals (Y. Zhu et al., 2014). Carnitine can also be converted into TMA in another pathway, which produces γ-butyrobetaine in the ileum, with subsequent conversion of γ-butyrobetaine to TMA in the cecum and colon (Koeth et al., 2014). Genes involved in

this conversion are a pair of genes called YeaW/YeaX that encode of oxygenase and oxidoreductase capable of having γ-butyrobetaine, L-carnitine, choline, and betaineas substrate (Zeisel et al., 2017). Many other strains of bacteria are able to produce homologs of CntA/CntB and YeaW/YeaX gene pairs, such as Gammaproteobacteria like *Klebsiella pneumoniae, E. coli, Citrobacter, Providencia*, and *Shigella*, Betaproteobacteria like *Achromobacter*, Firmicutes like *Sporosarcina*, and Actinobacteria while Bacteroidetes seem to not be able to produce anything similar (Flanagan et al., 2010).

After TMA is generated, it can be either be subjected to further microbial metabolism, it can be removed from the gut by simply be excreted though faeces or can re-absorbed into the systemic circulation. A large part of TMA is absorbed into the hepatic portal circulation by passive diffusion across the enterocyte membranes, and it gets converted into TMAO by flavin monooxygenase (FMOs), in particular FMO1 and FMO3 (Bennett et al., 2013). Roughly 95% of TMA is oxidized into TMAO (A. Q. Zhang et al., 1995) and, physiologically, plasma TMAO levels are roughly 10- to 20-fold higher than TMA (Seldin et al., 2016). FMO3 has a much higher specific activity, especially in the liver and it catalyses the NADPH-dependant oxygenation of TMA (Bennett et al., 2013). Alongside the oxygenation of TMA, FMO3 is capable utilising other molecules as substrates, including drugs such as cimetidine, chlorpromazine, ketoconazole, morphine, propranolol, ranitidine, sulindac, tamoxifen and tyramine (Mafune et al., 2016). TMA is a volatile gas and has a strong fish-like odour, while TMAO presents itself as a less volatile solid. In decomposing fish, TMAO is rapidly re-converted into TMA thanks to the bacterial activity, giving it its characteristic smell. Mutation in genes encoding for FMO3 in humans, result in the inability to properly oxidise TMA and its accumulation, leading to excretion of TMA in sweat and breath, in a condition referred to as trimethylaminuria. Patients affected by trimethylaminuria experience episodes of fishlike body odour, due to the excretion of TMA (Mackay et al., 2011). Expression of FMO3 can be modulated by different factors. In particular, oestrogen can induce the expression of FMO3, while testosterone suppresses its expression. As a consequence, activity of FMO3 is higher in female than in male, but while this effect is particularly marked in studies where mice where used, humans don’t have the same large difference (Bennett et al., 2013). As

evidenced by Obeid et al. (2016), women reportedly generate less TMAO than men, and while it is not possible to conclude what other factors may contribute to the different plasma levels of TMAO in the different genders, it is very likely that further studies on the distributions and expression of FMOs will be required. Although FMO3 and FMO1 genes are important in the production of TMAO, a very large study based on analysis of genome association did not find any significant association between genetic profile and circulating levels of TMAO, and justified variability in TMAO levels as the after-effect of different dietary factors and variability in the gut microbiome (Hartiala et al., 2014).

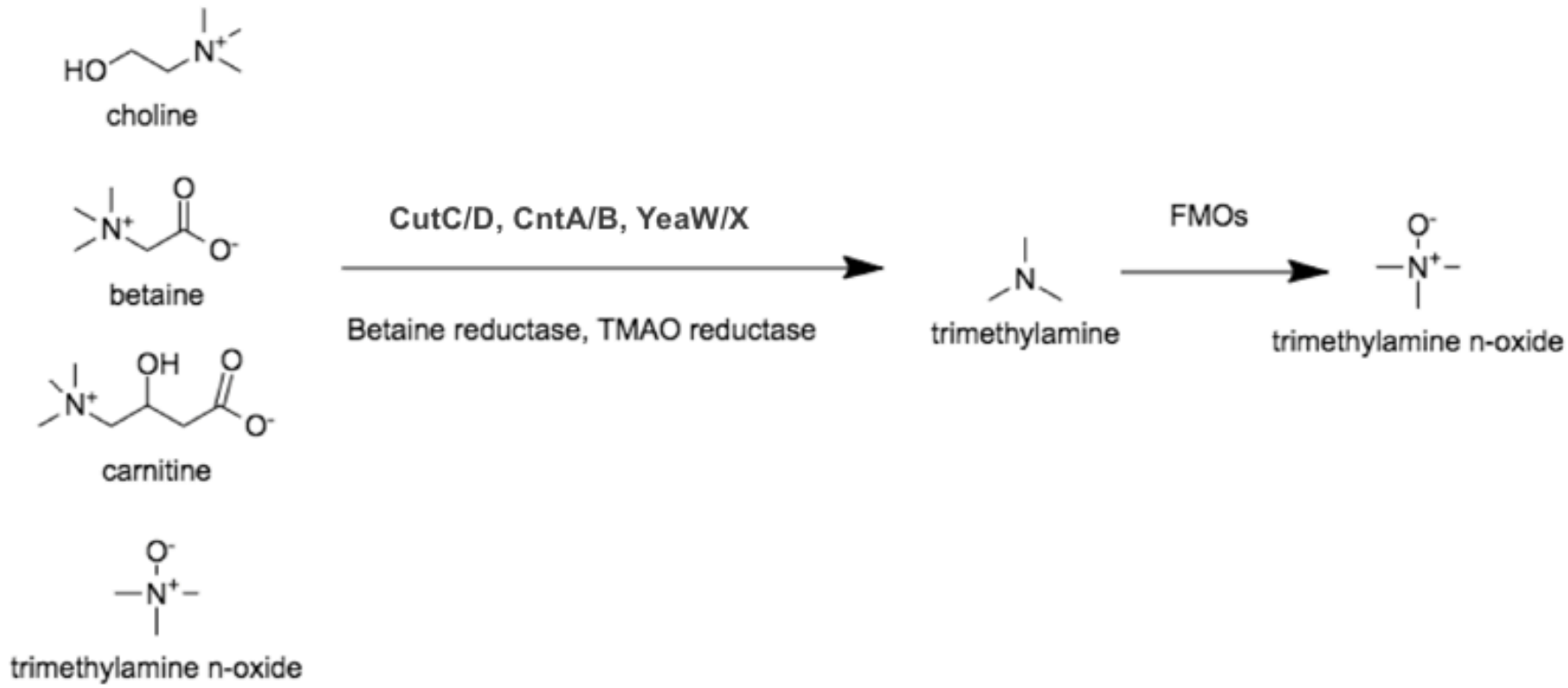

Figure 1.14. Chemical structure and biosynthesis of TMAO. Gut microbiota cleave some trimethylamine containing compounds to produce trimethylamine (TMA), which can be further oxidized as trimethylamine N-oxide (TMAO) in the host liver by flavin monooxygenase (FMOs). The pathway for the production of TMAO includes four enzymes involved in production of TMA, choline-TMA lyase (cutC/D), carnitine monooxygenase (cntA/B), betaine reductase, and TMAO reductase. Furthermore, yeaW/X. Besides carnitine, yeaW/X can also use choline, γ-butyrobetaine and betaine as substrates to produce TMAO. Image modified from Z. Wang et al. (2018).

The majority of studies measures TMAO levels in urine and plasma samples, although there are other studies that uses serum as a mean to compare TMAO levels. Mainly, TMAO is measured with LC-MS but it can be measured with other, more sophisticated version of LC-MS such as stable isotope dilution high performance liquid chromatography with electrospray ionization tandem mass spectrometry (DIS-HPLC-MS/MS), proton nuclear magnetic resonance spectrometry (1H-NMR), headspace gas chromatography (GC) and matrix-assisted laser desorption/ionization time-of-flight mass spectrometry (MALDI-TOF-MS). Another, less common, technique is Fast Atom Bombardment- mass spectrometry (FAB-SM) (Janeiro et al., 2018).

Plasma levels of TMAO show a very large inter- and intra-individual variations and these variations can be influenced by several factors (Velasquez et al., 2016). In a recent study by Gessner et al. (2020), plasma levels of TMAO in healthy patients ranged between 1.28–19.67 µmol/L for men and for women as 1.08–17.12 µmol/L. A first factor of variability is age. Studies have shown that plasma levels of TMAO increase with age, in both humans and rats (T. Li et al., 2017; Z. Wang, B. S. Levison, et al., 2014). Another important factor is diet. For example, a diet rich in vegetable can reduce FMO3 expression and, consequently, TMAO levels. In addition, vegetarians have a totally different composition of gut microbiota in comparison to omnivorous people and their production of TMA from L-carnitine is less (Koeth et al., 2013).

In contrast, high fat diets and wester-like diets increase plasma levels of TMAO (M. Wang et al., 2013). The amount of protein in the diet seems to have a positive correlation with TMAO excreted in urine (Rasmussen et al., 2012). Additionally, some studies suggest that a diet high in non-digestible carbohydrates can reduce production of TMAO by alteration and modulation of gut microbiota (C. Zhang et al., 2015), while other studies reports the opposite effect, suggesting that a diet high in non-digestible starch increases plasma TMAO levels in the short term (Bergeron et al., 2016). Finally, renal clearance may play a critical role in plasma TMAO levels. Other studies revealed that TMAO is augmented in renal insufficiency, but concentrations normalize following renal transplantation (Stubbs et al., 2016). However, there are also some studies suggesting that TMAO can contribute to the development of renal insufficiency (Janeiro et al., 2018; Tang et al., 2015).

1.12.1 Dietary sources of TMAO

As previously mentioned, TMAO and TMA can be introduced into the human body through the diet both as precursors and as final product. High concentrations of TMAO and TMA are found in fish and other seafoods. Comparatively, deep-sea fish like cod, haddock, halibut, herring and skate, contain higher concentrations of TMAO compared to freshwater fish (Bain et al., 2005) and are also higher than concentrations found in red meat and eggs, with 100g of cod containing roughly 300mg of TMAO while 100g of beef contains less than 1mg of TMAO (Cho et al., 2017). TMA is also contained in fish oil and in dietary supplements containing choline and choline-like compounds that have degraded during preparation or storage due to activity of bacteria (Zeisel et al., 1983). While fish have a high content of TMAO and TMA naturally, the biggest sources of carnitine and other precursors of TMAO remain animal products. It is important to note that only the stereoisomer L-carnitine is found in dietary sources. Meat, poultry, eggs and milk are the highest sources of carnitine, while plants contain little to none (Flanagan et al., 2010), with 100g of beef containing 39mg of carnitine, 100g of eggs containing less that 1mg of carnitine,

100g of cod containing 4mg of carnitine and 100g of asparagus containing 0.2mg of carnitine (Cho et al., 2017). While carnitine is found in these foods, it can also be synthesized endogenously from lysine and methionine (Koeth et al., 2013), mainly in tissues like brain, liver and kidney (Flanagan et al., 2010).

Apart from carnitine, TMA can be generated from dietary choline and other choline containing compounds, through bacterial activity. Foods that present high content of choline are, once again, animal products like eggs and liver but lower contents of choline and other choline-like compounds can be found in the majority of the foods we eat (Zeisel et al., 2003). Choline can be found both in its pure form but can also be ingested as esters of choline and both forms are absorbed in different ways in the intestine (Zeisel et al., 2003).

Lastly, TMA is also generated by bacterial activity from betaine (Z. Wang et al., 2014). Foods that present high content in betaine are mainly vegetables, particularly grains, spinach and beets that grow in highly osmotic environments (Zeisel et al., 2003),

because these plants use betaine as an osmolyte in their roots to help with hydrolytic retention (Craig, 2004). A database from the US Department of Agriculture evaluated foods based on betaine content and found that 100g of spinach contains 577mg of betaine, 100g of cod or beef contain 7mg of betaine and 100g of eggs contain less than 1mg of betaine.

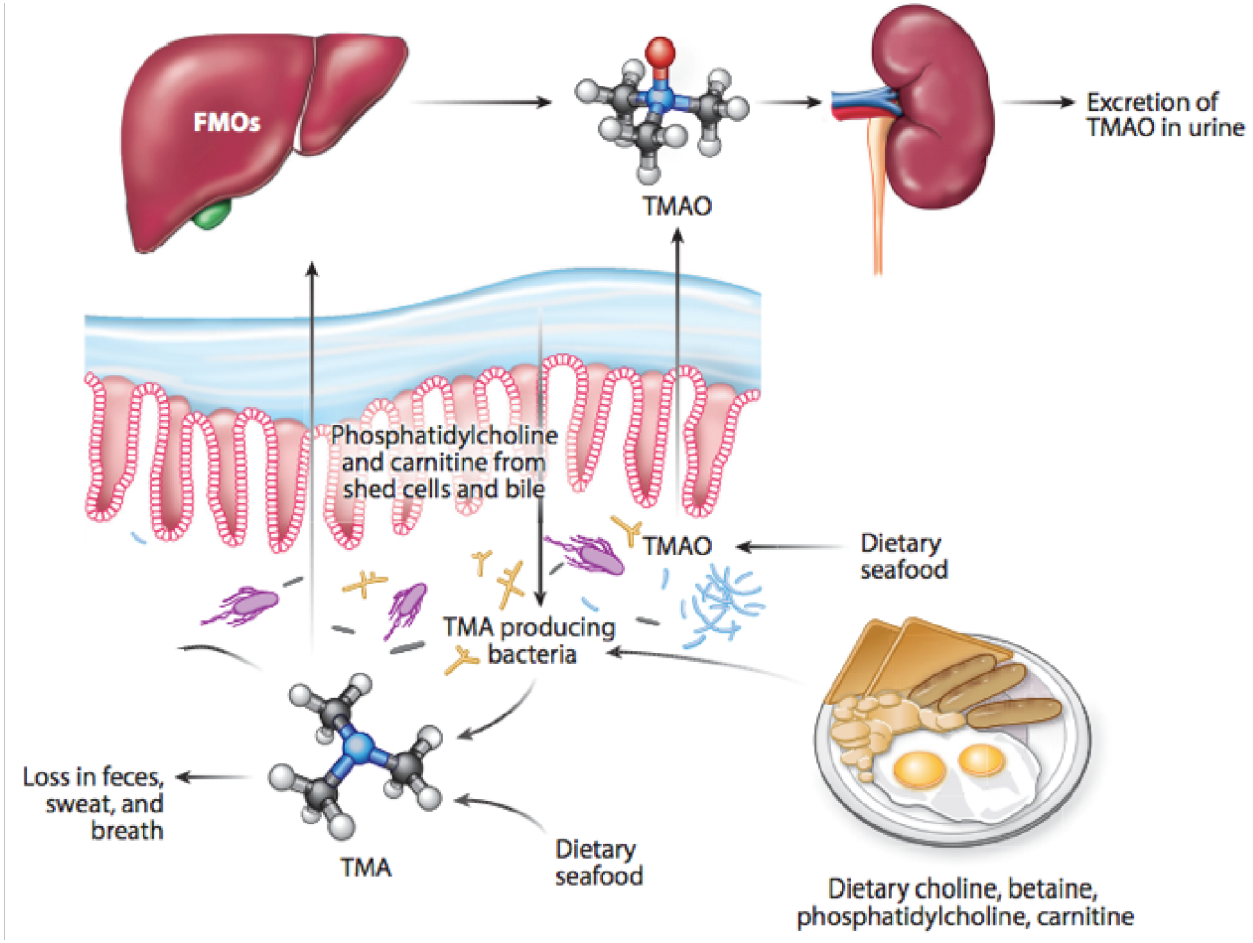

Figure 1.15. Dietary sources and biosynthesis of TMAO. Trimethylamine (TMA) is produced in the intestinal lumen when gut microbiota cleaves carnitine and other compounds from the diet. Dietary seafood contains large amounts of both TMA and TMAO. TMA can also be generated by gut microbiota in the bile or can be absorbed from the intestine. TMA is then re-absorbed from the intestine into the liver where flavin-dependent monooxygenase (FMO) isoforms 1 and 3 oxidize it to TMAO. TMAO is principally excreted by the kidney into urine while TMA is excreted also in faeces, breath and in sweat. Image modified from Zeisel and Warrier (2017).

1.12.2 Relationship between TMAO and CVD

Plasma and serum circulating levels of TMAO have been found to be associated with different CVD and are also linked to prediction of incident risk for adverse cardiovascular events, like myocardial infarction, stroke and eventually even death, when used in conjunction with other traditional cardiac risk factors and evaluation of renal function (Tang et al., 2013; Z. Wang et al., 2011). Alongside TMAO, plasma levels of choline, betaine and carnitine have also been used as predictors of adverse cardiac events and have been linked with increased CVD risk, but their relevance and predictive value seems to be almost totally dependent on the serum levels of TMAO (Koeth et al., 2013; Z. Wang, W. H. Tang, et al., 2014).

The link between TMAO and CVD has been investigated in different cohorts and in numerous studies (Schuett et al., 2017; Troseid et al., 2015) and it can be summarized in these key points that will be expanded upon in the following sections:

- TMAO is able to increase aortic lesion formation in Apolipoprotein E knockout (ApoE-null) mice, a standard model of spontaneous atherosclerosis, fed a diet supplemented with TMAO (Z. Wang et al., 2011).
- TMAO has been shown to have effects on thrombosis by increasing its risk via enhancement of platelet hyperreactivity (W. Zhu et al., 2016) confirmed by the fact that oral choline supplementation increased fasting TMAO levels and platelet aggregation (W. Zhu et al., 2017). The effect of TMAO on platelet aggregation were found to be mediated by increase in calcium release from the endoplasmic reticulum (W. Zhu et al., 2016).
- Peritoneal macrophages of mice fed with a TMAO-supplemented diet showed an increase in the expression level of receptors involved in atherosclerosis, an increase of cholesterol levels and enhanced foam cells formation (Z. Wang et al., 2011)

TMAO levels are not only linked to CVD but have also been found to be connected with renal insufficiency and mortality risk in patients with CKD, T2DM, insulin resistance, non-alcoholic fatty liver disease (NAFLD) and colorectal cancer (Kummen et al., 2017; Tang et al., 2015). These studies suggest that circulating TMAO levels can be used as a target

to manage TMAO related diseases intervention. In particular, by targeting the bacterial pathways that lead to the production of TMAO can be obtained through different routes: inhibition of cleavage by the gut bacteria of TMA containing compounds using specific enzymatic inhibitors, controlling the intake of TMAO precursors through regulation of diet or by inhibition of the oxidation of TMA into TMAO (Z. Wang & Zhao, 2018).

Despite these strong data that imply a direct link between TMAO and atherosclerosis, there are also plenty of inconsistencies. Clinical and epidemiological data by themselves are not enough to prove a causative link between TMAO and CVD. While several studies in mouse models and cell culture provide important evidence that there could be a causal relationship between TMAO and CVD, randomized intervention trials with TMAO are yet to be published, and there is an increasing body of literature suggesting that TMAO could be having little to none disruptive effect on the cardiovascular system (Zeisel & Warrier, 2017).

1.12.2.1 Role of TMAO as a biomarker in CVD

The link between TMAO levels and incidence of adverse cardiac events has been shown in several and numerous cohorts (Senthong, Wang, et al., 2016; Tang & Hazen, 2014; Tang et al., 2015; Tang et al., 2013; Z. Wang et al., 2011).

The first study suggesting a correlation was conducted in 2011, when a cohort of 1,800 stable cardiac patients undergoing coronary angiography showed the presence of high circulating TMAO levels and of other metabolites belonging to the same pathway of production of TMAO (choline, betaine and L-carnitine). It was suggested that these high levels were positively correlated with a prevalence of CVD and increase risk of adverse cardiovascular events (Z. Wang et al., 2011). Out of these compounds, TMAO was the one to show the strongest positive correlation, when the sizes of atherosclerotic plaques were compared (Z. Wang et al., 2011). Following this study, in another cohort of 4,000 patients undergoing elective coronary angiography, it was shown that elevated TMAO levels were linked to an increase in the incidence of adverse cardiac events,

myocardial infarction, stroke and even death, this time in a follow-up period of 3 years (Tang et al., 2013). In particular, patients with the highest levels of TMAO of the cohort were much more likely to be re-hospitalized due to severe cardiac events compared to patients with lower circulating levels of TMAO (Tang et al., 2013). The ability to predict the incidence of adverse cardiac event, in this study, was independent from any other traditional cardiac risk factors, lipids, C-reactive protein (an inflammatory marker used for prognostic purpose) and renal function. In addition, high circulating levels of TMAO were found to be more reliable in predicting the incidence of adverse cardiac events than other traditional markers, like low-density lipoprotein (LDL) cholesterol (Tang et al., 2013).

From these initial studies, additional evidence further suggests the existence of a correlation between high TMAO levels and CVD risks (Senthong, Wang, et al., 2016; Tang et al., 2015; Tang et al., 2013). A cross-sectional study of 227 patients undergoing cardiovascular surgery for coronary artery disease, valvular heart disease or aortic disease found that patients with the highest concentrations of plasma levels of TMAO were linked to an increased number of coronary infarctions compared to patients with lower concentrations of circulating TMAO (Mafune et al., 2016). Plasma concentrations of TMAO were also linked with long-term mortality risk in patients suffering from HF, advanced left-ventricular diastolic dysfunction and atherosclerotic development in patients suffering from atherosclerotic coronary artery disease (Senthong, Li, et al., 2016; Senthong, Wang, et al., 2016; Tang et al., 2015; Tang et al., 2013; Z. Wang, W. H. Tang, et al., 2014).

Lastly, high circulating TMAO levels were also associated with the presence of vulnerable coronary plaque, plaque rupture, and long-term risks of incident cardiovascular events in patients with acute coronary syndrome (Q. Fu et al., 2016; X. S. Li et al., 2017; Tang et al., 2017).

Overall, these findings indicate that increased levels and accumulation of TMAO has detrimental effects on CVD. It has been suggested that the introduction of TMAO measurements in routine clinical evaluation would be beneficial and these evaluations would benefit from increased accessibility of mass spectrometry within the clinical

laboratory, because of TMAO's potential as promising clinical biomarker (Heaney, 2020).

1.12.2.2 TMAO and atherosclerosis

Several human studies have supported the hypothesis that there is a strong correlation between high plasma levels of TMAO and the development of atherosclerotic plaque formation (J. M. Brown et al., 2015; Tang & Hazen, 2014).

A first study that focused on the link between TMAO and atherosclerotic plaque formation showed that germ-free mice or mice treated with short-term injection of antibiotics and fed with a TMAO or TMAO precursors-supplemented diet had an enhanced risk of developing atherosclerosis (Z. Wang et al., 2011). In particular, in this study, ApoE−/− C57BL/6J mice fed with a choline-rich diets and intact gut microbiota, and that showed high plasma levels of TMAO, were particularly prone to macrophage foam cell formation and enhanced aortic atherosclerotic plaques compared to the germ-free mice or the mice treated with short-term antibiotic for suppression of gut microbiota, in which production of TMAO was inhibited, and showed that the atherosclerotic burden was lessened (Z. Wang et al., 2011).

These effects were not unique to choline or phosphatidylcholine but have similarly been observed with other dietary nutrients that can generate TMAO downstream, including L-carnitine and γ- butyrobetaine (Koeth et al., 2014; Koeth et al., 2013).

A further study concluded that chronic choline supplementation of atherosclerosis prone low-density lipoprotein receptor (LDLR−/−) mice, leading to increased plasma levels of TMAO, resulted in an increase in the expression of inflammatory genes in vascular cells (Herlaar et al., 1999). In particular, these animals presented an increase in the expression of cytokines and adhesion molecules in the aorta and acute intraperitoneal administration of TMAO only reaffirmed these findings (Herlaar & Brown, 1999). Furthermore, when mice were fed a chemically defined diet supplemented with either 0.12% TMAO or 1% choline, platelet aggregation induced by adenosine diphosphate stimulation was significantly increased, potentially contributing to the worsening condition and development of atherosclerosis (W. Zhu et al., 2016).

Finally, while the evidence suggesting a causative relationship between TMAO and atherosclerosis is convincing, it is also important to remember the differences in atherogenesis between mice and humans. Humans carry about 75% of their plasma cholesterol in LDL particles, whereas mice carry most of their cholesterol in high-density lipoprotein (HDL) particles, thus possessing different pathways that lead to the formation of atherosclerotic plaques (Jawien et al., 2004). From this prospective, it would be reasonable to infer that TMAO may be affecting atherogenesis in mouse model in a different way to that in humans.

1.12.2.3 TMAO and heart failure

In addition to the previously described link between TMAO and atherosclerotic plaque formation, evidence of a correlation between high levels of TMAO and HF development and poor prognosis in these patients have emerged (Tang, Wang, et al., 2014; Tang et al., 2013; Z. Wang et al., 2011; Z. Wang, W. H. Tang, et al., 2014).

In particular, circulating TMAO levels were observed to be higher in patients affected by HF compared with healthy subjects of the same age and gender (Tang, Wang, et al., 2014). Additionally, high plasma levels of TMAO were found to be predictive of adverse events and worsening of the condition associated with HF, in a cohort of stable patients with HF with other risk factors, such as cardio-renal syndrome and systemic inflammation (Tang, Wang, et al., 2014). The link between high plasma levels of TMAO and HF progression is yet to be well-defined, and numerous studies have debated whether the nature of this relationship is purely correlation or if a causative component is present. More recent animal studies point to a connection between TMAO and HF of a more causative nature, by demonstrating that TMAO directly contributes to the development of adverse ventricular remodelling, which in turn could be a key component in the development of HF (Organ et al., 2016). In particular, Organ et al. (2016) used a trans-aortic constriction model of HF and mice fed with a high choline diet to prove that these animals not only showed higher TMAO levels, but were also affected by a much faster adverse ventricular remodelling, presenting a much bigger chamber dilation, thinning of the walls and a reduced shortening fraction compared to animals

that were fed a normal choline-level diet. Other parameters that were altered by the high choline-level diet was the significant increase in fibrosis and infiltration of foam cells (Tang et al., 2015).

It is not clear yet whether modulation of the gut microbiota pathway connected with TMAO, by inhibition of TMA production through suppression of the strains of bacteria, can help in lessening the detrimental effects of TMAO on HF development or if reduction of TMAO plasma levels in patients with HF can help in improving long term outcomes (Tang et al., 2017).

1.12.3 TMAO and chronic kidney disease

Cardiovascular and kidney disease are very closely correlated, and patients who suffer from what is commonly referred to as “cardio-renal” syndrome are usually associated with poor clinical outcomes (Ronco et al., 2008). Patients who suffer from CKD have a higher mortality-risk when it comes to complications from CVD (Gansevoort et al., 2013). There is evidence that non-traditional risk factors, like inflammation, oxidative stress and endothelial dysfunction play an important role into explaining this correlation (Schnabel et al., 2007).

A well-established fact, is that CKD patients have a rather largely altered gut microbiome composition, causing them to have a high influx of circulating urea and uremic toxins into the gut lumen (Vaziri et al., 2013; Wong et al., 2014). Urea gets normally hydrolysed by microbial ureases into the intestinal tract, resulting in a release of large quantities of ammonia, then converted into ammonium hydroxide. Both ammonia and ammonium hydroxide are capable of disrupting the intestinal epithelial tight junctions (Vaziri et al., 2013). It is hypothesized that the detrimental effect of ammonia is responsible for intestinal epithelial barrier dysfunction in CKD and that this, ultimately, is responsible for a systemic inflammation caused by bacterial DNA and uremic toxins released into systemic circulation (Szeto et al., 2008). As a confirmation of this altered status, DNA of gut microbiota was found in the plasma of CKD patients on chronic haemodialysis (Shi et al., 2014).

Another important factor is that TMAO has been found to accumulate in the plasma of patients with CKD and that high plasma levels of TMAO were associated with a progressive loss of kidney function and a higher degree of mortality (Tang et al., 2015; Tang et al., 2013). In the Framingham Heart Study, TMAO was one of the few metabolites that was able to be used as a biomarker for prediction of developments of CKD, when analysed in the plasma of healthy subjects (E. P. Rhee et al., 2013). Furthermore, Tang et al. (2015) highlighted how renal fibrosis and renal function were worsened by choline rich diet supplementation.

While TMAO concentrations are, indeed, reportedly higher in patients with CKD, it is not sufficient to state that TMAO has any role into causing or worsening CKD. Since renal clearance plays such an important role into determining plasma levels of TMAO, normal function of kidneys is essential into the link between TMAO and CKD, even if TMAO does not directly causes damage to the kidneys (Zeisel & Warrier, 2017).

1.12.4 Evidence of a protective effect of TMAO

Due to its chemical characteristics, such as the very small size and the combination of hydrophilic and hydrophobic features, TMAO has the ability to act as a chaotropic agent, meaning that it can alter the conformation of proteins and serve as a potential allosteric modulator to these (Schneck et al., 2013). In organisms that normally produce TMAO, (as opposed to having the molecule introduced in the system through the diet like it happens in the human body) such as aquatic animals and deep-sea fish, TMAO performs key physiological functions. Amongst these is the ability of TMAO to act as an osmolyte and to protect against protein destabilization caused by pressure (Kelly et al., 1999; Yancey et al., 2004). TMAO is largely used by these types of fish as an osmoregulatory and plasma levels of TMAO increase in fish with depth of sea levels (Yancey et al., 2014). Stabilization of proteins by TMAO has been shown to work not only in preventing the unfolding and loss of conformational and structural changes, like changes that usually occur during regulation of allosteric processes, but also to modulate intracellular molecular crowding (A. L. Miller et al., 2017; Yancey et al., 2004; Yancey et al., 1999).

Considering this, it isn't surprising that stabilization of proteins has been proposed as a potential mechanism in the protection of cardiomyocytes from hydrostatic pressure fluctuations during HF (Gawrys-Kopczynska et al., 2020). As such, several studies have tried to investigate this effect and have found controversial evidence that seem to contrast with previously mentioned studies. In particular, in studies where TMAO, or its metabolic precursors, were given in lower doses than the ones used in previous studies, TMAO was found to have a protective effect on cholesterol levels, atherosclerosis and hypertension (Collins et al., 2016; Huc et al., 2018; Martin et al., 2009; Zhao et al., 2019). Mice with a diet supplemented with 352 mg/kg L-carnitine, the equivalent to 2000 mg per day in humans, did not show signs of atherosclerotic plaques formation, despite the fact that plasma levels of TMAO were significantly higher compared to baseline (Collins et al., 2016). Furthermore, comparable results were also obtained with a modest supplementation of TMAO, roughly 6.7 mg TMAO/kg. In this case, despite plasma levels of TMAO where increased by four- to five-fold, TMAO was found to actually reduce diastolic dysfunction and help resolve pressure-overload in hearts of hypertensive rats (Huc et al., 2018). Finally, detrimental effects on atherosclerosis or inflammation could not be observed in any of the studies by Aldana-Hernandez (2019) and Lindskog Jonsson et al. (2018), even when levels of TMAO supplemented were higher.

1.13 Modulation of the gut microbiome as therapeutic target

Numerous studies have demonstrated the role of the human gut microbiome in the development of different diseases, as well as demonstrating the interaction between alterations of the human gut microbiome and their impact on diseases. Thus, manipulation of the human gut microbiome aims to treat these disorders by using different tools, such as diet, probiotics, prebiotics and faecal microbiota transplantation (FMT) (McCarville et al., 2016).

Studies suggest that some already existing drugs, like metformin, may exert their affect, at least partially, by modulating the human gut microbiome (H. Wu et al., 2017; X. Zhang et al., 2015).

As medicine is increasingly pursuing more precise disease treatment and health management, by producing drugs that are tailored to different populations and needs, it is essential that the human gut microbiome is considered into future therapeutic strategies (Kuntz et al., 2017; X. Zhang et al., 2019)

1.13.1 Dietary intervention

Several studies have shown a direct correlation between diet and the composition of the human gut microbiota and, in particular, the effects of diet in the production of microbial metabolites (David et al., 2014; G. D. Wu et al., 2011).

Alteration of the human gut microbiome caused by diet can play a role in the pathogenesis and development of IBS, obesity, T2DM, insulin resistance and NAFLD (Cani et al., 2016; Lee et al., 2015; Thorburn et al., 2014). Despite this, it not yet defined what an hypothetically ideal diet capable of promoting a healthy microbiome would be (McCarville et al., 2016). Dietary components such as fructo-oligosaccharides, galacto-oligosaccharides, soya-oligosaccharides, xylo-oligosaccharides, and pyrodextrins can cause an increase in the variability of the human gut microbiome (Bindels, Delzenne, et al., 2015; Gibson et al., 1995). Nondigestible foods are fermented by bacteria producing important metabolites in gut homeostasis such as SCFAs, ω-3 fatty acids or tryptophan derivate metabolites (Furusawa et al., 2013; Thorburn et al., 2014).

Diets rich in red meat and fat, in particular polyunsaturated fatty acids, can cause changes in the microbiota composition and may be involved in the pathogenesis of metabolic disorders, inflammatory bowel disease (IBD) or cancer (Daniel et al., 2014; Lee et al., 2015). Bacteria can metabolize meat proteins and produce nitrosamines, molecules related to carcinogenesis (Hughes et al., 2001; Paul et al., 2015). In addition, diets rich in red meat are the most responsible for the production of TMAO, as discussed in section 1.12.

Diet can also mediate positive effects on the pathogenesis of diseases. Cruciferous vegetables like cabbage, broccoli, kale, and cauliflower are rich sources of fibres, lutein, flavonoids, phytosterols, folic acid, and vitamin C, that are considered helpful in reducing the risk of cancer (Paul et al., 2015). Studies suggest a lower risk of IBD among

people with diets rich in fibre, fruits and vegetables. In particular, the Mediterranean diet has been considered as beneficial in terms of regulating the human gut microbiome and its production of metabolites (De Filippis et al., 2016). Finally, some dietary components have been shown to help regulate mucosal immune functions, such as vitamins, amino acids, and SCFAs (Brestoff et al., 2013).

1.13.2 Prebiotics and probiotics

The term prebiotics is normally used to refer to selectively fermented nondigestible food ingredients or substances able to promote the growth and activity of health promoting bacteria that colonize the gut (Bindels, Walter, et al., 2015). Deficiencies in bacterial flora may lead to IBD and interfere with host metabolic markers like rising body fat mass, inflammatory events and insulin resistance (Hansen et al., 2010; Le Chatelier et al., 2013). A fermented food ingredient needs to meet specific criteria to be considered as a prebiotic: it needs to be resistant to digestive enzyme hydrolysis and the acidity of the gastric secretions; it needs to be assimilated in the upper gastrointestinal portion and fermented by the gut bacterial flora; it needs to be able to stimulate advantageous bacterial processes (Cammarota et al., 2014).

In contrast, probiotics are actually live microorganisms which, when administered in sufficient quantity, provide a health benefit to the host. Several different strains of bacteria are commercially available to be used as probiotics, despite many of them lacking clinical evidence to back and support their relevance and importance in helping to alleviate and treat specific disease. It is hypothesized that probiotics are able to help with immunomodulation, restoration of barrier function, modulation of metabolic parameters, and modification of intestinal microbiota (Rijkers et al., 2011; Wolvers et al., 2010). Recommendations on probiotic bacteria assert that they should be preferably isolated from the human intestine, their safe use validated, stable genetically and able to cross through the gastrointestinal tract (McCarville et al., 2016)

1.13.3 Faecal microbiota transplantation

FMT, also referred to as ‘‘faecal infusion’’ or ‘‘faecal bacteriotherapy’’, is the introduction of liquid filtrate derived from stools of healthy donors into the into the gastrointestinal tract of a patient, done in order to treat ~~of~~ specific diseases (Cammarota et al., 2014).

Since numerous recent studies have highlighted how important is the role of gut microbiota in the pathophysiology on the human body, treatment with FMT has been given increasing attention, switching from being simply considered a mere treatment to a true organ transplantation (O'Hara & Shanahan, 2006). This particular approach and attention has led FMT to being used in the treatment of several diseases associated with the disruption of gut microbiota, such as IBD (Vrieze et al., 2012), metabolic syndrome (Anderson et al., 2012), obesity, infections caused by *Clostridium difficilis*, Chron’s disease and ulcerative colitis.

FMT has been proven to be more effective than probiotics in the restoration of altered gut microbiota, since a single faecal infusion is able to overcome one of the biggest limitations of the use of probiotics, which is quantity. Oral probiotic doses are usually more than 3-fold lower than the 100 trillion native micro-organisms existing in the large bowel. In addition, the administration of faecal flora alters the host gut bacteria almost permanently (Grehan et al., 2010), while probiotics are only able to colonize the gut lumen for a short-time period (Tannock et al., 2000).

1.14 Aims & Hypothesis

The primary aim of this study is to investigate whether TMAO is able to modulate cardiac function. By using isolated cardiomyocytes through to the intact myocardium, this study will be able to investigate the concentration-dependence of any TMAO-induced changes in cardiac function.

The primary model will be the Wistar rat isolated ventricular myocyte. In this, I will use the isolated cells, or the intact whole heart in coronary ligation measurements, to test

whether TMAO has a causative effect on functional dysregulation in the cardiomyocytes. Using patch clamp electrophysiological recording, fluorescence imaging, contractile function measurements and biochemical techniques for investigating metabolic function, a phenotypic and metabolic profile of the effects of TMAO on cardiomyocytes will be established.

It has been hypothesised that TMAO plays an important role in the progression of cardiovascular disease. In this study, the mechanisms of TMAO-induced dysregulation will be investigated.

Hypotheses:

1) TMAO will alter calcium regulation in the cardiac ventricular myocyte
2) TMAO will disrupt the mitochondrial fatty acid shuttle system and intermediary pathways in glycolytic metabolism

These hypotheses will be investigated in the following sections:

1) What is the acute effects of TMAO on the function of cardiomyocytes?

In this section of work, cardiac cells will be stimulated with acute treatments with TMAO to assess the short-term effects of the compound on contractile function. The modulation of ionic currents and calcium homoeostasis will initially be investigated. Given the close link between calcium homeostasis and the ischaemic damage that can be suffered during an infarction, cellular and whole heart models of ischaemia and reperfusion will be used.

2) What are the effects of up to 24h of culture with TMAO on cardiomyocyte function?

Freshly isolated cardiomyocytes can be cultured, short-term, in serum-free media without changing their morphology or proliferative status. Cardiomyocytes will be cultured for up to 24h with TMAO to investigate the effects of longer-term culture on functional behaviour of the cardiomyocytes.

3) What is the effect of TMAO on the cellular metabolism?

Using Seahorse respirometry, the effects of TMAO on metabolism, focusing on the impairment of mitochondrial metabolism in the heart and the possibility of TMAO being an important player that increases the severity of cardiovascular events or that enhances the progression of cardiovascular diseases by modulating bioenergetic pathways inside the cell will be investigated:

- As heart function is highly dependent on energy derived from ATP that is generated during oxidative phosphorylation in mitochondria, the altered cardiac energy metabolism and mitochondrial dysfunction play crucial roles in the development of cardiovascular diseases.
- Preliminary data suggests that TMAO is enhancing cardiac dysfunction in a concentration-dependent manner. This will be investigated to identify what mechanism are involved in this dysregulation. There are three potential points of modulation by TMAO that will be initially investigated:
    - Mitochondrial dysfunction: reducing ATP synthesis and reduced Ca^{2+} buffering capacity
    - Increased RyR activity do increasing intracellular Ca^{2+} release
    - Modulation of sarcolemmal ion currents to increase Ca^{2+} influx during the action potential therefore increasing CICR and intracellular Ca^{2+}

4) What is the effect of TMAO on pre-altered cellular metabolism?

To further investigate the potentially deleterious effects of TMAO on cardiomyocyte function and normal mitochondrial function, changes in the culture conditions and cotreatment of cardiac cells with different concentrations of TMAO and known modulators of cardiac function and energetic metabolism of the cells:

- Cardiac cells will be pre/co-exposed to environmental conditions that alter the normal mitochondrial function, like the culture in galactose-supplemented media, that push the cells to a metabolic shift that caused the cells to produce

ATP exclusively through OXPHOS. It is hypothesised that replacing glucose with galactose in the culture media of cardiac cells would increase their reliance on mitochondrial OXPHOS, thereby making them more sensitive to mitochondrial toxicants.

- Cardiac cells will be pre/co-exposed to short-time exposure to high glucose, that was shown to alter mitochondrial function. It is hypothesised that short-time exposure to high glucose would cause disruption of mitochondrial function implicated in the mechanism of damage to the myocardium, caused by overload of $[Ca^{2+}]_i$ and low levels of ATP.

Chapter 2

Materials & Methods

2 Materials and Methods

2.1 Introduction

The method section of this thesis can be divided into two different research topics: analysis of cardiomyocytes functionality and analysis of mitochondrial disruption. In the first section, experiments were designed with the intention of analysing the effects of TMAO on normal cardiac function, focusing on contractility of the cells and their electrical activity. In particular, the electrical activity of the cells and the currents underlying the cardiac action potential. This was investigated using electrophysiology techniques.

In the second section, experiments were designed with the intention of analysing the effects of TMAO on mitochondrial function. Evaluations of possible mitochondrial dysfunction was carried out through analysis of ATP production in different conditions, assessment of oxygen consumption rate and acidification rate of the cells and broad investigation of the sources of energy utilised during cellular respiration.

2.2 Solutions

The perfusion solutions described in this section were used all throughout the first experimental section (Table 2.1). Specifically, different variations of Normal Tyrode's (NT) solution were used to carry out isolation of ventricular cardiomyocytes, contractile function experiments, electrophysiological evaluation and fluorescent imaging.

Chemicals	Normal Tyrode's (mM)	Ca^{2+} free Tyrode's (mM)	Substrate-free Tyrode's (mM)	Substrate-free Metabolic Inhibition Tyrode's (mM)
KCl	5	5	5	5
NaCl	135	135	140	140
NaH_2PO_4	0.33	0.33	0.33	0.33
Na Pyruvate	5	5	--	--
HEPES	10	10	10	10
Mannitol	15	15	--	--
Glucose	5	5	--	--
Sucrose	--	--	20	20
$CaCl_2$	2	--	2	2
$MgCl_2$	1	1	1	1
EGTA	--	0.4	--	--
Sodium Cyanide	--	--	--	2
Iodoacetic acid	--	--	--	1

Table 2.1. List of chemicals and their concentrations used to make Normal Tyrode (NT) solution, Ca^{2+} free Tyrode's solution (Ca^{2+} free NT), substrate-free Tyrode's solution (SFT) and substrate-free metabolic inhibition Tyrode's solution (SFT-MI).

TMAO was prepared directly in NT or SFT-MI solutions according to what was required in the experiment. Unless otherwise specified, all reagents for cell isolation and experiments were purchased from Sigma-Aldrich (Sigma-Aldrich, Gillingham, UK).

2.3 Isolation of ventricular cardiomyocytes

Rat ventricular cardiomyocytes were isolated from adult male Wistar rats with a weight range of 300-400g. Animals were killed by concussion and cervical dislocation following the Home Office UK animals (Scientific procedures) Act 1986 (2012 amendment)

regulations. The heart was rapidly removed from the animal and placed into Ca^{2+} free-NT, then mounted on a Langendorff-type apparatus that allowed the heart to be perfused in a retrograde manner via the aorta. The heart was perfused with Ca^{2+} free-NT solution for ~5min at 37°C until all coronary flow was cleared of blood and solutions were able to perfuse all regions of the heart. The heart was then perfused with Ca^{2+} free- NT solution containing an enzyme mix comprising 0.5 $mg.ml^{-1}$ collagenase type II (Worthington, USA), 1.66 $mg.ml^{-1}$ bovine serim albumin (BSA) from factor V albumin and 0.6 $mg.ml^{-1}$ protease (type XIV 15 % Ca^{2+}) for 7-15 min (Brennan et al., 2019; Brennan et al., 2015; Sims et al., 2014). All solutions, during the isolation of the cardiomyocytes, were kept oxygenated with 95% O_2 and 5% CO_2. During this process, a plastic cannula was inserted in the atrioventricular gap to relieve any pressure building up during the perfusion. During the digestion, the heart was checked regularly. In particular, at the beginning of the digestion, the heart starts to swell and, as digestion proceeds, it gets softer to the touch, suggesting that the digestion process is almost over.

The heart was considered fully digested at the detection of rod-shaped cardiomyocytes in the perfusate and was then removed from the Langendorff apparatus for the collection of cells from the tissue. The heart was cut into smaller sections and the tissue was then transferred into a flask containing NT solution and shaken for 5 min in a water bath to allow the cardiomyocytes to be released from the tissue. The perfusate was then filtered to remove any residual tissue and allowed to settle in 15 mL falcon tubes to separate the cardiomyocytes. The pellet was re-suspended and stored in 75mm petri dishes containing fresh NT solution at room temperature until use or in 15 mL falcon tubes containing fresh NT solution at room temperature for culture.

This method, on average, generated ~80% of healthy rod-shaped cardiomyocytes for each preparation (Figure 2.1).

Figure 2.1. **Picture of freshly isolated rat cardiomyocytes.** Normal rod-shaped cardiomyocytes from Wistar rat after shortly after isolation. Image was captured using a JVC CCD camera and recorded to a DVD.

2.3.1 Culture of isolated ventricular cardiomyocytes

Freshly isolated cardiomyocytes were cultured in order to investigate the chronic effects of TMAO on cardiomyocytes. To culture the cardiomyocytes, following isolation, cells were suspended in NT and centrifuged at 300 revolutions per minute (rpm) for 1 min. The pellet was then re-suspended again, this time in complete 199 media and transferred into 6-well plates. Cells were maintained and cultured in media 199 (Life Technologies) supplemented with ITS+3 (2mg/100ml), 2mM carnitine, 5mM creatine, 5mM taurine, 1.5 pM T3, 100 Units pen/strep and 100mM sodium pyruvate at 37°C under a humidified 5% CO_2 atmosphere.

Cells were kept in culture for 24h in presence of TMAO (100 µM) to simulate long exposure to the metabolite and then used for the appropriate experiments.

2.4 Metabolic inhibition and reperfusion (MI/R) model and contractile function measurements

To investigate the effects of TMAO on cardiomyocytes contractile function, acutely and following 24h exposure to the metabolite, a metabolic inhibition and reperfusion (MI/R) model was used. Firstly, cells were perfused with NT solution at ~34°C and electrically stimulated to contract using a 1Hz electric field stimulation for 3 min. Subsequently, the perfusion solution was switched into a metabolic inhibition (MI) solution (as described in section 2.3 of this thesis) containing sodium cyanide and iodoacetic acid for 7 min, followed by 10 min of reperfusion with NT. The protocol was then carried out also in the presence of different concentrations of TMAO (0.3, 1, 3, 5, 10, 30, 50, 100, 300 and 1000 µM).

Sodium cyanide is responsible for blocking ATP synthesis at the level of oxidative phosphorylation and iodoacetic acid inhibits glycolysis (by inhibition of glyceraldehyde-3-phosphate dehydrogenase, GAPDH). Taken together, the metabolic inhibitors are responsible for leading the cells to enter a state of contractile failure caused by lack of substrates to use and depletion of intracellular ATP, thus creating a chemical simulation of ischaemia at a cellular level (Figure 2.2).

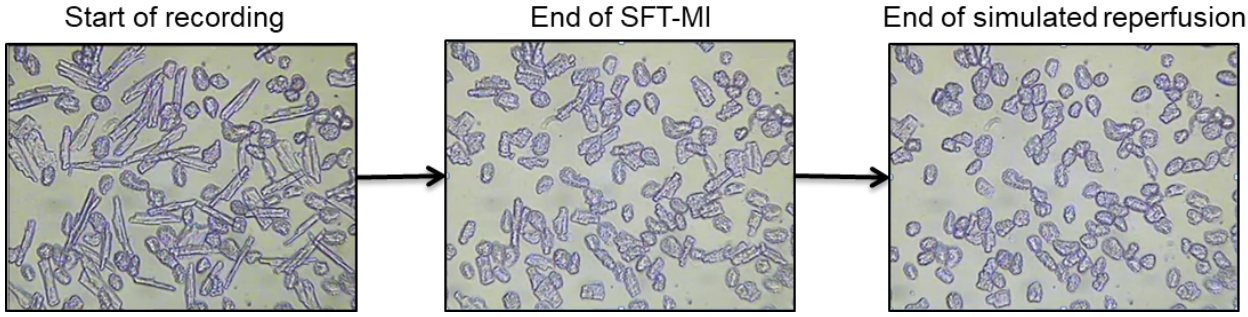

Figure 2.2. Pictures showing cardiomyocytes at different stages of the experiment. At the start of the recording the cells have the distinctive rod-shape typical of the cardiomyocytes. After MI perfusion, cells go into rigor due to lack of ATP and finally, at the end of the protocol, part of the cells are able to recover contractile functions thanks to the renewed presence of metabolic substrates.

Contractile function was observed via a JVC CCTV camera and recorded to DVD. Following reperfusion, part of the cardiomyocytes showed contractile recovery from the

stunned state, due to re-availability of metabolic substrates. Cells showing normal contractile function were identified as “recovered” and the percentage of contractile recovery was compared in the presence of different concentrations of TMAO. The times to contractile failure, times to rigor and time to contractile recovery were also recorded and compared in the presence of different concentrations of TMAO.

2.5 Patch-clamp electrophysiology

Patch clamp recording is an electrophysiology technique used to have a better understanding of ion channel behaviour in different type of cells, including cardiomyocytes. The method requires the isolation of a patch of membrane in the tip of a glass micropipette and to record the currents (Figure 2.3). Patch-clamp recording allows the investigation of the physiological role of ion channels, their conductance and kinetic and their behaviour in response to the use of modulators.

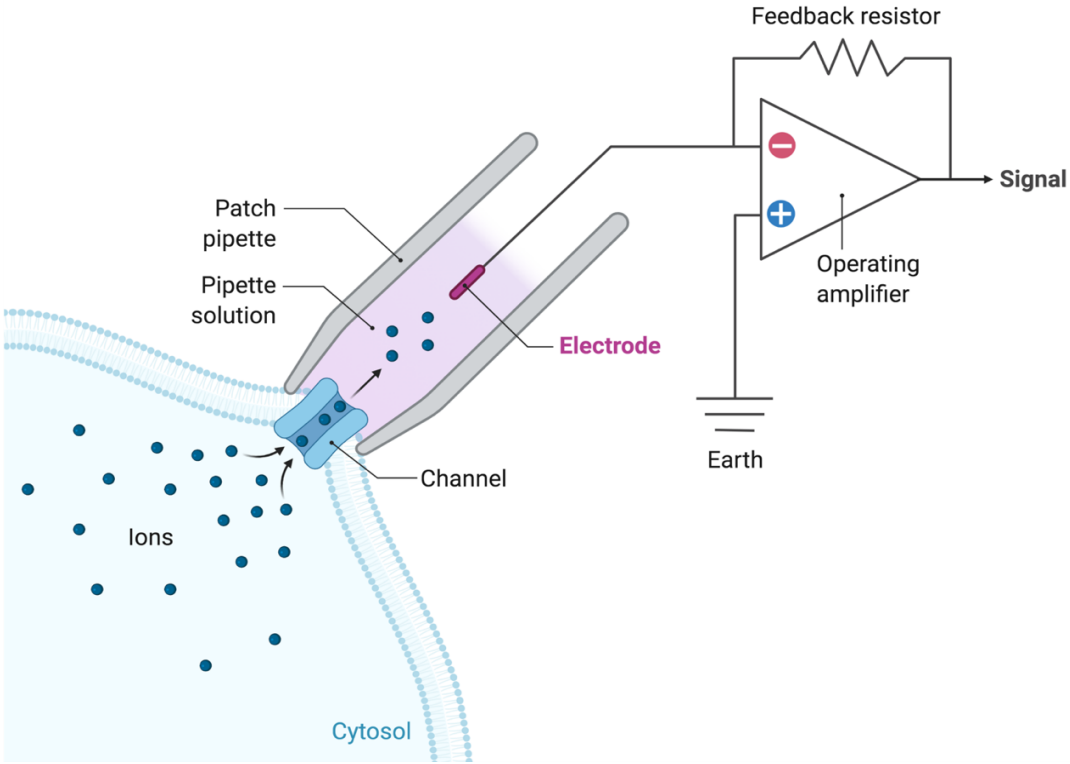

Figure 2.3. Schematic of patch-clamp electrophysiology recording. The technique uses a glass pipette containing an electrolyte solution that seals onto the cell membrane isolating electrically a patch of membrane. Through the patch pipette, currents produced by ion channels situated on to the isolated patch flows and can be recorder by an electrode connected to a highly sensitive amplifier. Created with BioRender.com.

This technique was used to understand how ion channels behave in freshly isolated ventricular myocytes when different concentrations of TMAO are present.

2.5.1 Bioelectricity

With the term "bioelectricity", we refer to the electrical currents and the electrical potentials generated by cells and tissues. Cells and tissue communicate with each other via movement of ions and the currents this generates. Generally, the electrical potential of a cell stems from the electrical properties of its membrane, in particular the ability of the membrane to allow ion fluxes to permeate. The electrical potential of a cell is due to a difference of electrical potential between the inside and the outside of the cell. The outside of the cell is always zero by convention.

In physiological conditions, the resting membrane potential of a cell is largely due to K^+ ions, present in much bigger concentrations inside the cell compared to the extracellular environment (140mM), leaving the cell moving down their electrochemical gradient. If the membrane was permeable to just K^+, the membrane potential of the cell would be exactly the same as the equilibrium potential for K^+. The equilibrium potential for an ion is the voltage at which the net flow of ions moving across the membrane balances the net flow of ions moving in the opposite direction, so that the resulting current for the ion across the membrane is zero. The equilibrium potential for any ion can be calculated with the Nernst equation:

$$Ex = \frac{RT}{zF} \ln \frac{[X]o}{[X]i}$$

In this equation, E_x is the equilibrium potential for an ion X, R is the universal gas constant (8.314 J K^{-1} mol^{-1}), T is the temperature expressed in Kelvin, z is the number of elementary charges of the ion, F is the Faraday constant (96.500 C mol^{-1}) and $[X]_o$ and $[X]_i$ are the concentrations of the ion outside and inside the cell, respectively.

However, because the cell is not permeable to just one ion at time, the membrane potential of the cell is generally established as a result of the relative contributions of several ions. When more than one ion channel is present (and open) in the plasma membrane, the membrane potential can be calculated by alternative methods.

As previously mentioned, in normal physiological conditions in cardiac cells, K^+ is the primary permeating ion at rest however, because the membrane is permeable to other ions as well, the resulting resting membrane potential is close to K^+ equilibrium potential (-89mV) but not exactly the same.

2.5.2 Electrophysiology set-up

The electrophysiology set-up used for patch-clamp experiments in this study included a Nikon TiU inverted microscope with a 20x objective and micromanipulator (Siskiyou), used to position the electrode in the rig. Both the patch-clamp rig and the recording chamber are shown in figure 2.3 and figure 2.4.

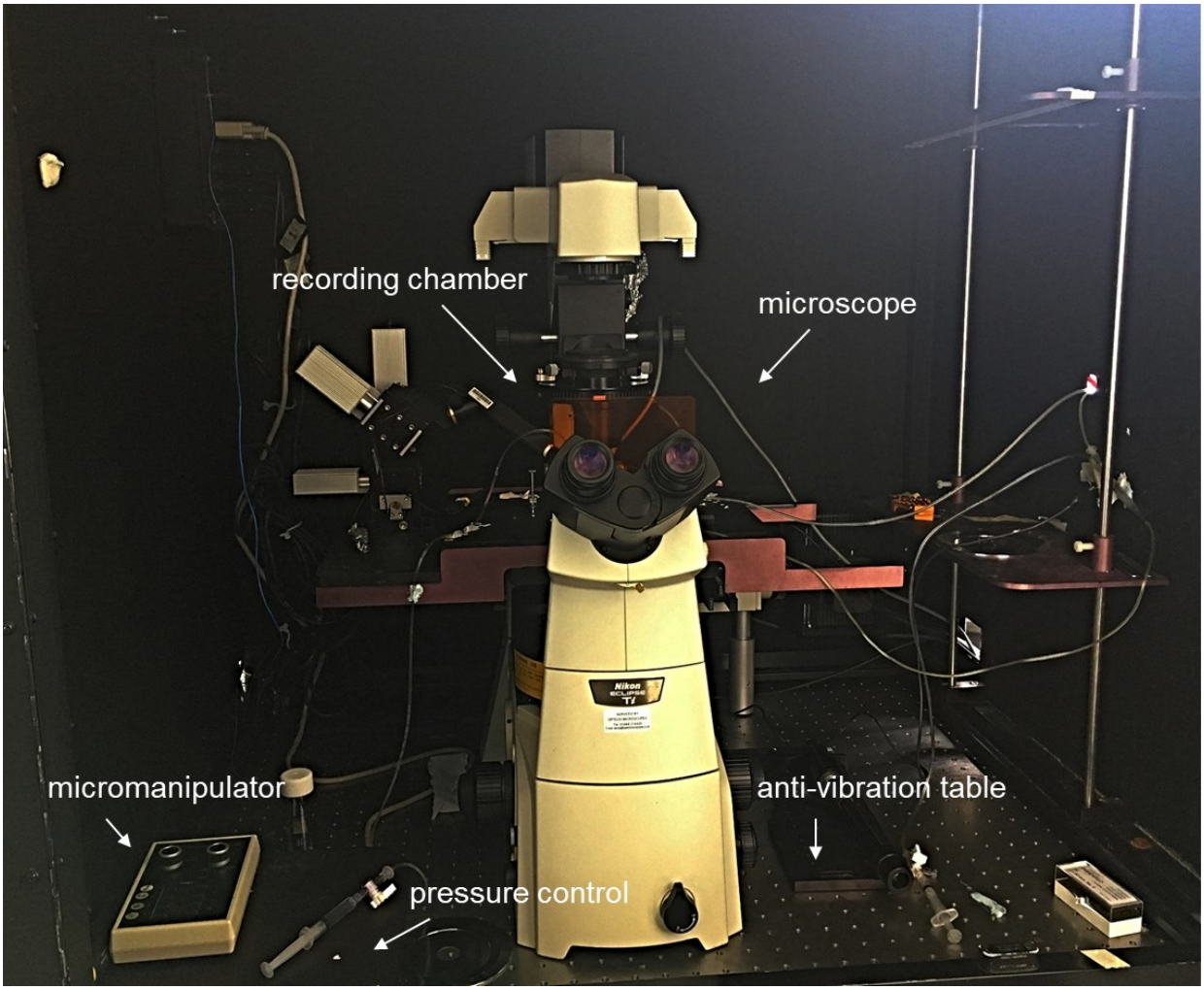

Figure 2.4. Picture and schematics of a patch-clamp electrophysiology rig. All of the equipment is placed on an air-table that prevents vibrations and into a Faraday cage used to shield microscope and chamber from electromagnetical interference that could cause noise in the recordings.

Electrical equipment that allowed patch-clamp recordings included an Axopatch 200B amplifier (Axon Instruments, Uckfield, UK) coupled to digital interface (Digidata 1440, Axon Instruments) and a computer that allowed acquisition and analysis of data by pCLAMP 10.7 software (Axon Instruments, Uckfield, UK).

The patch-clamp amplifier is used to amplify the signal recorded from the electrode. The amplifier connects to the cell via the Axopatch amplifier head stage (Figure 2.4). This is mounted on a micromanipulator which is used to position the electrode close to the cell. Lowpass filter was set on 2kHz. Sampling rate was set to 10 kHz.

The digitiser converts the signal from the amplifier into a digital signal that can be read and recorded by the computer. The digitiser is a vital component for patch clamp

recording as it is the interface between the analogue signals generated by the amplifier and the digital signals required for recording to the computer.

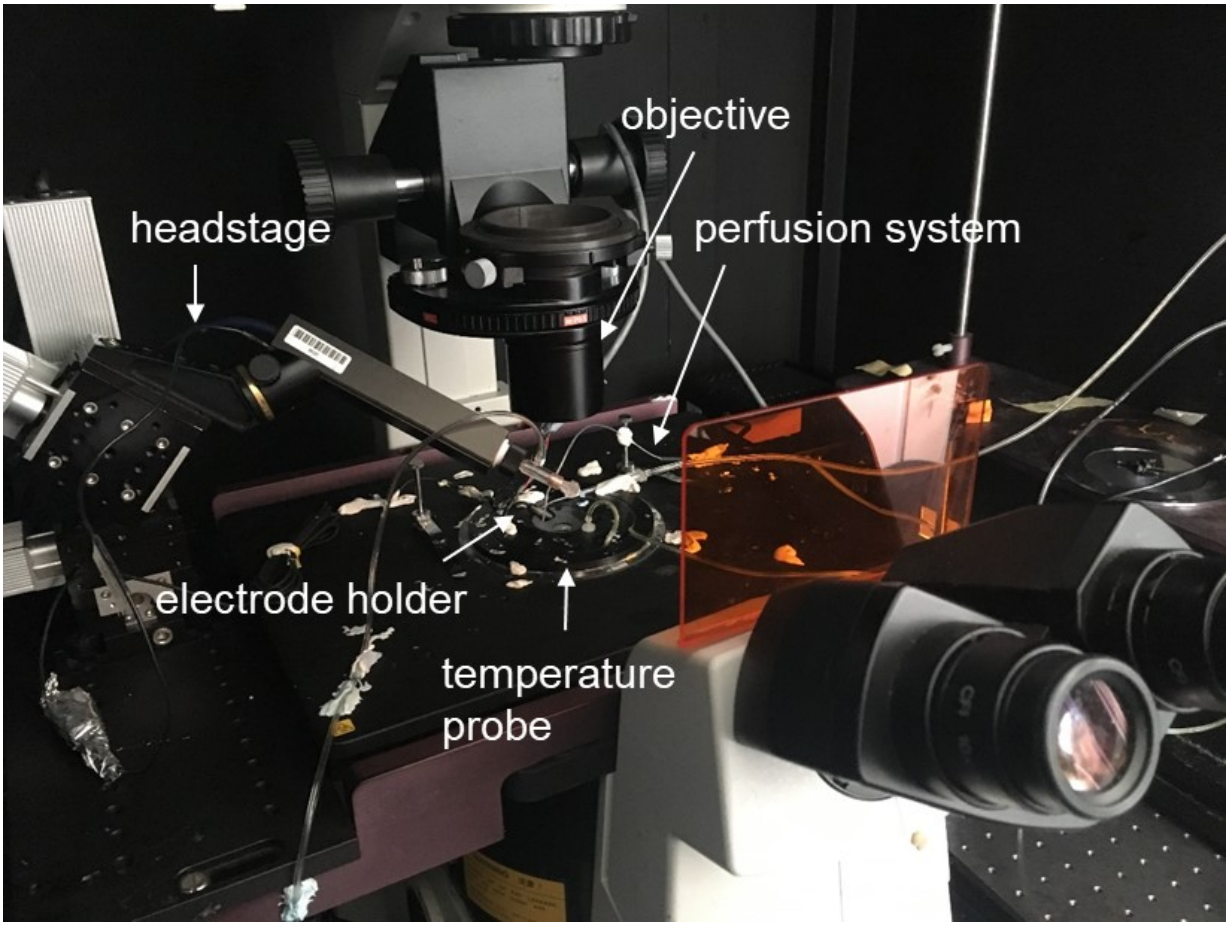

Figure 2.5. Close-up picture and schematics of the recording chamber in the patch-clamp electrophysiology rig. The recording chamber of the rig is where cells that will be used during the experiment will be used. The recording chamber comprises a perfusion system that allows to keep the cells in solutions and the easy replacement of extracellular solutions and a temperature probe used to keep extracellular solutions at a set temperature.

2.5.3 Microelectrodes

In patch-clamp experiments, microelectrodes used for all recordings were made from 1-2 mm borosilicate glass capillaries (Warner Instruments). To produce the microelectrodes, a dual-stage vertical electrode puller (Narishige PC-10 Dual Stage Glass Micropipette Puller) was used; the puller uses two different heating levels to produce thin-tip electrodes.

For both cell-attached recordings and whole-cell recordings, we used electrodes with a resistance ranging from 3 to 6 MΩ. The electrodes were made and used on the same day as the recordings.

2.5.4 Electrophysiology solutions

Solutions used in patch-clamp experiments were prepared as described in table 2.2. Different solutions were used in cell-attached experiments and whole-cell configuration experiments. These solutions were used to backfill the patch-pipette at the beginning of each experiment and were used to pass electrical signal from the electrode to the cell.

Extracellular solutions used in patch-clamp experiments were prepared as previously described (table 2.1). Extracellular solutions were perfused into the recording chamber through a dedicated perfusion system (Figure 2.4) by a Gilson Evolution peristaltic pump (Gilson) with a perfusion rate of 2.4 ml/min. Solutions in the perfusion chamber were heated to 34°-35°C by Dagan Heatwave perfusion chamber and the temperature was kept constant throughout the experiments. Extracellular solutions were swapped manually when needed.

Chemicals	Cell-attached configuration (mM)	Whole-cell configuration (mM)
KCl	140	110
KOH	--	30
HEPES	10	10
$CaCl_2$	1	0.61
$MgCl_2$	0.5	1
ATP	--	1
ADP	--	0.1
GTP	--	0.1
EGTA	--	5
pH	To 7.4 with KOH	To 7.2 with KOH

Table 2.2. List of chemicals and their concentrations used to make solutions for cell-attached and whole-cell recordings.

2.5.5 Cell-attached configuration

The cell-attached configuration is used to study single channel currents. In particular, with this technique, the activity of the $K_{ir}6.1$ and $K_{ir}6.2$ were studied and their modulation in response to the exposure to TMAO (100µM).

For a cell-attached recording, cardiomyocytes were allowed to adhere in the perfusion chamber of the patch-clamp rig for 10 min. The glass pipette was filled with an intracellular solution (table 2.2) and a silver/silver chloride (Ag/AgCl) electrode was inserted. The patch pipette if connected to an air-filled tube and to a syringe, to allow control of the pressure inside the pipette as shown in the electrophysiology set-up section (Figure 2.3). Using a micromanipulator, the patch pipette is inserted into the extracellular solution, typically NT or NT+TMAO and heated through a recording chamber plate containing a temperature probe, and maintained at 35°C. With the patch-pipette in the bath of the recording chamber, the Ag/AgCl electrode can serve as a reference electrode set to 0 mV as the extracellular potential.

While, the patch-electrode gets closer to the cardiomyocyte and touches the cell membrane, pressure was removed from the inside of the pipette and gentle suction was applied to the membrane in order to pull a small patch of membrane inside the pipette. As suctions gets applied, the resistance between the electrode and the bath increased forming the "giga-seal", necessary to start a recording in cell-attached configuration (Petersen, 2017), with the recording potential changed to +40mV. Assuming that the isolated cardiomyocytes had a resting membrane potential of -70mV, holding at +40mV means that the patch of membrane would be held around -110mV. In cell-attached recordings, the single channel activity was analysed as open probability (P_o) of the channel. P_o represents the fraction of time for which an ion channel is open, and a can be deduced from a histogram of a single channel recording as the total open time of the channel divided by the total time of the recording. For an ion channel that has a single open and a single closed state, the distribution of open probability fits a single exponential (Ogden et al., 1983). In these conditions:

$$To = \sum_{L=1}^{N} toL$$

In this equation, L represents the different open levels and t_oL represents the opening time for this type of ion channel in different opening levels (Fenwick et al., 1982; Sollini et al., 2002).

However, ion channels tend to have various open and closed states, which means that a single exponential no longer fits these distributions. Another complication is due to the fact that, usually, a single patch contains more than one channels opening in multiple levels. The open probability of the channel is better expressed in NP_o, calculated by the following equation where T represent the time of the recording (Roh et al., 2007; D. Q. Zhang et al., 2000):

$$NPo = \frac{To}{T}$$

2.5.6 Whole-cell configuration

The whole-cell configuration allows the patch electrode to record directly from the inside of the cell and is obtained by rupturing the patch of membrane isolated by the patch-pipette.

The glass pipette is filled with a different solution from the one used in cell-attached recordings (this solution will flow in direct contact with the intracellular space, thus is important that this solution is isosmotic to the intracellular compartment), as described in table 2.2.

To obtain a whole-cell configuration, after forming a giga-seal in cell-attached mode, rapid suction pulses were applied to the patch-pipette to rupture the membrane of the cell (Figure 2.5).

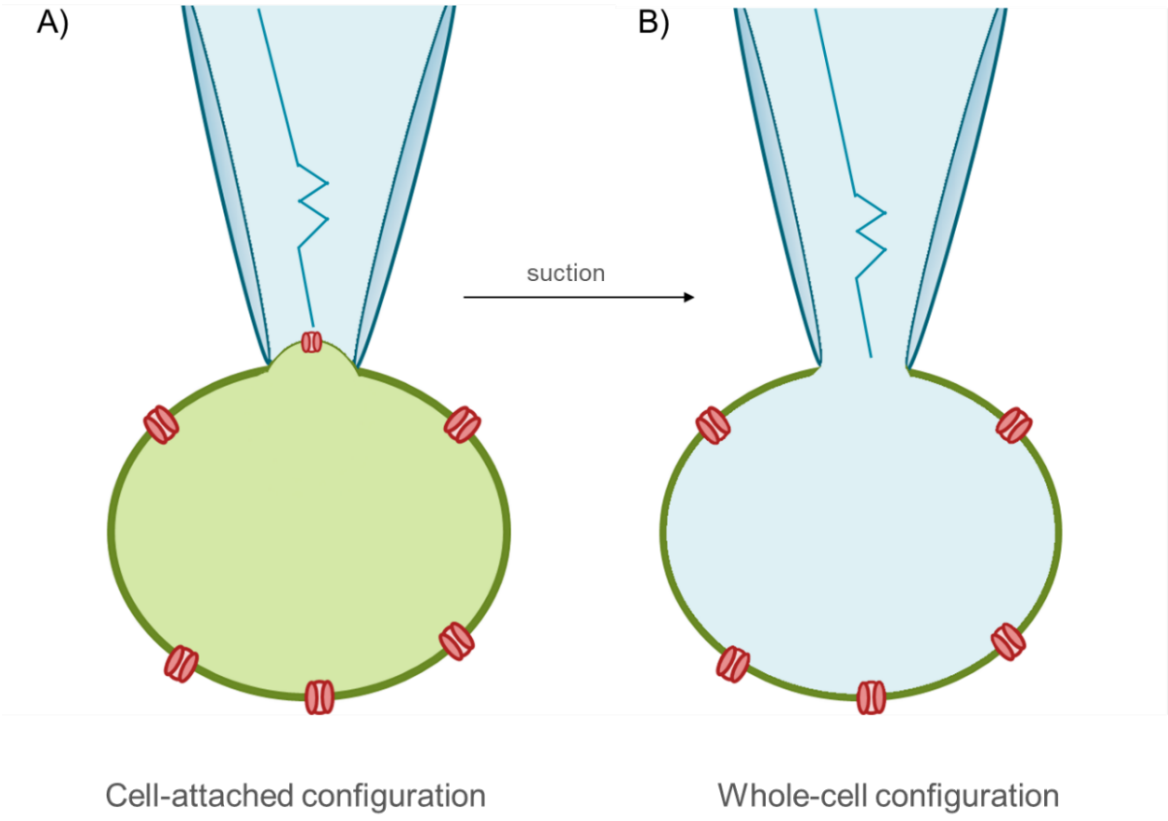

Figure 2.6. Cell-attached and whole-cell configuration. In cell-attached configuration, the patch pipette rests on the membrane of the cell and current is only recorder from the area of membrane included in the tip of the electrode (A). Cell-attached configuration is required to move on to whole-cell configuration. In whole-cell configuration, the membrane included in the tip of the patch pipette is ruptured by applying soft suction to the patch pipette when in cell-attached configuration (B).

The rupture of the membrane was identified by the appearance of large capacitance transients at the leading and trailing edges of the pulse. In whole-cell mode, voltage steps lead to large transient currents due to the charging and discharging of the membrane capacitance. The current flowing from the patch-pipette to the cell moves through a resistance in series. The series resistance represents the sum of all the resistances that currents existing between the source of the current and the inside of the cell and limits the amount of current that actually clamps the membrane. The series resistance can be compensated on the amplifier by adding a voltage pulse to correct for the membrane capacitance, thus correcting the error (Figure 2.6).

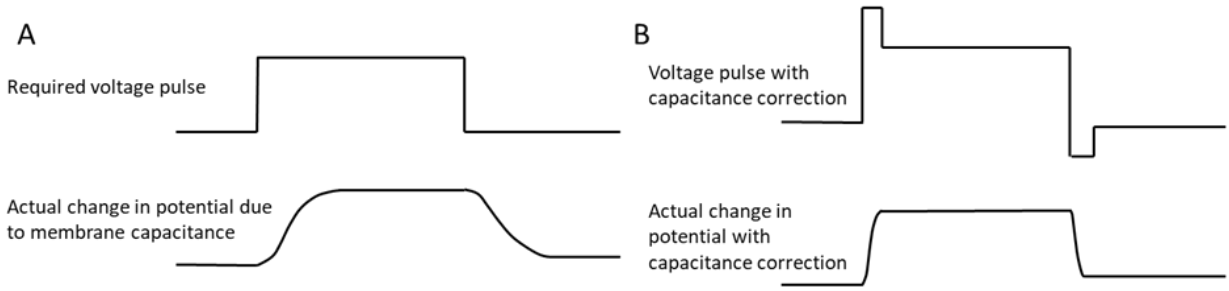

Figure 2.7. Series resistance compensation. Because in whole-cell recordings current flows through resistance in series, the voltage pulses are delayed (A). The series resistance compensation adds a voltage pulse proportional to the difference of the measured membrane potential to the set one is injected (B).

Whole-cell configuration was used, in this thesis, to investigate cardiomyocyte action potentials and detailed analysis of the ionic currents underlying the action potential.

2.5.6.1 Action potentials recordings

To investigate the effects of TMAO on the physiological electrical activity of cardiomyocytes, action potentials (AP) were recorded. AP recordings were measured in whole-cell configuration in current-clamp mode. Current is injected through the patch pipette and allows measurement of membrane excitability and firing of action potentials, via analysis of action potential duration (APD) and membrane voltage (V_m). Cardiomyocytes were stimulated via the injection of a small current (~2nA) to depolarise the resting membrane potential between 8 to 12 mV and to generate a cardiac action

potential. Thanks to the high stability of the technique, long-lasting recordings were possible. Generally, an AP recording consisted in 3min of control recording in NT solution, 7min of exposure of the cell to TMAO (100µM) and 5min of washout from TMAO in NT solution. At the end of each recording, the APD at 90% of repolarization and changes in the resting membrane potential (RMP) were calculated in the different phases of the recording.

2.5.6.2 Multi-currents protocol

A multi-step protocol was used in whole-cell configuration in voltage-clamp mode to measure the currents underlying the cardiac action potential. The separation and analysis of the ionic currents is possible because the currents have different kinetics, therefore it is possible to measure them at a suitable time during a voltage clamp pulse. The protocol constitutes of 4 sequential steps: a first step elicited by voltage commands from -100 to -70mV in 5mV steps during 10ms, in which I_{K1} current can be measured, a second step elicited by voltage commands from -70 to -40mV during 500ms, that allows isolation of the Na^+ spike, a third step from -40 to -50mV during 100ms, in which Ca^{2+} current can be measured and a final fourth step from -50 to -80mV in 10mV steps for 4000ms, in which I_{Ks} currents can be measured (Figure 2.7).

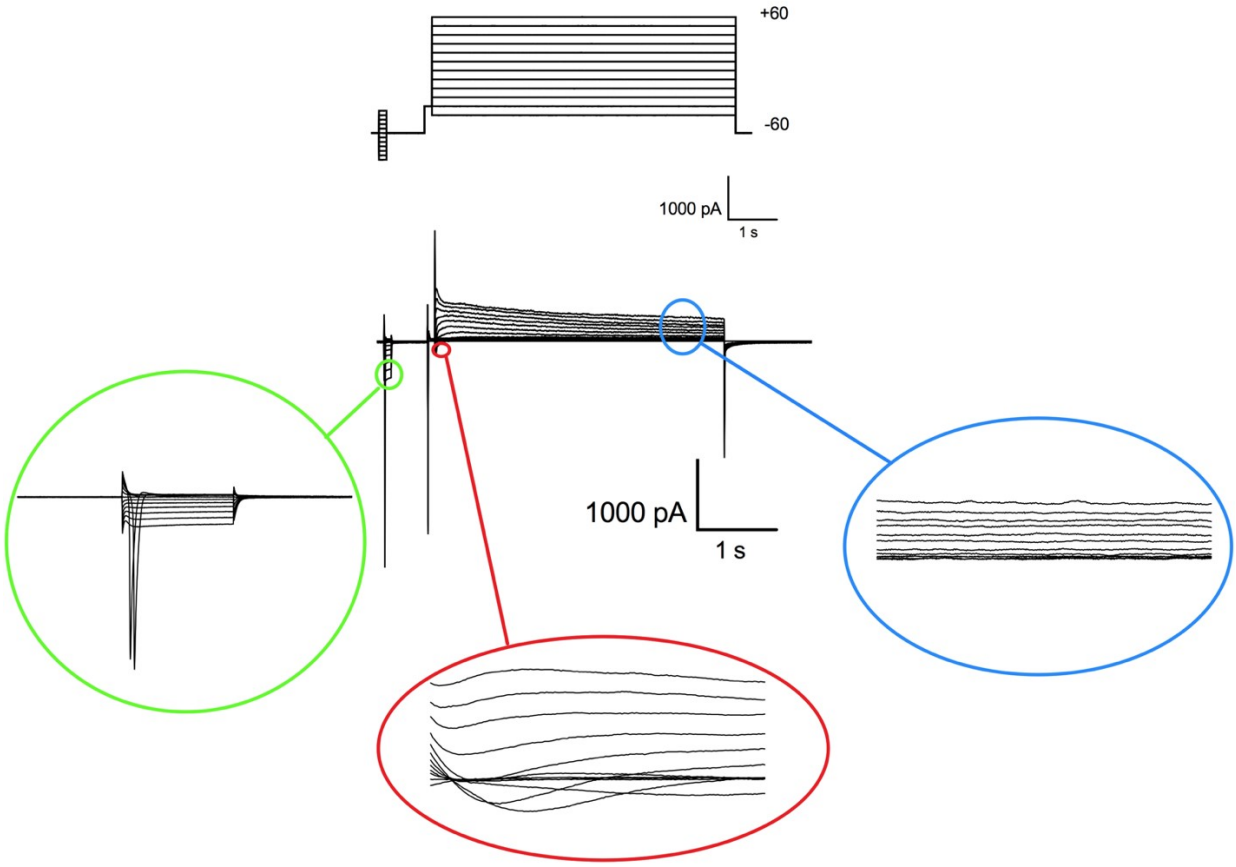

Figure 2.8. Example trace of current for a single patch clamp electrophysiology recording in whole cell configuration using the multi-step protocol. In the image, portions from which following analysis will be shown are highlighted.

2.5.6.3 Ca^{2+} current voltage-step protocol

Because of their kinetics, Na^{+} and Ca^{2+} current can be difficult to separate and measure individually in voltage-step protocol like the one described in section 2.5.6.2. In particular, opening of Ca^{2+} channels can sometimes happen while Na^{+} channels are opened and be "masked" by the latter.

To allow a more detailed look at Ca^{2+} current, a multi-step protocol was designed with the purpose to isolate Ca^{2+} current from other ionic currents that could potentially interfere. The protocol constitutes of 3 sequential steps followed by a final ramp. The first step is elicited by voltage commands from -70 to -40mV during 30ms, the second step from -40 to 0mV during 70ms, the third step holds the potential to 0mV for 300ms and the final ramp from 0 and -70mV holds to potential at -70mV until the end of the protocol (Figure 2.9).

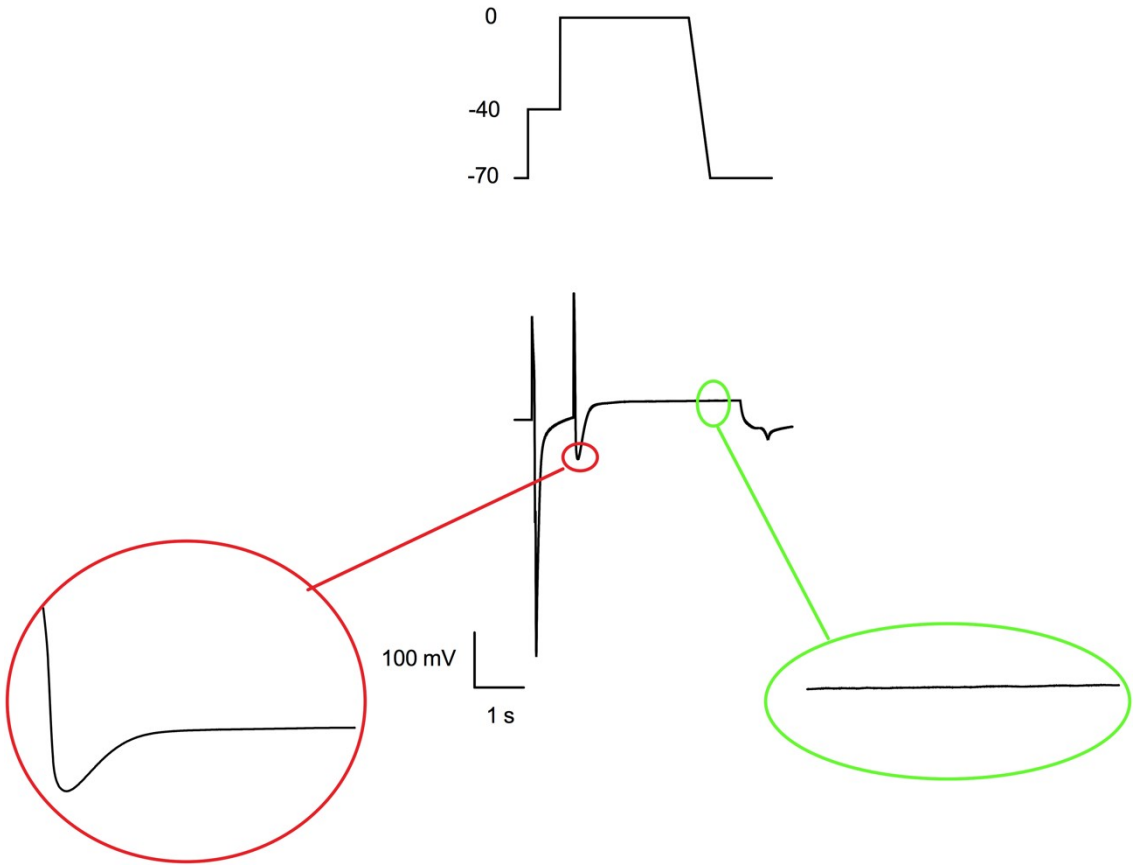

Figure 2.9. Example trace of current for a single patch clamp electrophysiology recording in whole cell configuration using the Ca^{2+} protocol. In the image, portions from which following analysis will be shown are highlighted.

2.6 Fluorescence imaging

Fluorescence imaging allows visualization of different events taking place in a cell. The technique takes advantage of the ability of fluorophores to absorb light forming a short-lived excited state and to emit light at a longer, lower energy wavelength.

A ratiometric dye, Fura-2- acetoxymethyl AM Cell Permeant (Invitrogen), was used to measure changes in intracellular Ca^{2+} and changes in Ca^{2+} transients when cardiomyocytes were exposed to TMAO. Recordings from Fura-2-AM dye were achieved by using excitation wavelengths of 340 nanometres (nm) (Ca^{2+} bound)/ 380 nm (Ca^{2+} free) and emissions collected at wavelengths above 520 nm. The advantage of using a ratiometric dye is that, rather than a single wavelength dye, is that by measuring a ratio

decreases the effects of photo-bleaching, inconsistent loading of the dye and changes in the shape and volume of the cells, which can be quite considerable in contractile cardiomyocytes. Fura-2-AM is one of the many dyes that uses AM esters as a way to cross the cell membrane. Due to their charged nature, calcium indicators are unable to cross the cell membrane. The protection of carboxylic group as AM esters render the dye neutral so that is able to load into the cell. Once inside the cytoplasm, esterases naturally present inside the cell will cleave the AM groups leaving the charged compound able to bond free Ca^{2+} inside the cell.

Briefly, cells were incubated in a lightproof tube with the appropriate dye for the experiment (5 µM of dye) and allowed 10-20 min to fully load the dye. Cells were than visualised through a Nikon 200 inverted microscope with a 20x objective and the images observed thanks to a Roper Cascade 512 B CCD camera (Photometrics, Arizona, USA). Fluorescent illuminator used for the experiment was a DeltaRAM X monochromator (PTI, New Jersey, USA) at 0.2 Hz for 40 ms and a 79001 – ET – Fura 2 Filter (Chroma Technology Corp, Vermont, USA) was set up to detect signals. Images were processed with EasyRatioPro software (PTI, New Jersey, USA) and analysed with Winfluor 4.0.2 software (Dr John Dempster, University of Strathclyde, Glasgow, UK).

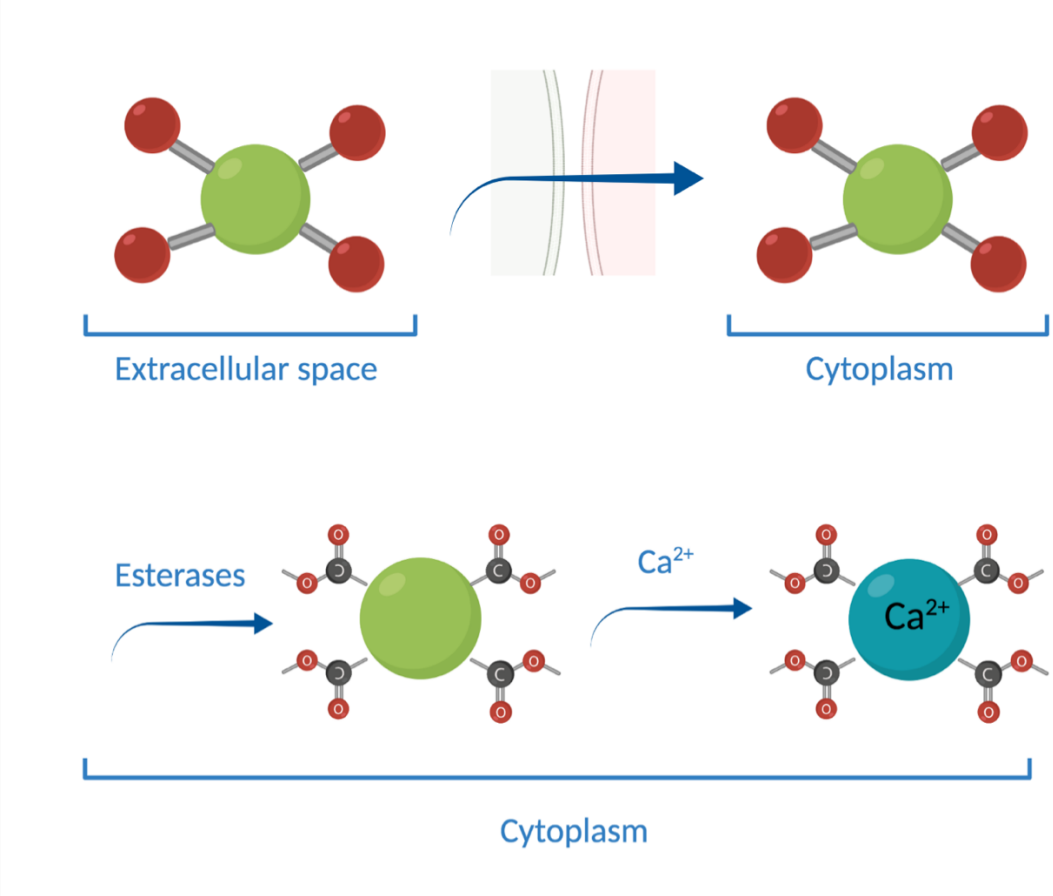

Figure 2.10. Scheme representing the process of internalization of AM-dyes. The AM dyes are able to enter the cytoplasm thanks to their neutral nature, where they get converted by the esterases into charged compounds that are able to create links with Ca^{2+}. Created with BioRender.com.

2.7 Langendorff-perfused heart and coronary artery ligation

To investigate the effects of TMAO on the whole heart, a Langendorff perfused heart model was used. In this model, ischaemia was induced by occluding the left anterior descending (LAD) coronary artery to cause localized injury (regional ischaemia) to the myocardium. Reperfusion was initiated by re-establishing coronary flow to the region at risk by removing the ligature. The Langendorff heart preparation was used to assess ischaemia–reperfusion injury, with or without the presence of TMAO. Infarct size following reperfusion was used as the end point of the experiment.

In this protocol, hearts were isolated from adult male Wistar rats (300-500g), cannulated via the aorta and retrogradely perfused in constant flow (8.5 ml/min) with oxygenated NT solution at ~37°C and suspended within a warmed organ bath/chamber (Figure 2.9).

The temperature of the solution was kept the same all throughout the experimental protocol.

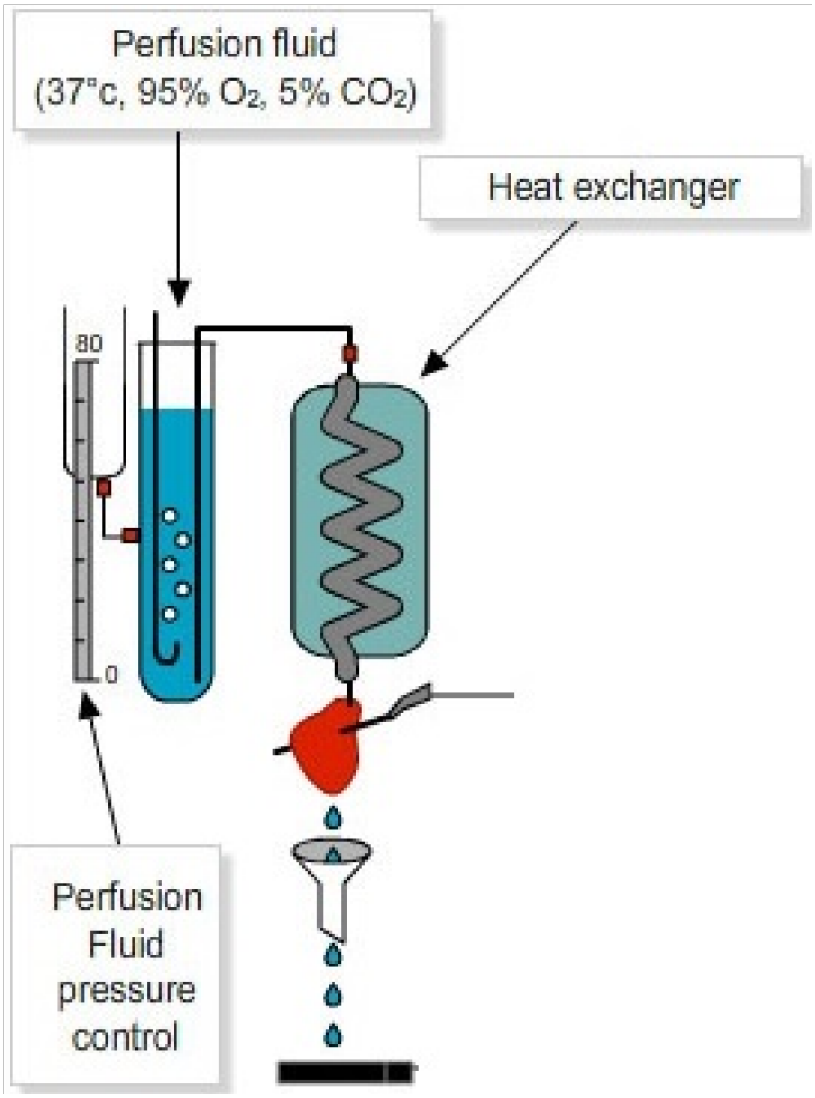

Figure 2.11. Simplified scheme of a Langendorff system in constant pressure or constant flow.

Before proceeding further with the protocol, the heart was left to equilibrate for ~1h to make sure that all the heart chambers were correctly perfused. Subsequently, the LAD was occluded by ligating it with using 5-0 USP braided silk suture to create a tie and two pipette tips to secure it in place for 40 min, in order to cause myocardial damage to the heart. After the 40 min, the ligation was released, and NT solution was then reperfused through the heart for 3h. At the end of reperfusion, the LAD was ligated once again and Evans blue dye (0.5% in NT solution), was infused via the cannula into the coronary

system. The dye coloured the non-risk zone dark blue, while the risk zone (in which the dye does not have access) remained pale pink. The area at risk was then stained using 2,3,5-triphenyltetrazolium chloride (TTC); the double staining allowed to distinguish between the infarcted tissue that remains near white whilst living tissue turned red. The heart slices were weighed, arranged from apex to base and compressed between two transparent coverslips and scanned on both sides on a flatbed scanner.

Finally, the sizes of the infarcted area, the area at risk and the non-risk zone were calculated using ImageJ and used to extrapolate the weight of those areas compare to the total weight of each slice. The final results were expressed as a percentage of area at risk and as a percentage of infarct size compared to the area at risk itself.

2.8 Cell Culture

The H9C2 cell line was derived through selective serial passaging of cells from the ventricular part of an embryonic E13 BDIX rat heart. H9C2 cells were purchased as an established cell line in a 1ml frozen ampule ($6.5x10^5$) from the American Type culture Collection (ATCC). The AC16 cell line is a human cardiomyocyte cell line derived from the fusion of primary cells from adult human ventricular heart tissue. AC16 cells were kindly provided by Dr Parveen Sharma, and originally purchased from Sigma-Aldrich. Nunc flasks and 96-well plates were purchased from Fisher Scientific (Loughborough, UK).

2.8.1 Culturing and passaging of cells

When H9C2 cells reach confluence, they will differentiate in non-proliferating myocytes/myotubes. Once cultures have differentiated, they cannot be recloned. Therefore, to prevent H9C2 cardiomyoblasts differentiating, H9C2 cells were subcultered at 80% confluence and if the cells reached 90-100% confluence, the cells were thrown away and a fresh batch cultured. Both AC16 and H9C2 cells were used between passages 10-30.

Cells were maintained and cultured in two different glucose level media, to better consider alterations to the metabolic environment; a low glucose (2.500 mg/L) Dulbecco's Modified Eagle's Medium (DMEM) media supplemented with 10% fetal bovine serum (FBS), 4mM glutamine and penicillin (100IU)/streptomycin (100mg/ml). Cells were kept at 37°C under a humidified 5% CO_2 atmosphere. Under these conditions, the cells achieved 80% to confluence.

Both AC16 and H9C2 cells used in this project were stored in liquid nitrogen. To culture, the cells were removed from liquid nitrogen storage and thawed for 2 minutes in a 37°C water bath. Once thawed, they were immediately pipetted into a 15 ml Falcon tube containing 9ml of pre-warmed (37°C) complete media and centrifuged at 1000rpm for 5 minutes. The supernatant was removed, and the cells were resuspended in 1ml of fresh media, in order to get rid of any dimethyl-sulfoxide (DMSO) present in the cryopreserving solution. The cells were sub-divided into T.75 flasks to the relevant density and fed with 10ml of fresh complete media. The cells were incubated in a 37°C humidified incubator with 5% CO_2 atmosphere and fed with fresh complete media every 48 hours.

Once the cells had reached the specified confluence in T.75 flasks, the media was removed. The cells were washed with 10ml phosphate-buffered saline (PBS) twice and then 3ml of pre-warmed (37°C) Trypsin-ethylenediaminetetraacetic acid (EDTA) 0.25% was added to the cell surface of the flask. The flask was placed into the 37°C incubator until the cells had displaced from the flask surface, as observed by microscopy. The trypsin was neutralised by addition of 7ml of the appropriate media (high or low glucose according to the growth medium) and the whole suspension (10ml) was added to the 15ml Falcon tube and centrifuged at 1000rpm for 5 minutes. The supernatant was discarded, and the cell was resuspended in 1ml of fresh media. The cells were either sub-cultured to the relevant ratio, or a cell count was performed using a haemocytometer. Specified cell numbers could then be seeded into T.75 flasks, or 96-well plates, as described in section 2.8.2.

Cells were frozen at low passage to maintain competent stock. Cells were frozen using cryopreservation medium, which consisted of complete culture medium supplemented with 10% DMSO. Briefly, once cells had reached desired confluence, they were

trypsinised and resuspended in 1ml of cryopreservation media. The cells were immediately transferred to a CoolCell and incubated at -80°C. After 24 hours, the cells were transferred for permanent storage in liquid nitrogen.

2.8.2 Changes to metabolic conditions of cell culture

In order to have a better understanding of the effects of TMAO in physiological conditions and in the altered conditions, growth media of the cells was modified to investigate possible differences that the change in metabolic conditions can cause to response of the cells to TMAO.

2.8.2.1 High-glucose media

Hyperglycaemia is associated with myocardial damage and worsening of cardiac parameters during acute coronary syndrome (Brennan et al., 2019). In particular, disruption of mitochondrial function is believed to be implicated in the mechanism of damage to the myocardium, caused by overload of $[Ca^{2+}]_i$ and low levels of ATP. High glucose levels can worsen this injury by boosting mitochondrial membrane depolarization in cardiomyocytes (Kumar et al., 2012).

H9C2 and AC16 cell lines were grown in DMEM containing high glucose (4.500 mg/L) supplemented with 10% FBS, 4mM glutamine and penicillin (100IU)/streptomycin (100mg/ml and kept in 5% CO2 at 37°C. Cells were maintained in

T.75 flasks and were subcultured at 70% confluence by trypsinization for experiments, as described in section 2.8.1.

2.8.2.2 Galactose media

Many tumour-derived cell lines prefer to produce the majority of their ATP via glycolysis instead of OXPHOS, despite having perfectly functioning mitochondria and normal,

physiological levels of glucose and oxygen (Rodriguez-Enriquez et al., 2001; Warburg, 1956).

To force cells to rely on their OXPHOS for the production of ATP and, therefore, being able to fully investigate if the compound in exam has any detrimental effects on normal mitochondrial function, culture media can be replaced with a galactose-supplemented media (Dott et al., 2014; Marroquin et al., 2007).

H9C2 and AC16 cell lines were cultured in DMEM containing 10mM galactose, 1mM sodium pyruvate, supplemented with 2mM glutamine (6mM final), 5mM HEPES, 10%FBS and penicillin-streptomycin and kept in 5% CO_2 at 37°C. Cells were maintained in T.75 flasks and allowed to adapt to galactose media for 2h before experiments, as described by Kamalian *et al.*, in which acute galactose conditioning for 2h prior to the treatments with the compound in exam is sufficient to allow the cells to be more prone to mitochondrial toxicity, as opposed to longer term treatment with galactose (Kamalian et al., 2015).

2.8.3 Cell plate seeding and treatments with TMAO

On day 1, H9C2 cells were seeded in a 96-well plate at their respective densities (table 2.3) in a final volume of 200 µl media. The plates were incubated in a 37°C humidified incubator with 5% C02 for 24 hours to reach 70-80% confluence.

	LDH Assay	ATP Determination Assay	SeaHorse XFe96 Measurements	BCA Assay
H9C2 cells	1 x 10^4 c/well	7.5 x 10^3 c/well	--	1 x 10^4 c/well
AC16 cells	1 x 10^4 c/well	1 x 10^4 c/well	1.5 x 10^4 c/well	1 x 10^4 c/well

Table 2.3. Table of the seeding densities for both H9C2 and AC16 cells used for the ATP bioluminescent assay, LDH determination assay, BCA assay and Seahorse XFe96 measurements.

On day 2, the compound to be used (TMAO) was dissolved into the media at its final concentrations. The treatments were carried on a clear 96-well plate. A media only negative control was included on each plate.

Media was warmed in a 37°C water bath and 100 µl of cells was added into 96-well plates for each treatment concentration. The media was then removed from the cell plate and 100 µl of compound/medium mixture was dispended into each well in triplicate for each treatment concentration. The plates were then incubated for a defined time in a 37°C humidified incubator with 5% CO_2.

2.8.4 Cell counting

The traditional cell counting method uses a haemocytometer, which is a thick, glass microscope slide with an indented chamber of precise dimensions. This allows a defined volume of cell suspension to be deposited in the chamber, where the cells can be counted.

Briefly, a suspension of cells was prepared approximately 1×10^6 cells/ml ensuring that the sample was thoroughly mixed. A mixture of the cell suspension and 0.4% trypan blue solution was prepared.

10 ml cell suspension was added to the edge of the haemocytometer chamber between the cover slip and the V-shaped groove in the chamber allowing the cell suspension to be drawn into the chamber by capillary action.

The counting chamber of a haemocytometer is delineated by grid lines that identify the chamber areas to be used in cell counting. It has a depth of 0.1 mm and the four corner regions are typically used for cell counting.

The number of cells – both viable (unstained) and nonviable (stained) was counted in each of the four corner quadrants and the average of these four readings was taken and multiplied by 10^4 to obtain the number of cells per ml in the sample applied to the haemocytometer.

The number was multiplied by two to take into account the 1:1 dilution of the sample in the trypan blue and multiplied by any dilutions in the original sample preparation of the cell suspension. The number of viable cells was calculated according to this formula:

$$\% \text{ Viable cells} = \frac{\text{Number of viable cells}}{\text{Total number of cells}}$$

2.9 Lactate Dehydrogenase Assay

Lactate dehydrogenase (LDH) is an oxidoreductase enzyme that catalyses the interconversion of pyruvate into lactate. The assay works on the premises that when cells are damaged or compromised, they release LDH into the bloodstream after the damage. Thanks to its enzymatic stability, LDH has frequently been used to evaluate the presence of damage to tissue and cells. Once released into the supernatant, LDH reduces NAD^+ to NADH by oxidation of lactate to pyruvate. Subsequently, the H^+ produced during the reduction of NAD^+ are transferred to the tetrazolium salt provided by the Cytotoxicity Detection kit to form the red formazan. Finally, the intensity of the red formazan is proportional to the amount of LDH release by the cells into the supernatant (Figure 2.12) (Decker et al., 1988). LDH is also elevated in certain pathological conditions.

H9C2 and AC16 cells were plated in 96-well cell culture plates at 10.000 cells/well and cultured as described (Section 2.8.3). Cells were than treated with different concentrations of TMAO, as described (Section 2.8.3).

Following this, the supernatant was collected and the content of LDH released by the cells into the media was measured using a Cytotoxicity Detection Kit in accordance with the manufacturer's instructions to evaluate the total LDH released into the supernatant. 40 µL supernatant and 40 µL of LDH catalyst-dye solution were added to a clear 96 well plate and incubated at room temperature in the dark for 30 min. The absorbance was read at 490 nm using a VarioskanTM Flash multimode plate reader with SkanItTM software.

Simultaneously, the remaining cells in the plate were lysed in 100 µL of somatic cell ATP releasing agent. 8 µL of cell lysate was added to a clear 96 well plate and diluted 1:5 with fresh media and 40 µL of LDH catalyst-dye solution was added to the plate. The plate was incubated in the dark at room temperature for 30 min and the absorbance read at 490 nm using a VarioskanTM Flash multimode plate reader with SkanItTM software.

The LDH retained within the cells was determined by the following formula:

Retained LDH = LDH in lysate / (LDH in lysate + LDH in supernatant)

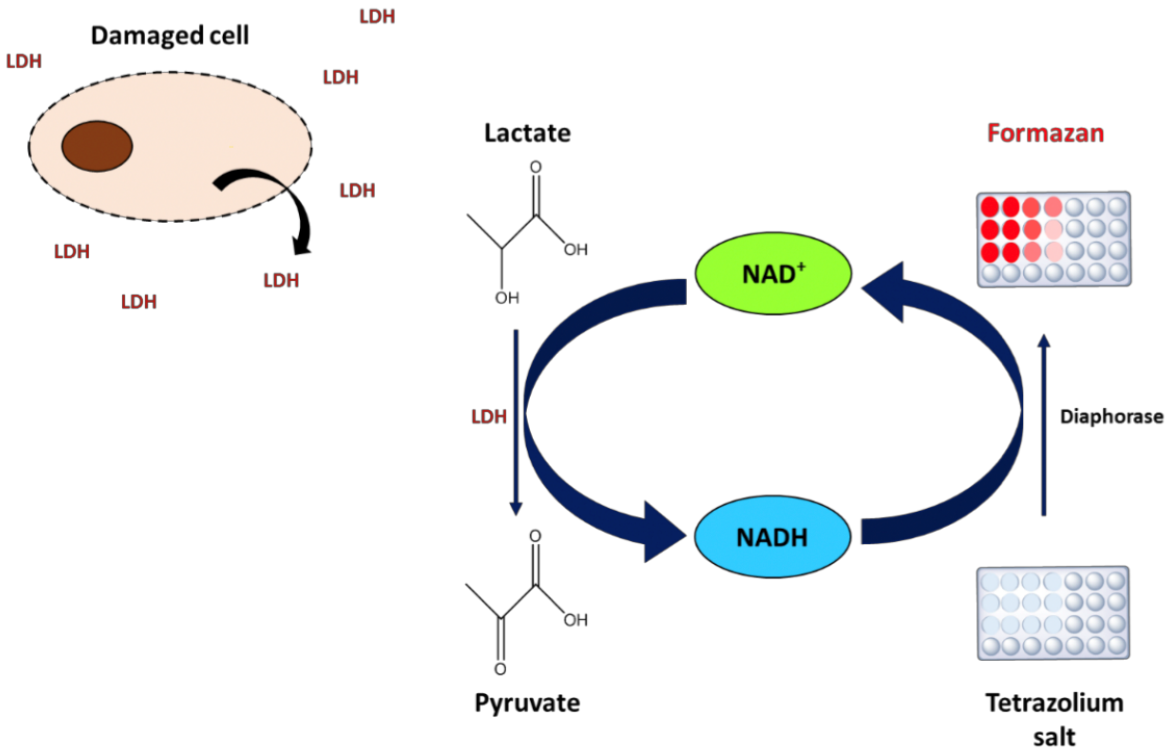

Figure 2.12. Scheme illustrating the workflow of the LDH Assay. Damaged cells with a compromised cell membrane release copious amounts of the enzyme LDH into the media. LDH catalyses the conversion of lactate to pyruvate leading to the reduction of NAD^+ to NADH. In a second reaction, H^+ serve as fuel for the conversion of tetrazolium salt, producing the red formazan dye that is proportional to the amount of LDH to be evaluated. Created with BioRender.com.

Following completion of the LDH assay, media was removed from all wells and cells were lysed in somatic ATP releasing agent (20 µL). 10 µL of cell lysates were transferred to a clear 96-well plate and a standard bicinchonic acid (BCA) assay was conducted as described in section 2.11. Protein content per well was used to normalise LDH released and retained by the cells.

2.10 ATP Bioluminescent Assay

To evaluate the content of ATP produced by the cells in presence of different concentrations of TMAO, a bioluminescent assay was performed. The ATP assay takes advantage of a particular reaction that requires ATP in order to work thus allowing to evaluate ATP content by analysis of light emitted at the end of the reaction. Luciferin, a photo-producing protein, and its oxidative specific enzyme, luciferase, are provided by

the assay kit. As mentioned before, in the presence of ATP and magnesium, luciferase oxidates luciferin to oxyluciferase and light is emitted (figure 2.12) (Chollet, 2012).
ATP content was assessed by the addition 10 µL of cell lysate and ATP standards to a white- walled 96-well plate. The ATP complete reaction solution was prepared according to the manufacturers guidelines by mixing ATP assay mix with ATP dilution buffer in a 1:25 ratio. 40 µL of the complete reaction solution was added to both the cell lysates and the standards and bioluminescence was measured (VarioskanTM, Thermo Scientific).

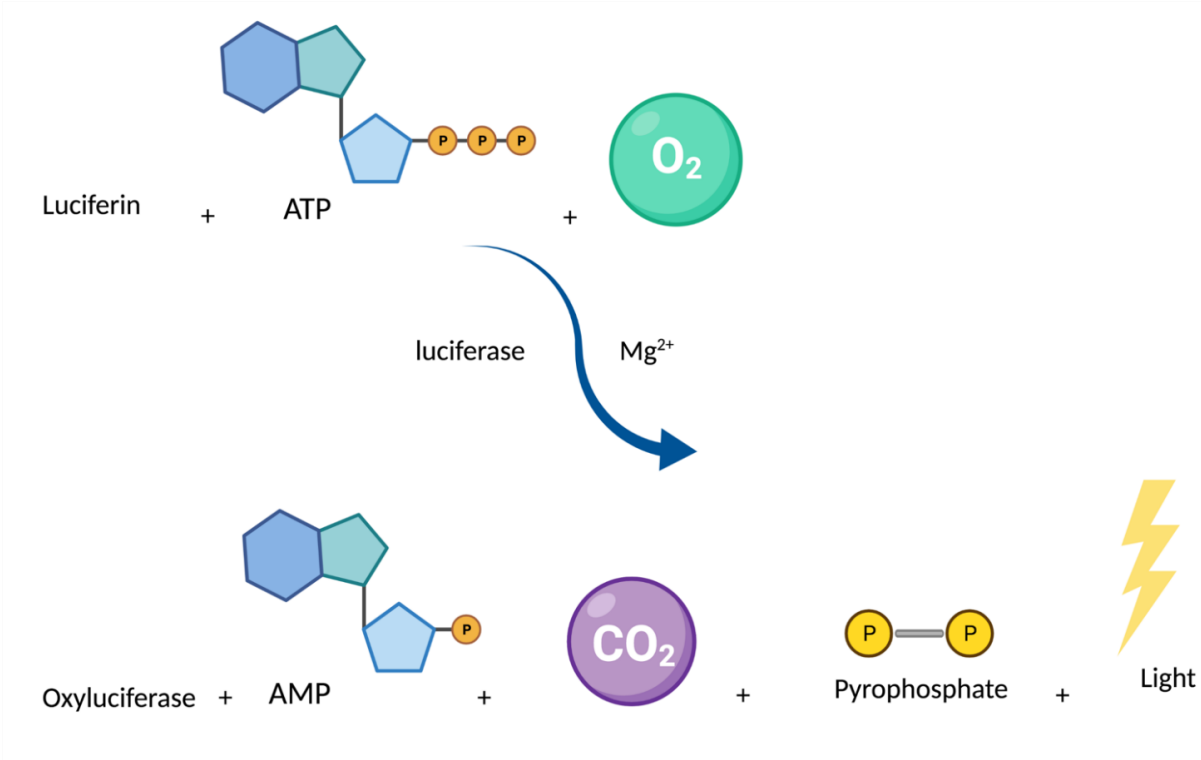

Figure 2.13. Chemical reactions undergone during the ATP bioluminescent assay. The luciferin supplemented by the assay gets converted by the enzyme luciferase to oxyluciferin. To work, this reaction requires ATP that gets converted into AMP and pyrophosphate and generates light. The light emitted during this reaction is directly proportional to the amount of ATP present in the cells. Created with BioRender.com.

Following completion of the ATP assay, media was removed from all wells and cells were lysed in somatic ATP releasing agent (20 µL). 10 µL of cell lysates were transferred to a clear 96-well plate and a standard BCA assay was conducted as described in section 2.11. Protein content per well was used to normalise ATP content.

2.11 Bicinchoninic acid protein quantification assay

In order to quantify the protein content of the cells, a BCA assay was used. The workflow of the assay includes two different step reactions, as shown in figure 2.13. In the first reaction, copper provided by the BCA assay gets chelated by proteins in an alkaline environment, forming a blue-coloured complex. In the second reaction, BCA reagent, a highly sensitive colorimetric detection reaction, react with the copper cation derived from the first reaction and produces a purple-coloured complex. The amount of the purple-coloured complex produced is directly proportional to the amount of proteins present in the sample evaluated (P. K. Smith et al., 1985).

Standards in the range of 0 – 1 mg/mL of BSA were added in duplicates to a 96-well plate and samples were diluted in the appropriate amount of diluent. The copper sulphate solution provided by the BCA assay was diluted 1:50 in the BCA solution and 200 µL of the working reagent was added to each well. The plate was incubated for 30 mins at 37 °C and the absorbance read at 562 nm using a VarioskanTM Flash multimode plate reader with SkanItTM software.

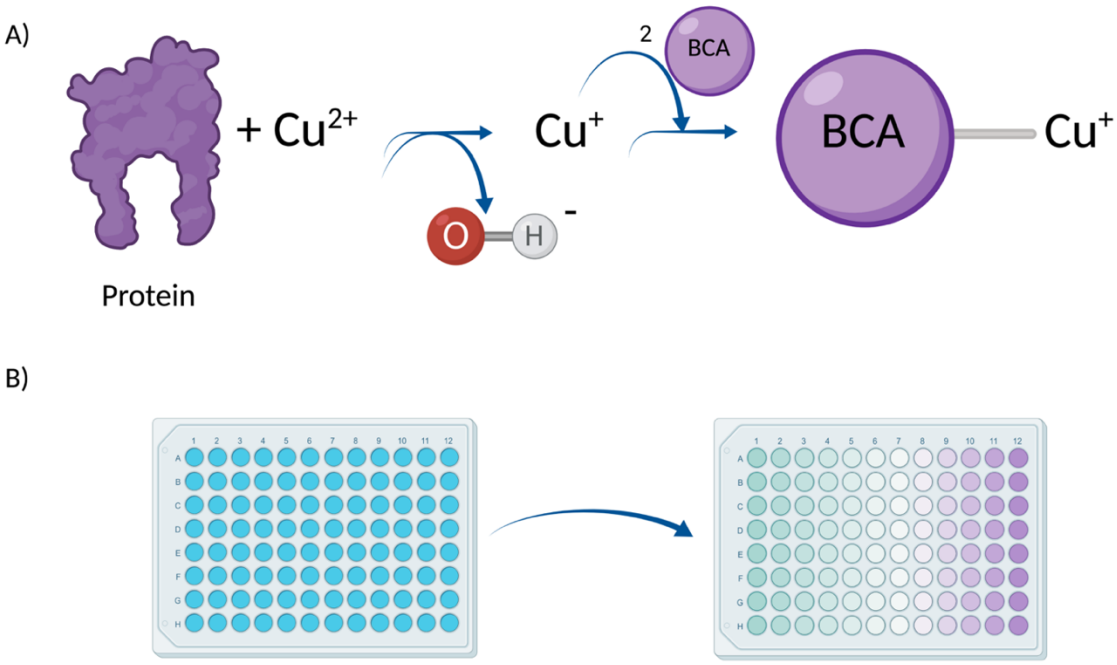

Figure 2.14. Illustration of the BCA assay used for protein quantification. Cu^{2+} is reduced by proteins in the cells and the free Cu^{+} than reacts with 2 molecules of BCA to form a complex visibly purple in colour (A). The purple complex produced this way by the cells is proportional to the amount of proteins within the sample (B). Created with BioRender.com

2.12 Seahorse XFe96 mitochondrial stress test

To evaluate respiratory function and possible alterations of normal bioenergetic pathways, one of the most widely used instruments is the extracellular flux analyser (Agilent Technologies). The Seahorse XFe96 analyser is capable of measuring simultaneously the oxygen consumption rate (OCR) and extracellular acidification rate (ECAR) as a mean to evaluate mitochondrial respiration and glycolysis respectively. Oxygen consumption by the cells (OCR) and proton excretion (ECAR) are responsible for rapid changes to the concentrations of oxygen and free protons inside each well that are measurable (Ferrick et al., 2008).

The XFe96 analyser is capable of measuring these changes by using a luminescent detector within the instrument (figure 2.15). Briefly, the 96-well cell culture microplates used are built with a sensor cartridge that supplies a sensor for each well. Each sensor has probes containing 2 separate polymer-embedded fluorophores that are sensitive to O_2 and H^{+} respectively.

During the experimental protocol, the sensor cartridge gets lowered inside the assay plate roughly 200 µm above the cell layer, thus creating a "transient microchamber" into which assessments can be made. In particular, inside the probe itself fibre optic bundles generate light that excites the fluorophores at the end of the probes. The light emitted from the fluorophores is proportional to the changes in O_2 and H^+ and is measured by a detector within the XFe96 instrument (figure 2.15) (Ferrick et al., 2008; Perry et al., 2011). After the measurements, the sensor cartridge is removed to allow the media to restore the cells to baseline (Koopman et al., 2016).

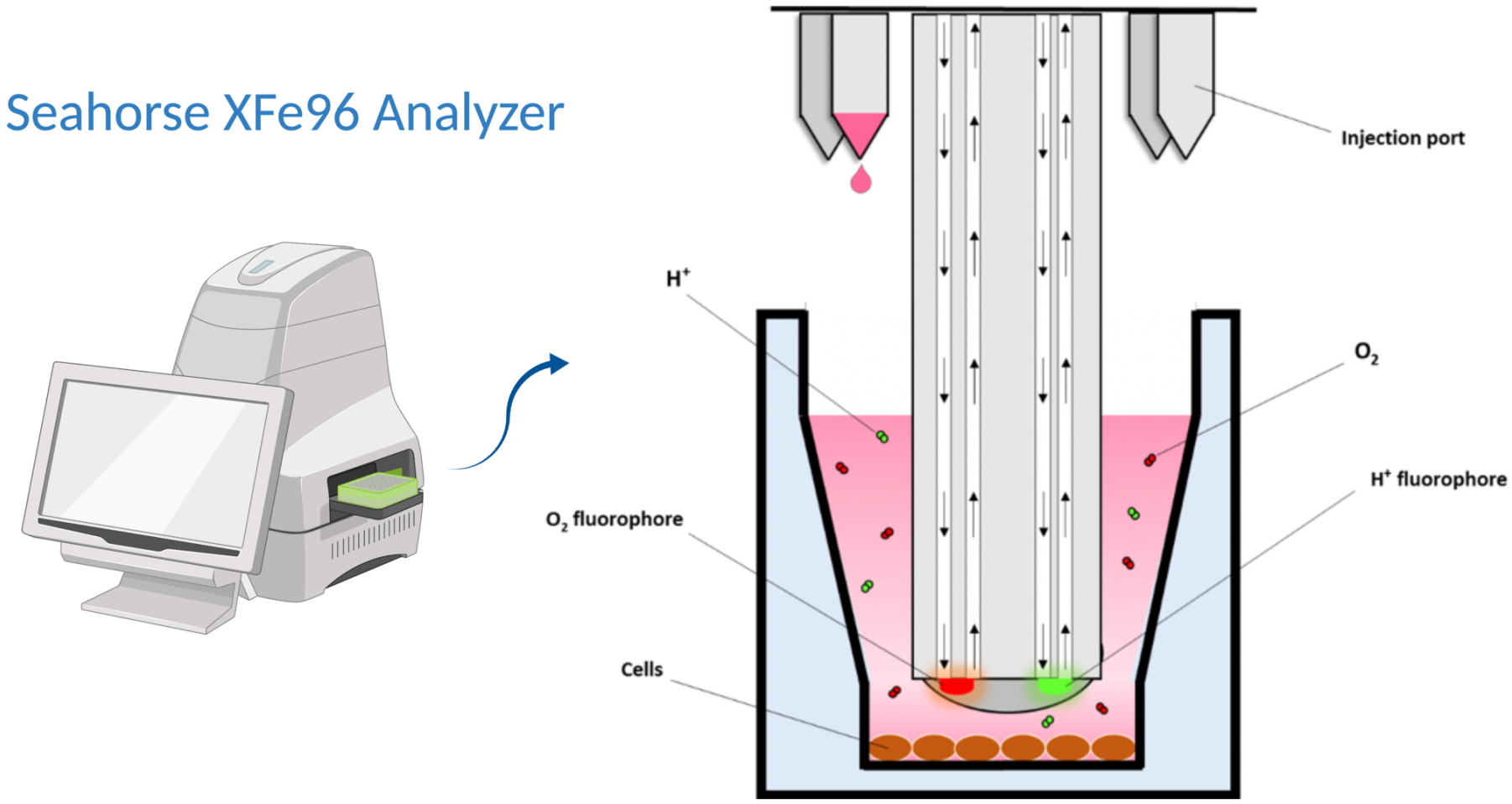

Figure 2.15. Scheme of the Seahorse XFe96 Analyzer and XFe sensor cartridge. Within each sensor probe present in the sensor cartridge of the assay plate provided by the Extracellular Flux Kit are 2 polymer-embedded fluorophores sensitive to O_2 and H^+. Inside the probe itself fibre optic bundles generate light that excites the fluorophores at the end of the probe, and a detector measures the emitted light thus collecting information about OXPHOS an glycolysis of the cells the probe is in contact with. Created with BioRender.com.

2.12.1 Assay workflow

Before the assay: Cells were seeded as described in section 2.8.3 in the Seahorse Bioscience 96-well plate. Background correction wells were left unseeded (A1, B4, C3 and D6) and only 100µl media was placed into these cells. The cells were incubated for 24h in a 37°C humidified incubator with 5% ($^{v}/_{v}$) CO_2. To hydrate the XFe96 sensor cartridge, 1 ml of Seahorse Bioscience Calibrant pH 7.4 media was added to each well of the utility 96-well plate. The sensor cartridge was placed back on top of the utility plate and stored at 37°C without CO_2 overnight.

Day of the assay: Before the start of the assay, culture media was removed and the cells were incubated at 37°C in 0% CO_2 in unbuffered Seahorse XFe base media (5mM or 25 mM glucose, according to the experimental conditions of the experiment, 1mM sodium pyruvate and 2mM l-glutamine) with the pH adjusted to 7.4. At the same time, different concentrations of TMAO were prepared in unbuffered Seahorse XFe base media with the pH adjusted to 7.4.

The XFe96 software and machine were switched on and the instrument stabilized to 37°C at least 2 hours before an experiment was run. An experimental template was designed for each experiment and the template loaded prior to running the experiment. Before the experiment itself, the XFe96 instrument had been programmed to mix the assay media in each well for 10 min to allow the oxygen partial pressure to equilibrate. Once the XFe96 sensor cartridge had reached right temperature, the assay was started, and the plate loaded into the machine in the correct orientation for calibration. At the end of the pre-programmed calibration procedure (30 min), the utility plate was replaced with the cell plate and the assay was started.

2.12.2 Mitochondrial Stress Test

The Mito Stress kit is derived from classical experiments to assess the physiological and pathophysiologic function of mitochondria, and to predict the ability of cells to respond to stress. In the assay, cells are treated with four compounds in succession, that each alters the bioenergetic profile of the cell. The first compound, Oligomycin, inhibits the

ATP synthase, providing an approximation on the coupling efficiency of the mitochondria. The second compound, uncoupling agent carbonyl cyanide p-[trifluoromethoxy]-phenyl-hydrazone (FCCP), introduces a high artificial proton conductance into the membrane, demonstrating the spare respiratory capacity of the mitochondria. The two final compounds, antimycin- and rotenone inhibit the electron transport chain and gives estimation of the non-mitochondrial respiration.

Compound preparation: The compounds and a 5ml aliquot of unbuffered media were stored at 37°C without CO_2 until loading of the sensor cartridge. The Mito Stress test compounds were made in the Seahorse media. The final optimised concentrations of the stress test compounds were oligomycin (1 µM), FCCP (0.25 µM), rotenone (1 µM) and antimycin-A (1µM).

Loading the XF Sensor cartridge with compounds: The Mito stress compounds and XF sensor cartridge were removed from the 37°C (without CO_2) incubator. 25 µL of the stress test compounds were added to the corresponding port on the sensor cartridge (figure 2.16) using a multi-channel pipette. The XF sensor cartridge was placed back in the 37°C incubator for 10 minutes prior to running the plate, to allow the plate to equilibrate to temperature.

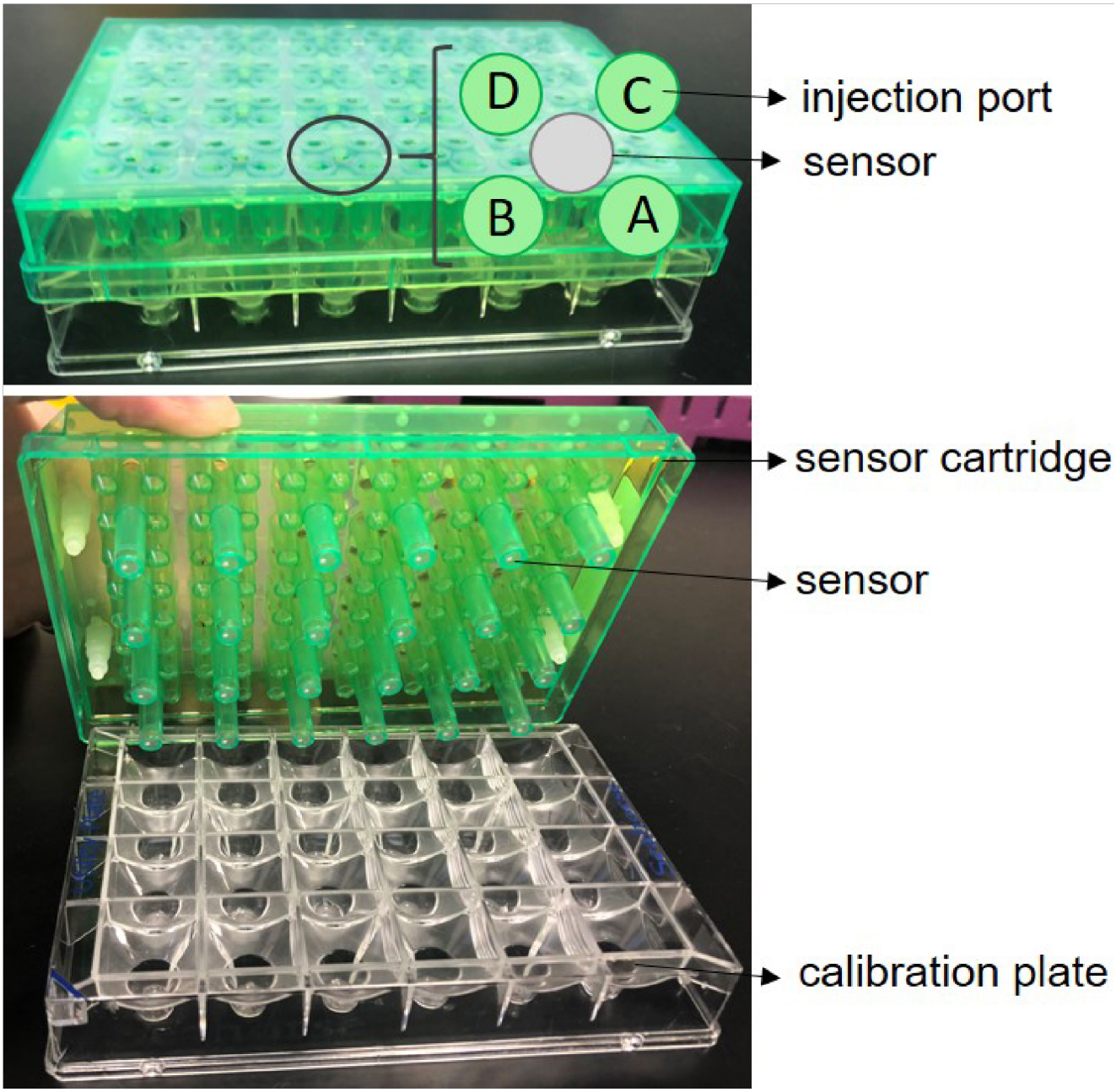

Figure 2.16. Image of the plate and sensor cartridge provided in the Extracellular Flux Assay Kit. 25 µl of stress test compounds can be loaded in the ports A-D. In these experiments TMAO was loaded into port A, oligomycin was loaded into port B, FCCP into port C and antimycin-A and rotenone into port D. Once loaded with the stress compounds, the cartridge gets moved from the calibration plate to the assay plate with the sensors facing the cells inside the wells. In this way the assay plate and the sensor cartridge can be inserted into the Seahorse XFe96 Analyzer.

2.12.2.1 Analysis of mitochondrial function

The mitochondrial stress test was used to dissect processes that were contributing to overall mitochondrial oxygen consumption. This technique uses selected mitochondrial inhibitors which allow for determination of six main parameters that describe key aspects of mitochondrial function in a cellular context: basal OCR, ATP- linked OCR, proton leak OCR, maximal OCR, reserve capacity, and non-mitochondrial OCR. These parameters were determined by measuring OCR after the sequential injection of oligomycin (to inhibit the ATP synthase), FCCP (introduces a high artificial conductance into the mitochondrial inner membrane, allowing for maximum electron flux through the ETC and uncoupling electron flow from OXPHOS), and antimycin-A (to inhibit complex III) and rotenone (to inhibit complex I) at the indicated time points.

Following completion of the XF stress test assay, media was removed from all wells and cells were lysed in somatic ATP releasing agent (20 µL). 10 µL of cell lysates were transferred to a clear 96-well plate and a standard BCA assay was conducted as described in section 2.11. Protein content per well was used to normalise ECAR and OCR values. Normalised data obtained combining XF stress test and BCA assay results, was analysed using the Seahorse XF Mito Stress Test Generator from Agilent. Normalised OCR values were used to calculate non-mitochondrial respiration (NMR = minimum rate measurement after rotenone/antimycin A injection, basal respiration (BR = last measurement before oligomycin injection – NMR), proton leak (PL = minimum measurement after oligomycin injection – NMR), ATP-linked respiration (ALR = BR – PL), maximum respiration (MR = maximum measurement after FCCP injection – NMR) and spare respiratory capacity (SRC = MR – BR).

2.13 Statistical analyses

Electrophysiology data was collected using Clampex 10.3 and analysed using Clampfit 10.3 (Axon Instruments) software. All data are presented as mean and standard error of the mean (SEM) or standard deviation (SD) as appropriate. Statistical analyses were performed using Graphpad Prism® 9 software (GraphPad Software, Inc., La Jolla, CA,

USA). Statistical significance of the data was assessed by paired student's t-test, unpaired t-test, one-way Analysis of Variance (ANOVA) and two-way ANOVA (with Dunnett's multiple comparison test). A P-value of < 0.05 was considered significant.

Chapter 3

Acute effects of TMAO on cardiac cell function and modulation of cardiac electrical parameters

3 Acute effects of TMAO on cardiac cell function and modulation of cardiac electrical parameters

3.1 Introduction

There is increasing evidence in the literature that the concentration of TMAO in the blood stream has a detrimental effect on myocardial function. This could mean development of heart failure, or contractile dysfunction. However, to date there has been no definitive investigation of the acute effects of TMAO on cardiac cells. This study aims to investigate whether TMAO has a directly cardiotoxic effect on cardiac cells. In order to investigate this, a number of different experimental approaches were taken, including electrophysiological recordings, calcium fluorescence imaging, contractile function measurements and Langendorff whole heart coronary ligation experiments. In this chapter, the acute effects of TMAO on freshly isolated cardiomyocytes will be studied.

3.2 Results

3.2.1 The effects of TMAO on freshly isolated rat cardiomyocytes contractile recovery and survival in a metabolic inhibition and reperfusion protocol (MI/R)

The effect of TMAO on contractile function of cardiomyocytes was investigated using a cellular model of metabolic inhibition and reperfusion (MI/R). The model, as previously described in section 2.4, uses cyanide and iodoacetic acid to block ATP synthesis in cardiomyocytes thus simulating ischaemia in the cells, and subsequently a washout phase to simulate reperfusion.

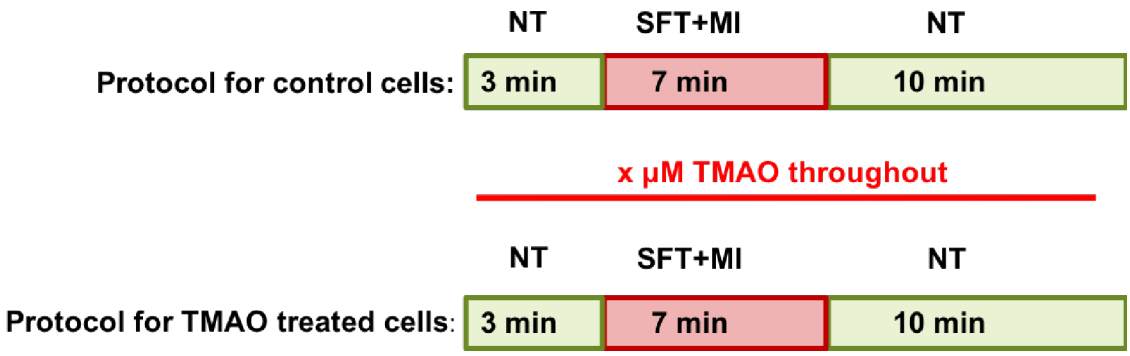

Figure 3.1. Schematic outlining the protocol for the (MI/R) experiment. Briefly, freshly isolated rat cardiomyocytes were perfused with NT solution for the first 3 minutes of the experiment. After which, the cells were exposed to a metabolic inhibition solution for the subsequent 7 minutes, during which contractions stop and the cell may enter a state of rigor. Finally, the cells were returned to NT solution for the final 10 minutes of the protocol, during which cells may regain the ability to contract on recovery from the metabolic inhibition. For TMAO experiments, the test concentration of TMAO was present throughout the experiment, affecting both the normal perfusion with NT and the metabolic inhibition stage.

The timeline of the MI/R protocol is shown in Figure 3.1. Freshly isolated cardiomyocytes were seeded onto the microscope for at least 10 min to allow the cells to adhere to the surface to avoid being washed out by perfusion. The cells are perfused with NT solution for the first 3 min of the experiment, in which rod-shaped cardiomyocytes normally contract in accordance with the 1 Hz EFS. After 3 mins, the cells are exposed to 7 min of metabolic inhibition, during which ATP synthesis is blocked and the cells lose the ability to properly contract. Finally, the cells are exposed to 10 min of washout, during which a portion of cells can recover contractile activity. Figure 3.2 A shows a pictorial representation of a field of view at the start of the recording, at the end of the metabolic inhibition and finally at the end of the reperfusion phase. In order to investigate the effects of TMAO on cardiomyocytes using the MI/R protocol, control cells (not exposed to TMAO) and cells exposed to different concentrations of TMAO during throughout the entirety of the experiment were recorded. Figure 3.2 B show a concentration response profile for TMAO, showing a loss of contractile recovery with increasing concentrations of TMAO. At the end of the experiment, cells were stained with trypan blue, a cellular dye used to selectively colour dead cells in blue. Figure 3.2 C shows that different concentrations of TMAO do not change the percentage of cells that survive the

experiment compared to the control, even at the same concentrations that caused loss of contractile recovery.

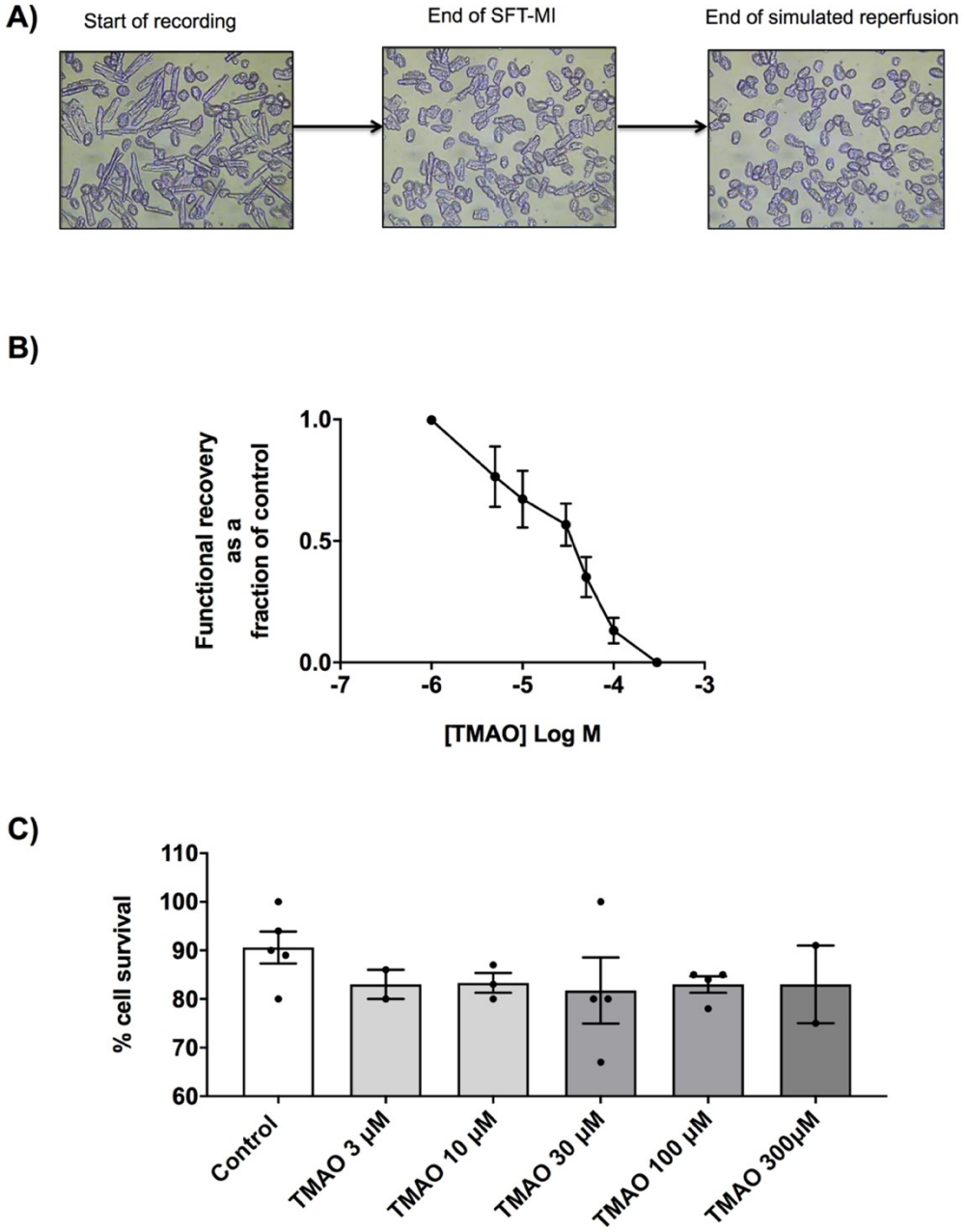

Figure 3.2. Effects of different concentrations of TMAO on functional recovery in cardiomyocytes. **A:** Pictures showing cardiomyocytes at different stages of the experiment; at the start of the recording the cells have the distinctive rod-shape typical of the cardiomyocytes. After MI perfusion, cells go into rigor due to lack of ATP and finally, at the end of the protocol, part of the cells are able to recover contractile function following the reintroduction of metabolic substrates. **B:** Concentration-response curve showing the functional recovery of the cells as a fraction of control following combined exposure to MI and different concentrations of TMAO. As shown in the figure, TMAO affects functional recovery of the cells in a concentration-dependant manner (n. 111 experiments from 23 animals). **C:** Bar chart showing the survival rate of the cells expressed as percentage of surviving cells (repeated-measures ANOVA; n. 20 experiments from 5 animals).

For each experiment, the times to contractile failure, time to rigor, time to contracture, time to hypercontracture and time to contractile recovery were recorded. The time to contractile failure indicates the time at which each cell has significantly reduced its ATP levels and as a result the K_{ATP} channel has opened. This causes shortening of action potential in the cells until complete action potential failure, visible in this experiment as contractile failure. Figure 3.3. A compares the time to contractile failure of cells exposed to different concentrations of TMAO to control cells. The time to rigor indicates the time of near complete ATP depletion inside the cell. As the cell can no longer sustain contraction and the actin and myosin crossbridges are broken down, it shortens into rigor. Figure 3.3. B compares the time to rigor of cells exposed to different concentrations of TMAO to control cells. The time to hypercontracture indicates the point at which the cells were reperfused with NT solution and was thus used as marker of precision of the experimental timings.

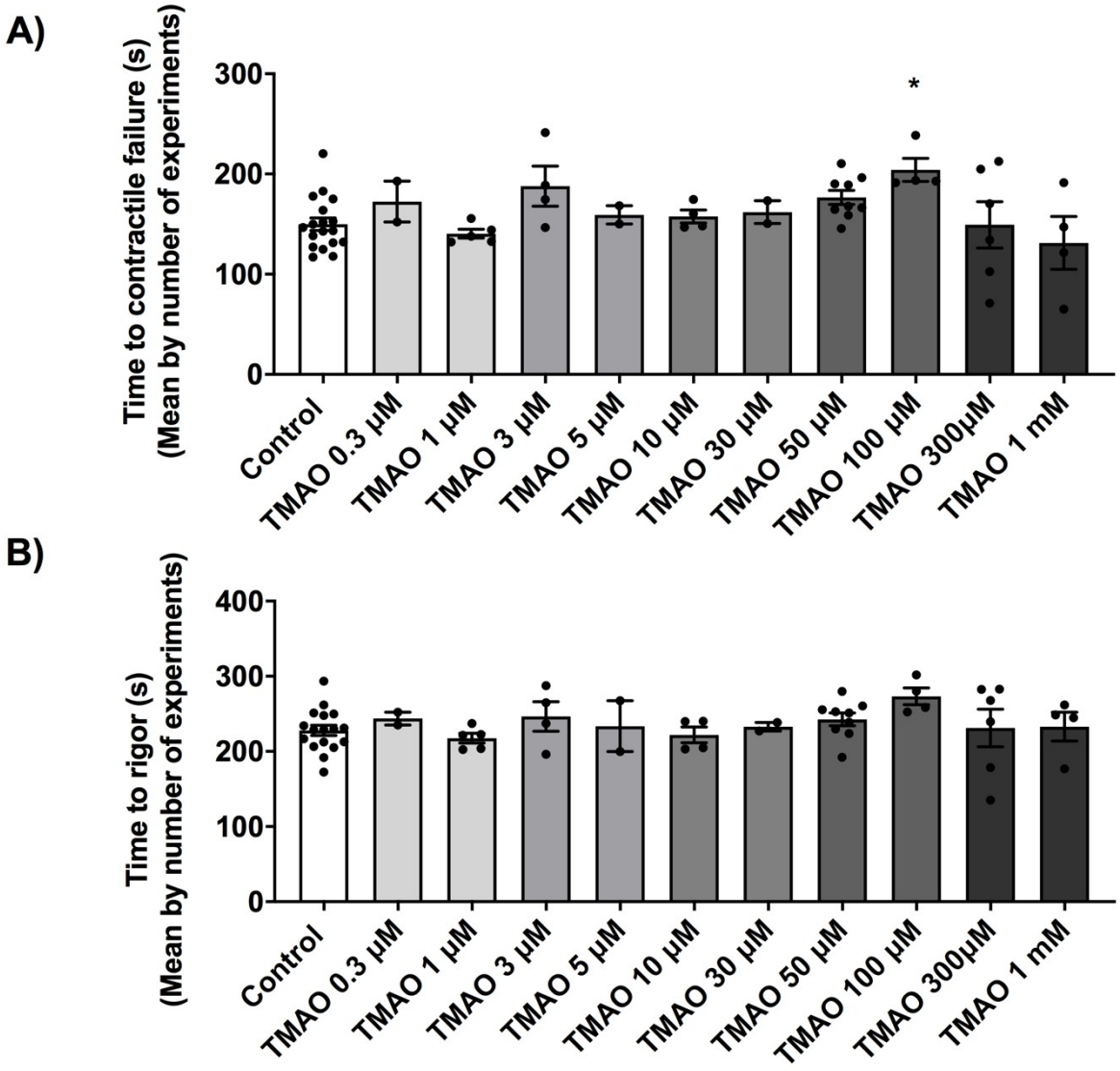

Figure 3.3. Effects of different concentrations of TMAO on cell functional recovery in cardiomyocytes. **A:** Bar chart comparing the time to contractile failure in control cells and in cells exposed to different concentrations of TMAO. **B:** Bar chart showing the time to rigor in control cells and in cells exposed to TMAO (* $P < 0.05$; repeated-measures ANOVA with Dunnett's post-test; n. 91 experiments from 18 animals).

Finally, the time to contractile recovery indicates the time at which the cell regains the ability to undergo normal calcium cycling, recovering its ability to contract. Figure 3.4 B compares the time to contractile recovery of cells exposed to different concentrations of TMAO to control cells. In a parallel to what happened with the percentage of cells recovering contractile function (Figure 3.4 A), the time to contractile recovery of cells gets delayed with increasing concentration of TMAO (30 to 100µM) and gets to the point of non-recovery at the highest concentrations (300 µM and 1 mM).

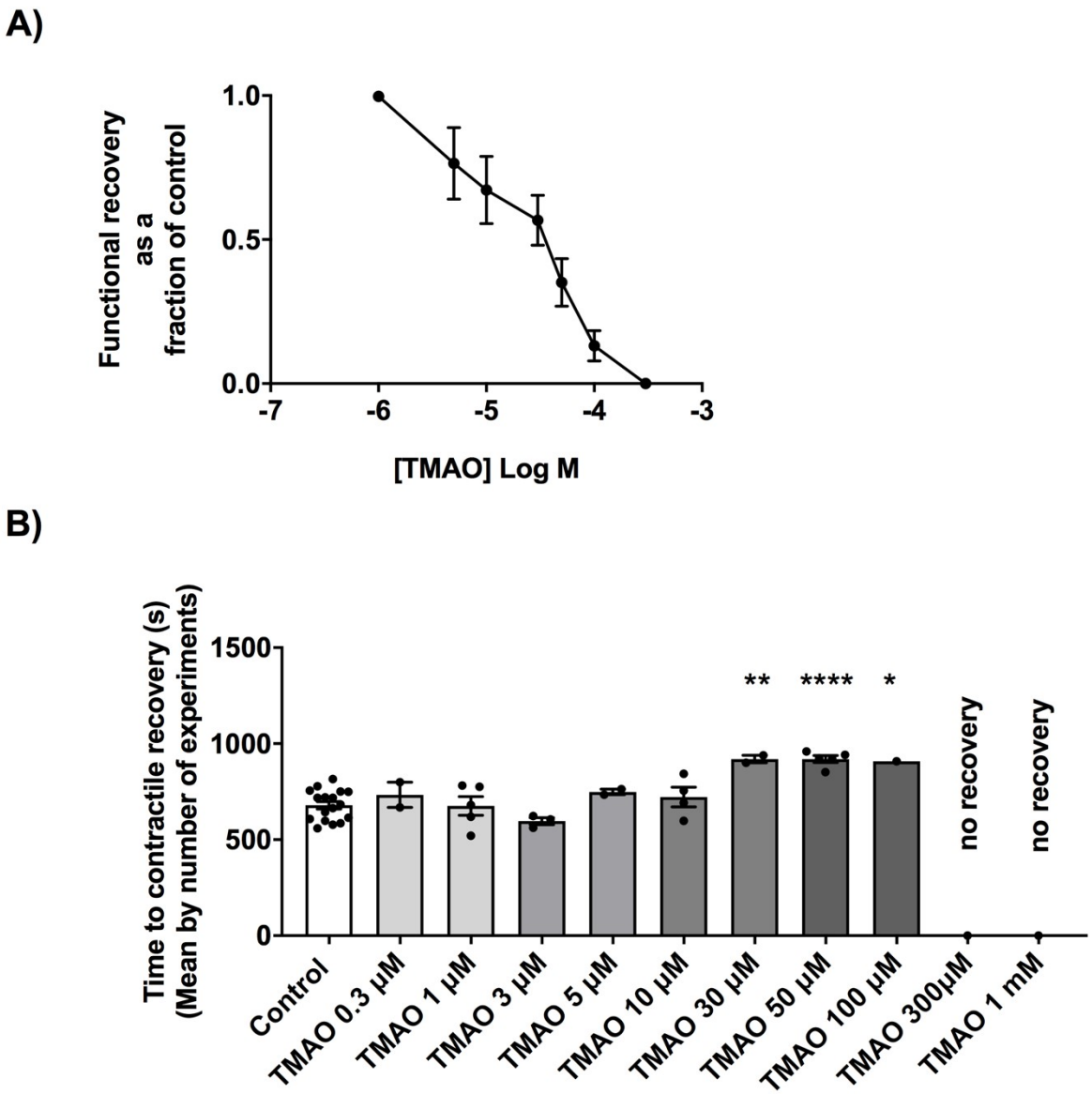

Figure 3.4. Effects of different concentrations of TMAO on cell functional recovery in cardiomyocytes. **A:** Reiteration of concentration-response curve showing the functional recovery of the cells as a fraction of control following combined exposure to MI and different concentrations of TMAO shown in Figure 3.2. High concentrations of TMAO result in cells not recovering their cell function after exposure to metabolic inhibitors. **B:** Bar chart showing the time to contractile recovery in control cells and in cells exposed to TMAO. High concentrations of TMAO (30 to 100µM) significantly prolong the time taken by the cells to recover from contractile failure if they recover at all (* $P < 0.05$; **$P < 0.01$; **** $P < 0.0001$; repeated-measures ANOVA with Dunnett's post-test n. 91 experiments from 18 animals).

3.2.2 The effects of TMAO on calcium transients in freshly isolated rat cardiomyocytes using calcium fluorescence imaging

Since the previous results suggest that TMAO is affecting cells ability to contract, the next step is to investigate the effects of TMAO on calcium homeostasis in cardiomyocytes. Since literature suggests that concentrations of TMAO that are found to be effective in cellular experiments range between 0.1 μM and 10mM (Jaworska et al., 2019; Savi et al., 2018; W. Zhu et al., 2016), with 10mM considered as an hyperphysiological concentration (Querio et al., 2019) and 100μM being the most used, and that previous experiments have found TMAO 100μM to be a suitable concentration (Figure 3.2 B), all experiments from here on are performed using TMAO 100μM unless stated otherwise.

As described in section 2.6, Fura-2-AM, a ratiometric Ca^{2+} binding dye that excited at 340-380 nm and emits at 520 nm, was used. In this experiment, cardiomyocytes were perfused with NT for 3 min, followed by 5 min treatment with TMAO 100μM. 1 Hz field stimulation was used to trigger the firing of action potential throughout each experiment, in order to investigate calcium transients.

Figure 3.5 A shows mean traces of Ca^{2+} transients triggered by 1Hz field stimulation in NT and TMAO 100μM of the duration of 1s. In the figure, TMAO 100μM caused an increase in the size of the calcium transients. To quantify the increase in the size of the calcium transients, two different parameters were used. First, the difference in size from peak to baseline of each calcium transients was analysed. In figure 3.5 B, ~~that~~ the presence of TMAO considerably affected the dimension of the peak reached during the transient. As a second parameter, the area under the curve for each transient was measured. Figure 3.5 C show the transient amplitude, measured as the percentage area under the curve in presence of 100μM of TMAO compared to control conditions. TMAO caused and increase in the AUC of the Ca^{2+} transients.

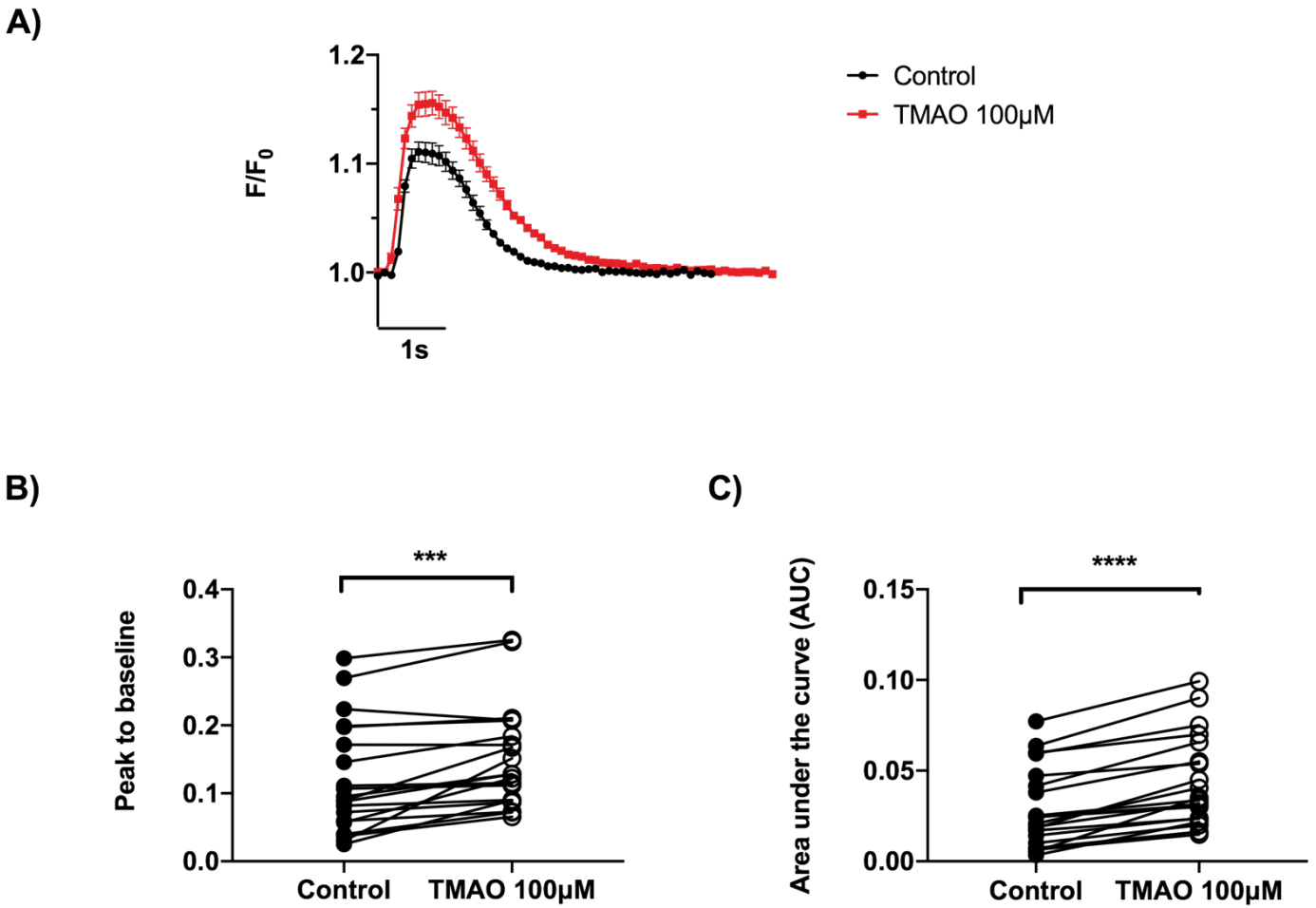

Figure 3.5. Effects of 100µM TMAO on calcium transients amplitude. **A:** Example mean traces showing the Ca^{2+} transients triggered by 1Hz field stimulation in NT and 100µM of TMAO. Side-by-side comparison of TMAO treatment showed a prolonged Ca^{2+} transient compared with control conditions. **B:** Bar chart showing the variability in the peak of the Ca^{2+} transients. The presence of TMAO considerably effected the dimension of the peak reached during the transient. **C:** Bar chart showing the transient amplitude, measured as the percentage area under the curve in presence of 100µM of TMAO compared to control conditions. TMAO increased the AUC of the Ca^{2+} transients (***P < 0.001; **** P < 0.0001; paired t-test; n. 20 cardiomyocytes from 3 animals).

3.2.3 The effects of TMAO on cardiac action potential duration and resting membrane potential in freshly isolated rat cardiomyocytes

Alterations in the calcium cycling inside the cardiomyocytes usually can lead to alterations in the duration of the action potential. As previous data suggests that TMAO causes an increase of intracellular calcium, action potential duration is expected to be altered to reflect these changes.

To investigate this, action potentials from isolated cardiomyocytes were recorded using the whole-cell patch-clamp technique as described in section 2.5.6. Action potentials were stimulated at a rate of 1 Hz until a steady- state was reached and recorded continuously for 3-6 minutes prior to perfusion with TMAO 100µM. APD_{90} and RMP for each condition was measured, calculated and analysed as described in section 2.5.6.1. Figure 3.6 A shows an example trace of cardiac action potential in control cells and in cells exposed to 100µM TMAO, recorded as previously described.

Figure 3.6 B shows a time-course plot of APD_{90}. TMAO was added after ~3min after the start of the recording ad was washed out after ~10min.

Figure 3.6 C shows the RMP of control cells and TMAO treated cells. TMAO caused no significant changes to the RMP of cells.

Figure 3.6 D shows the APD_{30} in control cells and in cells exposed to 100µM TMAO. Acute exposure to 100µM TMAO caused a prolonging of action potential but only while the cells remained exposed to it and Figure 3.6 E shows the APD_{50} in control cells and in cells exposed to 100µM TMAO confirmed and reinforced this effect on APD modulated by TMAO. Interestingly, figure 3.6 D shows the APD_{90} in control cells and in cells exposed to 100µM TMAO and in this case acute exposure to 100µM TMAO caused a shortening of action potential, while the cells remained exposed to the metabolite, suggesting that TMAO was very likely modulating different ion channels with distinct kinetics.

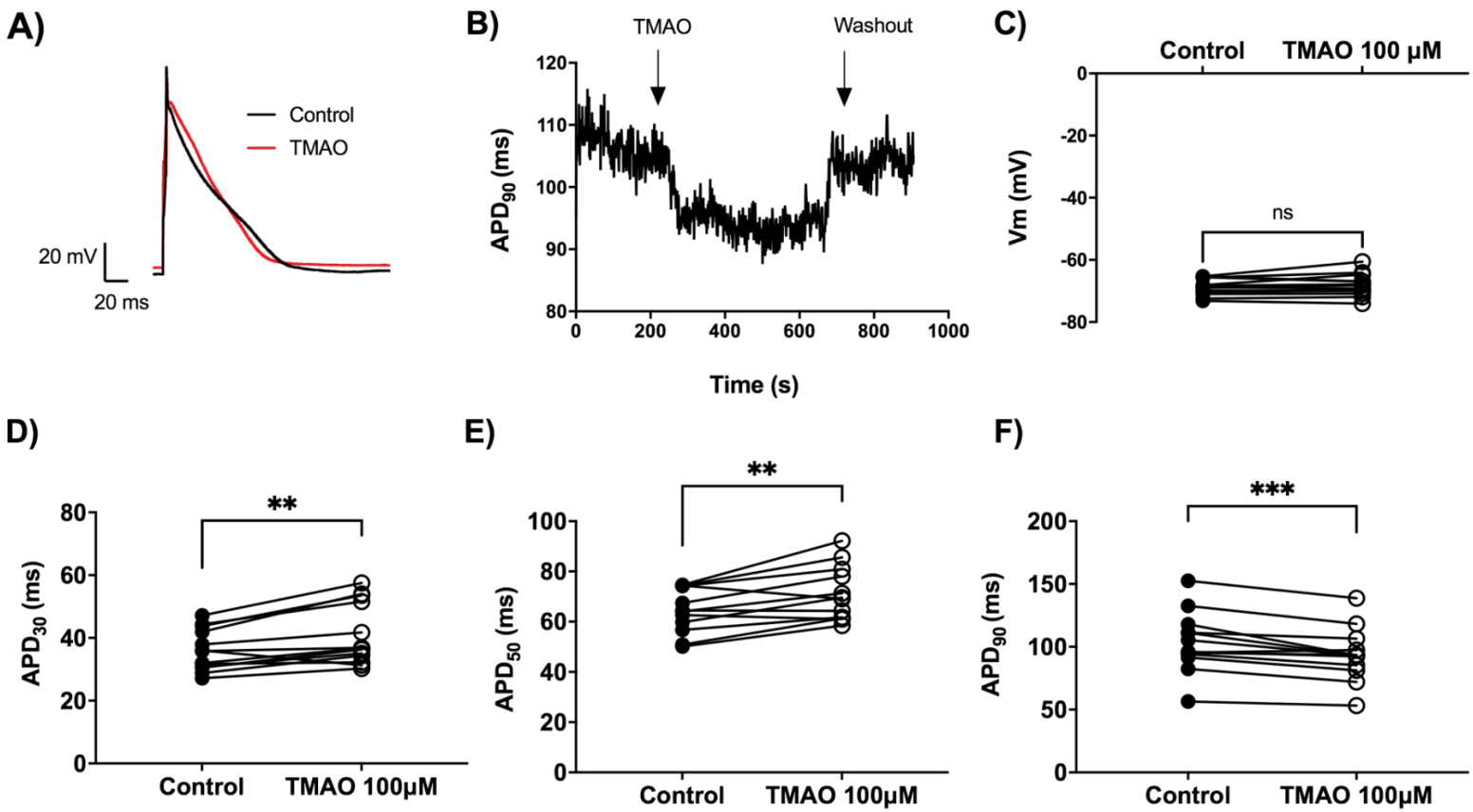

Figure 3.6. Effects of 100µM TMAO on membrane potential and action potential duration in cardiomyocytes. **A:** Example traces of cardiac action potential in control cells and in cells exposed to 100µM TMAO. **B:** Time-course plot of action potential to 90% repolarised (APD_{90}). TMAO was added after ~3min after the start of the recording ad was washed out after ~10min. **C:** Bar chart showing the resting membrane potential (RMP) of control cells and TMAO treated cells. TMAO caused no significant changes to the RMP of cells. **D**: Bar chart showing the duration of action potential at 30% repolarisation (APD_{90}) in control cells and in cells exposed to 100µM TMAO. **E:** Bar chart showing the duration of action potential at 90% repolarisation (APD_{90}) in control cells and in cells exposed to 100µM TMAO. Acute exposure to 100µM TMAO caused a prolonging of action potential duration. **F:** Bar chart showing the duration of action potential at 90% repolarisation (APD_{90}) in control cells and in cells exposed to 100µM TMAO. Acute exposure to 100µM TMAO caused a shortening of action potential. (**P < 0.01; ***P < 0.001; paired t-test; n. 18 cardiomyocytes from 9 animals).

3.2.4 The effects of TMAO on the ionic currents underlying the cardiac action potential in freshly isolated rat cardiomyocytes

The cardiac action potential is the key event that regulates the activity of cardiomyocytes. In normal physiological conditions, the cardiac action potential occurs by finely regulated movements of the ions across the membrane of the cells.

Amongst the currents that regulate the cardiac action potential, the I_{K1} current is of key importance for maintaining the resting membrane potential and for the final stages of repolarization. In order to fire an action potential, a cardiomyocyte needs to be depolarized above the action potential threshold. Following an excitation trigger, $Na_V1.5$ are opened, allowing the passage of Na^+ ions inside cell. This movement results in the upward stroke of the action potential. After, the membrane potential stabilizes itself in a plateau phase in which inward depolarizing currents are balanced by outward repolarizing currents. The main responsible for the depolarizing current is the influx of Ca^{2+} ions. The repolarizing phase constitutes in an increase in K^+ conductance and the K^+ currents are carried out by three different components, distinguished by their different kinetics.

As described in section 2.5.6.2, to investigate the effect of TMAO on the currents underlying the cardiac action potential a multi-step protocol was used in whole-cell configuration in voltage-clamp mode.

The separation and analysis of the ionic currents is possible because the currents have different kinetics, therefore is possible to measure them at a suitable time during a voltage clamp pulse. The protocol constitutes of 4 sequential steps: a first step elicited by voltage commands from -100 to -70mV in 5mV steps during 10ms, in which I_{K1} current can be measured, a second step elicited by voltage commands from -70 to 40mV during 500ms, that allows isolation of the Na^+ spike, a third step from -40 to 50mV during 100ms, in which Ca^{2+} current can be measured and a final fourth step from -50 to -80mV in 10mV steps for 4000ms, in which I_{Ks} currents can be measured (Figure 3.7). Figure 3.7 shows the protocol used and a correspondent example trace in which are highlighted the sections analysed to obtain information on how TMAO can modulate the different currents of the action potential.

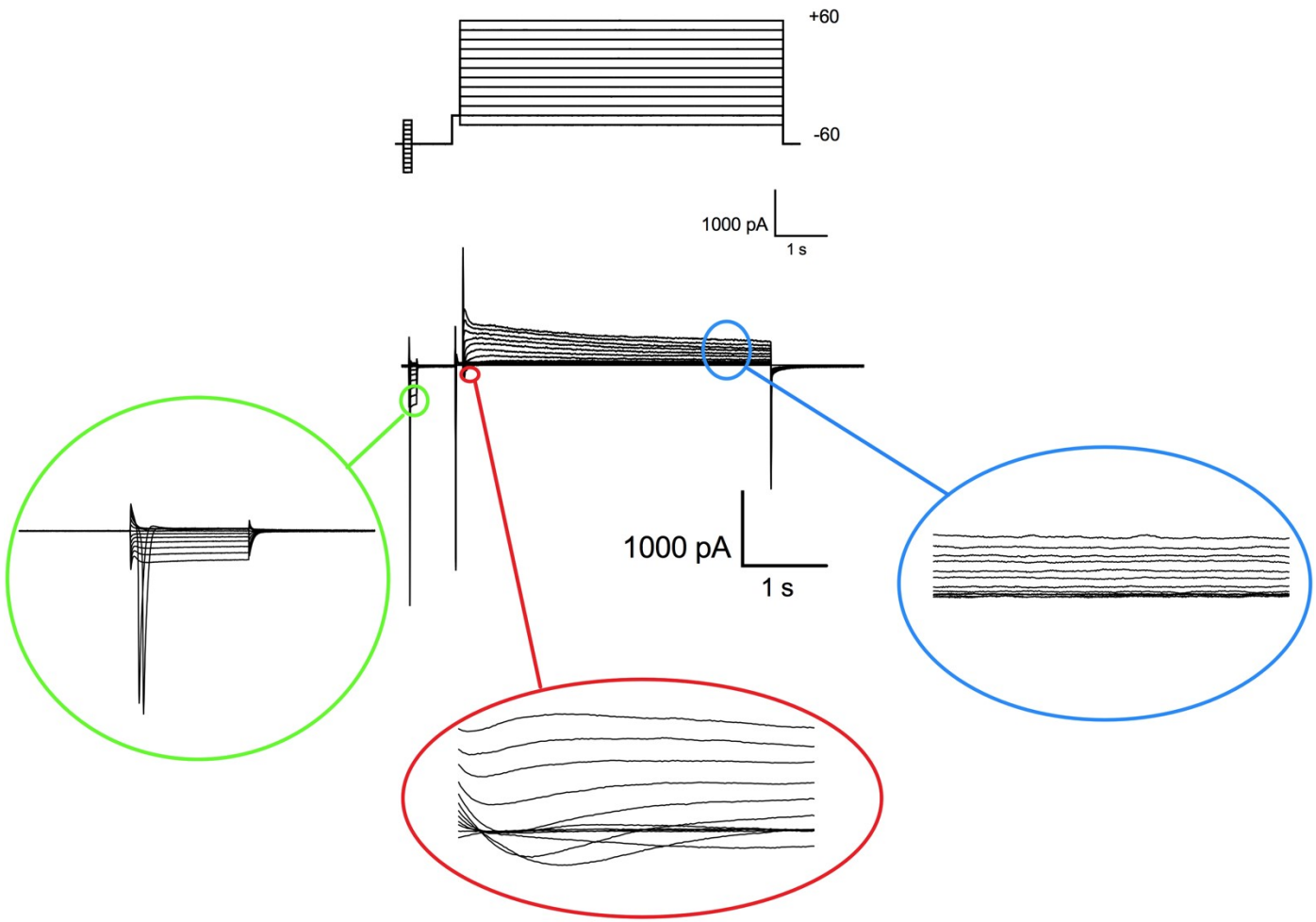

Figure 3.7 Example trace of a protocol that allows identification of changes in several different currents in a single patch clamp electrophysiology recording in whole cell configuration. To allow analysis of different ionic currents, namely IK1, Ca^{2+} and IKs current, a multi-step protocol was accurately designed. The protocol constitutes of 4 sequential steps: a first step elicited by voltage commands from -100 to -70mV in 5mV steps during 10ms to measure IK_1, a second step elicited by voltage commands from -70 to -40mV with a duration of 50ms to inactivate I_{Na}, a third step elicited by voltage commands from -40 to 50mV with a duration of 4000ms and a final fourth step back to the resting potential. In the image, portions from which following analysis will be shown are highlighted.

3.2.4.1 IK_1 current

K_{ir} channels are able to pass inward currents at potentials more negative than the equilibrium potential for K^+ (E_K) but as the membrane potential gets more positive, they progressively lose the ability to pass inward current and the current is minimal in the outward direction. The I_{K1} current is of crucial importance for maintaining the resting membrane potential and for the final stages of repolarization.

I_{K1} was measured by following the protocol exemplified in figure 3.8 A, in particular it was analysed in a first step elicited by voltage commands from -100 to -70mV in 5mV steps during 10ms, from the section enlarged in the image.

Figure 3.8 B shows a current-voltage (I-V) relationship comparing control, TMAO and washout I_{K1} current. Figure 3.8 C compares mean I_{K1} current in control and TMAO treated cells. TMAO caused no significant difference in I_{K1} current, as shown in both I-V plot and bar chart.

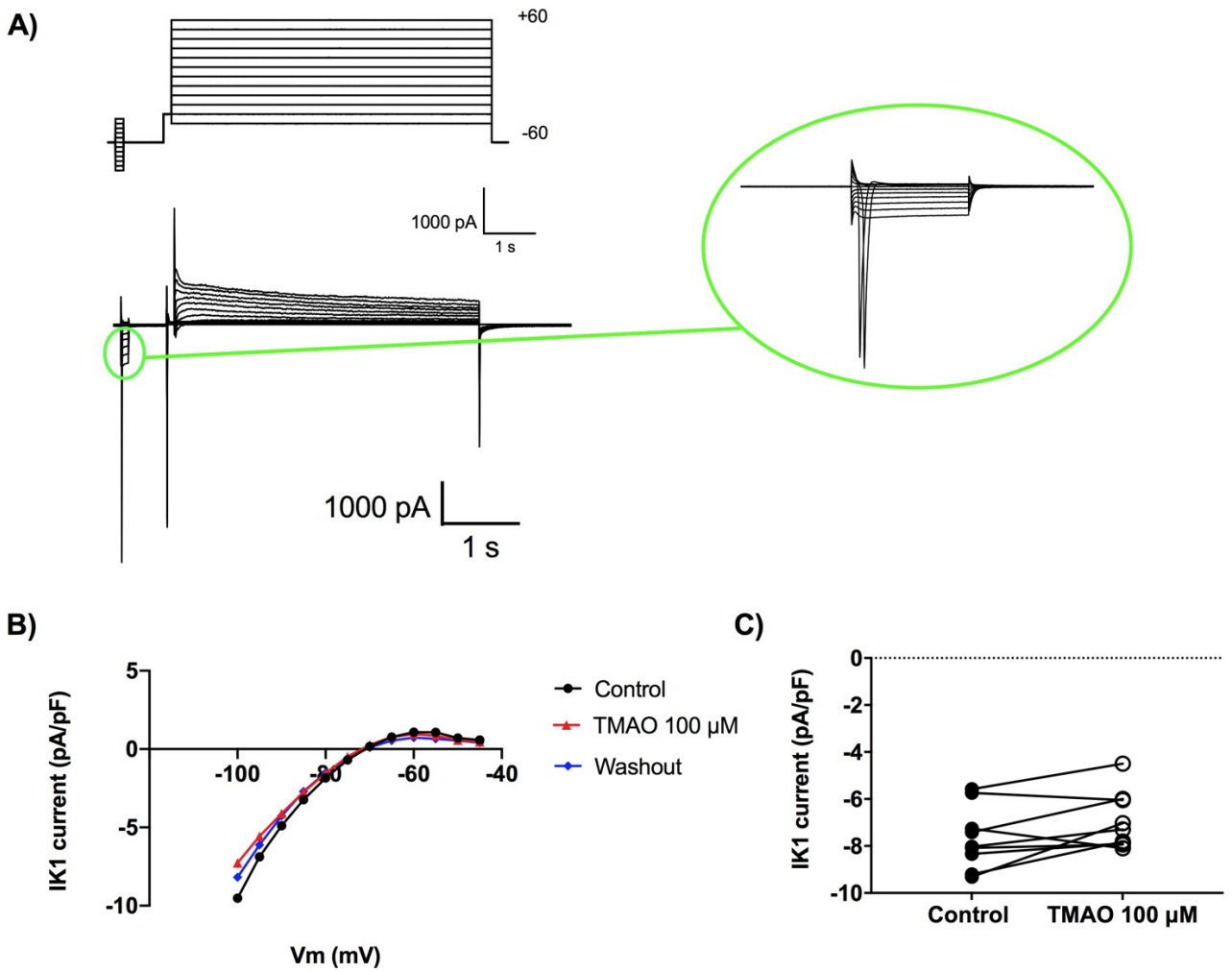

Figure 3.8. Effects of 100µM TMAO on IK1 current in cardiomyocytes exposed to TMAO during patch clamp electrophysiology whole cell configuration recording. **A:** Example trace of current for a single recording, made by following protocol shown in figure 3.7, showing the relevant area. **B:** Current-voltage relationship (I-V plot) comparing control, TMAO and washout IK1 current. **C:** Bar chart comparing mean IK1 current in control and TMAO treated cells. TMAO caused no significant difference in IK1 current, as shown in both I-V plot and bar chart (Paired t-test; n. 11 cardiomyocytes from 5 animals).

3.2.4.2 ICa^{2+} current

The membrane potential stabilizes itself in a plateau phase in which inward depolarizing currents are balanced by outward repolarizing currents, resulting in little changes in the membrane potential. The main responsible for the depolarizing current during the plateau phase of the action potential is the influx of Ca^{2+} ions through voltage gated Ca^{2+} channels.

Entrance of Ca^{2+} during the action potential plateau triggers Ca^{2+} release from the sarcoplasmic reticulum into the cytosol via activation of Ca^{2+}-release channels. Ca^{2+} influx through I_{CaL} is the regulatory point to maintain homeostasis of intracellular Ca^{2+}. ICa^{2+} was measured by following the protocol exemplified in figure 3.9 A, in particular it was analysed in a third step from -40 to -50mV during 100ms, from the section enlarged in the image.

Figure 3.9 B shows a current-voltage relationship (I-V plot) comparing control, TMAO and washout ICa^2 current. Figure 3.9 C compares mean ICa^2 current in control and TMAO treated cells. TMAO caused an increase in Ca^{2+} current, as shown in both I-V plot and bar chart, as well as a shift in the current, visible in the I-V plot.

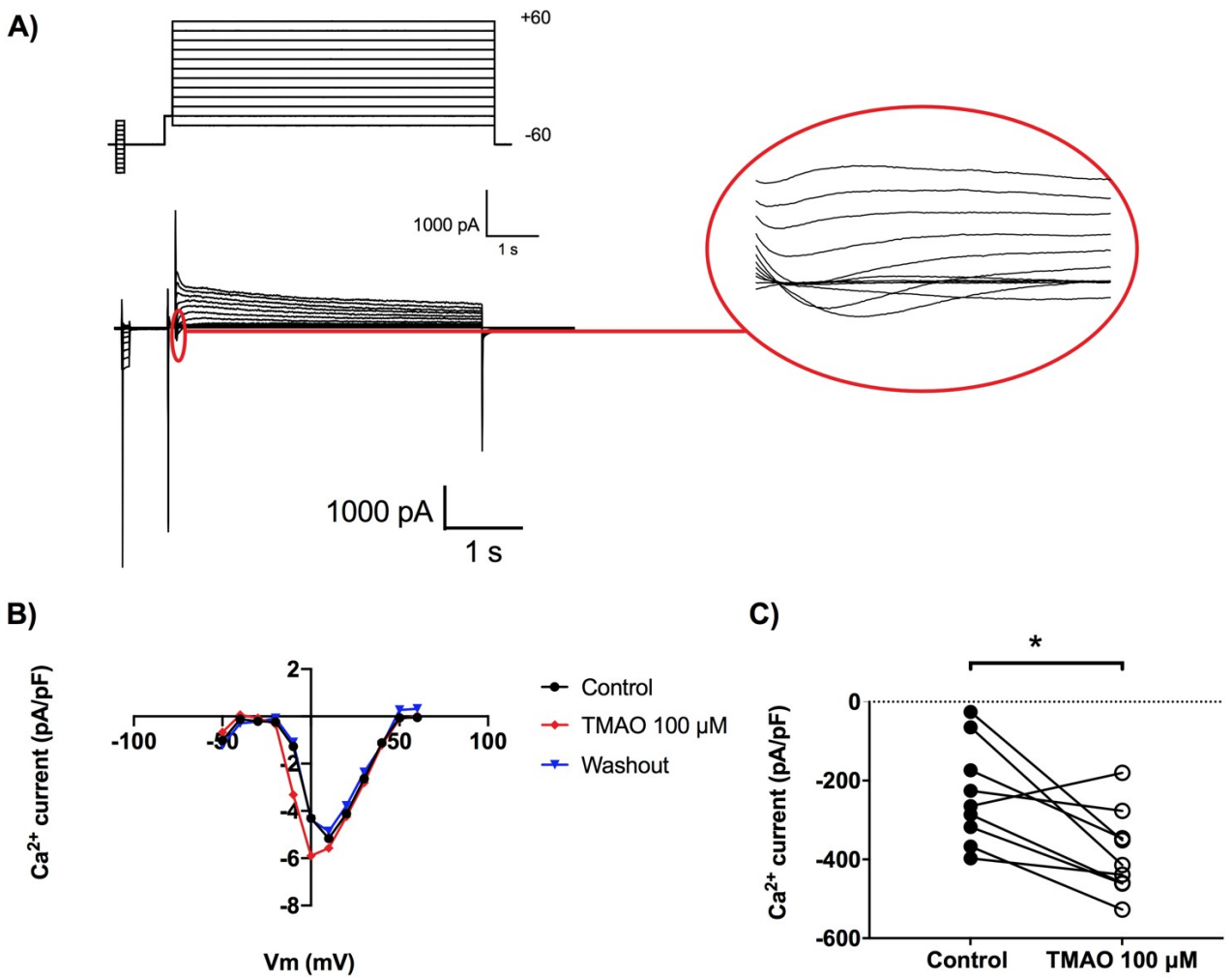

Figure 3.9. Effects of 100µM TMAO on Ca^{2+} current in cardiomyocytes exposed to TMAO. **A:** Example trace of current for a single recording, expanded from the protocol show in figure 3.7. **B:** Current-voltage relationship (I-V plot) comparing control, TMAO and washout Ca^{2+} current. **C:** Bar chartcomparing mean Ca^{2+} current in control and TMAO treated cells. TMAO caused an increase in Ca^{2+} current, as shown in both I-V plot and bar chart, as well as a shift in the current, visible in the I-V plot (*P < 0.05 paired t-test; n. 11 cardiomyocytes from 5 animals).

3.2.4.3 IKs current

The repolarizing phase constitutes in an increase in K^+ conductance and the K^+ currents are carried out by three different components, distinguished by their different kinetics. I_{Ks} is a current that activates extremely slowly when membrane depolarizes to potentials greater than -30 mV and reaches half-maximum activation close to +20 mV. I_{KS} has a very slow activation and deactivation kinetics to the point where it barely has any inactivation. I_{Ks} allows K^+ current to slowly increase during the plateau phase of the action potential therefore it contributes to the repolarizing current in the later stages of the action potential. I_{Ks} plays a key role in determining the shortening of the action potential during physiological increases in heart rate; during rapid heart rates the time of inactivation of I_{Ks} reduces causing the channel to accumulate and to contribute to a faster repolarization.

In addition, IK_s plays an important role in repolarization reserve. Repolarization reserve refers to the ability of the myocardium to compensate for the loss and/or alteration of a certain potassium current with modulation of the other potassium currents, in order to not affect repolarization duration (Baczko et al., 2016; Lengyel et al., 2001). This phenomenon was experimentally demonstrated in different species (Biliczki et al., 2002). The role of IKs in repolarization reserve is well characterized in humans, while the main repolarizing currents in mice and rats are It_o and IK_{ur} potassium currents.

I_{Ks} was measured by following the protocol exemplified in figure 3.10 A, in particular it was analysed in a final fourth step from -50 to -80mV in 10mV steps for 4000ms during 10ms, from the section enlarged in the image.

Figure 3.10 B shows a current-voltage relationship (I-V plot) comparing control, TMAO and washout I_{Ks} current. Figure 3.10 C compares mean I_{Ks} current in control and TMAO treated cells. TMAO caused no significant difference in I_{Ks} current, as shown in both I-V plot and bar chart.

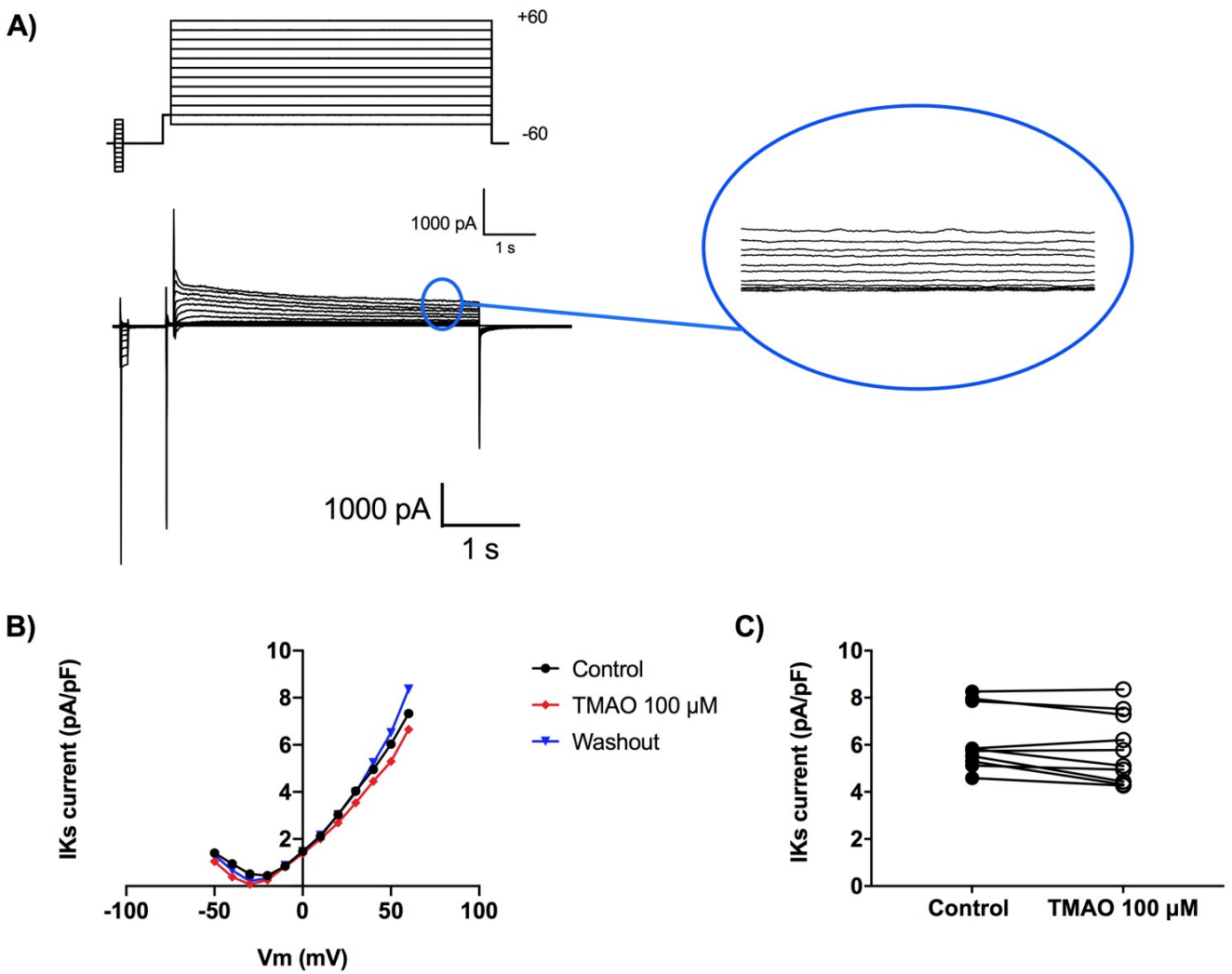

Figure 3.10. Effects of 100µM TMAO on IKs current in cardiomyocytes exposed to TMAO. A: Example trace of current for a single recording, made by following protocol outlined in figure 3.7. **B:** Current-voltage relationship (I-V plot) comparing control, TMAO and washout IKs current. **C:** Bar chart comparing mean IKs current in control and TMAO treated cells. TMAO had no significant effect on IKs current (Paired t-test; n. 11 cardiomyocytes from 5 animals).

3.2.5 The effects of TMAO on the ionic currents underlying the cardiac action potential in freshly isolated rat cardiomyocytes: a more detailed look at Ca^{2+} current

As outlined in section 2.5.6.3, because of their kinetics, Na^{+} and Ca^{2+} current can be difficult to separate and measure individually in voltage-step protocol as described previously. To allow a more detailed look at Ca^{2+} current, a multi-step protocol was designed with the purpose to isolate Ca^{2+} current from other ionic currents that could potentially interfere. The protocol constitutes of 3 sequential steps followed by a final ramp. The first step is elicited by voltage commands from -70 to -40mV during 30ms, the second step from -40 to 0mV during 70ms, the third step holds the potential to 0mV for 300ms and the final ramp from 0 and -70mV holds to potential at -70mV until the end of the protocol (Figure 3.11).

Another important reason for which this protocol was designed is to allow analysis of Ca^{2+} current over time. By nature, Ca^{2+} current runs down over time and can affect experiment designed to investigate its amplitude. Time-course experiment are important to infer information on the modulation of the current during the entire experiment.

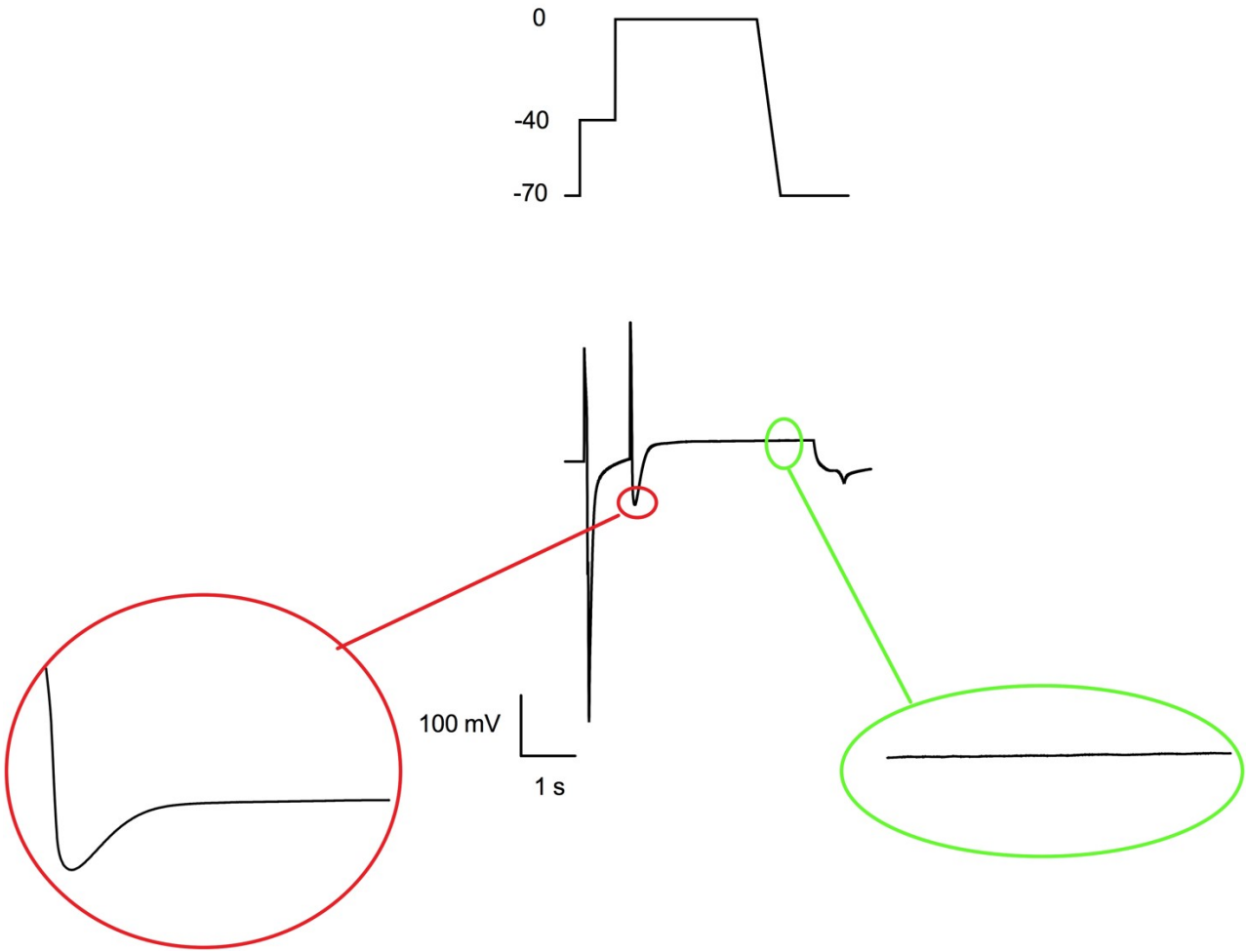

Figure 3.11. Example trace of current for a single patch clamp electrophysiology recording in whole cell configuration. The protocol constitutes of 3 sequential steps followed by a final ramp. The first step is elicited by voltage commands from -70 to -40mV during 30ms, the second step from -40 to 0mV during 70ms, the third step holds the potential to 0mV for 300ms and the final ramp from 0 and -70mV holds to potential at -70mV until the end of the protocol. In the image, portions from which following analysis will be shown are highlighted.

3.2.5.1 ICa^{2+} current

As shown in Figure 3.12, depolarising to 0mV activates a calcium current. The protocol was 2 s in duration and repeated until the end of the recording. TMAO was perfused as indicated. Calcium current was measured at the end of the normal Tyrode's solution perfusion and at the end of the TMAO perfusion. The mean current is shown in the bar chart (Figure 3.12B) comparing mean Ca^{2+} current in control and TMAO treated cells. TMAO caused a significant increase in Ca^{2+} current. The time –course of Ca^{2+} current for a single cell, showing how Ca^{2+} current rises after TMAO is perfused on the cell. As time progresses, Ca^{2+} current runs down and continues to do so after TMAO is no longer present in solution.

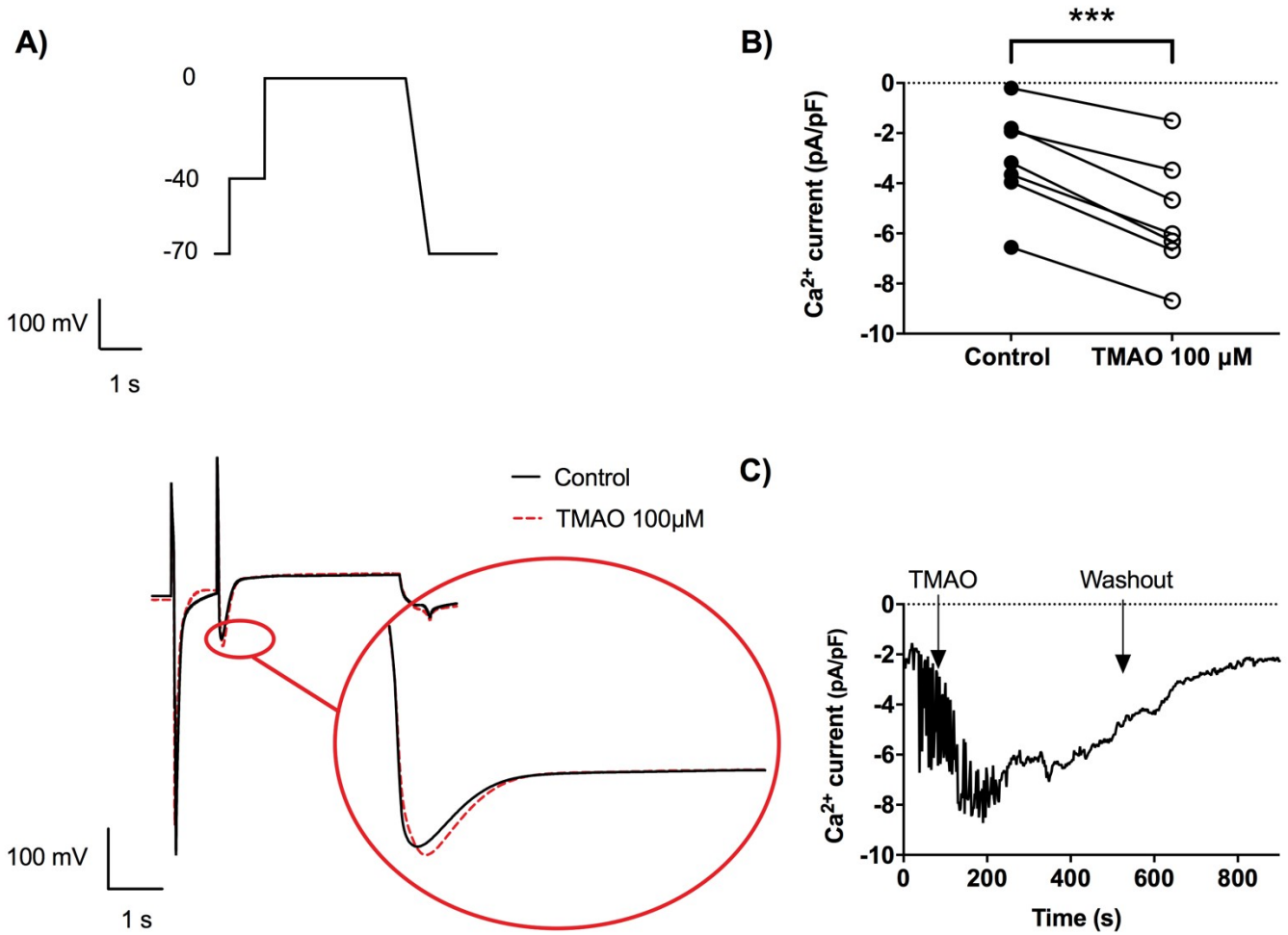

Figure 3.12. Effects of 100µM TMAO on Ca^{2+} current in cardiomyocytes exposed to TMAO. **A:** Example trace of current for a single recording elicited by voltage commands from -70 to 0mV in 2 steps and following ramp command back from 0 to -70mV. **B:** Bar chart comparing mean Ca^{2+} current in control and TMAO treated cells. TMAO caused a significant increase in Ca^{2+} current. **C:** Time –course of Ca^{2+} current for a single cell, showing how Ca^{2+} current rises after TMAO is perfused on the cell. As time goes on, Ca^{2+} current runs down and continues to do so after TMAO is no longer present in solution (***P < 0.001 paired t-test; n. 7 cardiomyocytes from 6 animals).

3.2.5.2 IKs current

The effects on IKs current was also investigated using this protocol as control.

Figure 3.13 A shows an example trace of current from a single recording from -70 to 0mV showing the general potassium currents of which, at this potential, IKs is likely to dominate.

The bar chart in figure 3.13 compares the mean IKs current in control and TMAO treated cells.

Figure 3.13 C shows a time–course of IKs current for multiple cells. TMAO caused no significant difference in IKs current, as shown in bar chart and time-course.

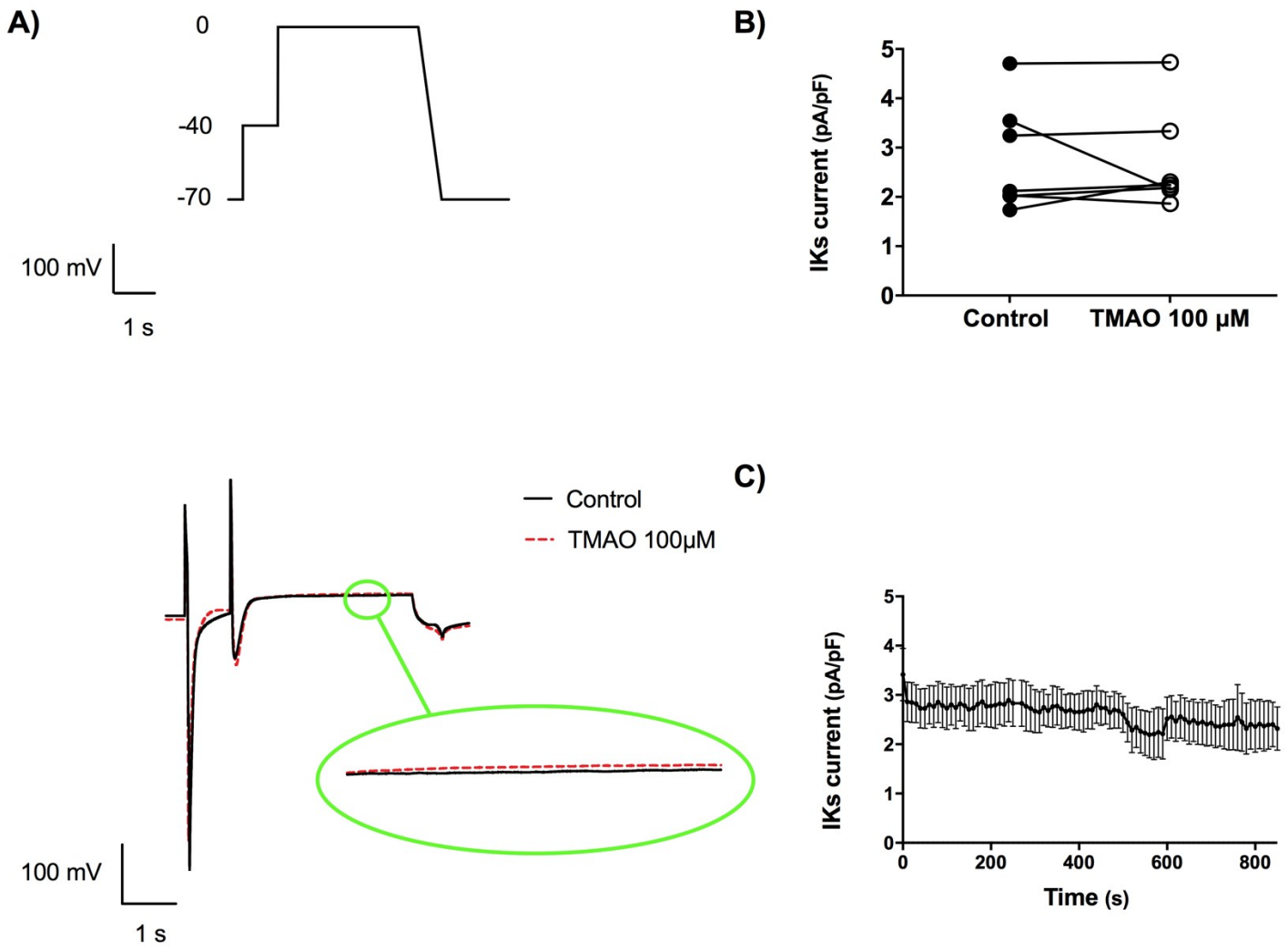

Figure 3.13. Effects of 100µM TMAO on IKs current in cardiomyocytes exposed to TMAO. **A:** Example trace of current from a single recording from -70 to 0mV showing potassium currents. **B:** Bar chart comparing mean IKs current in control and TMAO treated cells. **C:** Time–course of IKs current for multiple cells. TMAO caused no significant difference in IKs current, as shown in bar chart and time-course (Paired t-test; n. 7 cardiomyocytes from 6 animals).

3.2.6 The effects of TMAO on action potential duration and Ca^{2+} after exposure of TMAO in freshly isolated rat cardiomyocytes

Of further interest regarding the acute effects of TMAO is the time course of modulation of channels and APD in the presence of 100µM TMAO. While the electrophysiological protocols used (figure 3.7 and 3.11) to investigate the effects of TMAO on ionic currents was run, cells were perfused with TMAO for a longer period of time. In particular, for all electrophysiological experiments (action potential protocol, multi-current protocol and Ca^{2+}-detailed protocol), cells were perfused with NT for roughly 3 min to allow measurements for the "control" experimental group and were than perfused for 5-7 min with 100µM TMAO to allow complete perfusion and, in the end, a 10 min washout with NT was performed to remove all traces of TMAO.

When the experimental protocol made it possible, time-course of the activity of TMAO throughout the experiments was analysed. Figure 3.6 B showed a time-course of APD_{90} before, during and following cell's exposure to TMAO while figure 3.12 B. showed a time-course of Ca^{2+} current measured with Ca^{2+} current-detailed protocol before, during and following cell's exposure to TMAO; both figures highlight how quickly the cells respond to the exposure to TMAO and, interestingly, show that washout of TMAO on the cells remove the effects of TMAO analysed.

To investigate further, data from the washout phase of the experiments were also plotted in figure 3.14. Figure 3.14 A shows APD_{90} in control cells, in cells exposed to 100µM TMAO and washout Figure 3.14 B shows APD_{30} in control cells, in cells exposed to 100µM TMAO and washout. Figure 3.14 C shows APD_{50} in control cells, in cells exposed to 100µM TMAO and washout. Figure 3.14 D shows comparison mean Ca^{2+} current in control and TMAO treated cells. Acute exposure to 100µM TMAO caused a shortening of APD in APD_{90} and a prolongment of APD in APD_{30} and APD_{50} and an increase in Ca^{2+} current but only while the cells remained exposed to it. Washout of the cells resulted in a return to the initial state.

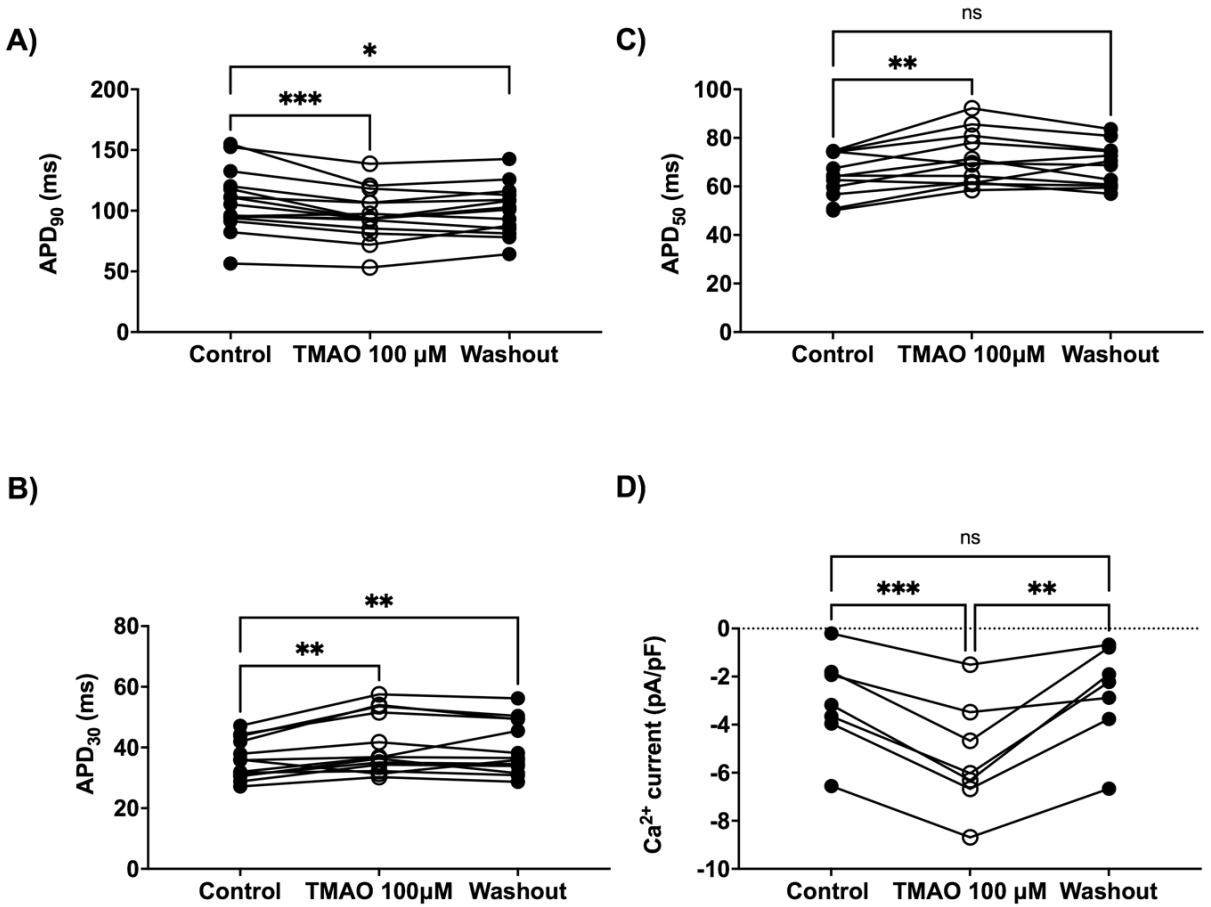

Figure 3.14. Effects of 100µM TMAO on APD and Ca^{2+} current after washout. **A:** Bar chart showing the duration of action potential at 90% repolarisation (APD_{90}) in control cells, in cells exposed to 100µM TMAO and washout. **B:** Bar chart showing the duration of action potential at 30% repolarisation (APD_{30}) in control cells, in cells exposed to 100µM TMAO and washout. **C:** Bar chart showing the duration of action potential at 50% repolarisation (APD_{50}) in control cells, in cells exposed to 100µM TMAO and washout (n. 18 cardiomyocytes from 9 animals). **D:** Bar chart comparing mean Ca^{2+} current in control and TMAO treated cells measured with Ca^{2+}-detailed current (* $P < 0.05$; ** $P < 0.01$; *** $P < 0.001$; repeated-measures ANOVA with Bonferroni post-test; n. 7 cardiomyocytes from 6 animals). Acute exposure to 100µM TMAO caused a shortening of APD and an increase in Ca^{2+} current but only while the cells remained exposed to it. Washout of the cells resulted in a return to the initial state.

3.2.7 The effects of TMAO on $K_{ir}6.1$ channel open probability measured using cell-attached recording in freshly isolated rat cardiomyocytes

As previous data have shown that TMAO can interfere with normal physiological pathways of the cardiomyocytes by altering their contractility, calcium handling and affecting the currents involved in the process of the cardiac action potential, the effects of TMAO on $K_{ir}6.1$ channel were also investigated.

While the majority of reports support the hypothesis that $K_{ir}6.2$/SUR2A channels are the predominant isoform of K_{ATP} channel in the heart (Nichols, 2016), recent findings of our research group evidence the presence of $K_{ir}6.1$ in the myocardium (manuscript currently under review). According to these findings, $K_{ir}6.1$ expressed by the cardiomyocytes can play a role, in normal physiological conditions, in the regulation on ADP inside the cells and, therefore, in Ca^{2+} handling. Activation of $K_{ir}6.1$ can result in shortening of ADP and a consequent reduction in Ca^{2+} influx. As a result, cardiomyocytes are more capable to preserve ATP and activation of Kir6.2/SUR2A is delayed. For these reasons, activation of $K_{ir}6.1$ is proposed as a cardioprotective mechanism and its possible modulation by TMAO was investigated.

To investigate the effects of TMAO on $K_{ir}6.1$ channel, the cell-attached patch configuration was used. The Kir6.1 channel activity is only able to be resolved using cell-attached patch recording. The current is constitutively active and so is difficult to resolve in the whole-cell configuration, however the characteristic single channel conductance allows it to be identified. Cardiomyocytes were perfused with NT to record channel activity. Following this, the solution was exchanged for TMAO 100 µM for the rest of the recording. The pipette potential was held at +40 mV with 140 mM K^+ in pipette solution, which, assuming a resting membrane potential of -70 mV, gives an approximate membrane potential of around -110 mV across the cell-attached patch. These parameters were applied in all cell-attached recordings. In every patch, a channel with a single channel current of ~5 pA can be observed in normal physiological resting conditions (Figure 3.15 A).

Figure 3.15 C shows the open probability of $K_{ir}6.1$ channel in control conditions and following treatment with 100µM TMAO while figure 3.15 D shows NP_o of $K_{ir}6.1$ channel in control conditions and following treatment with 100µM TMAO. In both these figures it is evident that TMAO caused an increase in both the open probability and NP_o of $K_{ir}6.1$ channel.

While the majority of cardiac action potential is carried out by univalent and divalent cations, important changes in action potential characteristics and the way other ionic currents behave can be caused by activation of chloride currents. Normally, changes in the extracellular concentration of chloride does not carry the power to cause differences in the resting membrane potential. However, activation of chloride currents can influence impulse formation and may play a role in arrhythmogenesis. Chloride currents normally show outward-going rectification or are largely activated at depolarized voltages, resulting in a plausible contribution of these to shortening of the ADP but not to the depolarization phase. The shortening of ADP caused by chloride activation may be a factor in the prevention of early afterdepolarization and protection by the detrimental effects of a prolonged action potential. Effects of chloride currents are, generally, limited by the presence of the predominant background potassium current (Hiraoka et al., 1998). Interestingly, during the cell-attached protocol used to detect activation of $K_{ir}6.1$ channel, it was noted that in a portion of the cells exposed to TMAO 100 µM there was activation of chloride current. Figure 3.15 B is a pie-chart showing the number of cells that exhibited Cl^- channels activation and the time after TMAO application that took for Cl^- channels to open.

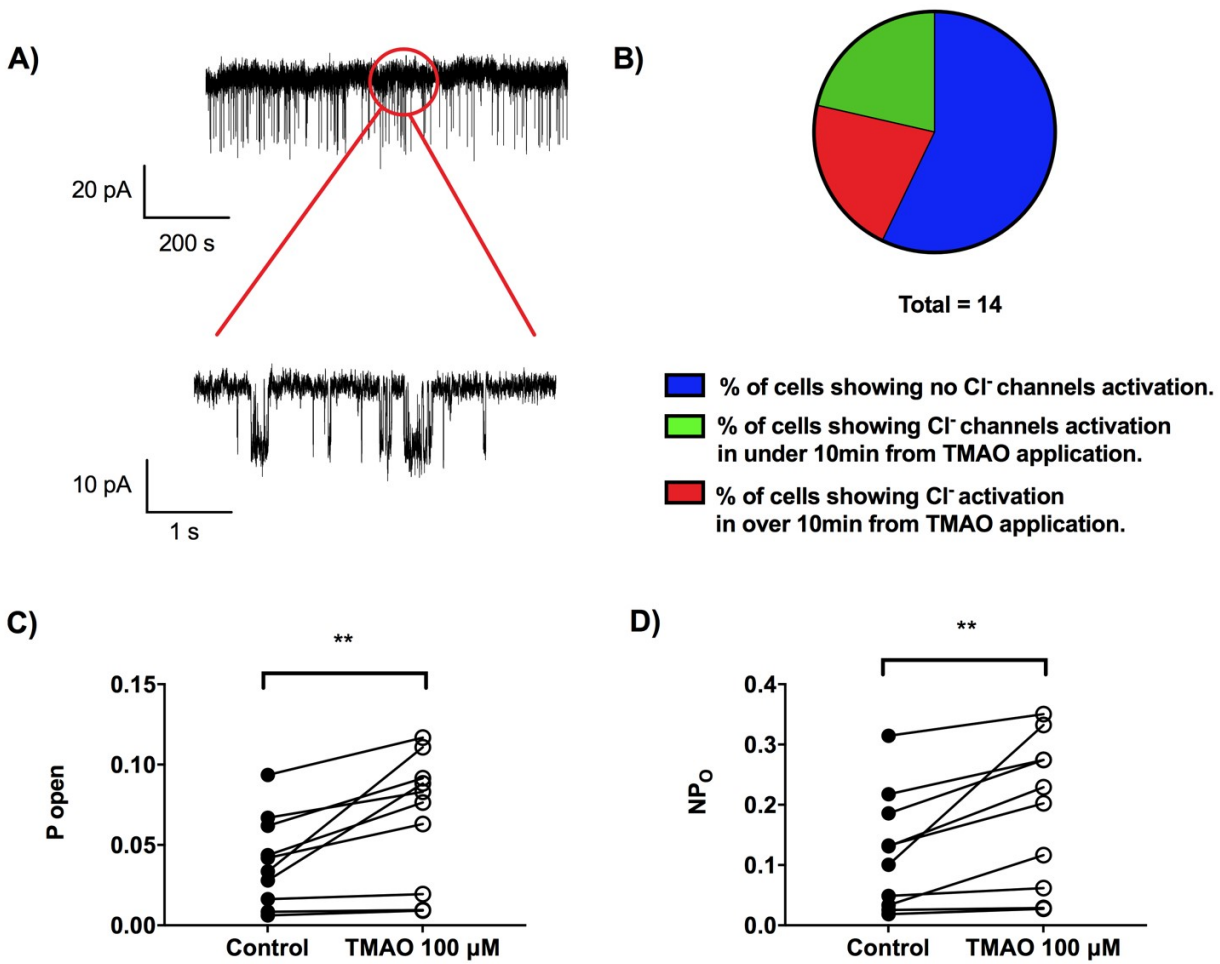

Figure 3.15. Effects of 100µM TMAO on K_{ir}6.1 channel open probability in cardiomyocytes exposed to TMAO. A: Example trace from a cell-attached patch recording, showing an expanded section for a more detailed view of the channel openings. **B:** Pie chart showing the number of cells that exhibited Cl^- channels activation and the time after TMAO application that took for Cl^- channels to open. **C:** Bar chart showing the open probability of K_{ir}6.1 channel in control conditions and following treatment with 100µM TMAO. TMAO caused an increase in the open probability of the Kir6.1 channel. **D:** Bar chart showing NP_o of K_{ir}6.1 channel in control conditions and following treatment with 100µM TMAO. TMAO caused and increase in the NP_o of the channel (**P <0.01 paired t-test; n. 10 cardiomyocytes from 7 animals).

3.2.8 The effects of TMAO on $K_{ir}6.2$ channels open probability in the MI-activated currents measured using cell-attached recording in freshly isolated rat cardiomyocyte

As previous data have shown that TMAO can interfere with normal physiological pathways of the cardiomyocytes by altering their contractility, calcium handling and affecting the currents involved in the process of the cardiac action potential, while also stimulating the opening of $K_{ir}6.1$, a potential cardioprotective pathway, the effects of TMAO on $K_{ir}6.2$ were also investigated.

In normal physiological conditions, $K_{ir}6.2$ is thought to be existing predominantly in a closed state that, consequently, does not contribute significantly to the membrane potential of the cardiomyocyte or the modulation and duration of the action potential. However, in case of the cells undergoing metabolic stress like in case of ischaemia or hypoxia, these channels switch to their opening state resulting in a reduction of the ADP and a decrease in the cell's ability to contract, in order to preserve the energetic resources, mainly ATP (Lederer et al., 1989). Opening of $K_{ir}6.2$ creates a hyperpolarizing K^+ current that decreases the time to repolarization of the cell and limits the plateau phase of the action potential, thus reducing Ca^{2+} influx and, altogether, causing a reduction of Ca^{2+} overload in cardiomyocytes (Brunner et al., 2003).

To investigate the effects of TMAO on $K_{ir}6.2$ channels, cell-attached patch configuration was used as described previously. Cardiomyocytes were perfused with either NT or TMAO 100 µM to record channel activity. Following this, the solution was exchanged for SFT+MI solution or SFT+MI and TMAO 100 µM for the rest of the recording. The metabolic inhibition causes ATP depletion and activation of $K_{ir}6.2$ channels. The pipette potential was held at +40 mV with 140 mM K^+ in pipette solution, which, assuming a resting membrane potential of -70 mV, gives an approximate membrane potential of around -110 mV across the cell-attached patch. These parameters were applied in all cell-attached recordings.

In every patch, a channel with a single channel current of ~10 pA can be observed in normal physiological resting conditions (Figure 3.16 A). Figure 3.16 A also shows the activation of the $K_{ir}6.2$ current (~10 pA) after MI due to the depletion of ATP and

increase of intracellular ADP and the activity of the $K_{ir}6.2$ highlighted by the two different levels of opening.

Traces were analysed by looking for bursts of activity which fitted the criteria of being >10pA and ≥100ms or ≥500ms, as this duration would exclude any spontaneous burst of activity that can occur which have not been induced by MI. Figure 3.16 B shows the mean time taken to detect a burst of $K_{ir}6.2$ activity lasting longer than 100ms in control cells and TMAO treated cells during MI perfusion while figure 3.16 C shows the mean time taken to detect a burst of $K_{ir}6.2$ activity lasting longer than 500ms in control cells and TMAO treated cells during MI. TMAO did not cause any significant difference in the activation of $K_{ir}6.2$, suggesting that enhancement of stress condition caused by TMAO evidenced in the previous experiments does not cause increase in $K_{ir}6.2$ channels opening, in these experimental conditions.

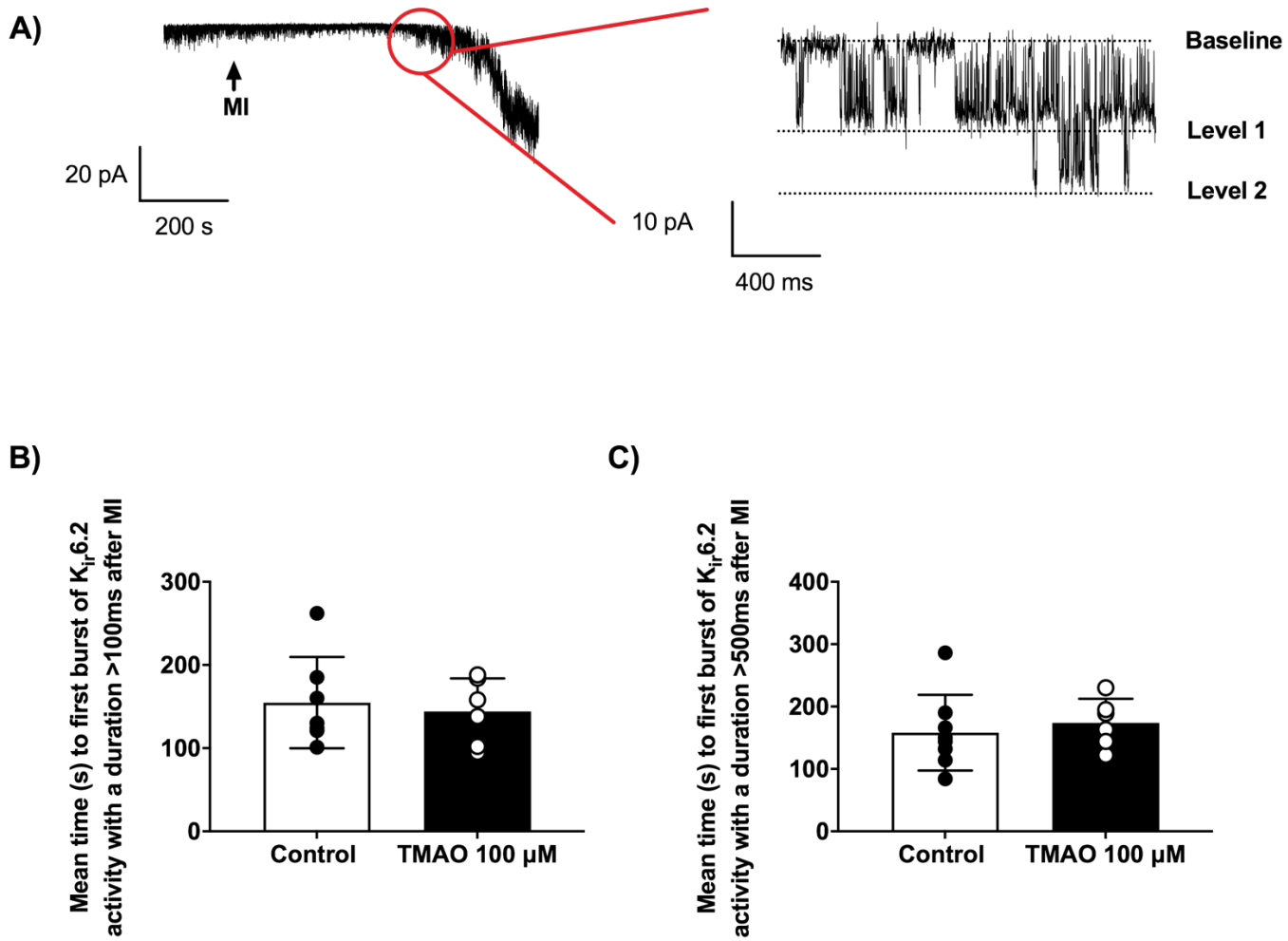

Figure 3.16. Effects of 100µM TMAO on the time to K_{ir}6.2 channel activity in cardiomyocytes exposed to TMAO. A: Example trace from a cell attached recording from a cardiomyocyte perfused with a metabolic inhibition (MI) solution. Following ~150 s of perfusion with MI, an inward K_{ATP} current is seen, consistent with Kir6.2/SUR2A activation, showing bursting behaviour. **B:** Bar chart showing the mean time taken to detect a burst of K_{ir}6.2 activity lasting longer than 100ms in control cells and TMAO treated cells during MI perfusion. **C:** Bar chart showing the mean time taken to detect a burst of K_{ir}6.2 activity lasting longer than 500ms in control cells and TMAO treated cells during MI. (Unpaired t-test, n.13 cardiomyocytes, 7 controls and 6 TMAO from 3 animals).

3.2.9 The effects of TMAO on the protection imparted by ischaemic preconditioning in freshly isolated rat cardiomyocytes

As previous data have shown that TMAO can interfere with normal physiological pathways of the cardiomyocytes by altering their contractility, calcium handling and affecting the currents involved in the process of the cardiac action potential, while also stimulating the opening of $K_{ir}6.1$, a potential cardioprotective pathway, TMAO was used on ischaemic preconditioned (IPC) cardiomyocytes to investigate its effects on a cardioprotective mechanism.

IPC is a cardioprotective mechanism elicited by a succession of brief periods of ischaemia or hypoxia exerted on the heart prior to the main ischaemic event that increases the ability of the myocardium to endure metabolic stress, thus having a protective effect on the myocardium. Briefly, in order to prepare IPC cardiomyocytes, hearts were perfused on a Langendorff canula where, to simulate short periods of ischaemia, perfusion was halted for three 5-min periods, with 5-min of normal perfusion between each break. The stopped perfusion has the effect of simulating the short periods of ischaemia, inducing the protective effects into the cells (Brennan et al., 2015). Cardiomyocytes that benefit from cardioprotection induced by IPC are characterized by specific effects: an increase in the percentage of contractile recovery and an increase in the percentage of cell survival following metabolic inhibition, when the MI/R model was applied, a delay in the time to contractile failure and a delay in the activation of $K_{ir}6.2$ (Brennan et al., 2015; Sims et al., 2014).

The timeline of the MI/R protocol is shown in Figure 3.1 IPC cardiomyocytes are seeded onto the microscope for at least 10 min to allow the cells to adhere to the surface as to avoid being washed out by perfusion. The cells sit for the first 3 min of the experiment in NT solution, in which rod-shaped cardiomyocytes normally contract according to the stimulation provided in the experiment. After, the cells are exposed to 7 min of metabolic inhibition, during which ATP synthesis is blocked and the cells lose the ability to properly contract. TMAO 100µM was used during the entire protocol, for the TMAO treated experiment.

Figure 3.17 A shows the percentage of functional recovery of IPC cells compared to TMAO treated cells. In a similar fashion to data show previously in figure 3.1, TMAO caused a reduction of the percentage of cell contractile recovery compared to the IPC cells, proving that TMAO is able to reverse the cardioprotection of the cardiomyocytes induces by the IPC treatment. Figure 3.17 B show a time course highlighting the reduction in functional recovery of IPC cells and TMAO treated IPC cells with respect to the time following IPC stimulus. Cardioprotection induced by IPC treatment is time-dependent and IPC cardiomyocytes rate of contractile recovery slowly decreases over time after isolation of the IPC cells. The time-dependency of contractile recovery rate is maintained in the TMAO-treated cells, but in this case TMAO-treated IPC cells consistently showed a further ~20% reduction in contractile recovery compared to the control IPC cells.

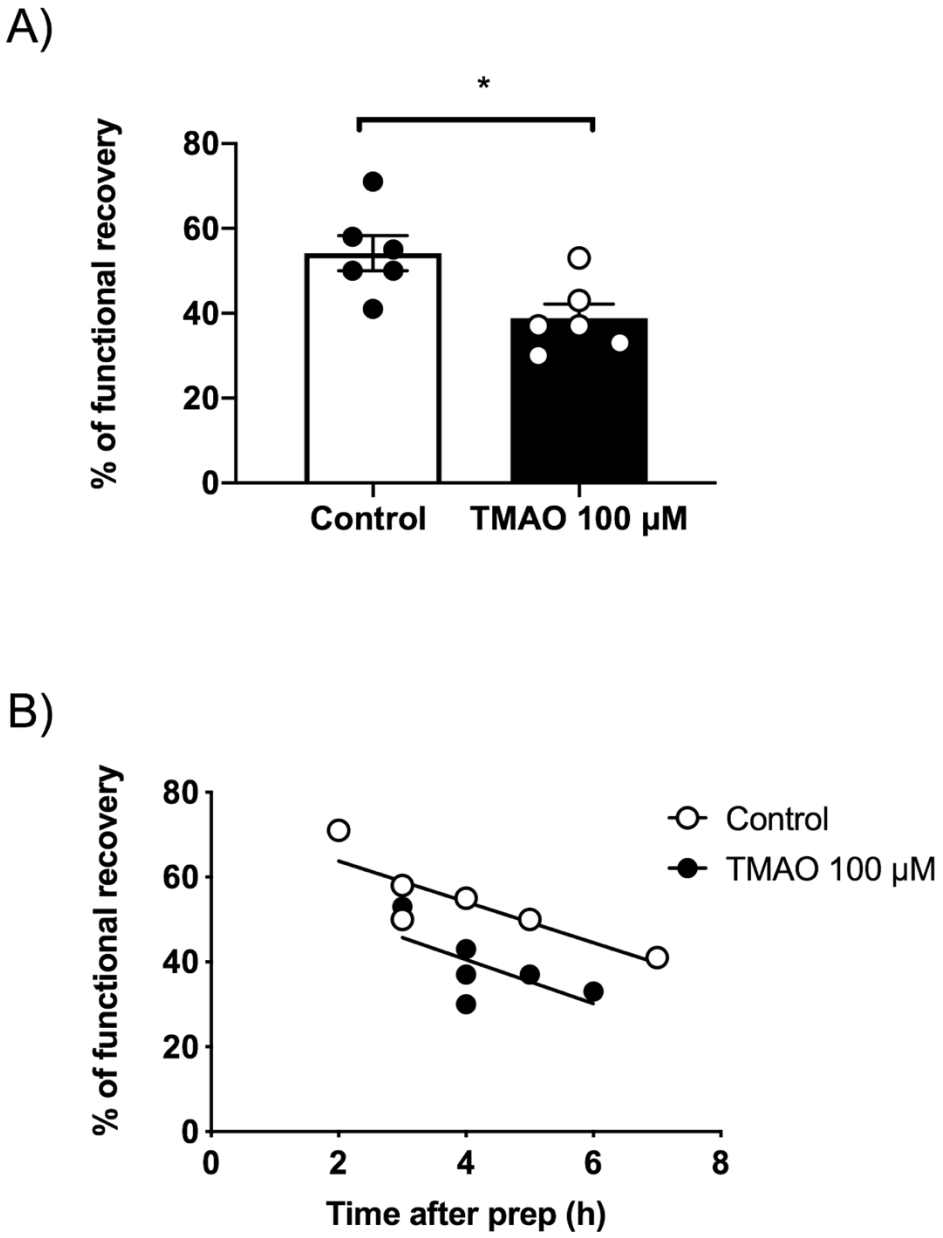

Figure 3.17. Effects of 100 µM TMAO on cell functional recovery in ischaemic-preconditioned cardiomyocytes. A: Bar chart showing the percentage of functional recovery of control cells and TMAO treated cells. TMAO treated cells showed a significant reduction in their cardioprotected status (*P < 0.05 unpaired t-test, n = 6 experiments for each condition from 3 animals). **B:** Time course showing the reduction in functional recovery of IPC cells and TMAO treated IPC cells with respect to the time following IPC stimulus. TMAO-treated IPC cells consistently showed a ~20% reduction in contractile recovery compared to the control IPC cells.

For each experiment, the times to contractile failure, time to rigor, time to contracture, time to hypercontracture and time to contractile recovery were also recorded. As mentioned in section 3.2.1 the time to contractile failure indicates the time at which

each cell has significantly reduced its ATP levels and K_{ATP} channel has opened. Figure 3.18 A compares the time to contractile failure of cells exposed to TMAO 100µM to preconditioned cells. The time to rigor indicates the time of near complete ATP depletion inside the cell. Figure 3.18 B compares the time to rigor of cells exposed to TMAO 100µM to preconditioned cells.

Finally, the time to contractile recovery indicates the time at which the cell regains the ability to undergo normal calcium cycling, recovering its ability to contract. Figure 3.18 C compares the time to contractile recovery of cells exposed to TMAO 100µM to preconditioned cells.

TMAO did not cause changes in time to contractile failure, time to rigor and time to contractile recovery in the ischaemic preconditioned cells.

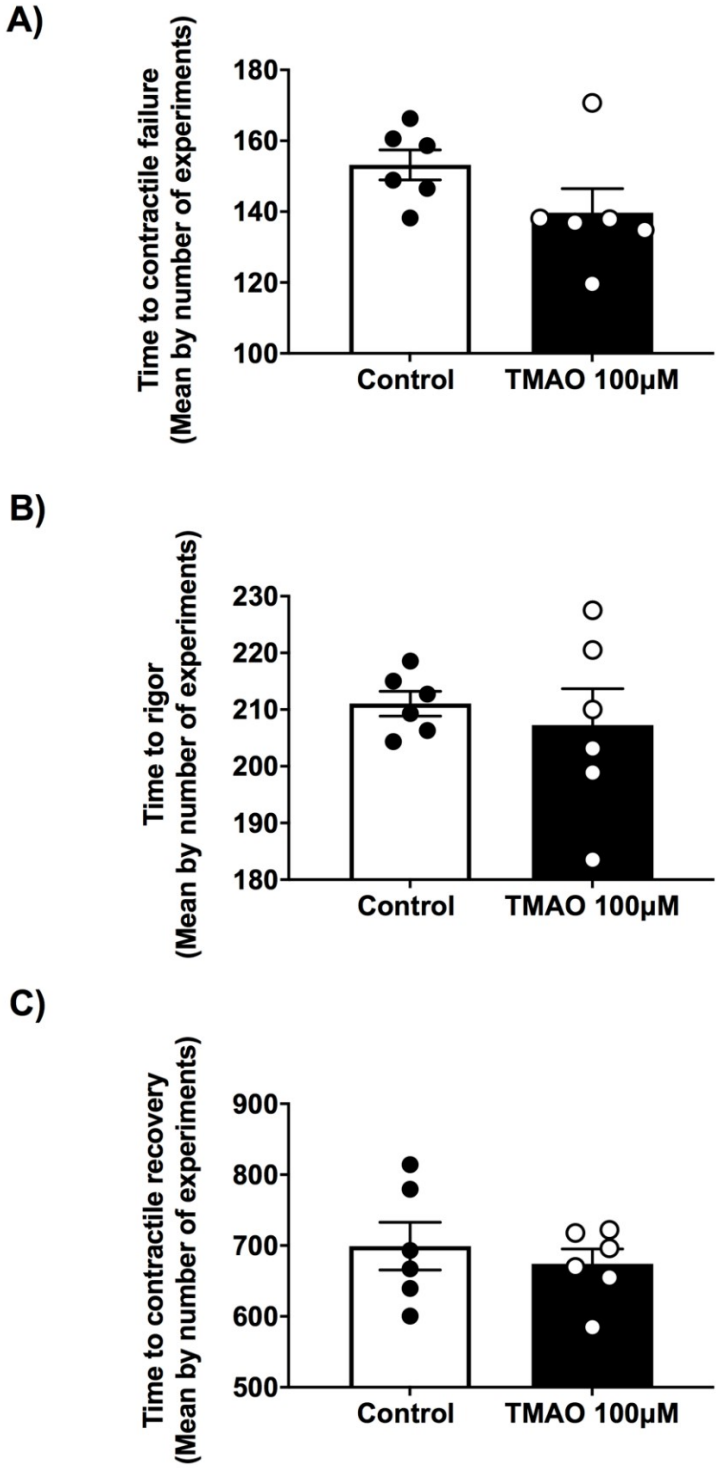

Figure 3.18. Effects of 100 µM TMAO on cell functional recovery in ischaemic-preconditioned cardiomyocytes. **A:** Bar chart comparing the time to contractile failure in control cells and in cells exposed to 100 µM TMAO. **B:** Bar chart showing the time to rigor in control cells and in cells exposed to 100 µM TMAO. **C:** Barc chart showing the time to contractile recovery in control cells and in cells exposed to 100 µM TMAO. TMAO caused no significant difference in the time to contractile failure, time to rigor and time to contractile recovery in ischaemic-preconditioned cardiomyocytes (Unpaired t-test; n. 12 experiments from 3 animals).

3.2.10 The effects of TMAO on ischaemia/reperfusion injury using Langendorff isolated whole heart model

To investigate the effects of TMAO on the whole heart, the Langendoff isolated whole heart model of ischaemia/reperfusion injury described in detail in section 2.7 was used. In this model, a region-specific injury of the myocardium was caused by occlusion of the LAD coronary artery in order to incite ischaemia. Later, removal of the ligation allows perfusate to normally flow again in the coronary cycle, thus re-establishing reperfusion. In this experimental model, TMAO 100 µM was perfused all throughout the protocol. At the end of the experiment, the dyes Evans blue and TTC were used to double stain slices of the whole heart to allow distinction between the areas analysed. Figure 3.19 A shows an example slice were the different areas analysed are highlighted. In the first image, the total slice displays all the three different areas of analysis: the blue area is the region stained by Evans blue and represents the non-ischaemic or healthy area, the red coloured area represents the regions in which Evans blue was incapable of penetrating, that is stained by TTC and represents the area at risk, and finally, the white unstained area represents the area of necrosis of the tissue. In the second image, the non-risk zone was cut out to record the area at risk. In the final image, only the area of necrosis was left behind.

To quantify the effects of TMAO on the areas analysed, the sizes of the infarcted area, the area at risk and the non-risk zone were calculated using ImageJ and used to extrapolate the weight of those areas compare to the total weight of each slice. The final results were expressed as a percentage of area at risk and as a percentage of infarct size compared to the area at risk itself. Figure 3.19 B shows the infarct size of whole heart expressed as percentage of area at risk while figure 3.19 C shows the area at risk of whole heart expressed as percentage of total heart. Both figures highlight the fact that TMAO caused no significant difference in the infarct size or in the percentage of area at risk of whole heart, suggesting that the detrimental effects of TMAO evidenced on the cardiomyocytes are not transferred to the whole heart.

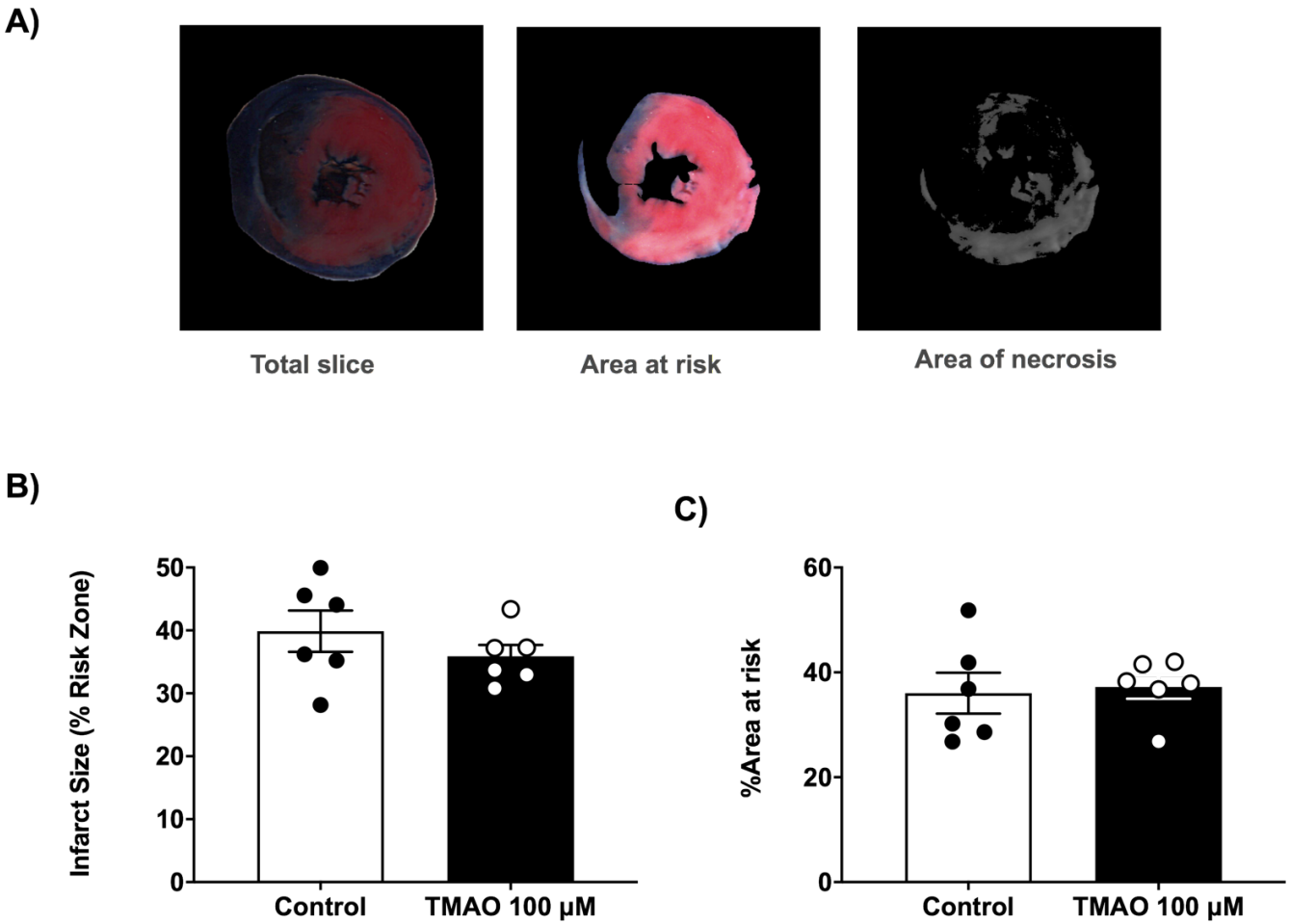

Figure 3.19. Effects of 100µM TMAO on ischemia/reperfusion injury in whole heart using Langendorff isolated heart model. **A:** Pictures showing the stages of analysis of each slice for this experiment. The total slice, before sections were cut out, shows three coloured areas: a blue area, where the Evans blue dye has penetrated, a red area identified as the area at risk and a final white area identified as the area of necrosis. Area at risk image shows the area of Evans Blue staining cut away from the image to record an area at risk. Finally, using ImageJ, the area of necrosis is measured. **B:** Bar chart showing the infarct size of whole heart expressed as percentage of area at risk. **C:** Bar chart showing area at risk of whole heart expressed as percentage of total heart. TMAO caused no significant difference in the infarct size or in the percentage of area at risk of whole heart (Unpaired t-test, n = 6 control and 6 TMAO treated hearts).

3.3 Discussion

In this chapter, data has been presented identifying a direct link between the gut-derived metabolite TMAO and altered cardiomyocyte function. Using electrophysiological and pharmacological tools, the effects of this metabolite have been investigated in freshly isolated cardiomyocytes.

In the literature, reports have primarily focused on the detrimental role of TMAO on endothelial cells. In particular, in these cells, TMAO was found to increase cellular aging, by upregulating specific markers (p53 and p21) that serve as senescence mediators, decrease cellular proliferation and alter cellular migration (Ke et al., 2018). TMAO has also been described to increase oxidative stress in these endothelial cells, through impairment of nitric oxide production, causing an altogether malfunctioning of the cells (T. Li et al., 2017). Another large part of the literature has focused its attention of the hypertensive effects of TMAO. In particular, TMAO was found to have a role in enhancing the activity of angiotensin II, mediator of hypertensive effects, by stabilizing its protein conformation and prolonging its hypertensive effects (Ufnal et al., 2014). Other reported effects of TMAO on the cardiovascular system have focused on the strong relationship between high TMAO plasma concentrations, caused by consumption of nutrients rich in precursors of TMAO, with the development of atherosclerosis (Koeth et al., 2013) and the correlation between high TMAO plasma concentrations with an increase of diabetes risk, through increase in body weight and insulin resistance (Dambrova et al., 2016). Despite being the focus of several studies, a comprehensive and cohesive description of the effects of TMAO is yet to be achieved and the function of TMAO is still being debated. Studies like the ones discussed above are often countered by evidences of a positive and protecting effect of TMAO, an argument that finds its root in the controversy surrounding fish-rich diets (Querio et al., 2019). It is well known that while fish and seafood do not yield large amounts of TMAO precursors, they are extremely rich in TMAO themselves and their effects on lowering the risk of complications in CVD is well-known. In addition, contrasting evidences are emerging on the link between high plasma concentrations of TMAO and development of

atherosclerosis, regarding the fact that TMAO does not seem involved in foam cell formation, key event in the development of atherosclerosis, even at concentrations higher than physiological ones (Collins et al., 2016). Other evidences that point to a positive correlation between TMAO and its involvement in the cardiovascular system are provided by a study performed by Huc et al. (2018), in which they highlighted a protective role of TMAO in reduction of fibrosis and diastolic dysfunction in pressureoverloaded hearts. Finally, another factor that heavily weighs in the discussion on whether TMAO can be considered as a protective or damaging factor in CVD, is the lack of a well-defined plasma concentration range of the metabolite, based on the contrasting data about TMAO plasma concentrations in healthy and pathological subjects (Querio et al., 2019).

This project aims to fits into this debate by providing new insights into the link between TMAO and CVD.

Although the link between TMAO and the cardiovascular system has been investigated, there are not many studies that turned their focus on the direct effects that the metabolite can have on cardiac cells. In these, TMAO has been presented as an agent that increases the severity of cardiovascular events and enhances the progression and development of cardiovascular diseases (Makrecka-Kuka et al., 2017). Consistently with these findings, in this project TMAO was found to enhance the damage to the contractile function of cardiomyocytes caused by a mixture of metabolic inhibitors, the which combined activity causes a depletion of ATP reserve in the cell, in a concentration-dependent manner (Figure 3.2 B). Indeed, TMAO by itself did not cause alterations of contractile function, even when used at the highest concentrations that were shown to permanently damage the cells when TMAO was used in combination with metabolic inhibitors (namely concentrations of TMAO higher than 100µM TMAO cause the cells to not be able to recover from the loss of contractility at all as shown in figure 3.2 B and in figure 3.4 B), but was only able to increase the damage caused by metabolic inhibition.

In addition, evidence from Querio et al. (2019) underlined that high concentrations of

TMAO caused no toxic effect in the cardiomyocytes. In their study they found that high concentrations of TMAO do not induce cardiac tissue loss and that there were no alterations in the cardiac structure of cardiomyocytes after exposure to TMAO, as emerged by evaluation of the sarcomere length and cytoskeletal organization. Besides this study, another study from Jaworska et al. (2019) found that TMA and not TMAO was responsible for the decrease in proliferation and viability of cardiomyocytes and that co-treatment with TMAO could be protective against the cytotoxic effects of TMA. Furthermore, they proposed that the detrimental effect they found TMA responsible for could be caused by an interference of this one in the degradation of proteins structure, since both albumin and cardiac LDH were degraded by 24h incubation with TMA in their study. These findings were similar to this study, as TMAO was found to not cause any differences in the cell survival rate compared to control conditions, even at the highest concentrations, as shown in figure 3.2 C. Our study took these findings a step further and confirmed that TMAO did not cause loss of cardiac issue not only in isolated cardiomyocytes but in the whole heart as well. In our study,
TMAO was used on the Langendoff isolated whole heart model of ischaemia/reperfusion injury and was shown to not cause any significant difference in the infarct size or in the percentage of area at risk of whole heart, as shown in figure 3.19 B and in figure 3.19 C.

Despite this evidence of a non-damaging role of TMAO on cardiomyocytes, there exists findings that make it clear that TMAO is able to directly impair cardiomyocyte contractile function and intracellular calcium dynamics. A first study that proposed Ca^{2+} handling as a possible mechanism to explain the effects of TMAO was conducted by W. Zhu et al. (2016). In this study, it was shown that TMAO was capable of increasing platelet hyperresponsiveness and increase thrombosis risk. In addition, they proved that this effect of TMAO on platelet hyperresponsiveness was strictly dependent on an increase in Ca^{2+} release from platelet intracellular stores, mediated by several agonists, in including ADP, thrombin, collagen, and arachidonic acid. Following on, Savi et al. (2018), showed a detrimental effect of TMAO in cardiomyocytes by finding it worsens intracellular calcium handling by a decrease in the efficiency of the cell to remove

intracellular calcium, with a consequent loss in cardiac function. In particular, they proposed that intracellular calcium handling was altered by TMAO via activation of protein sirtuin 1, which is known to increase SERCA2 expression. In this scenario, an increase of SERCA2 would lead to an increase in calcium store content explaining their findings of an increase in Ca^{2+} amplitude. Consistent with these findings, in this project TMAO was found to increase Ca^{2+} transients' amplitude, as shown in figure 3.5. The alteration of Ca^{2+} handling by TMAO was further confirmed in our study by electrophysiological studies. In two differently designed protocols, it was shown that TMAO caused an increase of Ca^{2+} current in cardiomyocytes, either by increasing influx of Ca^{2+} into the cells or by stimulating the release of Ca^{2+} from the intracellular stores, as shown in figure 3.9 and 3.12. Furthermore, in figure 3.16 it is clear that APD_{30} and APD_{50} are longer when TMAO is present on the cells, a clear reflection that the increase in intracellular Ca^{2+} was affecting the cardiac action potential by prolonging the plateau phase.

This study demonstrated that TMAO did not affect the other currents involved in modulating the cardiac action potential. As shown in figure 3.8, figure 3.10 and figure 3.13, TMAO did not cause any significant differences in IK_1 or IKs amplitude, suggesting that the detrimental effects of TMAO linked to alteration of Ca^{2+} handling do not cause further alterations in the other currents.

Ca^{2+} handling is not the only key point involved in the disruption and/or protection of cardiac function. In the cardioprotective signalling pathways, there are multiple molecules that are involved in the transmission of the protective signals from the trigger to the effectors (Murphy et al., 2008). Acute ischaemia-reperfusion injury has been described to involve ROS generation, reduction of nitric oxide supply, Ca^{2+} overload and disruption of the mitochondria leading to cell death (Kalogeris et al., 2014). In addition, it has been reported that an inflammatory response, mediated by NFκB and other transcription factor activation, is involved in enhancing the expression of cell adhesion molecules, leukocyte infiltration and, altogether, damage to the tissue. In contrast, specific signalling pathways can be activated to attenuate or prevent the damaging

effects caused by ischaemia-reperfusion injury (Kalogeris et al., 2012; Kalogeris et al., 2014).

Of these, ischaemic preconditioning (IPC) is an internal mechanism that can be triggered by a succession of short bursts of ischaemia that ultimately results in an improved cardiomyocyte survival rate and an equally improved cardiac function, after an episode of ischaemia (Murry et al., 1986; Suzuki et al., 2002). Effectors of the signalling pathways involved in mediating the cardioprotective response triggered by IPC include ROS generating pathways, nitric oxide and cyclic guanosine monophosphate (cGMP) pathway (Das et al., 2005; Solenkova et al., 2006). Cardiomyocytes protected by triggering of the IPC pathways were shown to be affected by exposure to TMAO. As shown in figure 3.17, TMAO caused a decrease in the percentage of cell recovery. Another interesting point was that while non-IPC cells treated with 100 µM TMAO showed differences in time to contractile recovery and time to contractile failure (fig 3.3 A and 3.4 B), the same differences in times could not be found in IPC cells treated with 100 µM TMAO (fig 3.18 A and C). These findings confirm that cardioprotection mediated by IPC results in an increased percentage of overall contractile recovery, and while the cardioprotection imparted is not entirely effective against the detrimental effects of TMAO, these results could be enough to suggest that TMAO may be involved in the same pathways that mediate cardioprotection by IPC .

An important role in the cardioprotection mediated by IPC is plated by K_{ATP} channels, however it is still unclear which of the isoforms of K_{ATP} channel is able to trigger the cardioprotective response. In normal physiological conditions, the $K_{ir}6.2$ channel, believed to be the main isoform expressed in the ventricular myocardium, remains predominantly closed and does not play important roles in either maintaining the resting membrane potential or the action potential duration. The situation changes in case of metabolic stress, such as an ischemic or hypoxia event, when reserves of ATP are depleted and K_{ATP} channels will open and cause a shortening of the APD in order to preserve ATP inside the cell (Lederer & Nichols, 1989). The idea that cardioprotection could be mediated by K_{ATP} channels was supported by findings from McPherson et al.

(1993), that suggested that cardioprotection could be achieved with the use a K_{ATP} opener, pinacidil, that caused a shortening of the APD and a decrease in cellular contractility that, altogether, served the purpose of preserving intracellular energy. A similar response was observed in cardiomyocytes exposed to TMAO, where TMAO caused a shortening of the APD_{90}, as shown in figure 3.6, suggesting that TMAO may be involved in the same cardioprotective pathway that involves K_{ATP} channels opening.

Although the $K_{ir}6.2$ channel is believed to be the main isoform expressed in ventricular cardiomyocytes (Suzuki et al., 2002), it is unlikely that this channel is involved in mediating the cardioprotection imparted by IPC, suggesting that there could be another isoform of K_{ATP} channel expressed at cardiac level. Brennan et al. (2015) found evidence that suggested that in cardiomyocytes protected by IPC the activation of $K_{ir}6.2$ channel was delayed after MI, effectively demonstrating that cardioprotection was not mediated by early activation of $K_{ir}6.2$ channels. Furthermore, this study showed evidence that activation of $K_{ir}6.2$ channel induced by MI actually caused contractile failure in the cardiomyocytes and that in cardiomyocytes protected by IPC the activation of $K_{ir}6.2$ channel was delayed (Brennan et al 2015).

Along with evidence that suggests against activation of $K_{ir}6.2$ channel as the main responsible for cardioprotection, there is evidence that suggesting that this role may be in part due to activity of $K_{ir}6.1$. Lawrence et al. (2002) demonstrated that ischaemia can cause an increase in the expression of $K_{ir}6.1$ and that transfection of a $K_{ir}6.1$ dominant negative subunit into cardiomyocytes caused a decrease of cell viability following the ischemic episode. In addition, Isidoro Tavares et al. (2007) proved that $K_{ir}6.1$ expression levels were upregulated following coronary ligation and that they were particularly high near the infarct zone. These findings were further demonstrated by our group in data, currently unpublished, that demonstrate that $K_{ir}6.1$ open probability was increased following a cardioprotective trigger. Further evidence showed that this activation was followed by a shortening of the action potential, reduction of Ca^{2+} accumulation and reduced ATP depletion during MI, overall improving contractile recovery and increasing the cell survival rate. Thus, the hypothesis is that there are two different protective

pathways in the heart: one mediated by activation $K_{ir}6.1$ channel, that is involved in the earliest stages of metabolic stress and a second one mediated by activation of $K_{ir}6.2$ channel, that is involved in prolonged ischaemia and the latest stages of metabolic stress that results in a late attempt of preserving ATP.

In accord with these findings, acute exposure to TMAO caused an increase in the activation of $K_{ir}6.1$ channel, as shown in figure 3.15, but was not involved in the modulation of activation of $K_{ir}6.2$ channel, as shown in figure 3.16. Although the mechanism is not clear, $K_{ir}6.1$ is seemingly activated by perfusion with TMAO.

These findings of activation of Kir6.1 current, coupled with the potentiation of calcium currents, suggest that there is an acute modulation of cardiomyocyte function by TMAO. This does not have a significantly deleterious effect on cell survival following ischaemia, however, does give increased calcium transient amplitude and so may have an acute positive ionotropic effect on the intact myocardium. Further investigations of intact myocardial function would be required to fully investigate this.

In conclusion, acute administration of TMAO to isolated cardiomyocytes can have an impact on modulation of ion channel function. These effects manifest as a change in the action potential and an effect on calcium homeostasis. Despite these changes in calcium homeostasis, the effects of ischaemia are not exaggerated in the whole heart, however contractile recovery following ischaemia is compromised in a single cell model of ischaemia and reperfusion. To further establish the potentially deleterious effects of TMAO on cardiomyocyte function, the effects of more chronic elevations of TMAO will be investigated in Chapter 4.

Chapter 4

The effects of 24-hour exposure with TMAO on cardiac cell function and modulation of cardiac electrical parameters

4 The effects of 24-hour exposure with TMAO on cardiac cell function and modulation of cardiac electrical parameters

4.1 Introduction

In the previous chapter, it was demonstrated that acute treatment of freshly isolated cardiomyocytes with TMAO cause an increased calcium current, increase $K_{ir}6.1$ channel activity and reduced contractile function following an ischaemia and reperfusion protocol. The effects identified in Chapter 3 were with a short 5-10-minute exposure of TMAO on the cardiac cells. It is plausible that there are differences between the acute effects of TMAO and those that are more chronic following prolonged exposure. To investigate the effects of longer-term exposure to TMAO on cardiomyocytes, freshly isolated rat cardiomyocytes were cultured for 24h following isolation with or without TMAO.

Experiments that yielded significant perturbations of cardiac cell behaviour, as described in chapter 3, were replicated to provide information and comparison between acute exposure and a prolonged exposure to TMAO.

4.2 Results

4.2.1 The effects of 24 exposure to TMAO on cardiac action potential duration and resting membrane potential in cultured rat cardiomyocytes

The first key experiment replicated to investigate the effects of TMAO on cultured cardiomyocytes was analysis of action potential duration.

To investigate this, action potentials from cultured cardiomyocytes were recorded using the whole-cell patch-clamp technique as described in section 2.5.6. Action potentials were stimulated at a rate of 1 Hz until a steady- state was reached and recorded

continuously for 3-6 minutes prior to perfusion with TMAO 100µM. APD_{90} and RMP for each condition was measured, calculated and analysed as described in section 2.5.6.1. Figure 4.1 A shows an example trace of cardiac action potential in control cells and in cells exposed to 100µM TMAO, recorded as previously described. The action potential morphology was significantly different following 24-hours in culture, showing a small depolarisation and prolonged action potential duration. Despite these different characteristics, there was no effect of TMAO on the action potential. Figure 4.1 B shows the RMP of control cells and TMAO treated cells. TMAO caused no significant changes to the RMP of cells. Figure 4.1 C shows the APD_{90} in control cells and in cells exposed to 100µM TMAO. From these data, it was concluded that longer-term exposure to 100µM TMAO did not cause any modulation of action potential duration in contrast to what was previously described for acute administration.

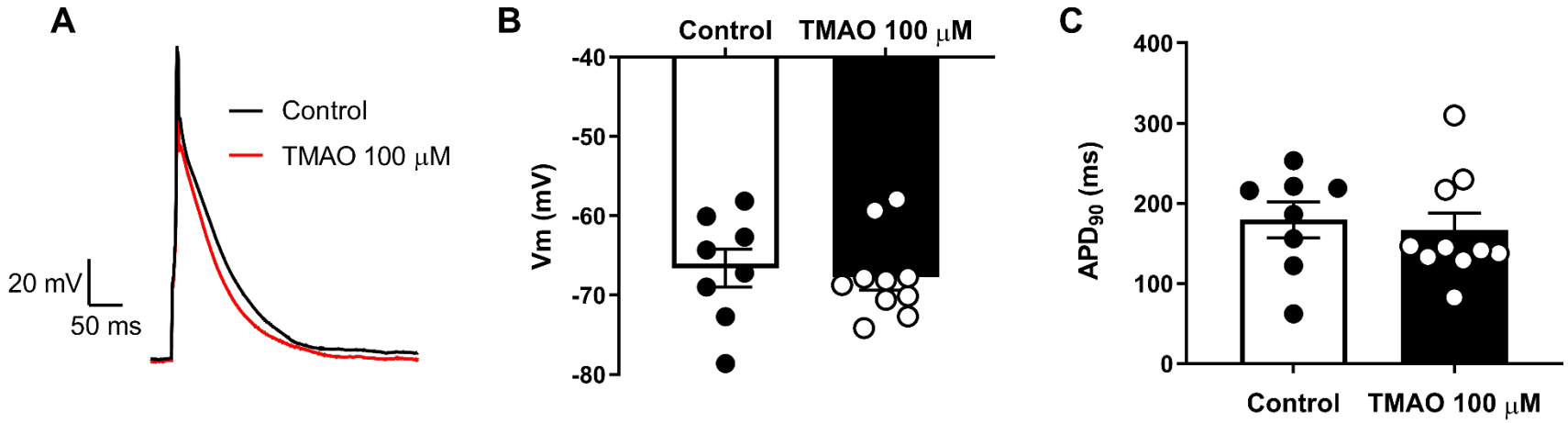

Figure 4.1. Effects of 24h exposure to 100μM TMAO on membrane potential and action potential duration. A: Example traces of cardiac action potential in control cells and in cells exposed to 100μM TMAO for 24h. **B:** Bar chart showing the resting membrane potential (RMP) of control cells and cells exposed to 100μM TMAO for 24h. Long exposure to TMAO caused no significant changes to the RMP of cells. **C:** Bar chart showing the duration of action potential at 90% repolarisation (APD_{90}) in control cells and in cells exposed to 100μM TMAO for 24h. While acute exposure to 100μM TMAO caused a shortening of action potential during the exposure, the effect was not present long-term. (Unpaired t-test, n = 8 control and 10 TMAO treated cells from 4 animals).

4.2.2 The effects of 24 exposure to TMAO on the ionic currents underlying the cardiac action potential in cultured rat cardiomyocytes: a more detailed look at Ca^{2+} current

Another important experiment that was chosen to be replicated on cultured cardiomyocytes exposed to 100µM TMAO for 24h, was the current protocol shown in figure 3.11 that allowed a more detailed analysis of the Ca^{2+} current. With acute exposure of cardiomyocytes to 100µM TMAO, Ca^{2+} current significantly increased by the presence of TMAO. To investigate whether this modulation was present in the cultured cardiomyocytes following 24-hour of treatment with TMAO, the multiple current protocol was used.

4.2.2.1 ICa^{2+} current

To investigate the effect of chronic treatment of TMAO on Ca^{2+} current, the inward current was measured from increasing depolarising steps, Figure 4.2 A. An example traces of Ca^{2+} current for a single recording is shown, together with the mean time course comparing mean Ca^{2+} current in control and TMAO treated cells. Finally, a bar chart showing mean Ca^{2+} current at 3 min from the start of the recording is shown (Figure 4.2C). These data demonstrate that more long-term (24-hour) exposure to TMAO caused no significant increase in Ca^{2+} current, as shown in bar chart and time course, unlike acute exposure to TMAO which caused an increase in Ca^{2+} current. It should be noted that there is a general trend of increased current, however it is not significant. This may be due to insufficient repeats given the variability of the data from cultured cardiomyocytes.

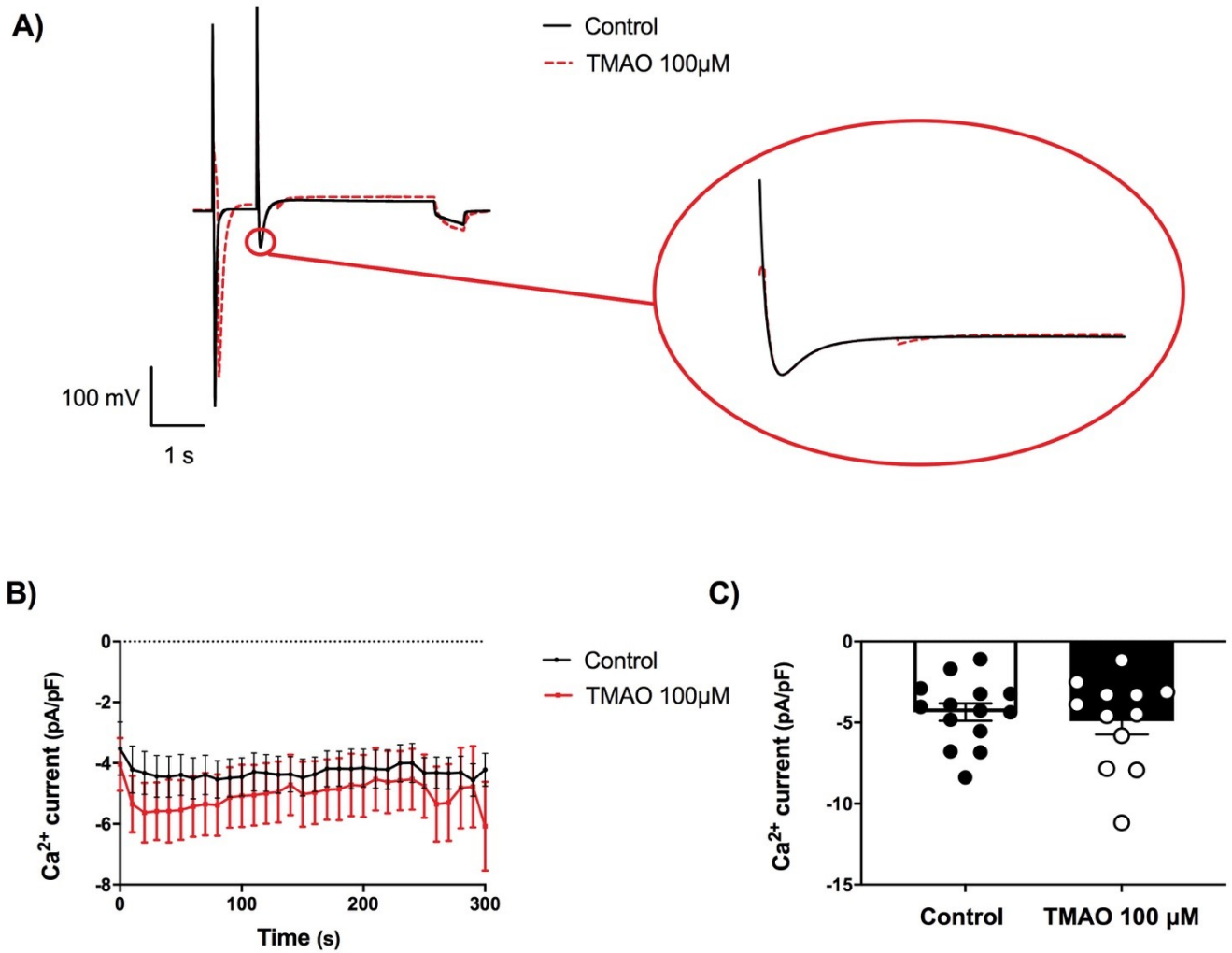

Figure 4.2. Effects of 24h exposure to 100µM TMAO on Ca^{2+} current in cardiomyocytes exposed to TMAO. **A:** Example trace of Ca^{2+} current for a single recording. **B:** Mean time course comparing mean Ca^{2+} current in control and TMAO treated cells. **C:** Bar chart showing mean Ca^{2+} current at 3 min from the start of the recording. Long exposure to TMAO caused no significant difference in Ca^{2+} current, as shown in bar chart and time-course, unlike acute exposure to TMAO which caused an increase in Ca^{2+} current (Unpaired t-test, n. 26 cardiomyocytes, 14 controls and 12 TMAO treated from 5 animals).

4.2.2.2 IKs current

To directly compare with the data investigating the acute effects of TMAO on currents, the effects of prolonged exposure of TMAO on the IKs current was investigated. These data, shown in figure 4.3, shows the time course of IKs current comparing mean IKs current in control and TMAO treated cells together with a bar chart showing mean IKs current at 3 min from the start of the recording. Consistent with the data investigating the acute effects of exposure to TMAO, long exposure to TMAO caused no significant difference in IKs current (Unpaired t-test, n. 26 cardiomyocytes, 14 controls and 12 TMAO treated from 5 animals).

In the cultured cardiomyocytes, the chronic effects of TMAO did not affect the calcium or the IKs currents. This may be due to the variability of the data acquired from the cultured myocytes.

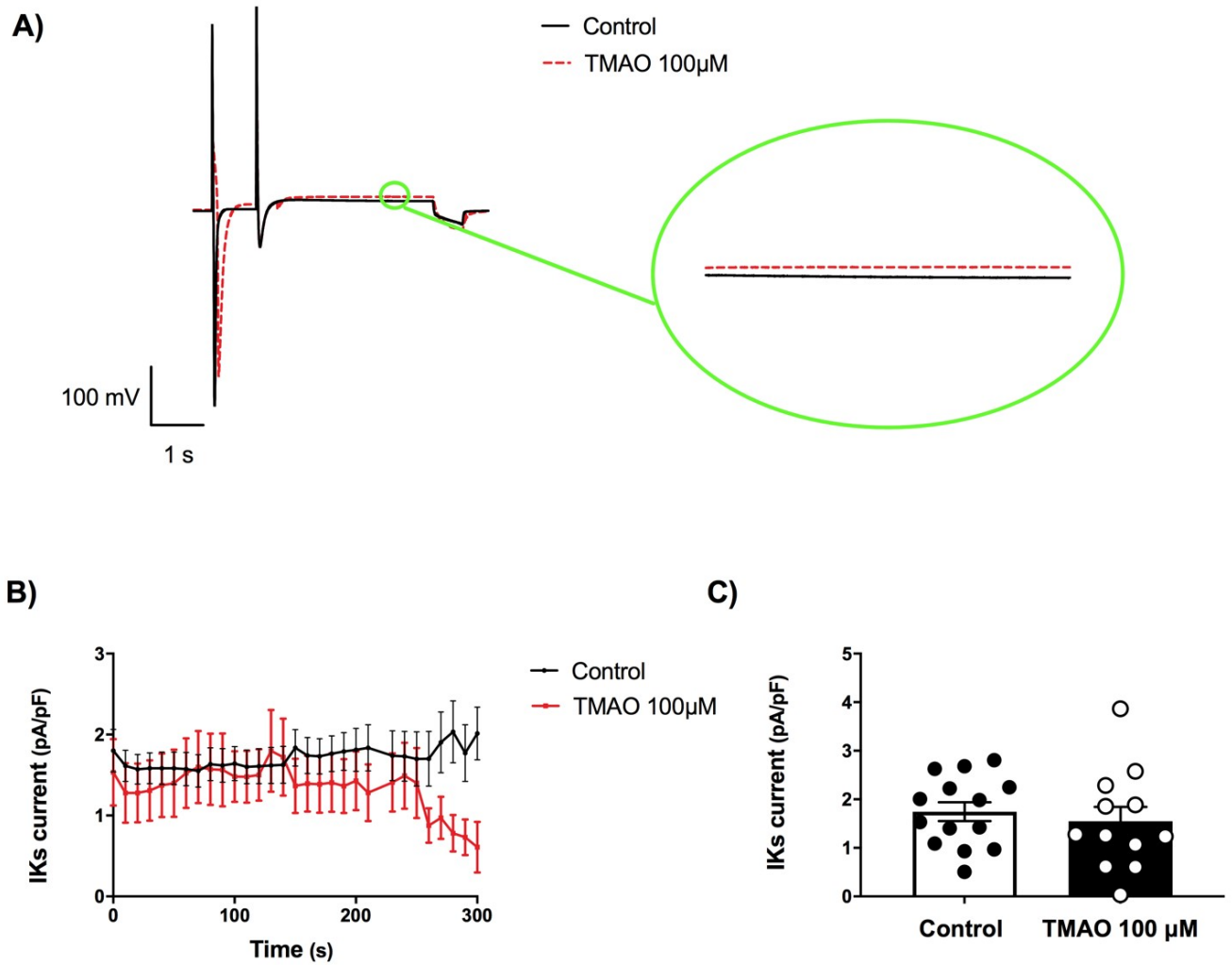

Figure 4.3. Effects of 24h exposure to 100µM TMAO on IKs current in cardiomyocytes exposed to TMAO. **A:** Example trace of current for a single. **B:** Time course of IKs current comparing mean IKs current in control and TMAO treated cells. **C:** Bar chart showing mean IKs current at 3 min from the start of the recording. Consistently to what happens with acute exposure to TMAO, long exposure to TMAO caused no significant difference in IKs current, as shown in both bar chart and time-course (Unpaired t-test, n. 26 cardiomyocytes, 14 controls and 12 TMAO treated from 5 animals).

4.2.3 The effects of 24 exposure to TMAO on K_{ir}6.1 channel open probability measured using cell-attached recording in cultured rat cardiomyocytes

With acute exposure to TMAO, it was shown that the activity of the Kir6.1 channel, as measured by the NP_o, was increased. To investigate whether the effects of longer-term exposure to TMAO on K_{ir}6.1 channel NP_o was similar, the cell-attached patch configuration was used. Cardiomyocytes were perfused with NT to record channel activity. Following this, the solution was exchanged for TMAO 100 µM for the rest of the recording. In these experiments the NP_o was measured in NT conditions (control was no incubation with TMAO). The pipette potential was held at +40 mV with 140 mM K^+ in pipette solution, which, assuming a resting membrane potential of -70 mV, gives an approximate membrane potential of around -110 mV across the cell-attached patch. These parameters were applied in all cell-attached recordings. In every patch, a channel with a single channel current of ~5 pA can be observed in normal physiological resting conditions (Figure 4.4 A).

Figure 4.4 B shows the open probability of K_{ir}6.1 channel in control cultured cells and in cells exposed to 100µM TMAO for 24h while figure 4.4 C shows NP_o of K_{ir}6.1 channel in control cultured cells and in cells exposed to 100µM TMAO for 24h. In both these figures it is evident that TMAO did not cause any significant increase in both the open probability and NP_o of K_{ir}6.1 channel.

In addition, during the cell-attached protocol used to detect activation of K_{ir}6.1 channel, it was noted that the cells exposed for 24h to TMAO 100 µM did not show any activation of chloride current, in contrast to what was found in the acute exposure of cardiomyocytes to TMAO.

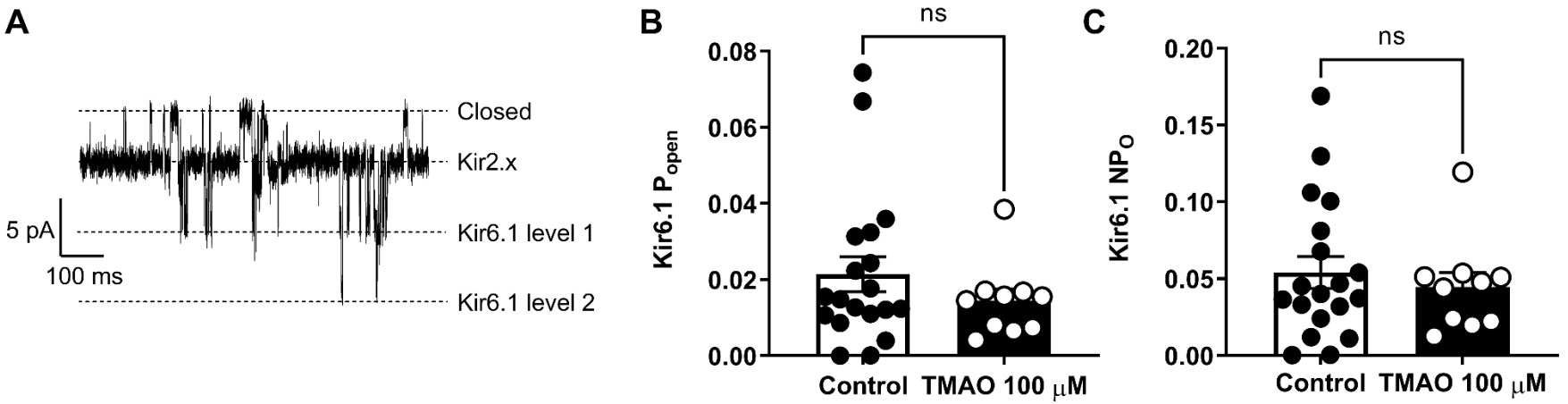

Figure 4.4. Effects of 24h exposure to 100μM TMAO on K_{ir}6.1 channel open probability. **A:** Example trace of a cell-attached patch recording with expanded segment on K_{ir}6.1 channel opening. **B:** Bar chart showing the number of openings of K_{ir}6.1 channels in control cells and in cells treated with 100μM TMAO for 24h. **C:** Bar chart showing the number of openings of K_{ir}6.1 channels in control cells and in cells treated with 100μM TMAO for 24h. TMAO caused no significant difference in the the NP_o of the channel. TMAO caused no significant difference in the open probabilities of the channel, unlike acute exposure to TMAO which caused an increase in the open probabilities of K_{ir}6.1 channel (Unpaired t-test, n. 19 controls and 10 TMAO treated from 4 animals)

4.2.3 The effects of 24-hour exposure to TMAO on K_{ir}6.2 channels open probability in the MI-activates currents measured using cell-attached recording in cultured rat cardiomyocytes.

With the acute-TMAO treatment, the activity of the Kir6.1 current was increased. In these experiments, it was hypothesised that the increased Kir6.1 activity would mean that the cell was partially cardioprotected and so would delay the opening of the Kir6.2/SUR2A complex that essentially acts as a metabolic sensor. From the data with the acute treatment of TMAO showing no change in Kir6.2 opening times, it was hypothesised that the increased calcium current counter-acted the calcium-sparing Kir6.1 activity. It was hypothesised that, given the lack off effect on Kir6.1 NP_o, the effects of long-term exposure to TMAO on K_{ir}6.2 activity would be minimal. To investigate this, the cell-attached patch configuration was to be used as described previously. Disappointingly, this data is only preliminary as the work was started just prior to laboratory closure due to the COVID pandemic and so was not completed.

Figure 4.5 A also shows the activation of the K_{ir}6.2 current (~10 pA) after MI due to the depletion of ATP and increase of intracellular ADP and the activity of the K_{ir}6.2 highlighted by the two different levels of opening.

Traces were analysed by looking for bursts of activity which fitted the criteria of being >10pA and ≥100ms or ≥500ms, as this duration would exclude any spontaneous burst of activity that can occur which have not been induced by MI. Figure 4.5 B shows the mean time taken to detect a burst of K_{ir}6.2 activity lasting longer than 100ms in control cultured cells and TMAO treated cells during MI perfusion while figure 4.5 C shows the mean time taken to detect a burst of K_{ir}6.2 activity lasting longer than 500ms in control cultured cells and TMAO treated cells during MI. These preliminary data show that long term exposure to TMAO did not cause any significant difference in the activation of K_{ir}6.2, re-confirming that K_{ir}6.2 activity is not modulated by the metabolite.

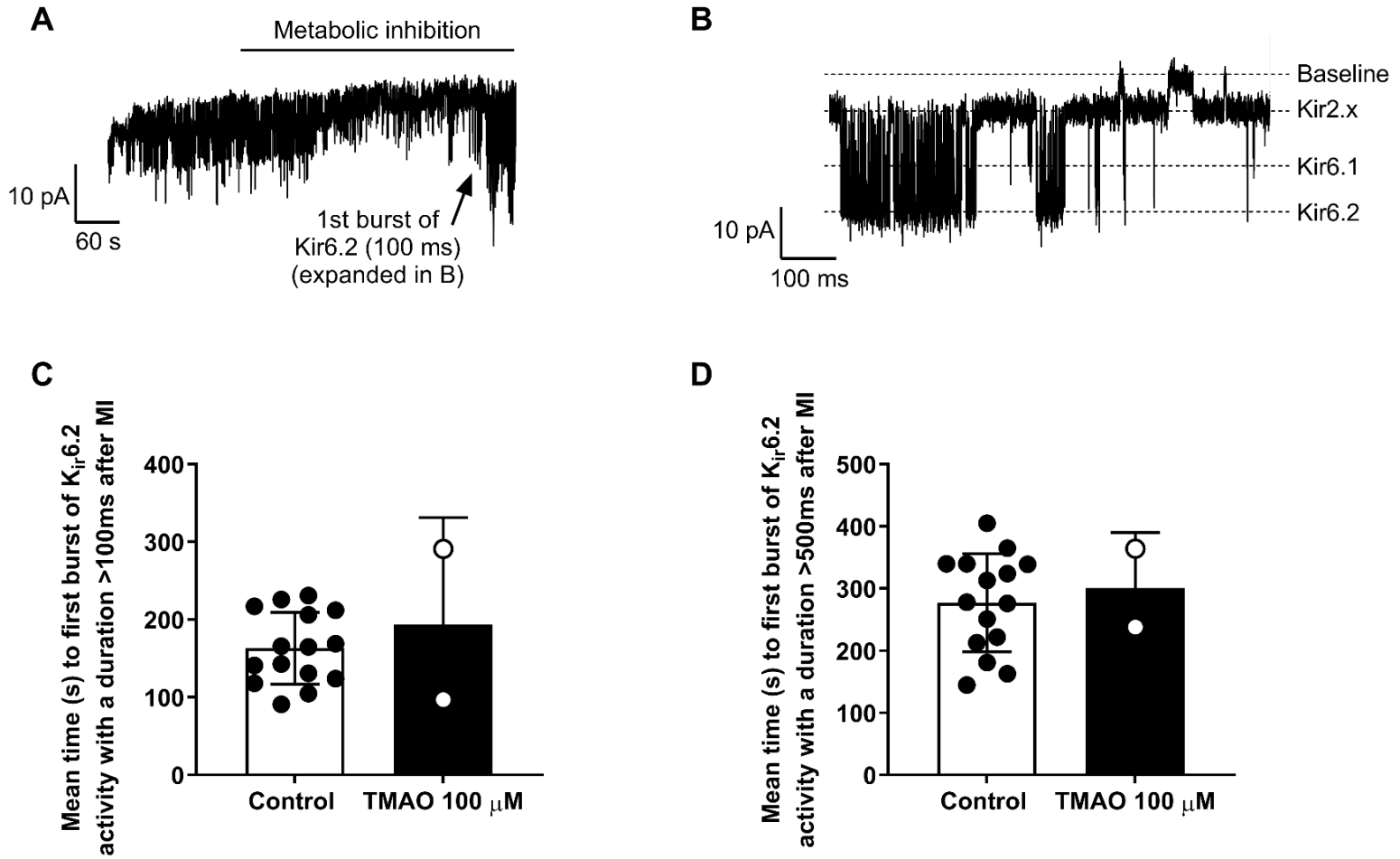

Figure 4.5. Effects of 24h exposure to 100µM TMAO on K_{ir}6.2 channels activity in cardiomyocytes exposed to TMAO during patch clamp electrophysiology cell-attached configuration recording. **A**: Example trace of single cell recording with **(B)** focus on first burst of activity of K_{ir}6.2 channels. **C:** Bar chart showing the average time taken to detect a burst of K_{ir}6.2 activity lasting longer than 100ms in control cells and TMAO treated cells after MI (or combination of MI and 100µM TMAO) perfusion. **D:** Bar chart showing the average time taken to detect a burst of K_{ir}6.2 activity lasting longer than 500ms in control cells and TMAO treated cells after MI (or combination of MI and 100µM TMAO) (Unpaired t-test, n. 15 controls and 2 TMAO from 5 animals).

4.3 Discussion

In this chapter, data have been presented to further investigate the direct effects of TMAO on cardiac cells, this time focusing on a longer exposure of the cells to the metabolite. Using electrophysiological and pharmacological tools, the effects of this metabolite have been investigated in freshly isolated cardiomyocytes, cultured for 24h with or without the presence of TMAO.

In the literature, studies have discussed the ranges of concentrations of TMAO present in both plasma and serum of healthy patients and of patients with CVD or at risk of developing CVD. This has been investigated in order to both establish a reliable range of concentrations of the metabolite to use as a biomarker for CVD risk and to identify a suitable protocol to investigate TMAO's activity.

Pharmacokinetics studies on TMAO, and on its renal clearance in healthy human patients, reveal that TMAO has a small volume of distribution inside the human body (resulting in being roughly half of the volume of distribution of urea), and that TMAO has a higher renal clearance compared to urea and creatinine (219 ± 78 mL/min for TMAO; 55 ± 14 for urea and 119 ± 21 mL/min for creatinine) (Akesson et al., 1989; Hai et al., 2015). This particularly high renal clearance of TMAO suggest that the metabolite is excreted both through glomerular filtration and through tubular secretion (50% of it at least) (Velasquez et al., 2016).

A study from Cho et al. (2017), based on previous findings, and their own evidence, concluded that TMAO has a plasma half-life of roughly 4h, and a human study by AlWaiz et al. (1987), performed with radio-labelled TMAO, concluded that TMAO was completely excreted within 24h from its synthesis, 94.5% in the urine, 4% in the faeces and less than 1% in breath. Based on these evaluations, it was concluded that an exposure to TMAO of 24h, corresponding to the time of complete excretion of TMAO from the human body, was the optimal way to investigate whether the effects of TMAO evidenced with acute exposure of the cardiomyocytes to the metabolite are sustained in a longer exposure, replicating a normal physiological condition.

Apart from the time of exposure, another important factor to consider in replicating normal physiological conditions are the range of concentrations of TMAO, based on diet and variability of plasma and serum levels found in the literature. Several studies have focused on describing TMAO levels. A study from C. A. Miller et al. (2014) described how a single intake of 6 egg yolks (roughly corresponding to 714 mg of choline) resulted in TMAO levels reaching between 2–20 μM after 8h from consumption and these levels returning to basal after 24h. Despite this, in a study with 30 healthy males, fasting plasma TMAO concentrations did not change after 4 weeks of regular ingestion of 400 mg/d choline (Lemos et al., 2018) confirmed by another study where 38 subjects consumed up to 3 eggs per day for 4 weeks, resulting in an increase in plasma levels of choline but not TMAO plasma levels (DiMarco et al., 2017). Other studies have focused on the levels of TMAO caused by sea food consumption. In particular, it was reported that sea food consumption caused an increase in postprandial urinary excretion of TMAO after 24 h equivalent to a diet with supplementation of 2100 mg choline, 2970 mg L-carnitine, or 1670 mg TMAO in healthy volunteers (A. Q. Zhang et al., 1999). Furthermore, in a study on 40 healthy young men, consumption of meals containing fish that produced TMAO, led to a significant increase in postprandial plasma TMAO levels, that reached its peak at roughly 150 μM, after 2 h post meals. However, egg or beef consumption, providing choline and L-carnitine, respectively, did not result in significant increase in TMAO plasma levels (Cho et al., 2017). Another study, on 113 heathy omnivore volunteers, showed that a diet high in red meat (which provided roughly 258 mg L-carnitine and 573 mg choline daily), consumed for 4 weeks, was enough to cause and increase in plasma levels of TMAO from a median level of 3.5 μM TMAO to 7 μM (Z. Wang et al., 2019). In this study, it was revealed that TMAO was mainly produced from L-carnitine, thanks to isotope tracing experiments, and that a diet rich in meat (both white and red meat) caused a minor decrease in fractional renal TMA excretion, which could be an explanation for the increase of plasma levels of TMAO (Z. Wang et al., 2019). Furthermore, it was reported that the Atkins diet, a diet particularly rich in red meat, caused an increase in plasma TMAO levels from 1.8 μM to 3.3 μM (Park et al., 2019). Finally, it was reported that a single consumption of 170 g of beefsteak did not result in a significant increase in postprandial mean plasma TMAO levels, which peaked only 1 h after consumption (Cho et al., 2017; Papandreou et al., 2020). In conclusion, it is likely

that there would be transient, but not sustained levels of TMAO under normal physiological conditions.

Several studies have focused on comparing levels of TMAO in healthy patients and patients affected by a different CVD. In a study, the reported serum levels of TMAO in stroke ranged from 0.5 to 18.3 μM, with a median value of 5.8 μM, which was reportedly higher than the serum levels detected in controls patients, that ranged between 2.6 to 6.1 μM, with a median value of 3.9 μM. On the other hand, the median level of serum TMAO content in those patients was significantly lower than in moderate-to-high stroke patients, reported to be between 4.1 μM vs. 9.1 μM (Rexidamu et al., 2019). Missailidis et al. (2016) compared plasma concentration of TMAO in 80 controls and 179 CKD patients and showed that elevated TMAO levels are strongly associated with degree of renal function. Another study that focused on CKD patients, Kaysen et al. (2015), in which they analysed serum levels of TMAO in 235 haemodialysis patients and showed that serum TMAO concentrations (28–67 μM) were higher in these patients compared to patients with normal or near normal kidney function (1.41 ± 0.49 μM). Furthermore, Bain et al. (2006) reported that plasma levels of TMAO in pre-dialysis patients (99.9 ± 31.9 μM) were significantly higher than the levels evaluated in healthy subjects (37.8 ± 20.4 μM). In addition, plasma levels of TMAO were decreased by roughly 60% with a single haemodialysis session and kidney transplantation caused a significant reduction in TMAO plasma levels (Stubbs et al., 2016; Velasquez et al., 2016).

Finally, in a more recent study by Gessner et al. (2020), in healthy patients the levels of TMAO were reported to be 1.28 to 19.67 μmol/L for men and for women as 1.08–17.12 μmol/L. Interestingly, these values were similar to levels of TMAO found in another group of healthy individuals in a study by Wang et al. (2014), but it also overlaps with values reported in patients with a confirmed cardiovascular event (Tang et al., 2013), or in patients with CKD (Stubbs et al., 2016).Thus, both plasma and serum levels of TMAO have been used in numerous different cohorts to fully define a range of active TMAO concentrations, but no unequivocal answer has emerged yet.

Cell culture experiments in the literature that aim to investigate the link between TMAO and CVD, both in acute treatments and in chronic treatment with the metabolite, have been performed using very different ranges of concentrations and different cell lines. Amongst these, the first studies aimed at delineating the effects of TMAO on the development of atherosclerotic plaques and its effects on endothelial cells. In cultured carotid artery endothelial cells, 30 μM TMAO was found to modulate different inflammatory pathways, such as an increase in caspase 1 activity, enhanced IL-1β production, which led to inflammasome formation that was hypothesized to be at the basis of the generation of atherosclerotic plaque formation (Boini et al., 2017). On a similar premise, Chou et al. (2019) showed that TMAO affected endothelial progenitor cells by promoting cellular inflammation and oxidative stress, while having detrimental effects on cellular function. These effects of TMAO were evident only when cells were cultured with 200 and 500 μM TMAO, while the same effects were not sustained by 2 μM or 100 μM TMAO. In addition, macrophages treated with increasing doses of TMAO up to 100 μM, showed no effect on atheroma formation, when its effect was evaluated on foam cell formation (Collins et al., 2016).

Interestingly, W. Zhu et al. (2016) in their study on the effects of TMAO on platelet hyperreactivity and thrombotic risk, found that plasma levels of TMAO in a cohort of sequential subjects undergoing elective diagnostic coronary angiography showed a "large dynamic range" of 0.06 to 312 μM, which has informed the choices of studies, and the experiments in this study, of performing experiments with a concentration of 100 μM of TMAO, which they determined to be "physiologically relevant".

Studies on a direct effect of TMAO on cardiomyocytes are just beginning to be published. The first work that treated cardiomyocytes with different concentrations of TMAO was published by Savi et al. (2018), in which 20 or 100 μM TMAO was used. Timings of treatment with TMAO were not mentioned, but it is likely that TMAO was used acutely, to prove that TMAO is able to affect cardiomyocyte contractility and intracellular Ca^{2+} handling and that co-treatment with Uro B-glucoronide, a molecule with anti-inflammatory properties, helped in the recovery of the cardiomyocyte functional properties, adding evidences of a possible modulation of inflammatory

pathways by TMAO. Another study performed in isolated rat cardiomyocytes, Querio et al. (2019), used 10 or 100 µM TMAO applied for 1 to 24h. In this study, TMAO was found to not have any significant effect on cell viability, sarcomere length, ROS production or mitochondrial membrane potential. Furthermore, the co-treatment with TMAO and molecules known to have a detrimental effect on cardiac cells function, like H_2O_2 and doxorubicin, did not cause any worsening of the negative effects caused by the cardiotoxic molecules.

Finally, in their study, Jaworska et al. (2019) demonstrated that neither 24h nor 72h treatment with TMAO were cytotoxic when used on the H9C2 cell line, a rat ventricular cardiac cell line, despite using concentrations of TMAO ranging from 0.1 to 100 mM These concentrations were notably much higher than the ones found in the plasma of both healthy patients (3.6 ± 0.4 µM) and in patients with severe aortic stenosis (5.5 ± 0.5 µM), in their own study and much higher than the concentration range observed in humans affected by CVD, as previously described. Furthermore, they proved that TMA, precursor of TMAO, at the same concentrations was not only affecting cell viability but was also causing cell shrinkage and detachment of the cells from the bottom of the plate, while TMAO was not capable of changing cell morphology and that cells maintained their normal morphology even after 10 days of treatment with TMAO. The only reputable effect they were able to associate with TMAO was that a lowered density of cell culture, suggesting that cell proliferation was affected, but not their survival.

Consistent with the literature, in this chapter we showed that the effects of 100 µM TMAO discussed in chapter 3, where acute exposure to the metabolite disrupted the normal contractile activity of cardiac cells, increased Ca^{2+} current inside the cells and modulated openings of $K_{ir}6.1$ channels, were no longer present when the experiments were performed following up to 24h exposure of the cardiac cells to the metabolite. Furthermore, in chapter 3, when the experimental protocol made it possible, time course of the acute exposure of TMAO throughout the experiments were analysed. These experiments showed that cells respond very quickly to the exposure to TMAO and, likewise, show that washout of TMAO on the cells remove the effects of TMAO as quickly. Combined with the data shown in chapter 4 on the absence of a significant

effect of TMAO during the 24h exposure, it is possible to infer hints on the mechanism behind the link between TMAO and its effects on cardiac cells.

When a signalling molecule binds to its extracellular receptor, usually the first reaction happens directly on ion channels and it affects their modulation and on molecular phosphorylation patterns of intra-cellular signalling molecules, and it is a very quick process. In contrast, modulation of signalling molecules and ion channel by alteration of gene expression by exogenous factors requires a longer time. Not only gene expression changes require a longer time to happen but the effects of a modulation of gene expression remain for a longer period of time. Taken these considerations into account, it is reasonable to infer that TMAO does not affect ion channel modulation by altering their gene expression, otherwise it would require a much larger window of time to execute its effects than shown in the time-course experiments on action potentials and on the ionic currents performed in chapter 3, and its effects would probably show in a long-exposure treatment like the ones performed in chapter 4.

Given the current data in this study, the mechanism(s) of the modulation of the currents are not clear. With additional time, further investigation of the molecular mechanism of the modulation of ionic currents would be carried out. Given the data recorded, and the speed at which the changes in calcium current were initiated on perfusion with TMAO, it is likely that there is either a direct modulation of the channel, or that there is an alteration of the lipid environment around the channels that promote their activity. On perfusion with TMAO, the calcium current, and action potential changes, occur within seconds of the beginning of perfusion. This immediacy suggests a direct effect that is independent of signalling processes. However, with limited further evidence this is currently supposition.

In conclusion, long-term (24h) administration of TMAO to cultured cardiomyocytes does not have an impact on modulation of ion channel function. The effects manifested in the acute administration of TMAO in isolated cardiomyocytes as a change in the action potential and an effect on calcium homeostasis, are no longer significant in a chronic model. To further investigate the potentially deleterious effects of TMAO on cardiomyocyte function and to analyse a possible mechanism of action that resolves he

link between TMAO and CVD, modulation of cardiac energy metabolism by TMAO and its effects on normal mitochondrial function will be investigated in Chapter 5.

Chapter 5

Cardiac energy metabolism and effects of TMAO on normal mitochondrial function

5 Cardiac energy metabolism and effects of TMAO on normal mitochondrial function

5.1 Introduction

In the previous chapters, it was demonstrated that acute treatment of freshly isolated cardiomyocytes with TMAO caused an increased calcium current, increased Kir6.1 channel activity and reduced contractile function following an ischaemia and reperfusion protocol. It was also demonstrated that isolated cardiomyocytes cultured for 24h with or without TMAO did not yield the same results as seen in the acute treatment with TMAO. Despite this lack of effect in chronic treatment with TMAO, there was a marked reduction of contractile recovery following ischaemia in freshly isolated cells treated with TMAO. This concentration-dependent effect of TMAO suggests that either TMAO was interfering with the contractile properties of the cardiomyocytes, or perhaps more likely, that TMAO is having an effect on mitochondrial function.

The findings in Makrecka-Kuka et al. (2017), suggest that mitochondrial function is modulated by TMAO, however other studies have not shown such alterations in mitochondrial function. It was hypothesised that the disruption of contractile recovery, but not a corresponding increase in cell death following ischaemia, could be explained by a reduction, but not complete abolition, of ATP synthesis during reperfusion in a TMAO concentration-dependent manner. Indeed, a reduction in ATP could cause a cessation of contraction whilst still retaining enough ATP to drive the Ca^{2+} homeostasis pathways.

Based on the results of this study so far, in this chapter, experiments are going to focus on further investigating the potentially deleterious effects of TMAO on cardiomyocyte function by analysing a possible mechanism of action that links TMAO and CVD. It is hypothesised that there is a modulation of mitochondrial function to yield a reduced ATP in the presence of TMAO. In this chapter the effects of TMAO on normal mitochondrial function, and therefore cellular energy metabolism, will be investigated.

5.2 Results

5.2.1 ATP determination in H9C2 cardiac cells exposed to increasing concentrations of TMAO

To investigate the effects of TMAO in pathways relating to mitochondrial dysfunction, a simple, high-throughput assay was employed to address this hypothesis *in vitro*. The quantitation of ATP is generally used as an index of both cell proliferation and viability. However, when data derived from these types of experiments are used in combination with other markers of cell viability, ATP content can be used to assess the effects of treatment on cellular bioenergetics and mitochondrial function. Since biosynthesis of ATP is a finely regulated process, any molecule or compound that is able to alter mitochondrial bioenergetics will most likely be able to lower ATP concentrations before a loss of cell viability or induction of cytotoxicity is detected (Mingatto et al., 2002)

In this study, the effects of TMAO on ATP content were compared to assess mitochondrial function following treatment. Experiments were carried out using an established rat cell line, H9C2 and cells were treated with different concentrations of TMAO ranging from 1-300 µM for the same duration (24 hours), and ATP content was indirectly determined. In this protocol, ATP production is directly correlated to the amount of light produced though the assay, as outlined in section 2.10. A negative control, represented by treatment of the cells with water that caused irreversible cell death, was included.

H9C2 cells were cultured in two different experimental environments: either in low glucose media or in high glucose media. Since hyperglycaemia is associated with myocardial damage and worsening of cardiac parameters during acute coronary syndrome through alteration of mitochondrial, caused by overload of $[Ca^{2+}]_i$ and low levels of ATP (Brennan et al., 2019), it was important to evaluate the effects of TMAO in both a more physiological environment (replicated by culturing the cells in low glucose

media) and in an altered environment were an excess of substrates was present (replicated by culturing the cells high glucose media).

Figure 5.1 A compares ATP production in H9C2 cells cultured in low glucose media and treated with different concentrations of TMAO ranging from 1-300 μM for 24h while figure 5.1 B compares ATP production in H9C2 cells cultured in high glucose with the same TMAO conditions. TMAO did not cause any significant differences in ATP production in either media environments (high glucose and low glucose media). Despite this, it is important to note that 300 μM of TMAO showed a reduction in ATP production, compared to the rest of the concentrations of TMAO, in both experimental conditions.

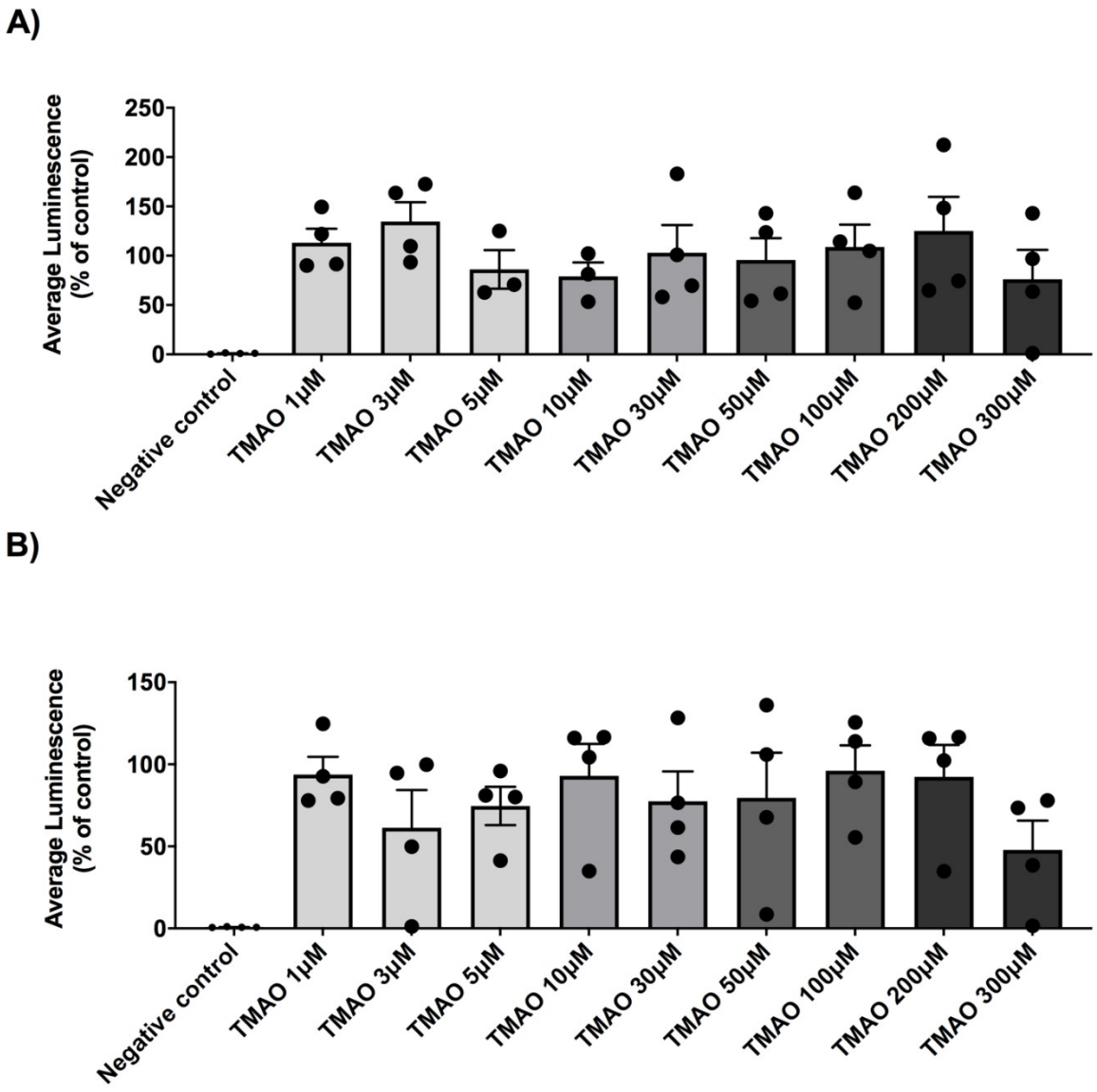

Figure 5.1. Effects of increasing concentrations of TMAO on ATP production in H9C2 cell line. A: Bar chart comparing ATP production in H9C2 cells cultured in low glucose media and treated with different concentrations of TMAO ranging from 1-300 µM for 24h. **B:** Bar chart comparing ATP production in H9C2 cells cultured in high glucose media and treated different concentrations of TMAO ranging from 1-300 µM for 24h. TMAO did not significantly affect ATP production in either media environments (high glucose and low glucose media). Despite changes in ATP production were not significant, it is of note that 300 µM of TMAO showed a reduction in ATP production, compared to the rest of the concentrations of TMAO, in both the experimental conditions. Data were presented as percentage of control (one-way ANOVA; n. 4 experiments for each treatment).

Lastly, a comparison between three selected concentrations of TMAO in both culture conditions was performed. These three concentrations were chosen as representative based both on results from previous chapters and considerations on the pharmacokinetics of TMAO and will be used in future experiments to compare the

effects of TMAO in different metabolic conditions. A concentration of TMAO of 3 µM was chosen to simulate physiological concentrations of TMAO found in the plasma of healthy patients, while 100 and 300 µM were chosen as physiologically relevant to simulate levels of TMAO found in patients with altered conditions and after a diet rich with TMAO and TMAO-precursors, as consistent with the literature.

Figure 5.2 compares side-to-side the effects of three different key concentrations (3, 100 and 300 µM) of TMAO on ATP production in H9C2 cells cultured in high glucose or in low glucose media. In all the concentrations of TMAO, ATP production was lower in the cells cultured in high glucose media compared to the corresponding concentration of TMAO in cells cultured in low glucose media, albeit in a non-significant manner.

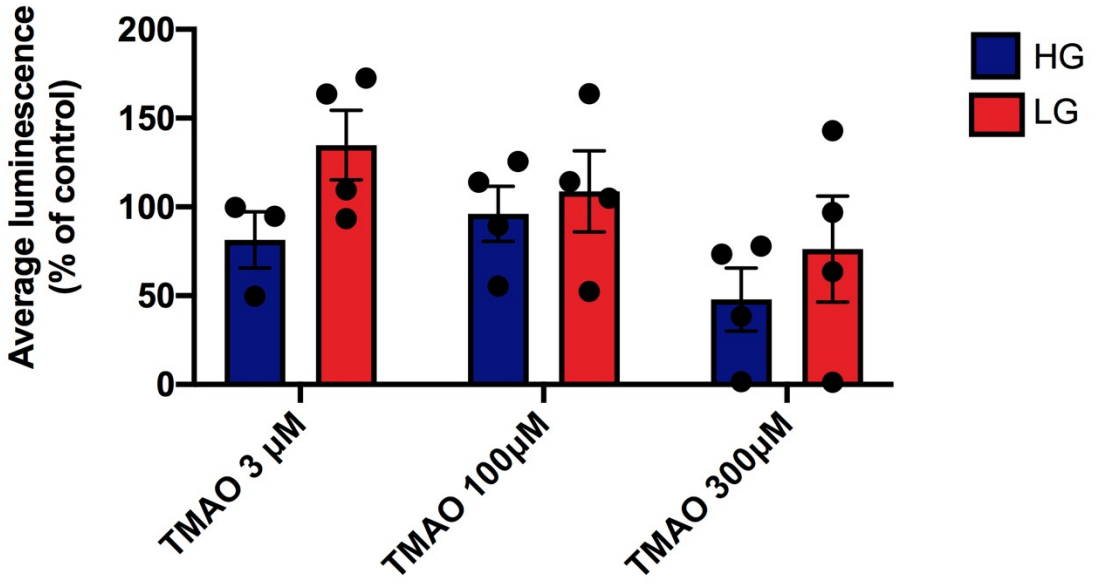

Figure 5.2. Side-to-side comparison of ATP production in H9C2 cells cultured in different media. Bar chart comparing the effects of three different key concentrations (3, 100 and 300 µM) of TMAO on ATP production in H9C2 cells cultured in high glucose or in low glucose media. In all the concentrations of TMAO, ATP production was lower in the cells cultured in high glucose media compared to the corresponding concentration of TMAO in cells cultured in low glucose media, albeit in a non-significant manner. Data were presented as percentage of control (two-way ANOVA; n. 4 experiments for each treatment).

5.2.2 Mitochondrial function of AC16 cardiac cells exposed to increasing concentrations of TMAO study using the Seahorse XF analyser

The mitochondrial stress test, fully described in section 2.12.1, was used to investigate the effects of TMAO on the mitochondrial function of AC16 cells cultured in high glucose and low glucose media.

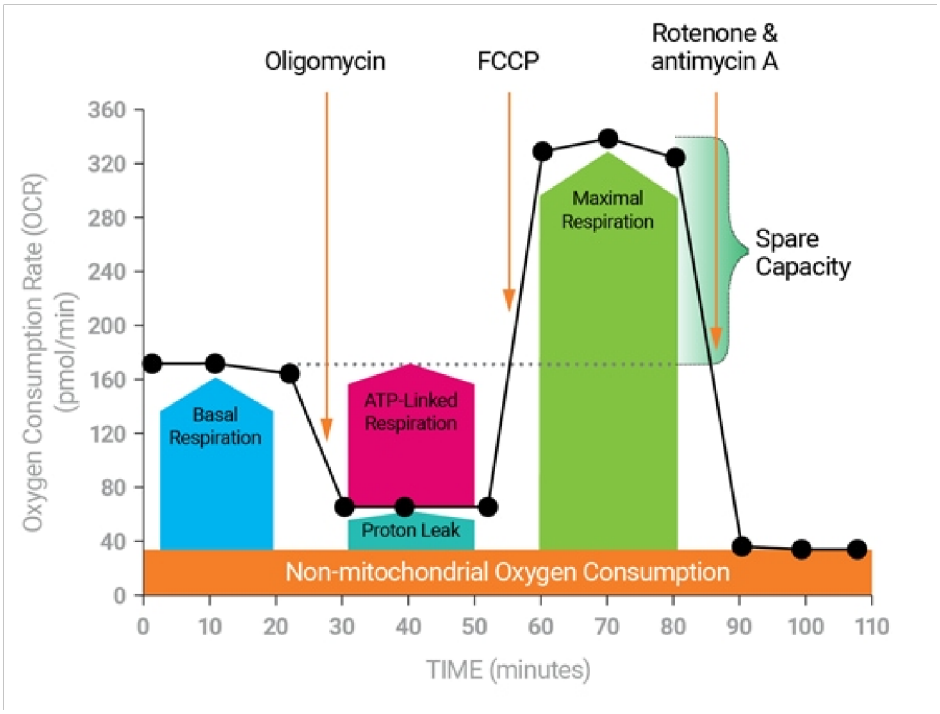

Figure 5.3. A typical profile of the mitochondrial stress test to assess mitochondrial function. In the first step, different concentrations of TMAO were injected on the plate and basal OCR was evaluated. Following the measurement of basal respiration, oligomycin was injected into each well, followed by 3 cycles of mix and wait and 3 min measurement to determine O_2 consumption resulting from proton leak. The difference between the basal OCR and the oligomycin-insensitive OCR, allow us to evaluate the amount of OCT that is ATP-linked. Then, FCCP was injected into each well, to determine the maximal respiration that is possible. The difference between FCCP rate and basal OCR allows us to estimate of the spare reserve capacity of the cells. Finally, a mixture of antimycin A and rotenone was injected into each well, allowing us to determine OCR from non-mitochondrial sites. Image modified from the Agilent Technologies website.

In the first step of the protocol, different concentrations of TMAO, ranging from 0.3 to 300 µM, were injected into the wells and the basal levels of OCR were measured. After basal OCR was established, AC16 cells treated with TMAO were exposed to the

metabolic inhibitors oligomycin, FCCP and a mixture rotenone and antimycin A at the timepoints indicated in figure 5.3. Figure 5.3 shows the typical profile of the mitochondrial stress test to assess mitochondrial function.

The measurements taken after each injection were used to calculate area under the curve (AUC) values for the mitochondrial function parameters, extrapolated as explained in figure 5.3; basal OCR, ATP-linked OCR, proton leak, maximal OCR, reserve capacity and non- mitochondrial OCR.

Figure 5.4 and figure 5.5 show real time measurements of OCR (figure 5.4 and figure 5.5 A) and ECAR (figure 5.4 and figure 5.5 B) for AC16 cells cultured in either high glucose (figure 5.5) or low glucose (figure 5.4) and treated with TMAO.

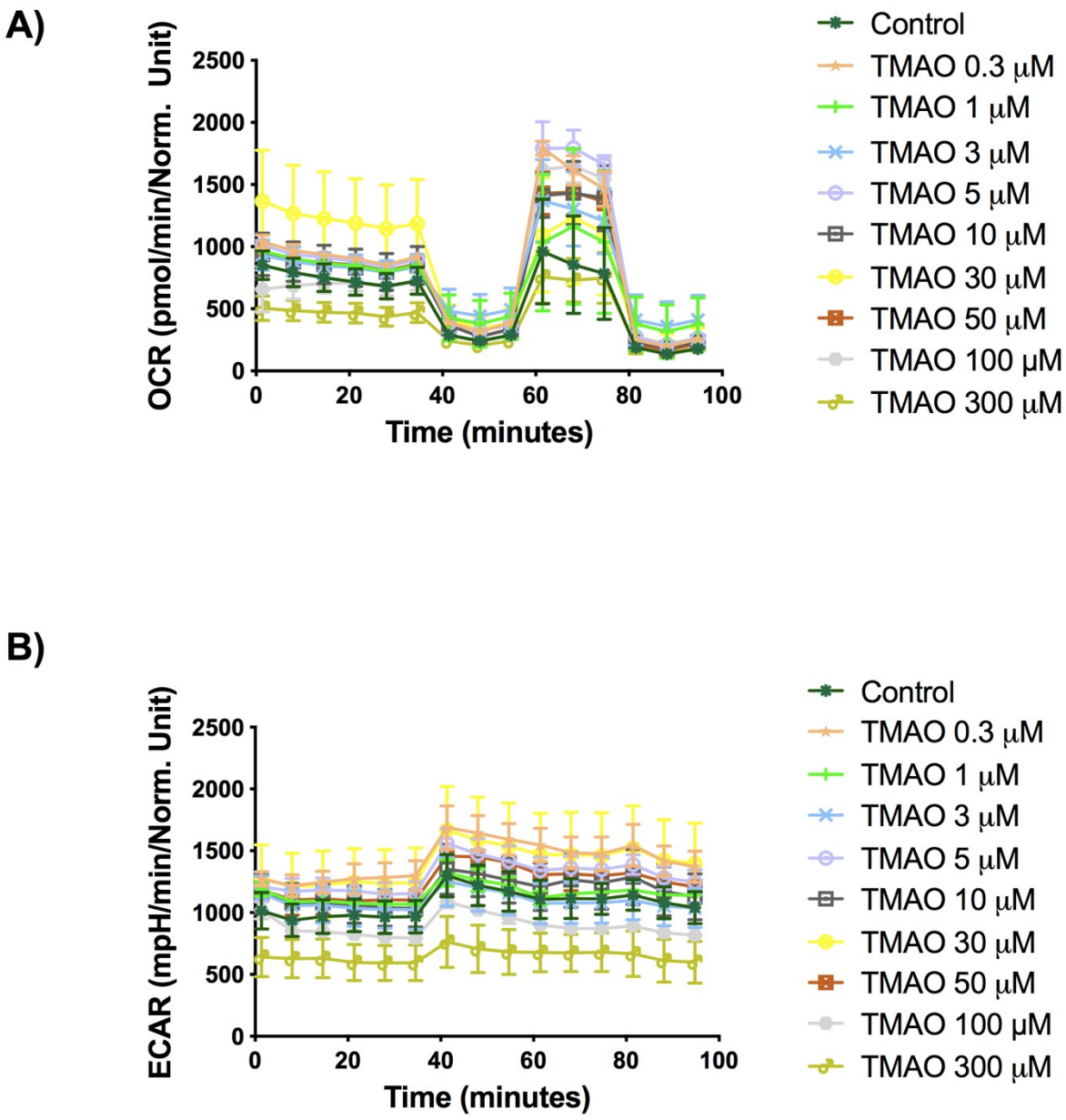

Figure 5.4. Effects of TMAO on cellular bioenergetics of AC16 cells cultured in low glucose media using the XF24 analyzer. AC16 cells were cultured for in low glucose media. Real time measurements of OCR **(A)** and ECAR **(B)** were measured and oligomycin, FCCP and antimycin A/rotenone were injected sequentially as shown (n. 3 experiments for each treatment).

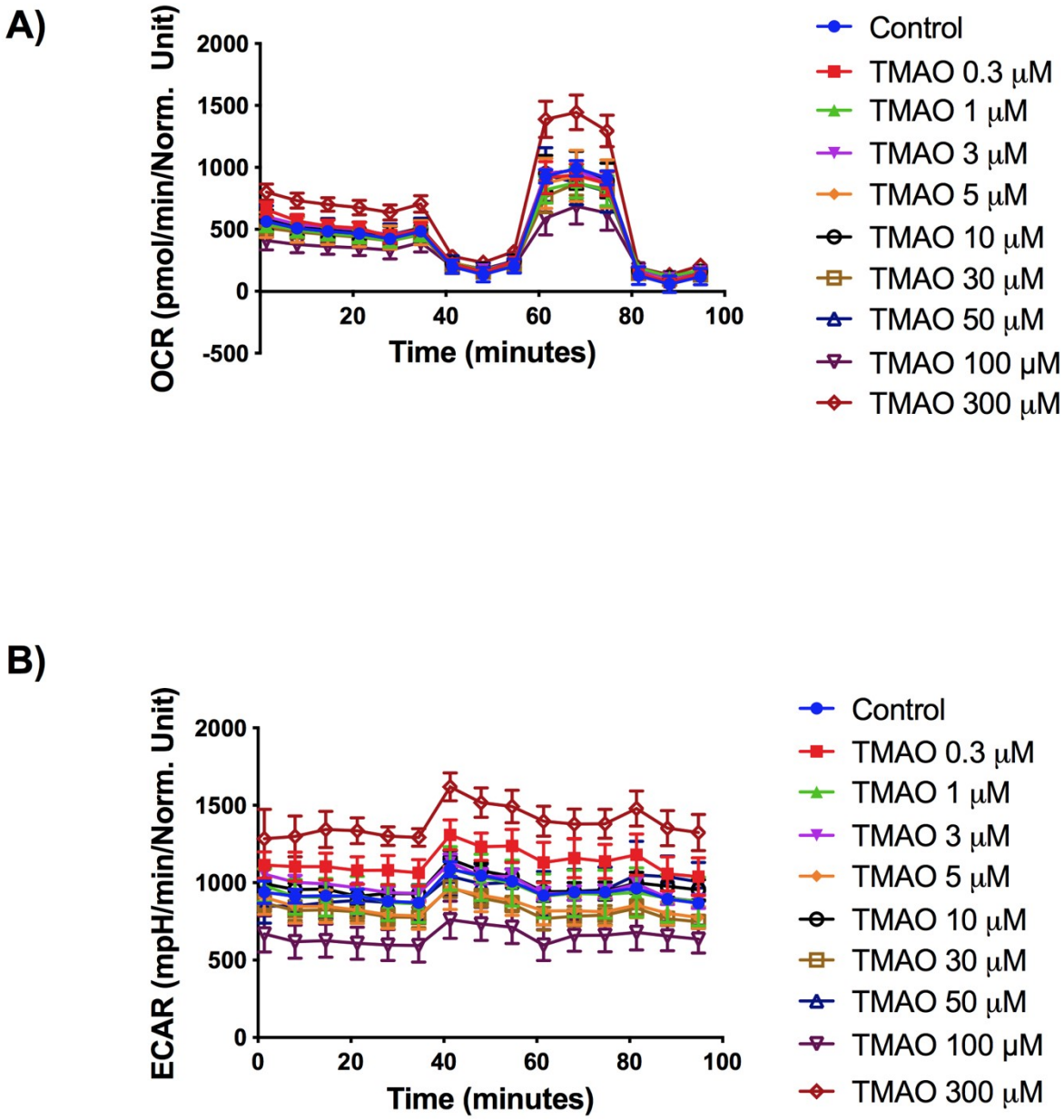

Figure 5.5. Effects of TMAO on cellular bioenergetics of AC16 cells cultured in high glucose media using the XF24 analyzer. AC16 cells were cultured for in high glucose media. Real time measurements of OCR **(A)** and ECAR **(B)** were measured and oligomycin, FCCP and antimycin A/rotenone were injected sequentially as shown (n. 3 experiments for each treatment).

Figure 5.6 shows the effects of increasing concentrations of TMAO on basal respiration in AC16 cell line; in panels A and B the effects of TMAO in high and low glucose media respectively, show that there were no significant changes in basal respiration. Despite non-significant changes in basal respiration, it is important to note that high concentrations of TMAO, in particular 100 and 300 μM of TMAO showed a reduction in

basal respiration compared to the rest of the concentrations of TMAO, in both the experimental conditions.

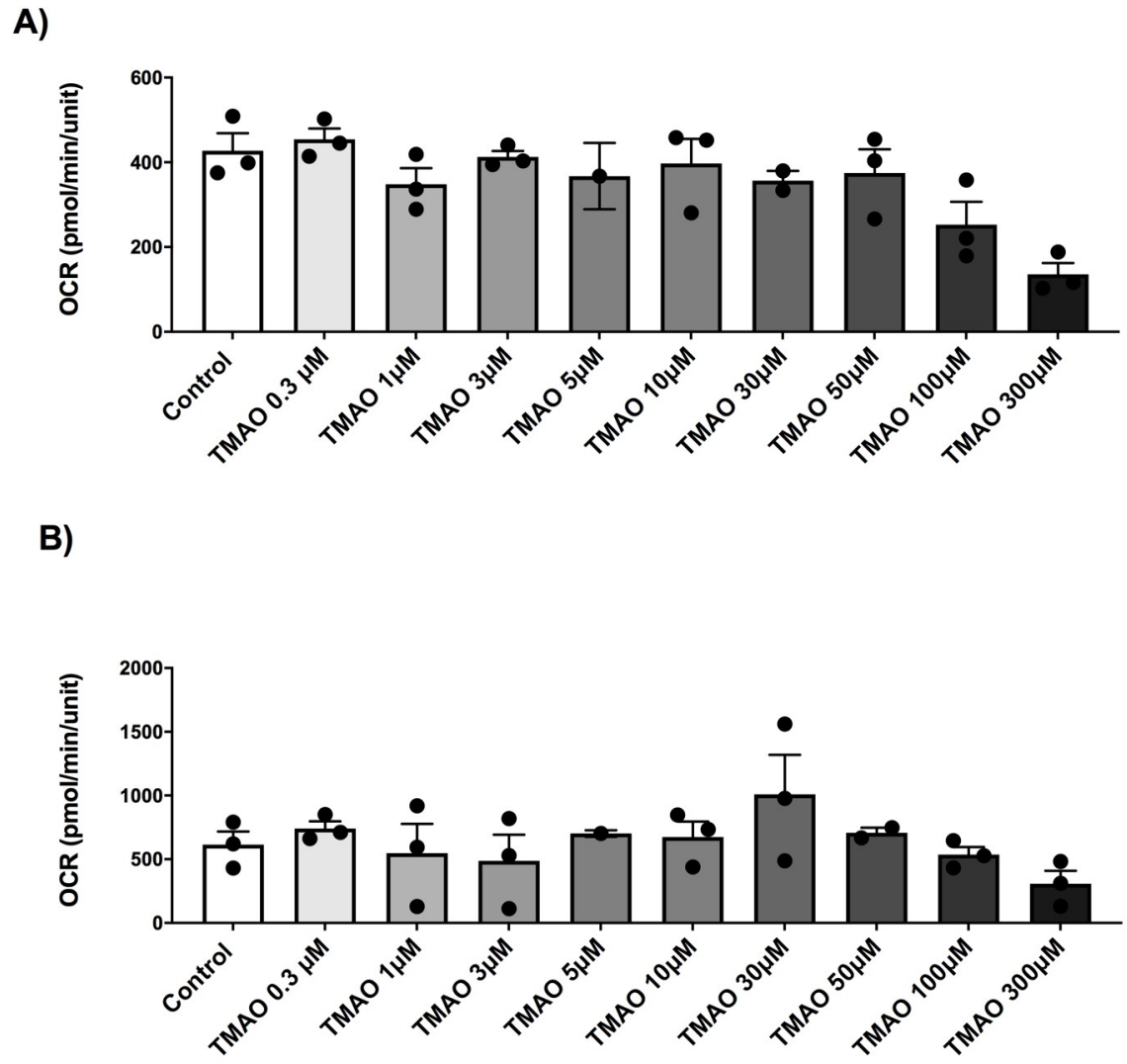

Figure 5.6. Effects of increasing concentrations of TMAO on basal respiration in AC16 cell line. A: Bar chart comparing basal respiration in AC16 cells cultured in high glucose media and treated with different concentrations of TMAO ranging from 0.3 to 300 µM. **B:** Bar chart comparing basal respiration in AC16 cells cultured in low glucose media and treated different concentrations of TMAO ranging from 0.3 to 300 µM. TMAO did not significantly affect basal respiration in either media environments (high glucose and low glucose media). Despite changes in basal respiration were not significant, it is of note that high concentrations of TMAO, in particular 100 and 300 µM of TMAO, showed a reduction in basal respiration, compared to the rest of the concentrations of TMAO, in both the experimental conditions (one-way ANOVA; n. 3 experiments for each treatment).

Figure 5.7 shows the effects of increasing concentrations of TMAO on maximal respiration in AC16 cell line; in panels A and B the effects of TMAO in high and low glucose media respectively, show that there were no significant changes in maximal

respiration. Similar to that shown in figure 5.6, 300 µM of TMAO showed a reduction in maximal respiration compared to the rest of the concentrations of TMAO, in both the experimental conditions.

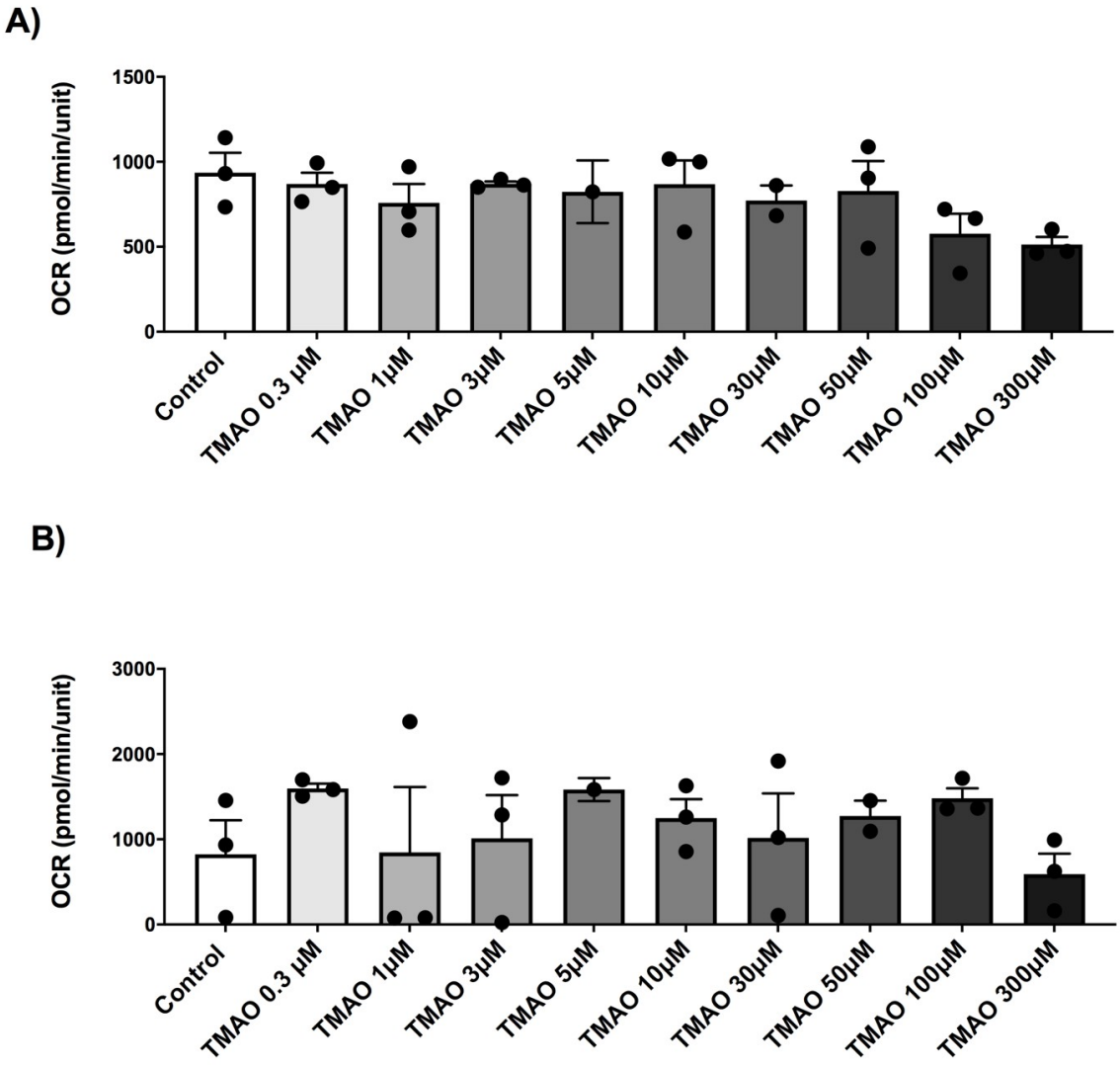

Figure 5.7. Effects of increasing concentrations of TMAO on maximal respiration in AC16 cell line. A: Bar chart comparing maximal respiration in AC16 cells cultured in high glucose media and treated with different concentrations of TMAO ranging from 0.3 to 300 µM. **B:** Bar chart comparing maximal respiration in AC16 cells cultured in low glucose media and treated different concentrations of TMAO ranging from 0.3 to 300 µM. TMAO did not significantly affect maximal respiration in either media environments (high glucose and low glucose media). Despite changes in maximal respiration were not significant, it is of note that high concentrations of TMAO, in particular 300 µM of TMAO, showed a reduction in maximal respiration, compared to the rest of the concentrations of TMAO, in both the experimental conditions (one-way ANOVA; n. 3 experiments for each treatment).

Figure 5.8 shows the effects of increasing concentrations of TMAO on ATP-linked respiration in AC16 cell line; in panels A and B the effects of TMAO in high and low glucose media respectively, show that there were no significant changes in ATP-linked respiration. In this case, two concentrations of TMAO, 100 and 300 µM, showed a reduction in ATP-linked respiration compared to the rest of the concentrations of TMAO, in both the experimental conditions.

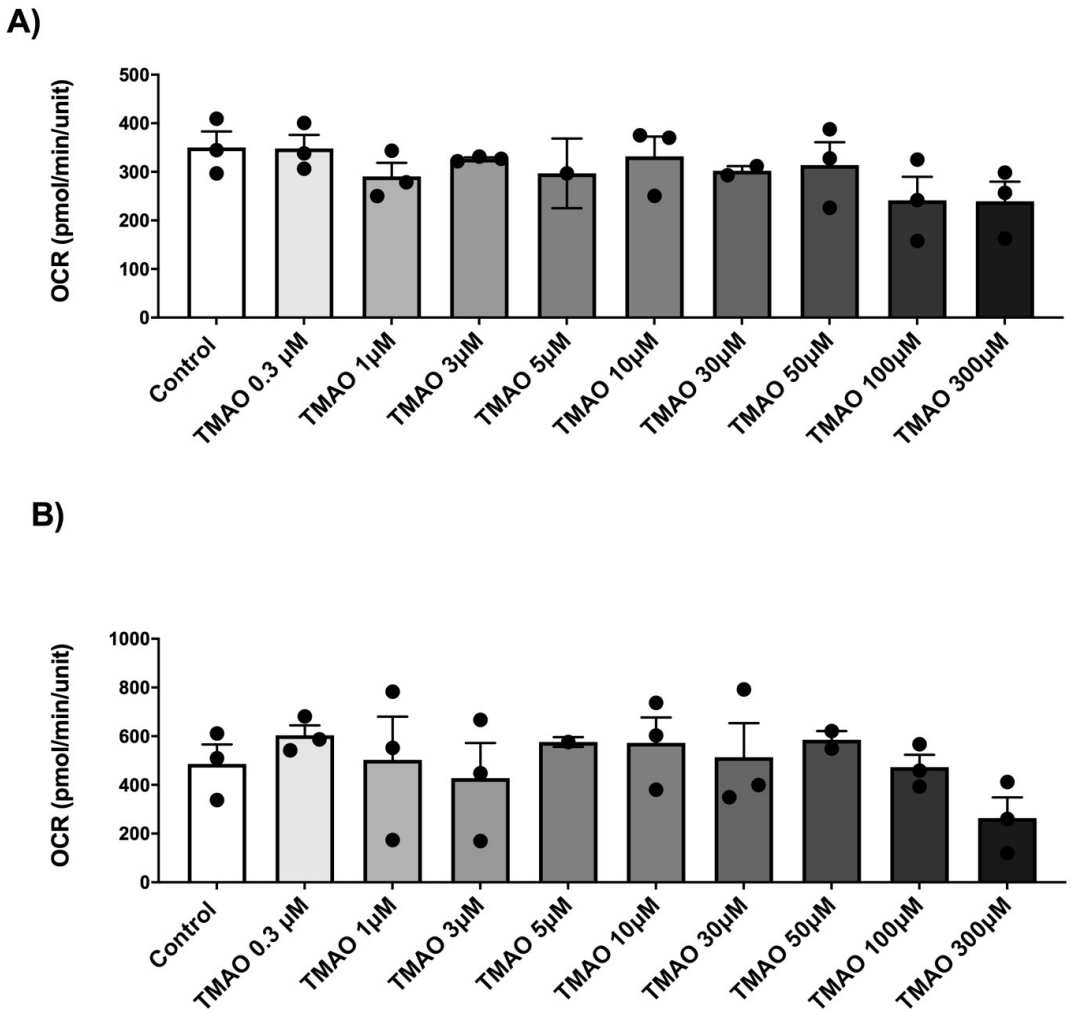

Figure 5.8. Effects of increasing concentrations of TMAO on ATP-linked respiration in AC16 cell line. A: Bar chart comparing ATP-linked respiration in AC16 cells cultured in high glucose media and treated with different concentrations of TMAO ranging from 0.3 to 300 µM. **B:** Bar chart comparing ATP-linked respiration in AC16 cells cultured in low glucose media and treated different concentrations of TMAO ranging from 0.3 to 300 µM. TMAO did not significantly affect ATP-linked respiration in either media environments (high glucose and low glucose media). Despite changes in ATP-linked respiration were not significant, it is of note that high concentrations of TMAO, in particular 100 and 300 µM of TMAO, showed a reduction in ATP-linked respiration, compared to the rest of the concentrations of TMAO, in low glucose environment (one-way ANOVA; n. 3 experiments for each treatment).

Figure 5.9 shows the effects of increasing concentrations of TMAO on spare respiratory capacity in AC16 cell line; in panels A and B the effects of TMAO in high and low glucose media respectively, show that there were no significant changes in spare respiratory capacity. In this case as well, 300 µM of TMAO showed a reduction in spare respiratory capacity compared to the rest of the concentrations of TMAO, in both the experimental conditions.

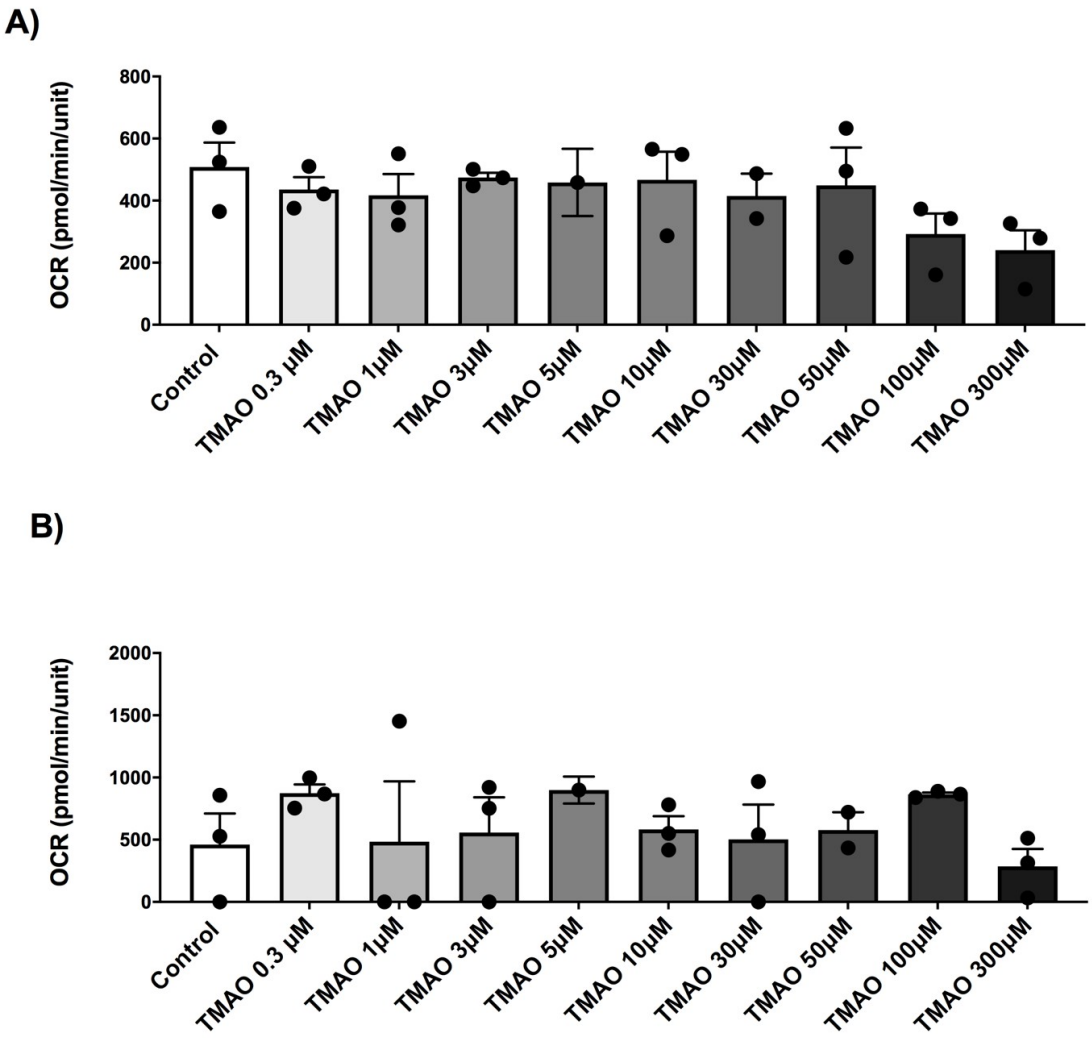

Figure 5.9. Effects of increasing concentrations of TMAO on spare respiratory capacity in AC16 cell line. A: Bar chart comparing spare respiratory capacity in AC16 cells cultured in high glucose media and treated with different concentrations of TMAO ranging from 0.3 to 300 µM. **B:** Bar chart comparing spare respiratory capacity in AC16 cells cultured in low glucose media and treated different concentrations of TMAO ranging from 0.3 to 300 µM. TMAO did not significantly affect spare respiratory capacity in either media environments (high glucose and low glucose media). Despite changes in spare respiratory capacity were not significant, it is of note that high concentrations of TMAO, in particular 300 µM of TMAO, showed a reduction in spare respiratory capacity, compared to the rest of the concentrations of TMAO, in both the experimental conditions (one-way ANOVA; n. 3 experiments for each treatment).

Figure 5.10 shows the effects of increasing concentrations of TMAO on proton leak in AC16 cell line; in panels A and B the effects of TMAO in high and low glucose media respectively, show that there were no significant changes in proton leak. Consistently with the rest of the results so far, high concentrations of TMAO, in particular 300 µM of TMAO, showed a reduction in proton leak, compared to the rest of the concentrations of TMAO, in both the experimental conditions.

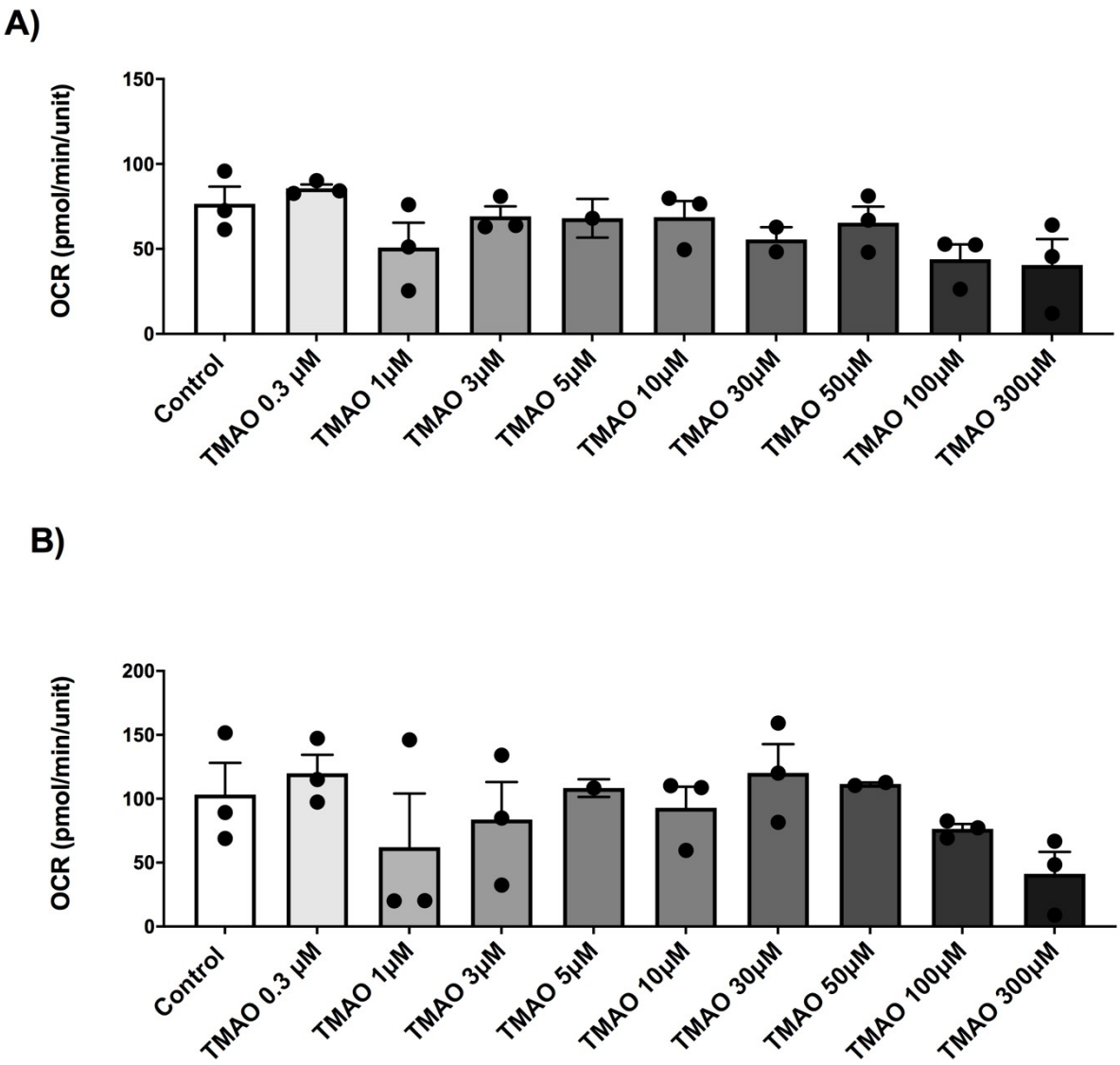

Figure 5.10. Effects of increasing concentrations of TMAO on proton leak in AC16 cell line. A: Bar chart comparing proton leak in AC16 cells cultured in high glucose media and treated with different concentrations of TMAO ranging from 0.3 to 300 µM. **B:** Bar chart comparing proton leak in AC16 cells cultured in low glucose media and treated different concentrations of TMAO ranging from 0.3 to 300 µM. TMAO did not significantly affect proton leak in either media environments (high glucose and low glucose media). Despite changes in proton leak were not significant, it is of note that high concentrations of TMAO, in particular 300 µM of TMAO, showed a reduction in proton leak, compared to the rest of the concentrations of TMAO, in both the experimental conditions (one-way ANOVA; n. 3 experiments for each treatment).

Lastly, in figure 5.11 shows a side-to-side comparison of the different parameters evaluated so far in this section in AC16 cells cultured in high glucose or in low glucose media, using three different key concentrations (3, 100 and 300 µM) of TMAO chosen based on previous results and evaluations. In particular, in figure 5.11 A shows the effects of TMAO on basal respiration, figure 5.11 B shows the effects of TMAO on proton

leak, figure 5.11 C shows the effects of TMAO on maximal respiration, and figure 5.11 D shows the effects of TMAO on ATP-linked. In all the concentrations of TMAO, the majority of parameters evaluated were lower in the cells cultured in high glucose media compared to the corresponding concentration of TMAO in cells cultured in low glucose media, albeit in a non-significant manner, except for proton leak in which the trend was reversed.

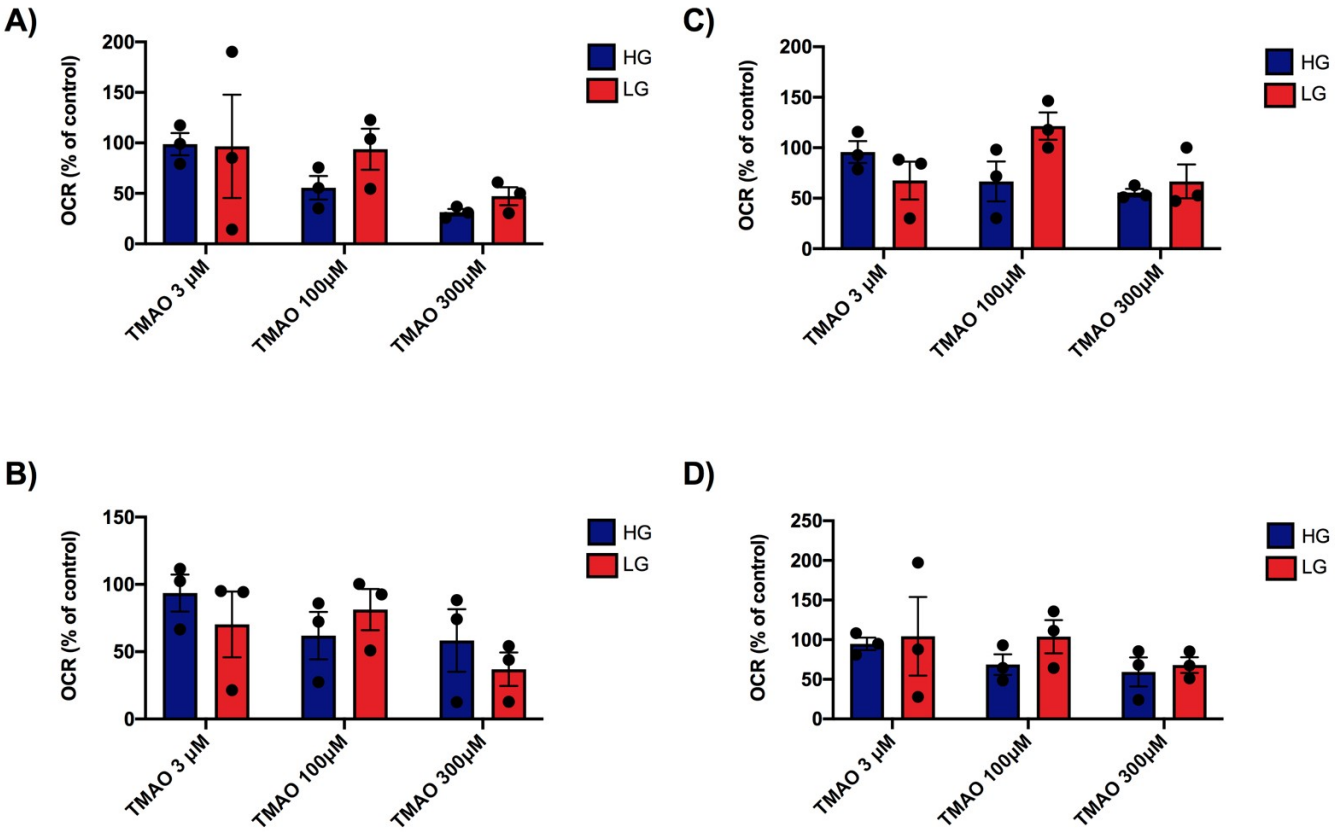

Figure 5.11. Side-to-side comparison of different parameters in AC16 cells cultured in different media. A: Bar chart comparing the effects of three different key concentrations (3, 100 and 300 µM) of TMAO on basal respiration in AC16 cells cultured in high glucose or in low glucose media. **B:** Bar chart comparing the effects of three different key concentrations (3, 100 and 300 µM) of TMAO on proton leak in AC16 cells cultured in high glucose or in low glucose media. **C:** Bar chart comparing the effects of three different key concentrations (3, 100 and 300 µM) of TMAO on maximal respiration in AC16 cells cultured in high glucose or in low glucose media. **D:** Bar chart comparing the effects of three different key concentrations (3, 100 and 300 µM) of TMAO on ATP-linked respiration production in AC16 cells cultured in high glucose or in low glucose media. In all the concentrations of TMAO, the majority of parameters evaluated were lower in the cells cultured in high glucose media compared to the corresponding concentration of TMAO in cells cultured in low glucose media, albeit in a non-significant manner, except for proton leak in which the trend was reversed. Data were presented as percentage of control (two-way ANOVA; n. 3 experiments for each treatment).

5.3 Discussion

In this chapter, data have been presented to further investigate the direct effects of TMAO on cardiac cells, focusing on the impairment of mitochondrial metabolism in the heart and the possibility of TMAO being an important player that increases the severity of cardiovascular events or that enhances the progression of cardiovascular diseases by modulating bioenergetic pathways inside the cell.

The first study that proposed that TMAO may have detrimental effects on mitochondrial activity was published by Makrecka-Kuka et al. (2017). In this study, it was highlighted that an increase in levels of TMAO was able to reduce both pyruvate and fatty acid oxidation, but was not able to cause any significant changes in modulation of the ETC. In particular, long-term administration of TMAO at a dose of 120 mg/kg for 8 weeks was found to increase TMAO concentration in plasma and cardiac tissues to about 15 µM (plasma levels) and 11 nmol/g (cardiac tissue) and was found to decrease mitochondrial substrate-dependent respiration by roughly 30% without affecting OXPHOS respiration. Furthermore, TMAO was found to be responsible for acting directly on fatty acid oxidation, by inhibition of β-oxidation and partial suppression of intake of energetic substrates by inhibition of pyruvate dehydrogenase enzymatic activity. Other important findings related to cardiac mitochondrial function that were brought to light in this study, were that no significant changes in mitochondrial ROS production were observed after acute exposure of cardiac fibres to TMAO under physiological conditions. In addition, it was found that TMAO does not inhibit citrate synthase, thus not affecting the Krebs cycle and because TMAO does not inhibit CPT I, –the authors inferred that TMAO exerts its activity by limiting fatty acid oxidation. The study concluded that increased levels of TMAO lead to impairment of pyruvate and fatty acid oxidation in cardiac mitochondria and was, thus, responsible for the accumulation of TMAO in cardiac tissues leading to disturbances in energy metabolism that can increase the severity of cardiovascular events.

On a similar premise, but with different conclusions, a more recent study from Querio et al. (2019) demonstrated that a long-term increase in plasma TMAO levels, up to 100 µM and a in cardiac tissue up to 140 nmol/g tissue, does not affect cardiac function. In this study, cardiomyocytes exposed to high concentrations of TMAO were found to show no cardiac tissue cell loss and no alterations of cardiac structure, as demonstrated from the evaluation of sarcomere length and cytoskeletal organization. Results from this study that were consistent with the previous findings from Makrecka-Kuka et al. (2017) were that they found no variation in ROS production, both in acute exposure and after 24 h of treatment and both in a cytoplasmic and a mitochondrial environment. Additionally, they demonstrated that TMAO had no effects on depolarization of mitochondrial membrane potential, reinforcing the narrative that TMAO had no direct detrimental effects on mitochondrial structure and function.

The results from this chapter confirm and reinforce these findings, further expanding and giving more detailed information as to what bioenergetic pathways are involved in explaining the effects of TMAO on cardiomyocytes. Furthermore, in this study different concentrations of TMAO ranging from 0.3 to 300 µM were used, giving a more comprehensive outline of the concentration-dependence of TMAO effects commonly found, according to the extensive literature, physiologically in the human body. These data partially address one of the concerns that Querio et al. (2019) cited as one of the "weaknesses" of their study. In particular, this study demonstrated that concentrations of TMAO ranging from 1-300 µM for 24h did not cause significant alterations of ATP production in two different lines of cardiomyocytes, H9C2, a rat cardiac cell line, and AC16, a human cardiac cell line. Furthermore, we demonstrated that TMAO did not cause significant changes in ATP production in two different experimental environments: one considered more similar to a physiological environment, replicated by culturing the cells low glucose media, and one considered more similar to an altered environment where an excess of substrates was present, replicated by culturing the cells high glucose media. Since changes in ATP production from exposure of the cells to TMAO were not significant, mitochondrial disruption intended as profound alterations of structure and function of the mitochondria can be excluded as a target for

mechanistic analysis of TMAO's activity. Only a concentration of 300 µM of TMAO, considered as an hyperphysiological concentration, showed a non-statistically significant reduction in ATP production in both the experimental conditions, compared to the lower concentrations of TMAO used and considered as more similar to physiological levels of TMAO, suggesting that only very high concentrations of TMAO could, potentially, be involved in mitochondrial dysfunction.

The use of ATP evaluation as an indicator of mitochondrial function, albeit useful in detecting alterations in cell viability, does not provide insight into the bioenergetic pathways involved into the possible dysfunction occurring. For this reason, extracellular flux analysis was used to provide more insight into the mechanisms of possible mitochondrial toxicity caused by TMAO, as changes in OCR are an established sensible tool to evaluate mitochondria function (Brand & Nicholls, 2011).

The treatment of AC16 cells with different concentrations of TMAO ranging from 0.3 to 300 µM did not result in significant changes in any of the OCR parameters measured, supporting the previous findings that the TMAO does not induce mitochondrial dysfunction in cardiac cells. In particular, out of all the data presented in this chapter, spare respiratory capacity is considered as the most sensitive parameter to mitochondrial dysfunction, and is usually reduced in experimental conditions that cause mitochondrial liability (Kamalian et al., 2018), and it was demonstrated that there was no significant decrease in spare respiratory capacity in cells treated with TMAO.

In these experiments it is of note that despite the changes in OCR parameters measured not being significant, it was found that the highest concentrations of TMAO used in the experiments (100 and 300 µM) showed a reduction in all of the OCR parameters, compared to lower concentrations of TMAO, in both the experimental conditions, reinforcing the hypothesis that only very high concentrations of TMAO could, potentially, be involved in mitochondrial dysfunction. This finding may shed light on whether TMAO is a protectant or toxic to cardiac cells.

Another important piece of information emerging from the study was found by comparing the effects of three different key concentrations (3, 100 and 300 µM) of

TMAO all of the OCR parameters in AC16 cells cultured in high glucose or in low glucose media. In all the concentrations of TMAO, the parameters evaluated were lower in the cells cultured in high glucose media compared to cells cultured in low glucose media. Although this data was not significant, these finding suggests that alteration in the cardiac cell's environment can also be of fundamental importance when investigating the effects of TMAO. Additional replicates of these experiments were planned prior to the laboratory lockdown due to coronavirus, however this was not able to be completed.

Lastly, a very recent study that expands on the findings from the results published by Makrecka-Kuka et al. (2017), concluded that long-term TMAO administration shifted mitochondrial energy substrate utilization from fatty acid oxidation to glucose metabolism (Videja et al., 2020). The basis of this study and of the conclusion published in this work are based on the heart shifting from fatty acid oxidation as a primary source of energetic substrates to glucose metabolism, as a way to react to pathophysiological stimuli (D. A. Brown et al., 2017). In normal conditions, this shift in metabolic resources in considered as preparation by the heart for possible future stress events, such as hypoxia caused by an adverse cardiac event. These preparations are aimed at preserving energy metabolism and subsequently improving cardiac function recovery after injury (Karwi et al., 2018). The study describes cardiac cells entering this stage of preparation after long-term administration of TMAO, when fatty acid oxidation was decreased in favour of pyruvate metabolism but without overall changes in cardiac functionality, suggesting that it is the increase in TMAO concentration to induce the previously described metabolic shift, through direct inhibition of β-oxidation, toward more efficient substrate metabolism.

The concluding observation of the study was that TMAO administration was responsible for cardioprotection of cells during HF, by preserving fatty acid oxidation and by being able to induce the cells to enter the metabolic switch, both of key importance in maintaining healthy cardiac bioenergetic in the event of ischaemic damage (Karwi et al., 2018; Kolwicz et al., 2012). The overall findings suggest that long-term increase in TMAO levels in both plasma and cardiac tissue do not exert detrimental effects on cardiac

function and could be interpreted as preservation of cardiac energy metabolism, possibly explaining protective effects of TMAO.

In conclusion, administration of different concentrations of TMAO to cultured cardiomyocytes (established cell line) does not have a significant impact on modulation of mitochondrial function. High concentrations of TMAO (300 µM and in some cases 100 µM) show a non-statistical difference in mitochondrial parameters that could, potentially, point to a possible detrimental effect of TMAO on normal mitochondrial function. Furthermore, alterations in the environmental conditions, specifically culture of the cardiac cells in media supplemented with hyper-physiological concentrations of glucose, exacerbated the effects of the higher concentration of TMAO on mitochondrial function. To further investigate the potentially deleterious effects of TMAO on cardiomyocyte function and normal mitochondrial function, changes in the culture conditions and co-treatment of cardiac cells with different concentrations of TMAO and known modulators of cardiac function and energetic metabolism of the cells will represent the scope of investigation in Chapter 6.

Chapter 6

Cardiac energy metabolism and effects of TMAO on mitochondrial function altered by changes in metabolic conditions

6 Cardiac energy metabolism and effects of TMAO on mitochondrial function altered by changes in metabolic conditions

6.1 Introduction

In the previous chapters, it was demonstrated that while administration of different concentrations of TMAO to cultured cardiac cells does not have a significant impact on modulation of mitochondrial function, high concentrations of TMAO (300 μM and in some cases 100 μM) show a difference in mitochondrial parameters that point to a possible detrimental effect of TMAO on normal mitochondrial function.

Based on the results of this study so far, in this chapter, experiments are going to focus on further investigating the potentially deleterious effects of TMAO on cardiomyocyte function and normal mitochondrial function, changes in the culture conditions and cotreatment of cardiac cells with different concentrations of TMAO and known modulators of cardiac function and energetic metabolism of the cells. In particular cardiac cells are pre/co-exposed to environmental conditions that alter the normal mitochondrial function, like the culture in galactose-supplemented media, that push the cells to a metabolic shift that caused the cells to produce ATP exclusively through OXPHOS or short-time exposure to high glucose, that was shown to alter mitochondrial function.

6.2 Results

6.2.1 Acute metabolic switch of energetic source from glucose to galactose on AC16 cardiac cells in presence of TMAO

Many tumour-derived cell lines prefer to produce the majority of their ATP via glycolysis instead of OXPHOS, despite having perfectly functioning mitochondria and normal, physiological levels of glucose and oxygen (Rodriguez-Enriquez et al., 2001; Warburg, 1956).

To force cells to rely on their OXPHOS for the production of ATP and, therefore, being able to fully investigate whether the compound under investigation has any detrimental effects on normal mitochondrial function, culture media can be replaced with a galactose-supplemented media (Dott et al., 2014; Marroquin et al., 2007). In this way, the assessment of ATP content and LDH retention in cells cultured in galactose media acts as an early marker of mitochondrial function.

AC16 cells were allowed to adapt to galactose media for 2h before experiments, as described by Kamalian *et al*., in which acute galactose conditioning for 2h prior to the treatments with the compound under investigation was sufficient to allow the cells to be more prone to mitochondrial toxicity (Kamalian et al., 2015).

In order to detect a possible TMAO-induced mitochondrial toxicity in the absence of significant cell death, cellular ATP content and LDH content were measured in AC16 cells acutely conditioned to glucose or galactose media, as described in section 2.9 and section 2.10. Figure 6.1 shows that while TMAO did not significantly affect LDH retention in either media environments (glucose and galactose media), high concentrations of TMAO (especially 300 µM of TMAO) caused an evident reduction in ATP production, compared to the rest of the concentrations of TMAO, in galactose supplemented media.

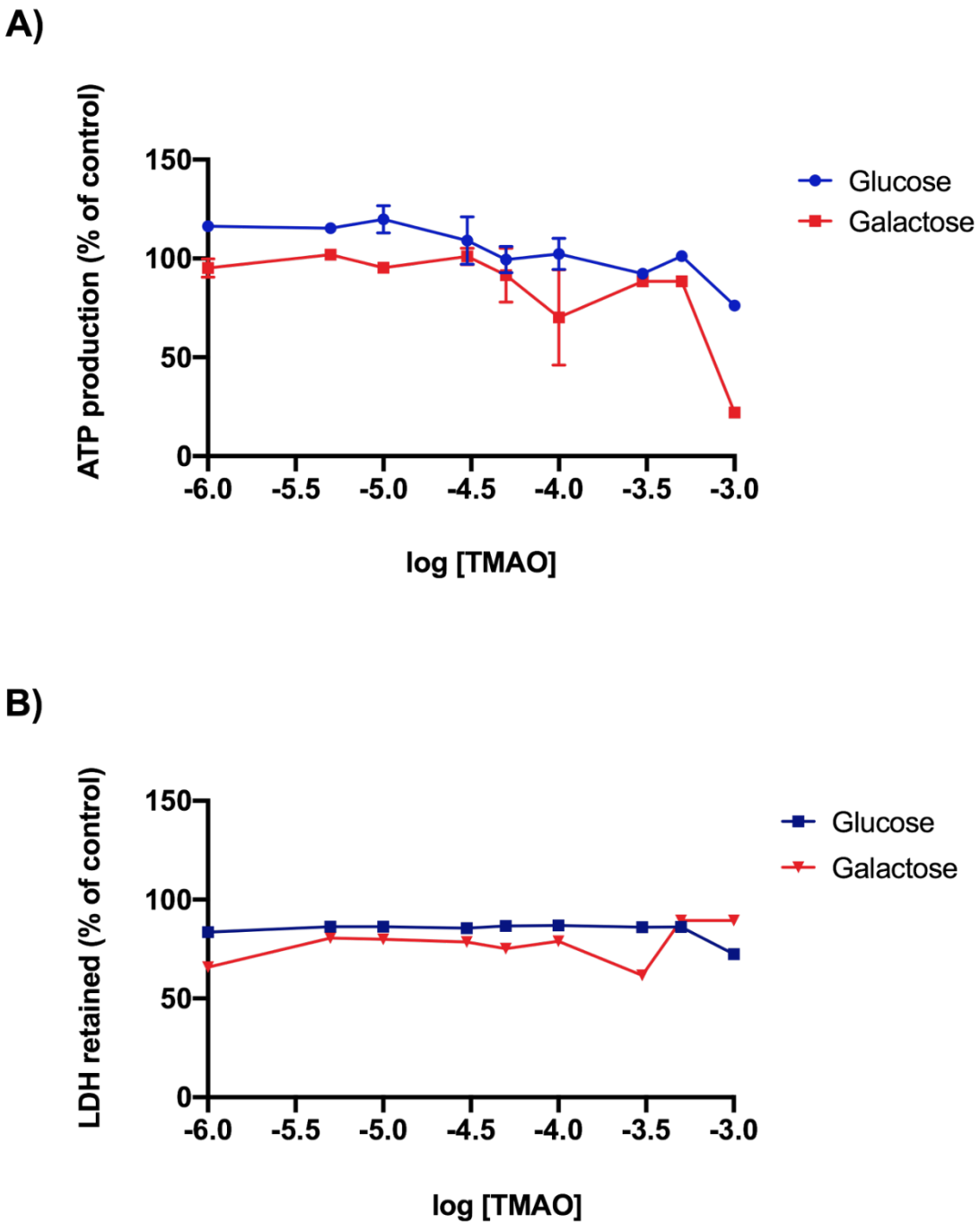

Figure 6.1. Effects of increasing concentrations of TMAO on ATP and production and in AC16 cell line. **A:** Line chart comparing ATP production in AC16 cells cultured in either glucose- or galactose supplemented media for 4h and treated with different concentrations of TMAO ranging from 0.3-300 µM. **B:** Line chart comparing LDH retention in AC16 cells cultured in either glucose- or galactose-supplemented media for 4h and treated with different concentrations of TMAO ranging from 0.3-300 µM. TMAO did not significantly affect LDH retention in either media environments (glucose and galactose media). Despite the fact that there were no changes in LDH retention, it is of note that 300 µM of TMAO showed a distinct reduction in ATP production, compared to the rest of the concentrations of TMAO, in galactose-supplemented media. Data were presented as percentage of control (n. 3 experiments for each treatment).

6.2.2 Acute metabolic switch of energetic source from low glucose to short-term high glucose on AC16 and H9C2 cardiac cells in presence of TMAO

Acute hyperglycaemia is associated with myocardial damage and worsening of cardiac parameters during acute coronary syndrome through alteration of mitochondrial function, caused by overload of $[Ca^{2+}]_i$ and low levels of ATP (Brennan et al., 2019; Squire et al., 2010). To further investigate the potentially deleterious effects of TMAO on cardiomyocyte function and normal mitochondrial function it was interesting to evaluate the effects of TMAO on co-treatment with 100 µM of TMAO and short-term treatments of high glucose on ATP production in H9C2 and AC16 cells.

In this section of the study, the effects of TMAO on ATP content were compared to assess mitochondrial function following treatment. Experiments were carried out using H9C2 and AC16 cells cultured in low glucose media and then treated with 100 µM TMAO (concentration chosen to maintain consistency with the results shown in previous chapters) and short-term treatments (5, 15 and 30 min) of high glucose. After treatment, ATP content was indirectly determined. In this protocol, ATP production is directly correlated to the amount of light emitted in the assay, as outlined in section 2.10.

Figure 6.2 A compares ATP production in AC16 cells cultured in low glucose media and following short-term treatments (5, 15 and 30 min) of high glucose while figure 6.2 B compares ATP production in the same conditions with 100 µM of TMAO. Similarly, figure 6.2 C compares ATP production in H9C2 cells cultured in low glucose media with short-term treatments (5, 15 and 30 min) of high glucose while figure 6.2 D as in C, however with 100 µM of TMAO. In all the conditions, short-term treatments with high glucose altered ATP production in a time-dependent manner; all time points longer than 5 min showed a distinct decrease in ATP production, especially when short-treatment with high glucose reached 30 min.

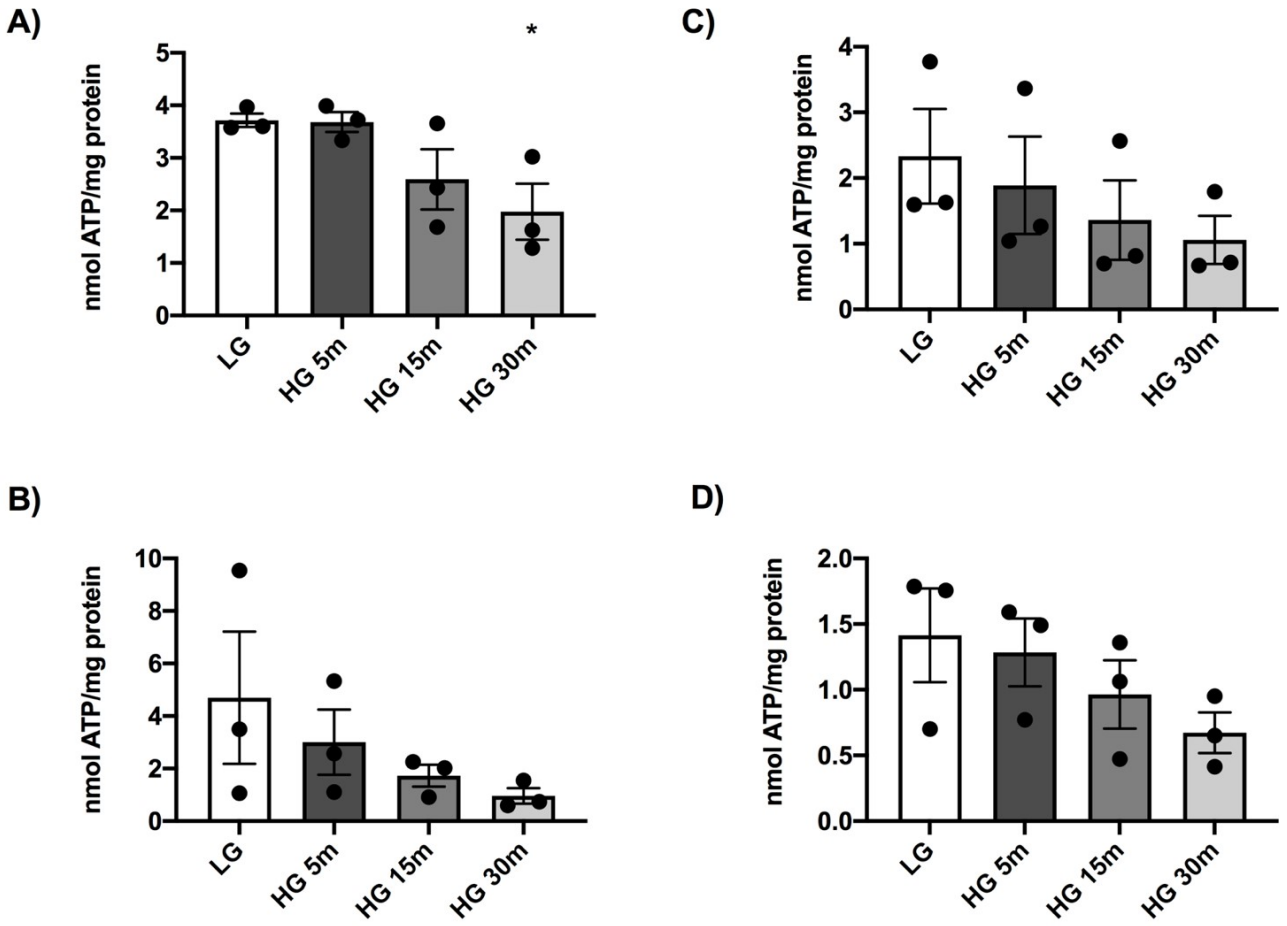

Figure 6.2 Effects of co-treatment with 100 µM of TMAO and short-term treatments of high glucose on ATP production in H9C2 and AC16 cells. A: Bar chart comparing the effects of short-term treatments (5, 15 and 30 min) of high glucose on ATP production in AC16 cells. **B:** Bar chart comparing the effects of co-treatment of 100 µM of TMAO as in A. **C:** Bar chart comparing the effects of short-term treatments (5, 15 and 30 min) of high glucose on ATP production in H9C2 cells. **D:** Bar chart comparing the effects of co-treatment of 100 µM of TMAO as in C, (* $P < 0.05$; one-way ANOVA with Dunnett's post- test; n. 3 experiments for each treatment).

In order to evaluate the effects of TMAO on co-treatment with 100 µM of TMAO and short-term treatments of high glucose on ATP production, figure 6.3 compares side-by side the cells exposed to only short-term treatments of high glucose with the cells exposed to both high glucose and co-treatment with 100 µM of TMAO. In section A, the effects co-treatment with 100 µM of TMAO and short-term treatments of high glucose on ATP production on AC16 cells are shown, while in section B, the effects on H9C2 cells are shown. In both cell lines and in all the time points evaluated, co-treatment with 100 µM of TMAO and short-term treatments of high glucose caused a further decrease in ATP production compared to cells not treated with TMAO.

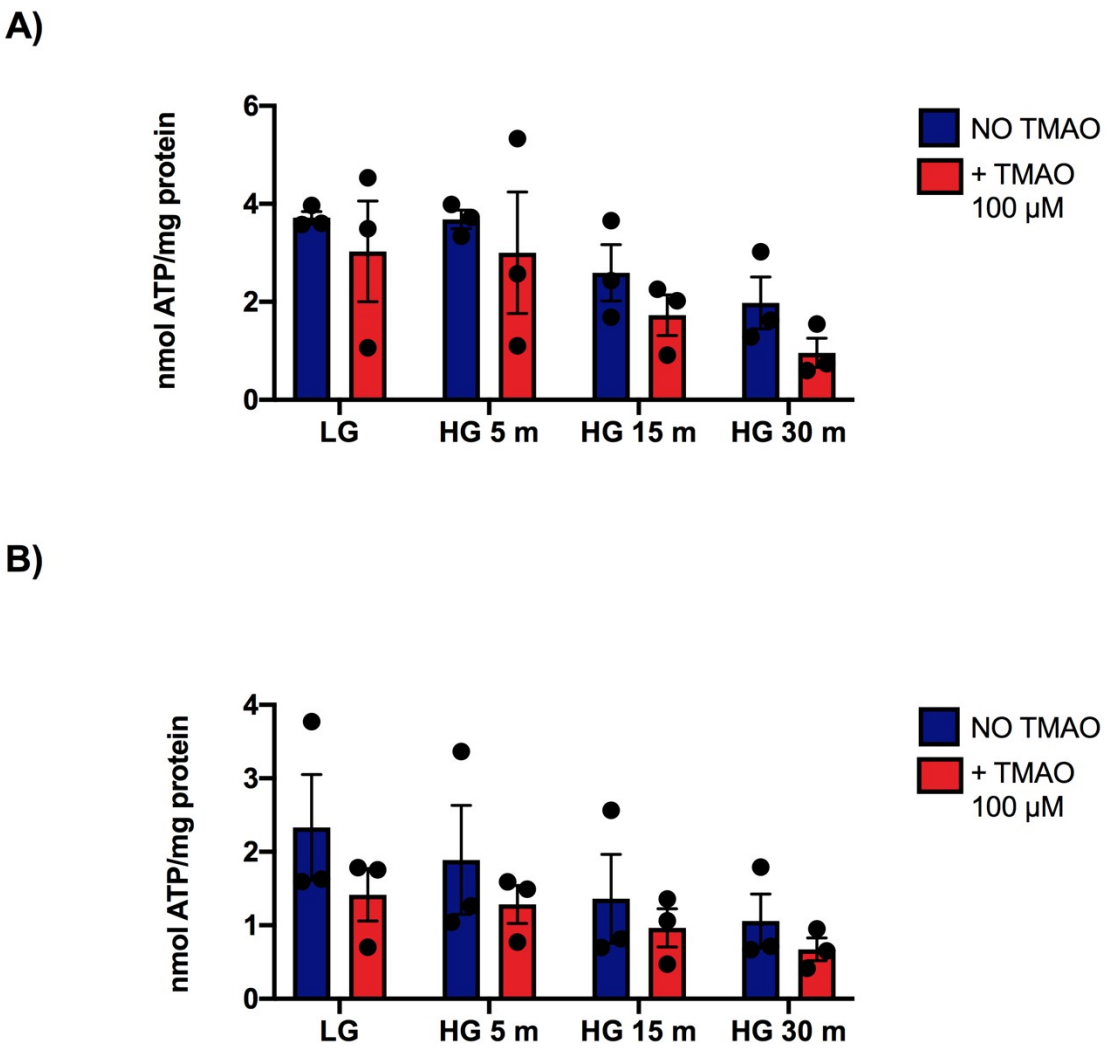

Figure 6.3. Side-to-side comparison of co-treatment with 100 µM of TMAO and short-term treatments of high glucose on ATP production in H9C2 and AC16 cells. A: Bar chart comparing the effects of TMAO and short-term treatments (5, 15 and 30 min) of high glucose on ATP production in AC16 cells. **B:** Bar chart comparing the effects of TMAO and short-term treatments (5, 15 and 30 min) of high glucose on ATP production in H9C2 cells. In both cell lines and in all the time points evaluated, treatment with 100 µM of TMAO caused a further decrease in ATP production compared to cells non-treated with TMAO (two-way ANOVA; n. 3 experiments for each treatment).

Together with evaluation of ATP production, LDH release was also evaluated. As described in section 2.9, damaged cells release LDH into the media, thus LDH retention in the cells is an indirect way to evaluate damage caused to the cells.

Figure 6.4 A compares LDH retention in AC16 cells cultured in low glucose media and treated short-term treatments (5, 15 and 30 min) of high glucose while figure 6.4 B compares ATP production in AC16 cells in the same conditions with 100 µM of TMAO. Figure 6.4 C compares LDH retention in H9C2 cells cultured in low glucose media and treated short-term treatments (5, 15 and 30 min) of high glucose while figure 6.4 D

compares LDH retention in H9C2 cells in the same conditions with 100 µM of TMAO. As in the data shown in figure 6.2, figure 6.4 A suggests that short-term treatments with high glucose altered LDH retention in a time-dependent manner; all time points longer than 5 min showed a distinct decrease in LDH retention. These data show significance when short treatment with high glucose reached 30 min, while similar results were not confirmed in co-treatment with 100 µM of TMAO.

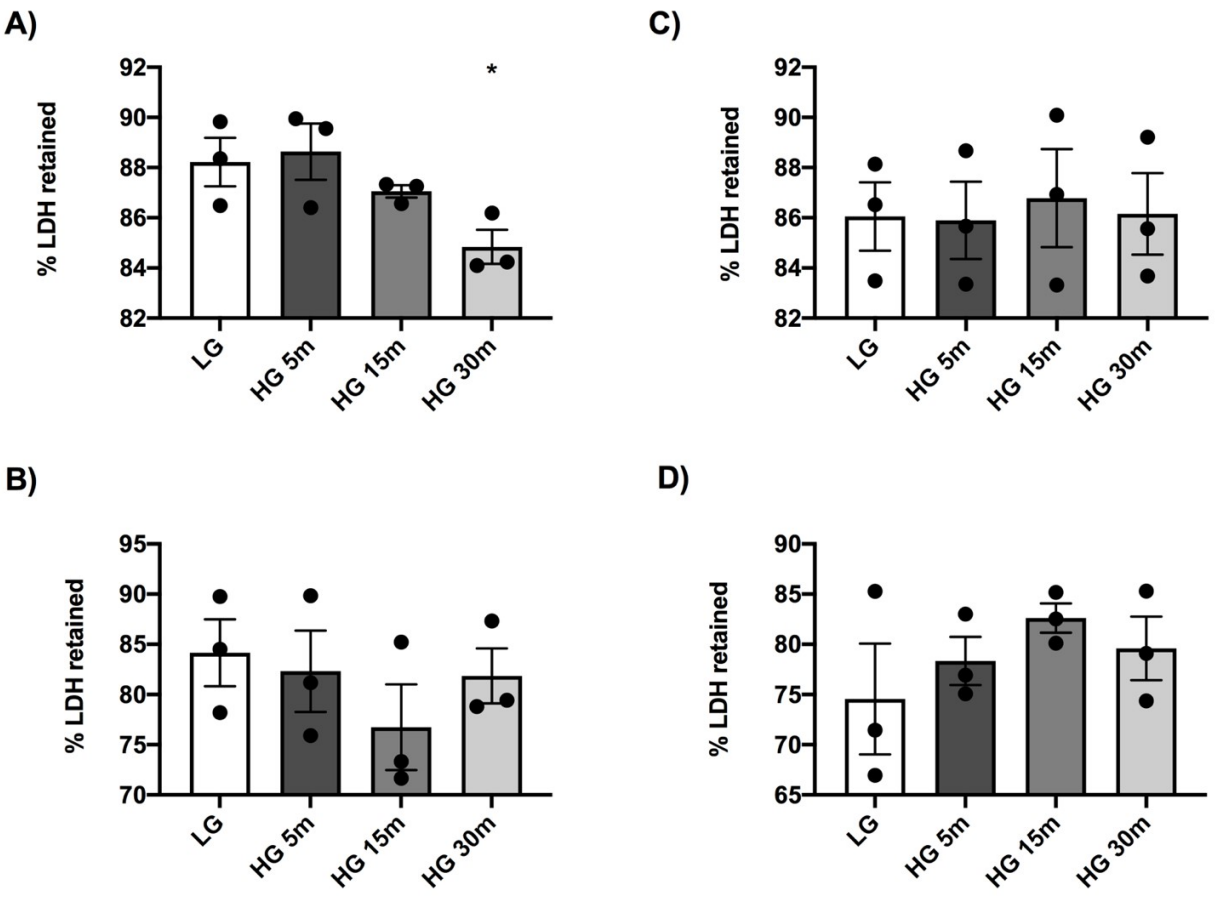

Figure 6.4. Effects of co-treatment with 100 µM of TMAO and short-term treatments of high glucose on LDH retention in H9C2 and AC16 cells. A: Bar chart comparing the effects of short-term treatments (5, 15 and 30 min) of high glucose on LDH retention in AC16 cells. **B:** Bar chart comparing the effects of co-treatment of 100 µM of TMAO, with glucose treatments in A, on LDH retention in AC16 cells. **C:** Bar chart comparing the effects of short-term treatments (5, 15 and 30 min) of high glucose on LDH retention in H9C2 cells. **D:** Bar chart comparing the effects of co-treatment of 100 µM of TMAO, with glucose treatments in C, on LDH retention in AC16 cells. In all the conditions, short-term treatments with high glucose altered LDH retention in a time-dependent manner, while co-treatment with TMAO did not affect ATP production (* $P < 0.05$; one-way ANOVA with Dunnett's post-test; n. 3 experiments for each treatment).

Lastly, figure 6.5 compares side-to-side the cells exposed to only short-term treatments of high glucose with the cells exposed to co-treatment with 100 µM of TMAO and short-term treatments of high glucose. In section A, the effects co-treatment with 100 µM of TMAO and short-term treatments of high glucose on LDH retention on AC16 cells are shown, while in section B, the effects co-treatment with 100 µM of TMAO and short-term treatments of high glucose on LDH retention on H9C2 cells are shown. Like what is shown in figure 6.3, in both cell lines and in all the time points evaluated, co-treatment with 100 µM of TMAO and short-term treatments of high glucose caused a further decrease in LDH retention compared to cells not treated with TMAO.

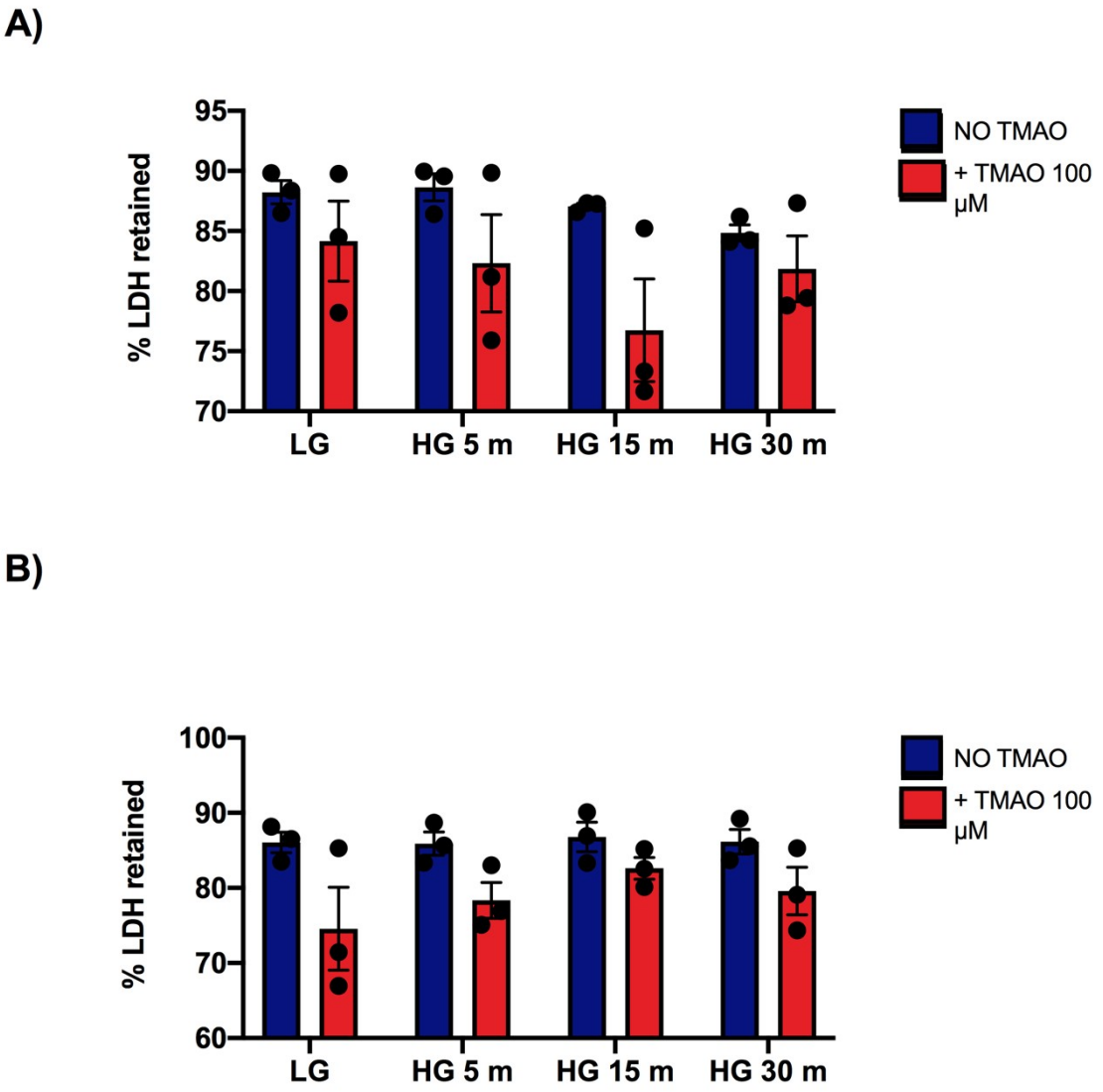

Figure 6.5. Side-to-side comparison of co-treatment with 100 µM of TMAO and short-term treatments of high glucose on LDH retention in H9C2 and AC16 cells. A: Bar chart comparing the effects of TMAO and short-term treatments (5, 15 and 30 min) of high glucose on LDH retention in AC16 cells. **B:** Bar chart comparing the effects of TMAO and short-term treatments (5, 15 and 30 min) of high glucose on LDH retention in H9C2 cells. In both cell lines and in all the time points evaluated, treatment with 100 µM of TMAO caused a further decrease in LDH retention compared to cells not treated with TMAO (Two-way ANOVA; n. 3 experiments for each treatment).

6.2.3 Mitochondrial function of AC16 and H9C2 cardiac cells exposed to a combination of short-time exposure to high levels of glucose and TMAO study using the Seahorse XF analyser

To evaluate the effects of TMAO on cells exposed to a combination of short-time exposure to high levels of glucose and TMAO on mitochondrial cardiac function of AC16 and H9C2 using the Seahorse XF analyser, an altered version of the mitochondrial stress test described in section 2.12.1 was used.

In this protocol, cells cultured in low glucose media were exposed to short-term treatments (5, 15 and 30 min) of high glucose alone, or a co-treatment with 100 µM of TMAO, on the Seahorse XF analyser, to evaluate in real-time changes in the OCR and ECAR of the cells. In particular, short-term treatments of high glucose or a co-treatment with 100 µM of TMAO and short-term treatments of high glucose were injected on the plate and basal OCR was evaluated. Following the measurement of basal respiration, oligomycin was injected into each well, followed by 3 cycles of mix and wait and 3 min measurement to determine O_2 consumption. Oligomycin inhibits ATP synthase (complex V) and is injected in the final stage of this modified protocol following basal measurements. It decreases electron flow through the ETC, resulting a reduction in mitochondrial respiration or OCR. This decrease in OCR allows the quantification of the portion of OCR which is linked to ATP-production (ATP-linked respiration) to cellular ATP production and was compared to the basal OCR in all the experimental conditions.

Figure 6.6 shows the effects co-treatment with 100 µM of TMAO and short-term treatments of high glucose on OCR of AC16 cells cultured in low glucose. All of the short-term treatments with high glucose cause a slight decrease in basal levels of OCR, that was not sustained after oligomycin injection. Cells exposed to only short treatments of high glucose and cells exposed to both 100 µM of TMAO and short-term treatments of high glucose have similar OCR profiles, suggesting that TMAO is not altering OCR in these conditions.

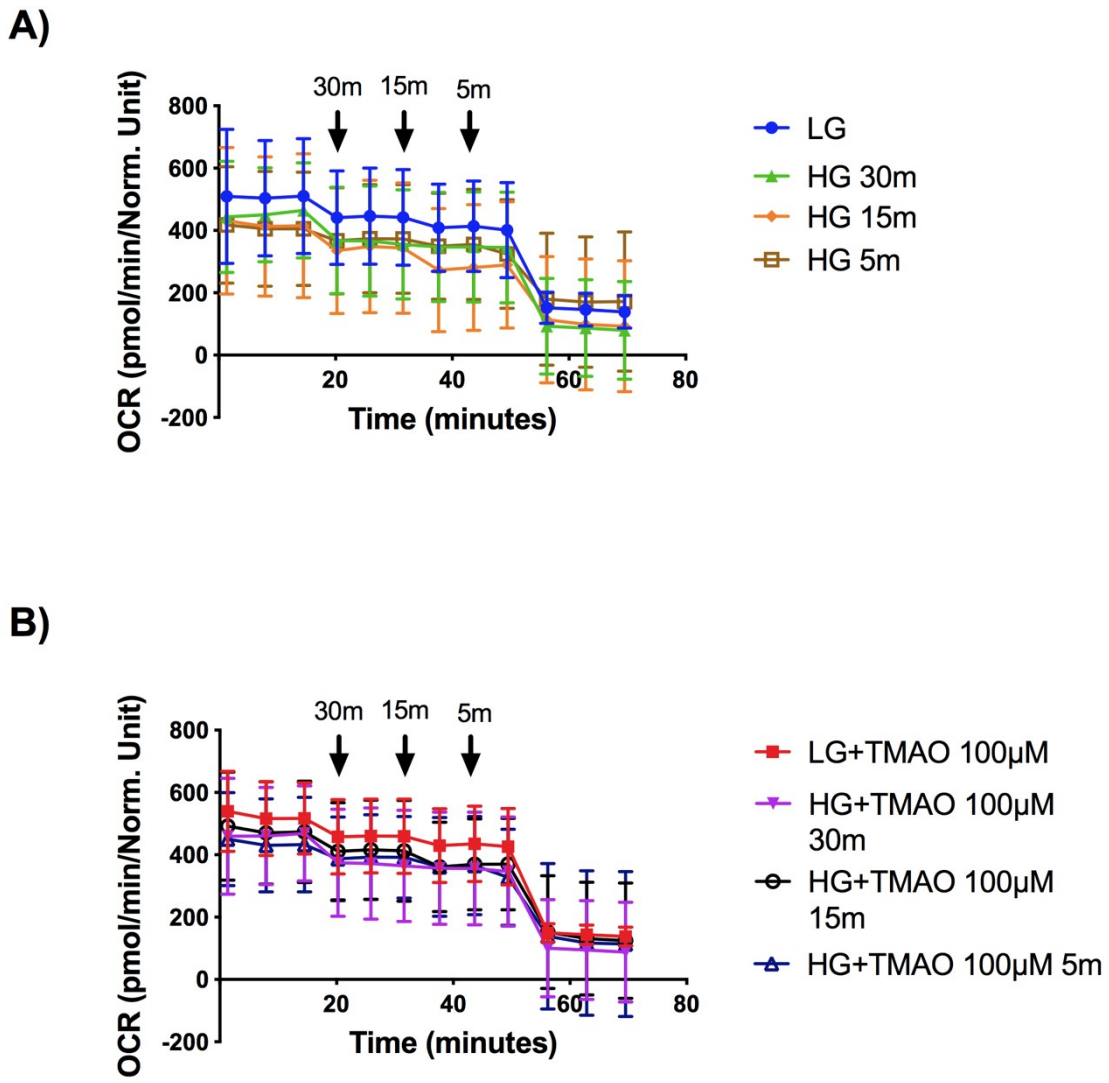

Figure 6.6. Effects of co-treatment with 100 µM of TMAO and short-term treatments of high glucose on OCR of AC16 cells cultured in low glucose media using the XF24 analyzer. A: AC16 cells were cultured for 24h in low glucose media. Real time measurements of OCR were performed while short-term injections of high glucose at 30, 15 and 5 min were done. **B:** AC16 cells were cultured for 24h in low glucose media in the presence of 100 µM TMAO. Real time measurements of OCR were performed while short-term injections of high glucose at 30, 15 and 5 min were done. At the end of the protocol, an injection with oligomycin was performed as shown (n. 3 experiments for each treatment).

Figure 6.7 shows the effects co-treatment with 100 µM of TMAO and short-term treatments of high glucose on OCR of H9C2 cells cultured in low glucose. Results obtained from this cell line are consistent with the findings shown in figure 6.6, in that TMAO does not seem to be altering OCR in these conditions and that short-term treatments with high glucose cause an increase in basal levels of OCR that was not sustained after oligomycin injection.

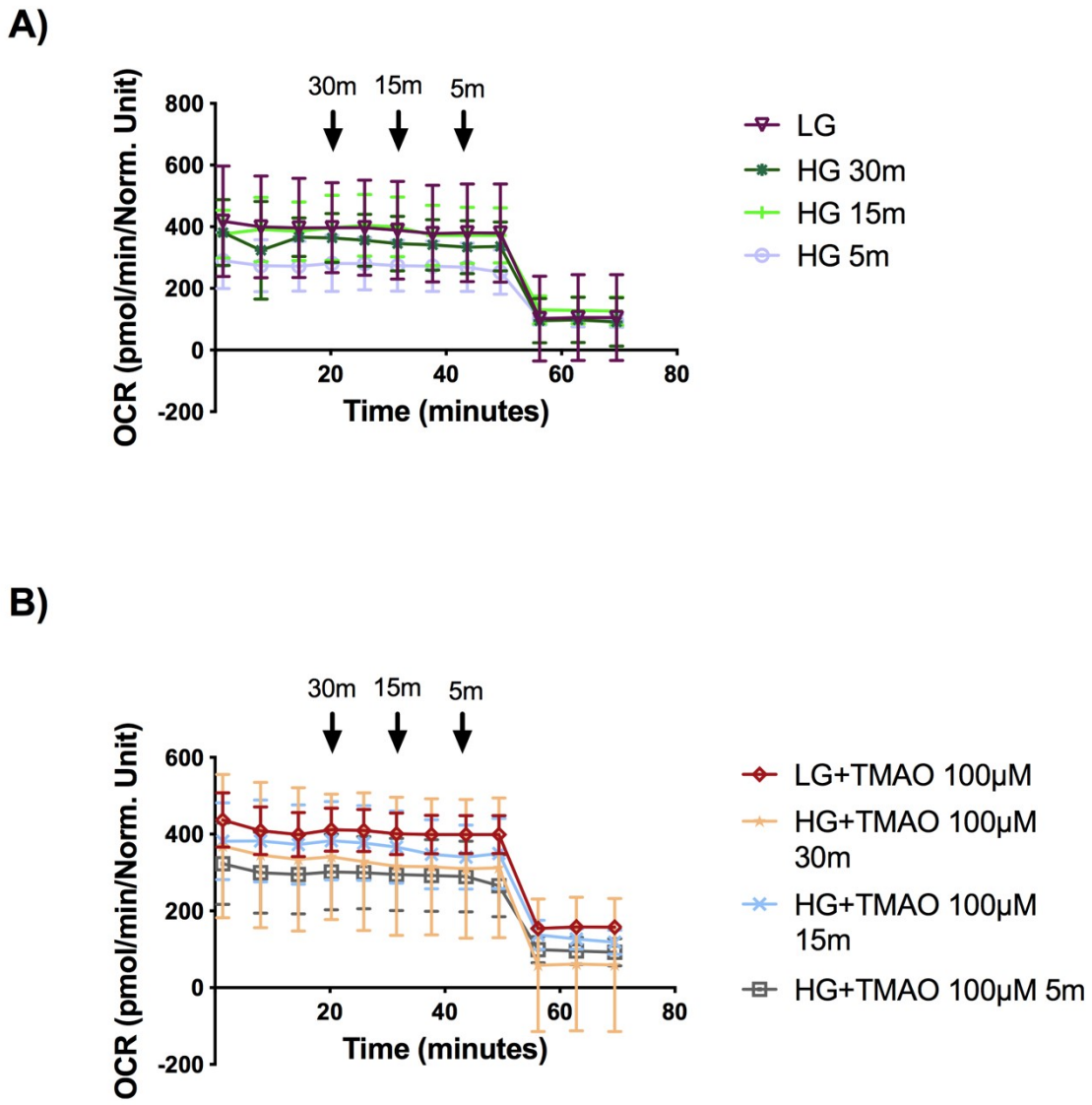

Figure 6.7. Effects of co-treatment with 100 µM of TMAO and short-term treatments of high glucose on OCR of H9C2 cells cultured in low glucose media using the XF24 analyzer. A: H9C2 cells were cultured for 24h in low glucose media. Real time measurements of OCR were performed while short-term injections of high glucose at 30, 15 and 5 min were done. **B:** H9C2 cells were cultured for 24h in low glucose media in the presence of 100 µM TMAO. Real time measurements of OCR were performed while short-term injections of high glucose at 30, 15 and 5 min were done. At the end of the protocol, an injection with oligomycin was performed as shown (n. 3 experiments for each treatment).

Figure 6.8 shows the effects co-treatment with 100 µM of TMAO and short-term treatments of high glucose on ECAR of AC16 cells cultured in low glucose. Consistently with the OCR profile, cells exposed to only short treatments of high glucose and cells exposed to both 100 µM of TMAO and short-term treatments of high glucose have similar ECAR profiles, suggesting that TMAO is not altering ECAR in these conditions.

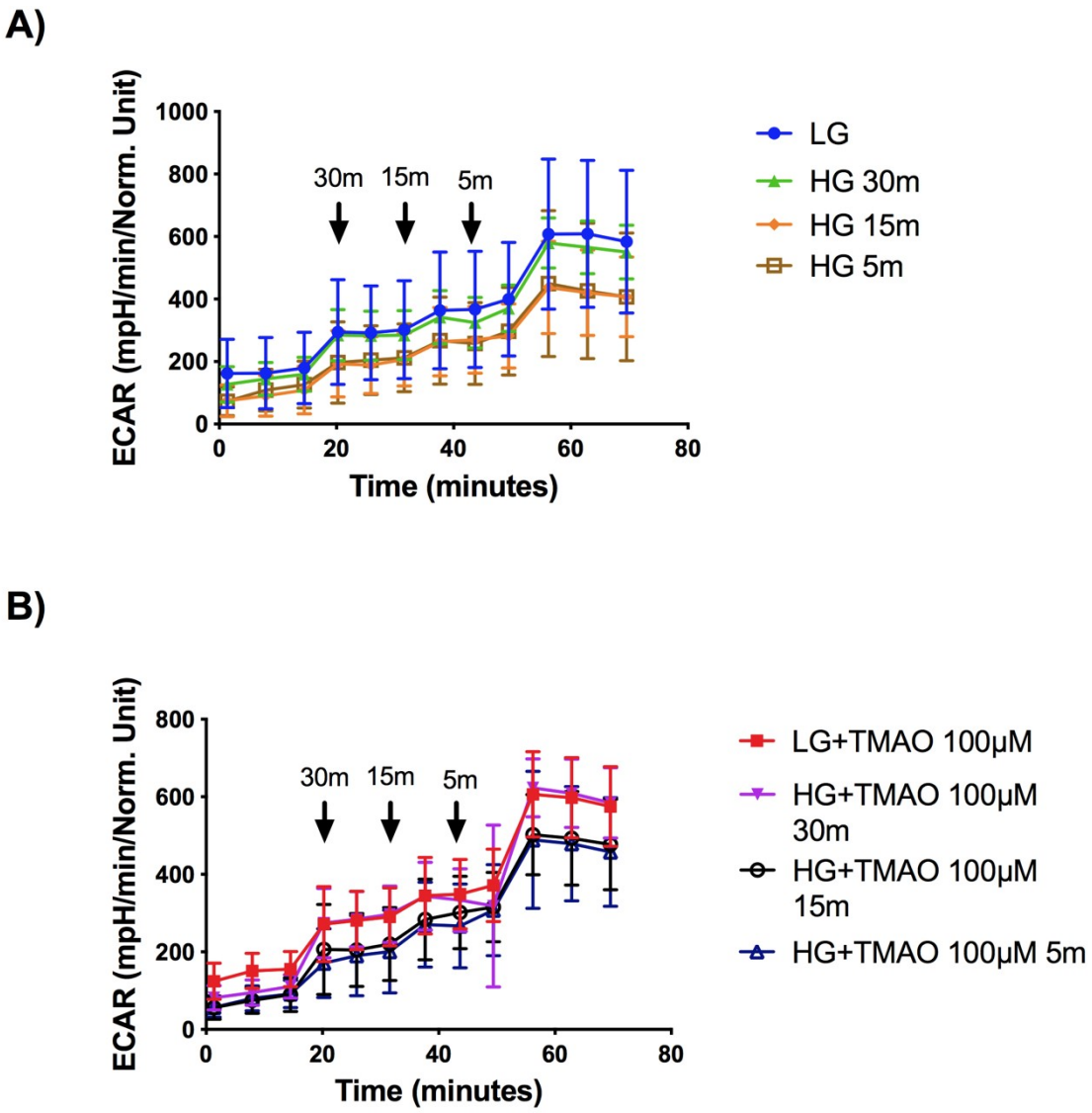

Figure 6.8. Effects of co-treatment with 100 µM of TMAO and short-term treatments of high glucose on ECAR of AC16 cells cultured in low glucose media using the XF24 analyzer. A: AC16 cells were cultured for 24h in low glucose media. Real time measurements of ECAR were performed while short-term injections of high glucose at 30, 15 and 5 min were done. **B:** AC16 cells were cultured for 24h in low glucose media in the presence of 100 µM TMAO. Real time measurements of ECAR were performed while short-term injections of high glucose at 30, 15 and 5 min were done. At the end of the protocol, an injection with oligomycin was performed as shown (n. 3 experiments for each treatment).

Figure 6.9 shows the effects co-treatment with 100 µM of TMAO and short-term treatments of high glucose on ECAR of H9C2 cells cultured in low glucose. These results confirm the findings of figure 6.8, in that TMAO does not seem to be altering ECAR in these conditions.

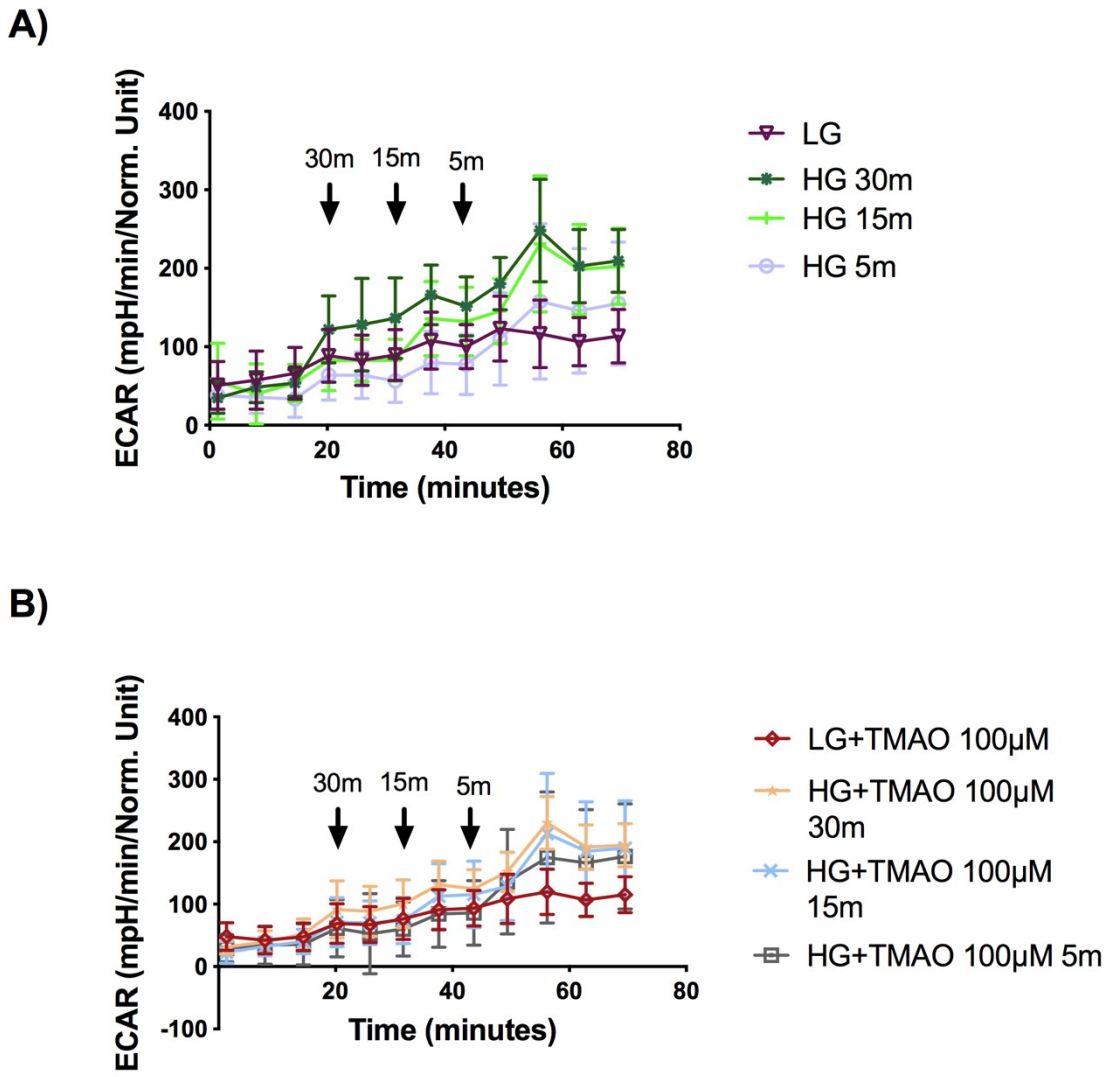

Figure 6.9. Effects of co-treatment with 100 µM of TMAO and short-term treatments of high glucose on ECAR of H9C2 cells cultured in low glucose media using the XF24 analyzer. A: H9C2 cells were cultured for 24h in low glucose media. Real time measurements of ECAR were performed while short-term injections of high glucose at 30, 15 and 5 min were done. **B:** H9C2 cells were cultured for 24h in low glucose media in the presence of 100 µM TMAO. Real time measurements of ECAR were performed while short-term injections of high glucose at 30, 15 and 5min were done. At the end of the protocol, an injection with oligomycin was performed as shown (n. 3 experiments for each treatment).

Figure 6.10 shows the effects of short-term treatments of high glucose OCR/ECAR of AC16 cells cultured in low glucose media. This figure highlights and reinforces the findings of figure 6.6 and 6.7, confirming that indeed all of the short-term treatments with high glucose cause an increase in basal levels of OCR, that was not sustained after oligomycin injection, alluding to the fact that maybe high glucose treatment caused a decrease in the rate of ATP-linked respiration. To explain the OCR/ECAR profile in terms of differences between the time of the exposure to high glucose, it could be that over

time the presence of high glucose causes a biphasic response in OCR, initially decreasing basal respiration, reaching its peak after 15 mins, before returning to level similar to levels measured in low glucose after 30 mins. Intriguingly, the same pattern is seen in basal ECAR, with a biphasic response to high glucose and with low glucose treatment having the highest levels.

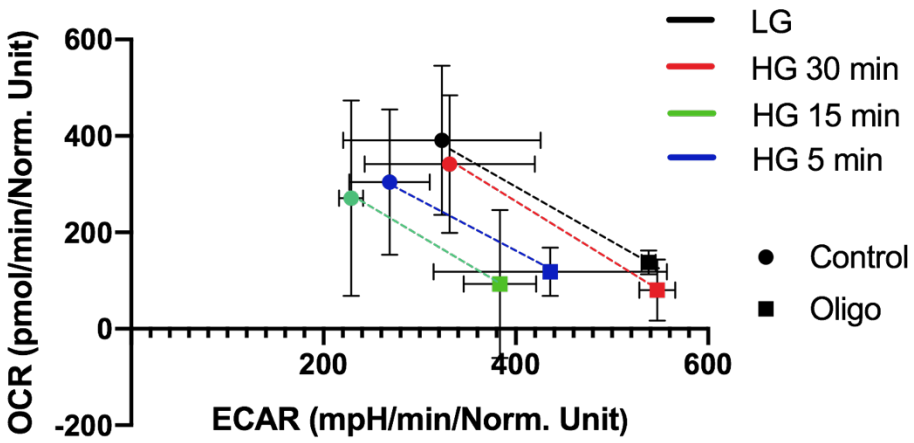

Figure 6.10. Effects of short-term treatments of high glucose on OCR/ECAR of AC16 cells cultured in low glucose media using the XF24 analyzer. Short-term treatments with high glucose caused an increase in basal levels of OCR, that was not sustained after oligomycin injection. All short-term treatment with high glucose caused a similar shift in the OCR/ECAR ration, however there is a transient decrease in the starting ratio. Short-term treatment with highglucose for 5 min and 15 min caused a decrease in OCR that returned to levels similar to low glucose with the 30 min treatment, suggesting a possible adaptive response of the cells to the high glucose environment, after 30min of treatment.

6.3 Discussion

In this chapter, data has been presented to expand on the investigation on the direct effects of TMAO on cardiac cells, focusing on the impairment of mitochondrial metabolism in the heart. Using assays to assess mitochondrial function, the possibility of TMAO being an important player that increases the severity of cardiovascular events or that enhances the progression of cardiovascular diseases by modulating bioenergetic pathways inside the cell, discussed in chapter 5. The focus of this chapter is to investigate the effects of TMAO on cardiac cells that are subjected to changes in the culture conditions and co-treatment of cardiac cells in different concentrations of TMAO and known modulators of cardiac function and energetic metabolism of the cells, to replicate a condition of pre-existing stress in the cardiac cells. Based on our previous findings, it is hypothesized that, in these conditions, TMAO would exacerbate an already altered bioenergetic metabolism, leading to an increase in adverse outcome for cardiac cells function.

The first metabolic stress model that was used is a model that has been developed to improve detection of mitochondrial toxicants and that utilizes cells grown in two types of media, one supplemented with high glucose and the other with galactose (glucose/galactose model) (Dykens et al., 2008; Marroquin et al., 2007; P. Rana et al., 2011). Normally, cells grown in glucose media are considered more resistant to the activity of mitochondrial toxins because they can easily shift metabolic resources from regular ATP synthesis through OXPHOS to utilizing glycolysis for ATP generation, thus compensating for an eventual mitochondrial impairment. Despite the fact that glycolysis is not a very efficient way of energy production, capturing as ATP only 5-6% of potential energy in the glucose substrate when fully oxidized via OXPHOS, the inefficiency of the process can be balanced by an increase in the availability of substrates, resulting in an accelerating pathway that functionally compete with OXPHOS (Marroquin et al., 2007; Robinson et al., 1992). On the other hand, cells grown in galactose media as the only available substrate for energy productions are forced to rely on OXPHOS for ATP generation (Gohil et al., 2010; Robinson et al., 1992). Galactose gets converted very

slowly into glucose-1-phosphate, which means that cells grown in galactose-supplemented media get 98% of their ATP from glutamine (Reitzer et al., 1979; Wagner et al., 1991). As a consequence, cells grown in galactose-supplemented media show an increased OCR and decreased levels of glycolysis, compared to cells cultured in high glucose (Aguer et al., 2011; Marroquin et al., 2007).

Since cells grown in galactose-supplemented media generate ATP almost exclusively through OXPHOS, their dependency on a normally functioning mitochondrial activity is more acute and they are more prone to be affected by stimuli and toxins that can cause mitochondrial disfunction than cells maintained in high glucose (Dykens et al., 2008; Marroquin et al., 2007). Conversely, when cells cultured in high glucose are affected by stimuli and toxins while cells grown in galactose-supplemented media are not, it is usually considered as a sign that the compound is affecting the glycolytic pathway (Gohil et al., 2010). The glucose/galactose model has been successfully used on cardiac (H9C2) cell lines to identify mitochondrial toxicants (Dykens et al., 2008; Marroquin et al., 2007; P. Rana et al., 2011). In this chapter, it is shown that TMAO affected cells grown in galactose-supplemented media in a concentration-dependant manner. In particular, high concentrations of TMAO caused a reduction of ATP production that was evident when the cells were grown in galactose-supplemented media. Consistent with results show in previous chapters, 300 µM of TMAO was the concentration where the detrimental effects of TMAO on ATP production were extremely evident, suggesting that the change in metabolic substrates was useful in exposing the effects of TMAO on mitochondrial activity.

The second metabolic stress model that was used is a model of acute hyperglycaemia. Acute hyperglycaemia refers to elevations in blood glucose and is an extremely common factor in the onset of acute coronary syndrome and CVD in general. (Fujino et al., 2014; Squire et al., 2010). It is also associated with poor outcome of these patients, even when the elevations in blood glucose are not drastic (above 8.2mmol/L)(Al Jumaily et al., 2015; Gardner et al., 2015; Squire et al., 2010). Disruption of mitochondrial function plays an important role in in the damage of the myocardium that occurs during acute coronary syndrome. In particular, overload of $[Ca^{2+}]i$, dissipation of the mitochondrial membrane

potential and low levels of ATP are considered to be responsible for cardiac cell death and necrosis of the tissue, through formation of mitochondrial permeability transition pore (Briston et al., 2019; Nesci, 2018). This particular event is, in turn, responsible for generating a constant flux of ROS into the cytoplasm that stimulates even more release of ROS from the matrix of the mitochondria. The accumulation of ROS thus created inside the cell is responsible for the cellular damage and the initiation of the apoptotic stimuli from the cells located in the affected area (Penna et al., 2009). Studies have demonstrated that this process is exacerbated by the cell's exposure to acute hyperglycaemia, either by promoting mitochondrial membrane depolarisation in H9C2 cells (Kumar et al., 2012), or by increasing ROS generation, increasing caspase activity and so infarct area in the hyperglycaemic myocardium (Su et al., 2013).

In different studies published by Hreiche et al. (2009), Sims et al. (2014) and Brennan et al. (2019), it was demonstrated that acute hyperglycaemia was responsible for prolonging cellular APD, increasing $[Ca^{2+}]i$, and eliciting spontaneous contraction of cardiomyocytes. Furthermore, the time course of decay in numbers of contractile cardiomyocytes was found to be correlated to the increase in spontaneous contractions in high extracellular glucose and, lastly, IPC- imparted cardioprotection was attenuated by increases in extracellular glucose concentrations. Based on these findings, in this chapter a co-treatment of cardiac cells with 100 μM of TMAO and short-time acute treatment with high glucose was performed to investigate whether TMAO was capable of further exacerbating the already compromised situation caused by hyperglycaemia. From the results shown in this chapter, two important findings emerged. The first one was that the detrimental effects of hyperglycaemia on cardiac cells are greatly dependent on the duration of the exposure to the elevations in glucose. Acute high glucose was capable of causing a decrease in ATP production and in LDH retention when the exposure to high glucose was longer than 5 min. The second important findings that emerged regarded the co-treatment of cardiac cells with 100 μM of TMAO. The results demonstrated that co-treatment of cardiac cells with 100 μM of TMAO and short-time acute treatment with high glucose caused a further decrease in ATP production and in LDH retention when the exposure to high glucose was longer than 5 min, suggesting that TMAO was able to exacerbate the mitochondrial dysfunction caused by hyperglycaemia.

In conclusion, co-treatment of cardiac cells with different concentrations of TMAO and known modulators of cardiac function and energetic metabolism of the cells, to replicate a condition of pre-existing stress in the cardiac cells has an impact on modulation of mitochondrial function. High concentrations of TMAO show a difference in mitochondrial parameters that point to a possible detrimental effect of TMAO on normal mitochondrial function. When cardiac cells are pre/co-exposed to environmental conditions that alter the normal mitochondrial function, like the culture in galactose-supplemented media, that pushed the cells to a metabolic shift that caused the cells to produce ATP exclusively through OXPHOS or short-time exposure to high glucose, that was shown to alter mitochondrial function, high concentrations of TMAO (100 and 300 μM) worsened the mitochondrial parameter evaluated, suggesting that the detrimental effects of TMAO on mitochondrial function are more evident when mitochondria are already altered.

Chapter 7

General Discussion

7 General Discussion

Cardiovascular diseases are the leading cause of mortality and disability in the modern era, and it becomes particularly prevalent with increasing age (Lopez et al., 2006). Amongst these, CAD, MI, stroke, HF and atrial fibrillation are all known to be closely associated with both T2DM and CKD, as well as with atherosclerosis (Miura et al., 2019). In recent years, the has been an increasing literature focusing on the importance of the role performed by the gut microbiota in affecting a wide range of systemic conditions, including CVD, T2DM and metabolic syndrome and how these conditions, in turn, are able to modulate the gut microbiota (Lau et al., 2017). Particular importance has been put on one gut microbiota-dependent metabolite, TMAO, for its association with CVD and atherosclerosis, highlighting the importance of gut microbiome-metabolism in cardiometabolic health (Senthong, Li, et al., 2016; Z. Wang et al., 2011). Elevated plasma TMAO levels have been linked with major adverse CVD events (Papandreou et al., 2020; Tang & Hazen, 2014) and the link between TMAO and CVD has been investigated in different cohorts and in numerous studies (Schuett et al., 2017; Troseid et al., 2015). While there are evidence suggesting that TMAO may be both a marker and a mediator in lifestyle diseases, several studies have also shown a protective role for TMAO and suggested that the correlation between elevated blood TMAO level and the risk of CVD is not as immediate as previously described (Nowinski et al., 2018).

It is evident, then, that a better understanding of the biological role of TMAO in health and disease is required and is of key importance in order to determine whether investing in TMAO as a potential therapeutic target and/or using TMAO as a routine biomarker is feasible and cost-effective.

In this study, the primary aim was to investigate whether TMAO can modulate cardiac function by having a direct effect on cardiac cells. By using isolated cardiomyocytes through to the intact myocardium, this study was able to investigate the concentration dependence of any TMAO-induced changes in cardiac function.

7.1 TMAO: diagnostic biomarker, potentially harmful or a protective agent?

TMAO first started to attract the attention of the scientific community when it was proposed that it could serve as a diagnostic and prognostic marker of many pathological conditions. High plasma levels of TMAO were quickly associated with risk of development of T2DM and cardiovascular complications (Dambrova et al., 2016; Lever et al., 2014; Obeid et al., 2016). Furthermore, high plasma levels of TMAO were also found to be correlated with negative outcomes in metabolic patterns (Obeid et al., 2016). High plasma levels of TMAO were also found to be positively associated with further progression of atherosclerosis and mortality, in patients affected by CAD (Lever et al., 2014; Senthong, Wang, et al., 2016) and were also found in patients with poor prognosis after events associated with acute coronary syndromes (X. S. Li et al., 2017). However, there are several clinical studies questioning the positive correlation between TMAO blood level and CVD. For example, TMAO levels showed no correlation with coronary artery calcification in young adults (K. A. Meyer et al., 2016). In addition, increases in TMAO plasma levels were not complemented by a rise of highly sensitive C-reactive protein and LDL levels (Kuhn et al., 2017; C. A. Miller et al., 2014).

Considering this evidence, the use of TMAO as a biomarker is not as straightforward and reliable as it was initially suggested (Nowinski & Ufnal, 2018).

Limitations to the usefulness of TMAO as a biomarker could be summarized by 1) significant intra-individual variety of TMAO plasma levels (Kuhn et al., 2017), 2) TMAO synthesis and its dependency on a diet rich in TMAO precursors, and 3) influence of the gut microbiota composition (which is affected by diet as well as other factors, such as age, ethnicity and sex) on TMAO plasma levels.

Other factors to consider are that increases in plasma levels of TMAO during progression of CVD and T2DM could be caused by dysbiosis associated with the disease themselves and the limitations linked to the methodology of evaluation of plasma levels (Papandreou et al., 2020). For example, several studies report plasma levels of TMAO only without taking into consideration TMA levels or urinary secretion. Papandreou et al. (2020) suggested that a solution could be to consider the plasma TMA/TMAO ratio

as a marker, that would be more reliable and reflective of the actual levels of circulating metabolites. It is also important to consider the possibility that high TMAO levels are a result of injuries caused by disease, which will induce TMAO up-regulation to promote the healing process, suggesting that increased levels of TMAO may be a compensatory mechanism in response to disease rather than cause (Papandreou et al., 2020). While the potential of TMAO as a useful biomarker for CVD is currently still debated, several studies point to a positive correlation between elevated plasma TMAO level and an increased cardiovascular risk and a possible involvement of TMAO in the prognosis of CVD (Senthong, Wang, et al., 2016; Tang et al., 2013; Troseid et al., 2015; Z. Wang, W. H. Tang, et al., 2014). Furthermore, studies have emerged that show that TMAO is able to alter lipid homeostasis, corroborating the theory that TMAO could be involved in the development of CVD.

TMAO is able to enhance lesion development in Apolipoprotein E knockout (ApoE-null) mice, a standard model of spontaneous atherosclerosis, fed a diet supplemented with TMAO (Z. Wang et al., 2011). Furthermore, TMAO was found to modulate cholesterol and sterol metabolism and promoting progress of atherosclerosis (Koeth et al., 2013). Peritoneal macrophages of mice fed with a TMAO-supplemented diet showed an increase in the expression level of receptors involved in atherosclerosis, an increase of cholesterol levels and enhanced foam cells formation (Z. Wang et al., 2011). It is hypothesized that TMAO is able to exacerbate inflammatory reactions of vascular wall, by activating NLRP3 inflammasome and by increasing ROS production, but also by altering cholesterol reverse transport (X. Sun et al., 2016).

TMAO has been shown to have effects on thrombosis by increasing the thrombosis risk through enhancement of platelet hyperreactivity (W. Zhu et al., 2016) confirmed by the fact that oral choline supplementation increased fasting TMAO levels and platelet aggregation (W. Zhu et al., 2017). The effect of TMAO on platelet aggregation were found to be mediated by increase in calcium release from the endoplasmic reticulum (W. Zhu et al., 2016).

Data presented in this study shows that TMAO has a direct effect on cardiac cells, by altering key components of their physiological function. TMAO was found to alter functional recovery of cardiac cells in an *in vitro* model of MI/R in a concentration

dependent manner (figure 3.2), and high concentrations of TMAO result in cells not recovering their cell function after exposure to metabolic inhibitors. Furthermore, high concentrations of TMAO significantly prolong the time taken by the cells to recover from contractile failure if they recover at all (figure 3.4). Based on literature that suggests that concentrations of TMAO that are found to be effective in cellular experiments range between 0.1 µM and 10mM (Jaworska et al., 2019; Savi et al., 2018; W. Zhu et al., 2016), with 10mM considered as an hyperphysiological concentration (Querio et al., 2019) and 100µM being the most used, concentrations of TMAO higher than 50 µM are considered as high, and well above physiological concentrations (see section 7.2 for a more detailed discussion on physiological relevance of TMAO levels).

Consistently with studies like the previously mentioned study by W. Zhu et al. (2016) and another study by Savi et al. (2018), TMAO was found to alter calcium homeostasis by increasing the AUC of the Ca^{2+} transients (figure 3.5) and increasing Ca^{2+} current in an electrophysiological model of action potential (figure 3.9 and figure 3.12). As a result of this alteration in calcium homeostasis, APD_{30} and APD_{50} were found to be increased by exposure to TMAO (figure 3.6 D-E).

Additionally, TMAO has been found to interfere with normal cell bioenergetics by inhibiting the substrate dependent respiration, thus leading to a decrease in beta-oxidation of fatty acids by cardiac cells (Makrecka-Kuka et al., 2017). The effects of TMAO on the mitochondrial function of cardiac cells were the focus of both chapter 5 and chapter 6 of this study, and it was confirmed that only particularly high concentrations of TMAO (from 100 µM) were capable of alter mitochondrial parameters (figure 5.1, figure 5.6-5.10) and that when cardiac cells are pre/co-exposed to environmental conditions that alter the normal mitochondrial function, high concentrations of worsened the mitochondrial parameter evaluated.

There is evidence that supports the hypothesis that TMAO may have a positive effect in the human body and on the prognosis and development of CVD. For the most part, these evidence take root in the observation that fish, rich in TMAO, are fundamental components of the Mediterranean diet, considered to have a beneficial effect on the

circulatory system (Widmer et al., 2015), and from the well-known knowledge that TMAO acts as an osmolyte in marine animals, particularly in deep-sea ones (Yancey et al., 2004). Marine animals use TMAO to counteract protein-destabilizing effects of osmotic and hydrostatic pressures and studies show that TMAO is able to stabilize protein folded state and nucleic acids. Furthermore, it has been found that TMAO counteracts the effects of various protein denaturants, such as urea, heat and pressure (Granata et al., 2006; Lin et al., 2009; Yancey et al., 2004; Yancey & Siebenaller, 1999).
Other and more recent evidence in support of a possible protective role for TMAO were published by Collins et al. (2016), in which TMAO was found to slow aortic lesion formation in a mouse model.
This current study provided a novel insight into the possibility that TMAO could have a cardioprotective role in cardiac cells and a plausible mechanism for this activity. Acute exposure to TMAO caused an increase in the activation of $K_{ir}6.1$ channel, as shown in figure 3.15 and there is evidence that suggests that the activity of $K_{ir}6.1$ is a potential mediator of cardioprotection. In accord with these findings, TMAO caused a shortening of the APD and a decrease in cellular contractility that, it is hypothesised, preserve intracellular energy. TMAO caused a shortening of the APD_{90}, as shown in figure 3.6 F, suggesting that TMAO may be involved in the same cardioprotective pathway that involves K_{ATP} channels opening.

7.2 Concentrations of TMAO

The apparent contradictions previously discussed and the results from animal studies have to be interpreted in light of several factors. One of the most important factors that were considered in the planning of the experiments performed in this study was trying to replicate normal physiological conditions of the range of concentrations of TMAO, based on diet and variability of plasma and serum levels found in the literature.
Both plasma and serum levels of TMAO have been used in numerous different cohorts to fully define a range of active TMAO concentrations, but no unequivocal answer has emerged yet. While several studies have focused on describing TMAO levels, in different cohorts and conditions, it was quickly evident that there existed a discrepancy between

range of concentrations found in published papers describing plasma and/or serum levels of TMAO found in healthy patients and the range of concentrations used to perform *in vivo* and *in vitro* experiments.

In a single study, the reported serum levels of TMAO in stroke ranged from 0.5 to 18.3 μM, with a median value of 5.8 μM, which was reportedly higher than in controls patients, found to be with a median value of 3.9 μM. On the other hand, the median level of serum TMAO content in those patients was significantly lower than in moderate-to-high stroke patients, reported to be between 4.1 μM vs. 9.1 μM (Rexidamu et al., 2019). Another study published by Missailidis et al. (2016) compared plasma concentration of TMAO in CKD patients and showed that elevated TMAO levels are strongly associated with degree of renal function.

Cell culture experiments in the literature that aim to investigate the link between TMAO and CVD, both in acute treatments and in chronic treatment with the metabolite, have been performed using very different ranges of concentrations and different cell lines. In cultured carotid artery endothelial cells, 30 μM TMAO was found to modulate different inflammatory pathways, that was hypothesized to be at the basis of the generation of atherosclerotic plaque formation (Boini et al., 2017). Chou et al. (2019) showed that 200 and 500 μM TMAO promoted cellular inflammation and oxidative stress, while having detrimental effects on cellular function, while 2 μM or 100 μM TMAO did not have the same effects, suggesting that the detrimental effects of TMAO were linked to the concentrations of TMAO used in the experiments. Furthermore, macrophages treated with increasing concentrations of TMAO up to 100 μM, showed no effect on atheroma formation, when its effect was evaluated on foam cell formation (Collins et al., 2016).

To the best of our knowledge, the first and only study that suggested that concentrations of TMAO close to 100 μM of TMAO could be considered “physiologically relevant” were W. Zhu et al. (2016). In their study on the effects of TMAO on platelet hyperreactivity and thrombotic risk, they found that plasma levels of TMAO in a cohort showed a “large dynamic range” of 0.06 to 312 μM, which prompted the decision of performing the experiments of the study with a concentration of 100 μM of TMAO. Successive studies on a direct effect of TMAO on cardiomyocytes followed these concentrations of TMAO for their studies. Savi et al. (2018) showed that 20 or 100 μM TMAO affected cardiomyocyte contractility and intracellular Ca^{2+} handling. Another

study performed in isolated rat cardiomyocytes, Querio et al. (2019) used 10 or 100 µM TMAO applied for 1 to 24h to show that TMAO did not have any significant effect on cell viability, sarcomere length, ROS production and mitochondrial membrane potential. In this study, the lack of use of a wider range of concentrations of TMAO that could include concentrations more similar to the ones found in healthy patients and in patients affected by CVD was described by the author themselves as one of the "weaknesses" of their study. Another interesting point made in this study was the duration of the treatment with TMAO. Based on pharmacokinetics studies on TMAO, and on its renal clearance in healthy human patients, reveal that TMAO has a small volume of distribution inside the human body, and it was concluded that TMAO has a plasma half-life of ~4h (Cho et al., 2017), and that TMAO was completely excreted within 24h from its synthesis (Al-Waiz et al., 1987). Based on these evaluations, it was concluded that an exposure to TMAO of 24h, corresponding to the time of complete excretion of TMAO from the human body, was the optimal way to investigate whether the effects of TMAO evidenced with acute exposure of the cardiomyocytes to the metabolite are sustained in a longer exposure, replicating a normal physiological condition.

More recently, Jaworska et al. (2019) proved that neither 24h nor 72h treatment with TMAO were cytotoxic on cardiac cells, despite using concentrations of TMAO ranging from 0.1 to 100 mM, notably much higher concentrations than the ones found in the plasma of both healthy patients (3.6 ± 0.4 µM) and in patients with severe aortic stenosis (5.5 ± 0.5 µM), in their own study.

Despite the inconsistency between ranges of TMAO found in the different cohorts and conditions explored, it was evident that in vitro and in vivo experiments performed with excess amounts of TMAO or its precursors and/or in distress-suffering animal models are far from the normal situation and cannot explain a causal relationship between TMAO and disease development (Papandreou et al., 2020).

In this current study, a large range of concentrations of TMAO was used to highlight the differences in the effects caused by concentrations of TMAO similar to the ones found in healthy patients, in patients affected by CVD and concentrations of TMAO commonly used in the literature for *in vivo* and *in vitro* experiments with the metabolite.

It quickly emerged from the experiments we performed, that the impact of TMAO on modulation of cardiac functionality in cardiac cells was strictly dependent of the concentrations of TMAO used to perform the experiments (figure 3.2 and figure 3.4). Concentrations of TMAO similar to that found in healthy patients and in patients affected by CVD were not responsible for having detrimental effects on the contractile function of cardiac cells, while higher concentrations of TMAO negatively impacted cardiac function. Another important aspect that emerged from this study and was never presented before, was that the harmful effects of TMAO on cardiac cells were only present while the cells were exposed to TMAO. As evidenced in figure 3.14, alteration of APD and Ca^{2+} homeostasis, both negative for the health of the cells, were quickly reversed by washing out of these.

The correlation between harmful effects of TMAO and the concentrations of the metabolite used to perform the experiments was further explored in Chapter 5 of this study. An in-depth exploration of the effects of TMAO on the mitochondrial function of cardiac cells confirmed that only particularly high concentrations of TMAO (from 100 µM) were capable of alter mitochondrial parameters (figure 5.1, figure 5.6-5.10).

Furthermore, chapter 4 addressed the importance of the duration of the administration of TMAO. As previously mentioned, 24h exposure was identified as a realistic time of exposure based on plasma half-life and excretion of TMAO in the human body and in chapter 4 were presented evidence that even the effects of concentrations of TMAO higher than the ones found in healthy patients and in patients with CVD did not cause detrimental effects on cardiac cells in a 24h exposure.

7.3 Future work

The work presented in this thesis aimed to investigate whether TMAO can modulate cardiac function by having a direct effect on the cardiac cell, it provided a better understanding of the biological role of TMAO in health and disease, and addressed important question in order to determine whether investing in TMAO as a potential therapeutic target.

However, in order to further clarify TMAO's clinical relevance and/or if using TMAO as a routine biomarker is feasible and cost-effective as well as its physiological role, there are still questions to answer.

Firstly, further research and intervention studies with relatively low levels of TMAO may be needed, as *in vivo* and *in vitro* studies published so far could be faulted for applying excessive amounts of TMAO, far from the normal physiological levels and are not enough to explain a causal relationship between TMAO and disease development.

Secondly, investigations on a possible cardioprotective role for TMAO could be the direction for future works. Although this study has provided a plausible mechanism involved in mediating cardioprotection, by presenting data that showed how TMAO was able to modulate K_{ATP} channels and affect the duration of the action potential, this can be further expanded upon and the possibility of TMAO enhancing other known mechanism of cardioprotection could be investigated.

Lastly, while research is including other precursors of TMAO and other carnitine-like metabolites, there is definitely a need for comparative works that take into consideration the effects of other small molecules and the possibility of these metabolites potentially interacting and influencing one another, in order to attribute univocal clinical relevance to TMAO.

7.4 Conclusion

In this study, TMAO was found to be able to modulate cardiac function by having a direct effect on cardiac cells. Targets of TMAO inside the cardiac cells were both electrical modulation of the cardiac action potential and alteration of bioenergetic pathways of importance to cardiac cells.

This study shows that acute administration of high concentrations of TMAO to isolated cardiomyocytes can have an impact on modulation of ion channel function. These effects manifest as a change in the action potential and alterations of calcium

homeostasis. Despite these changes in calcium homeostasis, the effects of ischaemia are not exaggerated in the whole heart, however contractile recovery following ischaemia is compromised in a single cell model of ischaemia and reperfusion. These detrimental effects of TMAO were present only at higher concentrations and lasted only while TMAO was present on cardiac cells. Additionally, data presented in this study suggest a plausible role for TMAO in cardioprotection, by increasing opening of the $K_{ir}6.1$ channel.

In contrast, long-term (24h) administration of TMAO to cultured cardiomyocytes does not have an impact on modulation of ion channel function. The effects manifested in the acute administration of TMAO in isolated cardiomyocytes are no longer significant in a chronic model.

Furthermore, administration of different concentrations of TMAO to cultured cardiomyocytes (established cell line) does not have a significant impact on modulation of mitochondrial function. Only high concentrations of TMAO show a difference in mitochondrial parameters that point to a possible detrimental effect of TMAO on normal mitochondrial function. Furthermore, alterations in the environmental conditions, specifically culture of the cardiac cells in media supplemented with hyperphysiological concentrations of glucose, exacerbated the effects of the higher concentration of TMAO on mitochondrial function. Finally, co-treatment of cardiac cells with different concentrations of TMAO and known modulators of cardiac function and energetic metabolism of the cells, to replicate a condition of pre-existing stress in the cardiac cells has an impact on modulation of mitochondrial function. High concentrations of TMAO show a difference in mitochondrial parameters that point to a possible detrimental effect of TMAO on normal mitochondrial function. When cardiac cells are pre/co-exposed to environmental conditions that alter the normal mitochondrial function, high concentrations of worsened the mitochondrial parameter evaluated, suggesting that the detrimental effects of TMAO on mitochondrial function are more evident when mitochondria are already altered.

References

Adler, A., & Viskin, S. (2016). Clinical Features of Genetic Cardiac Diseases Related to Potassium Channelopathies. *Card Electrophysiol Clin, 8*(2), 361-372. doi:10.1016/j.ccep.2016.02.001

Adnan, S., Nelson, J. W., Ajami, N. J., Venna, V. R., Petrosino, J. F., Bryan, R. M., Jr.et al. (2017). Alterations in the gut microbiota can elicit hypertension in rats. *Physiol Genomics, 49*(2), 96-104. doi:10.1152/physiolgenomics.00081.2016

Aguer, C., Gambarotta, D., Mailloux, R. J., Moffat, C., Dent, R., McPherson, R.et al. (2011). Galactose enhances oxidative metabolism and reveals mitochondrial dysfunction in human primary muscle cells. *PLoS One, 6*(12), e28536. doi:10.1371/journal.pone.0028536

Aguiar-Pulido, V., Huang, W., Suarez-Ulloa, V., Cickovski, T., Mathee, K., & Narasimhan, G. (2016). Metagenomics, Metatranscriptomics, and Metabolomics Approaches for Microbiome Analysis. *Evol Bioinform Online, 12*(Suppl 1), 5-16. doi:10.4137/EBO.S36436

Agus, A., Clement, K., & Sokol, H. (2020). Gut microbiota-derived metabolites as central regulators in metabolic disorders. *Gut*. doi:10.1136/gutjnl-2020-323071

Akesson, B., Vinge, E., & Skerfving, S. (1989). Pharmacokinetics of triethylamine and triethylamine-N-oxide in man. *Toxicol Appl Pharmacol, 100*(3), 529-538. doi:10.1016/0041-008x(89)90300-1

Al Jumaily, T., Rose'Meyer, R. B., Sweeny, A., & Jayasinghe, R. (2015). Cardiac damage associated with stress hyperglycaemia and acute coronary syndrome changes according to level of presenting blood glucose. *Int J Cardiol, 196*, 16-21. doi:10.1016/j.ijcard.2015.05.143

al-Waiz, M., Mikov, M., Mitchell, S. C., & Smith, R. L. (1992). The exogenous origin of trimethylamine in the mouse. *Metabolism, 41*(2), 135-136. doi:10.1016/00260495(92)90140-6

Al-Waiz, M., Mitchell, S. C., Idle, J. R., & Smith, R. L. (1987). The metabolism of 14Clabelled trimethylamine and its N-oxide in man. *Xenobiotica, 17*(5), 551-558. doi:10.3109/00498258709043962

Aldana-Hernandez, P. L., K.A.; Zhao, Y.Y.; Curtis, J.M.; Field, C.J.; Jacobs, R.L. (2019). Dietary Choline or Trimethylamine N-oxide Supplementation Does Not Influence Atherosclerosis Development in Ldlr-/- and Apoe-/- Male Mice. *J. Nutr*.

Amin, A. S., Asghari-Roodsari, A., & Tan, H. L. (2010). Cardiac sodium channelopathies.

Pflugers Arch, 460(2), 223-237. doi:10.1007/s00424-009-0761-0

Amin, A. S., Tan, H. L., & Wilde, A. A. (2010). Cardiac ion channels in health and disease. *Heart Rhythm, 7*(1), 117-126. doi:10.1016/j.hrthm.2009.08.005

Anders, H. J., Andersen, K., & Stecher, B. (2013). The intestinal microbiota, a leaky gut, and abnormal immunity in kidney disease. *Kidney Int, 83*(6), 1010-1016. doi:10.1038/ki.2012.440

Anderson, J. L., Edney, R. J., & Whelan, K. (2012). Systematic review: faecal microbiota transplantation in the management of inflammatory bowel disease. *Aliment Pharmacol Ther, 36*(6), 503-516. doi:10.1111/j.1365-2036.2012.05220.x

Antzelevitch, C., & Burashnikov, A. (2011). Overview of Basic Mechanisms of Cardiac Arrhythmia. *Card Electrophysiol Clin, 3*(1), 23-45. doi:10.1016/j.ccep.2010.10.012

Backhed, F., Ley, R. E., Sonnenburg, J. L., Peterson, D. A., & Gordon, J. I. (2005). Hostbacterial mutualism in the human intestine. *Science, 307*(5717), 1915-1920. doi:10.1126/science.1104816

Baczko, I., Jost, N., Virag, L., Bosze, Z., & Varro, A. (2016). Rabbit models as tools for preclinical cardiac electrophysiological safety testing: Importance of repolarization reserve. *Prog Biophys Mol Biol, 121*(2), 157-168. doi:10.1016/j.pbiomolbio.2016.05.002

Bain, M. A., Faull, R., Fornasini, G., Milne, R. W., & Evans, A. M. (2006). Accumulation of trimethylamine and trimethylamine-N-oxide in end-stage renal disease patients undergoing haemodialysis. *Nephrol Dial Transplant, 21*(5), 1300-1304. doi:10.1093/ndt/gfk056

Bain, M. A., Fornasini, G., & Evans, A. M. (2005). Trimethylamine: metabolic, pharmacokinetic and safety aspects. *Curr Drug Metab, 6*(3), 227-240. doi:10.2174/1389200054021807

Balmer, M. L., Schurch, C. M., Saito, Y., Geuking, M. B., Li, H., Cuenca, M.et al. (2014). Microbiota-derived compounds drive steady-state granulopoiesis via MyD88/TICAM signaling. *J Immunol, 193*(10), 5273-5283. doi:10.4049/jimmunol.1400762

Barth, E., Stammler, G., Speiser, B., & Schaper, J. (1992). Ultrastructural quantitation of mitochondria and myofilaments in cardiac muscle from 10 different animal species including man. *J Mol Cell Cardiol, 24*(7), 669-681. Retrieved from http://www.ncbi.nlm.nih.gov/pubmed/1404407

Beaumont, M., Goodrich, J. K., Jackson, M. A., Yet, I., Davenport, E. R., Vieira-Silva, S.et al. (2016). Heritable components of the human fecal microbiome are associated with visceral fat. *Genome Biol, 17*(1), 189. doi:10.1186/s13059-016-1052-7

Begriche, K., Massart, J., Robin, M. A., Borgne-Sanchez, A., & Fromenty, B. (2011). Druginduced toxicity on mitochondria and lipid metabolism: mechanistic diversity and deleterious consequences for the liver. *J Hepatol, 54*(4), 773-794. doi:10.1016/j.jhep.2010.11.006

Behr, E. R., Dalageorgou, C., Christiansen, M., Syrris, P., Hughes, S., Tome Esteban, M. T.et al. (2008). Sudden arrhythmic death syndrome: familial evaluation identifies inheritable heart disease in the majority of families. *Eur Heart J, 29*(13), 1670-1680. doi:10.1093/eurheartj/ehn219

Bennett, B. J., de Aguiar Vallim, T. Q., Wang, Z., Shih, D. M., Meng, Y., Gregory, J.et al. (2013). Trimethylamine-N-oxide, a metabolite associated with atherosclerosis, exhibits complex genetic and dietary regulation. *Cell Metab, 17*(1), 49-60. doi:10.1016/j.cmet.2012.12.011

Bergeron, N., Williams, P. T., Lamendella, R., Faghihnia, N., Grube, A., Li, X.et al. (2016). Diets high in resistant starch increase plasma levels of trimethylamine-N-oxide, a gut microbiome metabolite associated with CVD risk. *Br J Nutr, 116*(12), 2020-2029. doi:10.1017/S0007114516004165

Bernini, P., Bertini, I., Luchinat, C., Nepi, S., Saccenti, E., Schafer, H.et al. (2009). Individual human phenotypes in metabolic space and time. *J Proteome Res, 8*(9), 4264-4271. doi:10.1021/pr900344m

Berrill, J. W., Gallacher, J., Hood, K., Green, J. T., Matthews, S. B., Campbell, A. K.et al. (2013). An observational study of cognitive function in patients with irritable bowel syndrome and inflammatory bowel disease. *Neurogastroenterol Motil, 25*(11), 918-e704. doi:10.1111/nmo.12219

Bers, D. M. (2008). Calcium cycling and signaling in cardiac myocytes. *Annu Rev Physiol, 70*, 23-49. doi:10.1146/annurev.physiol.70.113006.100455

Biliczki, P., Virag, L., Iost, N., Papp, J. G., & Varro, A. (2002). Interaction of different potassium channels in cardiac repolarization in dog ventricular preparations: role of repolarization reserve. *Br J Pharmacol, 137*(3), 361-368. doi:10.1038/sj.bjp.0704881

Bindels, L. B., Delzenne, N. M., Cani, P. D., & Walter, J. (2015). Towards a more comprehensive concept for prebiotics. *Nat Rev Gastroenterol Hepatol, 12*(5), 303-310. doi:10.1038/nrgastro.2015.47

Bindels, L. B., Walter, J., & Ramer-Tait, A. E. (2015). Resistant starches for the management of metabolic diseases. *Curr Opin Clin Nutr Metab Care, 18*(6), 559-565. doi:10.1097/MCO.0000000000000223

Boini, K. M., Hussain, T., Li, P. L., & Koka, S. (2017). Trimethylamine-N-Oxide Instigates NLRP3 Inflammasome Activation and Endothelial Dysfunction. *Cell Physiol Biochem, 44*(1), 152-162. doi:10.1159/000484623

Borlaug, B. A. (2014). The pathophysiology of heart failure with preserved ejection fraction. *Nat Rev Cardiol, 11*(9), 507-515. doi:10.1038/nrcardio.2014.83

Boyer, P. D. (1993). The binding change mechanism for ATP synthase--some probabilities and possibilities. *Biochim Biophys Acta, 1140*(3), 215-250. doi:10.1016/0005-2728(93)90063-l

Brand, M. D., & Nicholls, D. G. (2011). Assessing mitochondrial dysfunction in cells. *Biochem J, 435*(2), 297-312. doi:10.1042/BJ20110162

Brennan, S., Chen, S., Makwana, S., Martin, C. A., Sims, M. W., Alonazi, A. S. A.et al. (2019). A novel form of glycolytic metabolism-dependent cardioprotection revealed by PKCalpha and beta inhibition. *J Physiol, 597*(17), 4481-4501. doi:10.1113/JP278332

Brennan, S., Jackson, R., Patel, M., Sims, M. W., Hudman, D., Norman, R. I.et al. (2015). Early opening of sarcolemmal ATP-sensitive potassium channels is not a key step in PKC-mediated cardioprotection. *J Mol Cell Cardiol, 79*, 42-53. doi:10.1016/j.yjmcc.2014.10.016

Brestoff, J. R., & Artis, D. (2013). Commensal bacteria at the interface of host metabolism and the immune system. *Nat Immunol, 14*(7), 676-684. doi:10.1038/ni.2640

Briston, T., Selwood, D. L., Szabadkai, G., & Duchen, M. R. (2019). Mitochondrial Permeability Transition: A Molecular Lesion with Multiple Drug Targets. *Trends Pharmacol Sci, 40*(1), 50-70. doi:10.1016/j.tips.2018.11.004

Brown, D. A., Perry, J. B., Allen, M. E., Sabbah, H. N., Stauffer, B. L., Shaikh, S. R.et al. (2016). Expert consensus document: Mitochondrial function as a therapeutic target in heart failure. *Nat Rev Cardiol*. doi:10.1038/nrcardio.2016.203

Brown, D. A., Perry, J. B., Allen, M. E., Sabbah, H. N., Stauffer, B. L., Shaikh, S. R.et al. (2017). Expert consensus document: Mitochondrial function as a therapeutic target in heart failure. *Nat Rev Cardiol, 14*(4), 238-250. doi:10.1038/nrcardio.2016.203

Brown, J. M., & Hazen, S. L. (2015). The gut microbial endocrine organ: bacterially derived signals driving cardiometabolic diseases. *Annu Rev Med, 66*, 343-359. doi:10.1146/annurev-med-060513-093205

Brunner, F., Maier, R., Andrew, P., Wolkart, G., Zechner, R., & Mayer, B. (2003). Attenuation of myocardial ischemia/reperfusion injury in mice with myocytespecific overexpression of endothelial nitric oxide synthase. *Cardiovasc Res, 57*(1), 55-62. doi:10.1016/s0008-6363(02)00649-1

Budas, G. R., Churchill, E. N., & Mochly-Rosen, D. (2007). Cardioprotective mechanisms of PKC isozyme-selective activators and inhibitors in the treatment of

ischemiareperfusion injury. *Pharmacol Res, 55*(6), 523-536. doi:10.1016/j.phrs.2007.04.005

Cammarota, G., Ianiro, G., Bibbo, S., & Gasbarrini, A. (2014). Gut microbiota modulation: probiotics, antibiotics or fecal microbiota transplantation? *Intern Emerg Med, 9*(4), 365-373. doi:10.1007/s11739-014-1069-4

Cani, P. D., & Delzenne, N. M. (2007). Gut microflora as a target for energy and metabolic homeostasis. *Curr Opin Clin Nutr Metab Care, 10*(6), 729-734. doi:10.1097/MCO.0b013e3282efdebb

Cani, P. D., & Everard, A. (2016). Talking microbes: When gut bacteria interact with diet and host organs. *Mol Nutr Food Res, 60*(1), 58-66. doi:10.1002/mnfr.201500406

Candelli, M., Franza, L., Pignataro, G., Ojetti, V., Covino, M., Piccioni, A.et al. (2021). Interaction between Lipopolysaccharide and Gut Microbiota in Inflammatory Bowel Diseases. *Int J Mol Sci, 22*(12). doi:10.3390/ijms22126242

Capaldi, R. A., & Aggeler, R. (2002). Mechanism of the F(1)F(0)-type ATP synthase, a biological rotary motor. *Trends Biochem Sci, 27*(3), 154-160. doi:10.1016/s09680004(01)02051-5

Carabotti, M., Scirocco, A., Maselli, M. A., & Severi, C. (2015). The gut-brain axis: interactions between enteric microbiota, central and enteric nervous systems. *Ann Gastroenterol, 28*(2), 203-209. Retrieved from https://www.ncbi.nlm.nih.gov/pubmed/25830558

Carmody, R. N., Gerber, G. K., Luevano, J. M., Jr., Gatti, D. M., Somes, L., Svenson, K. L.et al. (2015). Diet dominates host genotype in shaping the murine gut microbiota. *Cell Host Microbe, 17*(1), 72-84. doi:10.1016/j.chom.2014.11.010

Chambers, E. S., Morrison, D. J., & Frost, G. (2015). Control of appetite and energy intake by SCFA: what are the potential underlying mechanisms? *Proc Nutr Soc, 74*(3), 328-336. doi:10.1017/S0029665114001657

Chan, K., Truong, D., Shangari, N., & O'Brien, P. J. (2005). Drug-induced mitochondrial toxicity. *Expert Opin Drug Metab Toxicol, 1*(4), 655-669. doi:10.1517/17425255.1.4.655

Chau, C. H., Rixe, O., McLeod, H., & Figg, W. D. (2008). Validation of analytic methods for biomarkers used in drug development. *Clin Cancer Res, 14*(19), 5967-5976. doi:10.1158/1078-0432.CCR-07-4535

Chaudhary, K., Poirion, O. B., Lu, L., & Garmire, L. X. (2018). Deep Learning-Based MultiOmics Integration Robustly Predicts Survival in Liver Cancer. *Clin Cancer Res, 24*(6), 1248-1259. doi:10.1158/1078-0432.CCR-17-0853

Chen, L., Sampson, K. J., & Kass, R. S. (2016). Cardiac Delayed Rectifier Potassium Channels in Health and Disease. *Card Electrophysiol Clin, 8*(2), 307-322. doi:10.1016/j.ccep.2016.01.004

Chen, Y. T., Wong, L. L., Liew, O. W., & Richards, A. M. (2019). Heart Failure with Reduced Ejection Fraction (HFrEF) and Preserved Ejection Fraction (HFpEF): The Diagnostic Value of Circulating MicroRNAs. *Cells, 8*(12). doi:10.3390/cells8121651

Cho, C. E., Taesuwan, S., Malysheva, O. V., Bender, E., Tulchinsky, N. F., Yan, J.et al. (2017). Trimethylamine-N-oxide (TMAO) response to animal source foods varies among healthy young men and is influenced by their gut microbiota composition: A randomized controlled trial. *Mol Nutr Food Res, 61*(1). doi:10.1002/mnfr.201600324

Chollet, R., Ribault, S.b.,. (2012). Use of ATP Bioluminescence for Rapid Detection and Enumeration of Contaminants: The Milliflex Rapid Microbiology Detection and Enumeration System.

Chou, R. H., Chen, C. Y., Chen, I. C., Huang, H. L., Lu, Y. W., Kuo, C. S.et al. (2019). Trimethylamine N-Oxide, Circulating Endothelial Progenitor Cells, and Endothelial Function in Patients with Stable Angina. *Sci Rep, 9*(1), 4249. doi:10.1038/s41598-019-40638-y

Chung, H., Pamp, S. J., Hill, J. A., Surana, N. K., Edelman, S. M., Troy, E. B.et al. (2012). Gut immune maturation depends on colonization with a host-specific microbiota. *Cell, 149*(7), 1578-1593. doi:10.1016/j.cell.2012.04.037

Cohen, B. H. (2010). Pharmacologic effects on mitochondrial function. *Dev Disabil Res Rev, 16*(2), 189-199. doi:10.1002/ddrr.106

Collins, H. L., Drazul-Schrader, D., Sulpizio, A. C., Koster, P. D., Williamson, Y., Adelman, S. J.et al. (2016). L-Carnitine intake and high trimethylamine N-oxide plasma levels correlate with low aortic lesions in ApoE(-/-) transgenic mice expressing CETP. *Atherosclerosis, 244*, 29-37. doi:10.1016/j.atherosclerosis.2015.10.108

Conly, J. M., Stein, K., Worobetz, L., & Rutledge-Harding, S. (1994). The contribution of vitamin K2 (menaquinones) produced by the intestinal microflora to human nutritional requirements for vitamin K. *Am J Gastroenterol, 89*(6), 915-923. Retrieved from http://www.ncbi.nlm.nih.gov/pubmed/8198105

Craciun, S., & Balskus, E. P. (2012). Microbial conversion of choline to trimethylamine requires a glycyl radical enzyme. *Proc Natl Acad Sci U S A, 109*(52), 21307-21312. doi:10.1073/pnas.1215689109

Craig, S. A. (2004). Betaine in human nutrition. *Am J Clin Nutr, 80*(3), 539-549. doi:10.1093/ajcn/80.3.539

Dambrova, M., Latkovskis, G., Kuka, J., Strele, I., Konrade, I., Grinberga, S.et al. (2016). Diabetes is Associated with Higher Trimethylamine N-oxide Plasma Levels. *Exp Clin Endocrinol Diabetes, 124*(4), 251-256. doi:10.1055/s-0035-1569330

Daniel, H., Gholami, A. M., Berry, D., Desmarchelier, C., Hahne, H., Loh, G.et al. (2014). High-fat diet alters gut microbiota physiology in mice. *ISME J, 8*(2), 295-308. doi:10.1038/ismej.2013.155

Das, S., Cordis, G. A., Maulik, N., & Das, D. K. (2005). Pharmacological preconditioning with resveratrol: role of CREB-dependent Bcl-2 signaling via adenosine A3 receptor activation. *Am J Physiol Heart Circ Physiol, 288*(1), H328-335. doi:10.1152/ajpheart.00453.2004

David, L. A., Maurice, C. F., Carmody, R. N., Gootenberg, D. B., Button, J. E., Wolfe, B. E.et al. (2014). Diet rapidly and reproducibly alters the human gut microbiome. *Nature, 505*(7484), 559-563. doi:10.1038/nature12820

De Filippis, F., Pellegrini, N., Vannini, L., Jeffery, I. B., La Storia, A., Laghi, L.et al. (2016). High-level adherence to a Mediterranean diet beneficially impacts the gut microbiota and associated metabolome. *Gut, 65*(11), 1812-1821. doi:10.1136/gutjnl-2015-309957

Debarry, J., Garn, H., Hanuszkiewicz, A., Dickgreber, N., Blumer, N., von Mutius, E.et al. (2007). Acinetobacter lwoffii and Lactococcus lactis strains isolated from farm cowsheds possess strong allergy-protective properties. *J Allergy Clin Immunol, 119*(6), 1514-1521. doi:10.1016/j.jaci.2007.03.023

Decker, T., & Lohmann-Matthes, M. L. (1988). A quick and simple method for the quantitation of lactate dehydrogenase release in measurements of cellular cytotoxicity and tumor necrosis factor (TNF) activity. *J Immunol Methods, 115*(1), 61-69. doi:10.1016/0022-1759(88)90310-9

Deluca, H. F., & Engstrom, G. W. (1961). Calcium uptake by rat kidney mitochondria. *Proc Natl Acad Sci U S A, 47*, 1744-1750. doi:10.1073/pnas.47.11.1744

Denham, N. C., Pearman, C. M., Caldwell, J. L., Madders, G. W. P., Eisner, D. A., Trafford, A. W.et al. (2018). Calcium in the Pathophysiology of Atrial Fibrillation and Heart Failure. *Front Physiol, 9*, 1380. doi:10.3389/fphys.2018.01380

Dhamoon, A. S., & Jalife, J. (2005). The inward rectifier current (IK1) controls cardiac excitability and is involved in arrhythmogenesis. *Heart Rhythm, 2*(3), 316-324. doi:10.1016/j.hrthm.2004.11.012

DiMarco, D. M., Missimer, A., Murillo, A. G., Lemos, B. S., Malysheva, O. V., Caudill, M. A.et al. (2017). Intake of up to 3 Eggs/Day Increases HDL Cholesterol and Plasma Choline While Plasma Trimethylamine-N-oxide is Unchanged in a Healthy Population. *Lipids, 52*(3), 255-263. doi:10.1007/s11745-017-4230-9

Doenst, T., Nguyen, T. D., & Abel, E. D. (2013). Cardiac metabolism in heart failure: implications beyond ATP production. *Circ Res, 113*(6), 709-724. doi:10.1161/CIRCRESAHA.113.300376

Dolphin, A. C. (2016). Voltage-gated calcium channels and their auxiliary subunits: physiology and pathophysiology and pharmacology. *J Physiol, 594*(19), 53695390. doi:10.1113/JP272262

Donohoe, D. R., Garge, N., Zhang, X., Sun, W., O'Connell, T. M., Bunger, M. K.et al. (2011). The microbiome and butyrate regulate energy metabolism and autophagy in the mammalian colon. *Cell Metab, 13*(5), 517-526. doi:10.1016/j.cmet.2011.02.018

Donohoe, D. R., Wali, A., Brylawski, B. P., & Bultman, S. J. (2012). Microbial regulation of glucose metabolism and cell-cycle progression in mammalian colonocytes. *PLoS One, 7*(9), e46589. doi:10.1371/journal.pone.0046589

Dott, W., Mistry, P., Wright, J., Cain, K., & Herbert, K. E. (2014). Modulation of mitochondrial bioenergetics in a skeletal muscle cell line model of mitochondrial toxicity. *Redox Biol, 2*, 224-233. doi:10.1016/j.redox.2013.12.028

Douglas, G. M., Hansen, R., Jones, C. M. A., Dunn, K. A., Comeau, A. M., Bielawski, J. P.et al. (2018). Multi-omics differentially classify disease state and treatment outcome in pediatric Crohn's disease. *Microbiome, 6*(1), 13. doi:10.1186/s40168-018-0398-3

Dudkina, N. V., Sunderhaus, S., Boekema, E. J., & Braun, H. P. (2008). The higher level of organization of the oxidative phosphorylation system: mitochondrial supercomplexes. *J Bioenerg Biomembr, 40*(5), 419-424. doi:10.1007/s10863008-9167-5

Dumas, M. E., Barton, R. H., Toye, A., Cloarec, O., Blancher, C., Rothwell, A.et al. (2006). Metabolic profiling reveals a contribution of gut microbiota to fatty liver phenotype in insulin-resistant mice. *Proc Natl Acad Sci U S A, 103*(33), 12511-12516. doi:10.1073/pnas.0601056103

Dykens, J. A., Jamieson, J. D., Marroquin, L. D., Nadanaciva, S., Xu, J. J., Dunn, M. C.et al. (2008). In vitro assessment of mitochondrial dysfunction and cytotoxicity of nefazodone, trazodone, and buspirone. *Toxicol Sci, 103*(2), 335-345. doi:10.1093/toxsci/kfn056

Dykens, J. A., & Will, Y. (2007). The significance of mitochondrial toxicity testing in drug development. *Drug Discov Today, 12*(17-18), 777-785. doi:10.1016/j.drudis.2007.07.013

Eisner, D. A., Caldwell, J. L., Kistamas, K., & Trafford, A. W. (2017). Calcium and Excitation-Contraction Coupling in the Heart. *Circ Res, 121*(2), 181-195. doi:10.1161/CIRCRESAHA.117.310230

Erickson, A. R., Cantarel, B. L., Lamendella, R., Darzi, Y., Mongodin, E. F., Pan, C.et al. (2012). Integrated metagenomics/metaproteomics reveals human hostmicrobiota signatures of Crohn's disease. *PLoS One, 7*(11), e49138. doi:10.1371/journal.pone.0049138

Ethanic, M., Stanimirov, B., Pavlovic, N., Golocorbin-Kon, S., Al-Salami, H., Stankov, K.et al. (2018). Pharmacological Applications of Bile Acids and Their Derivatives in the Treatment of Metabolic Syndrome. *Front Pharmacol, 9*, 1382. doi:10.3389/fphar.2018.01382

Evans, J. M., Morris, L. S., & Marchesi, J. R. (2013). The gut microbiome: the role of a virtual organ in the endocrinology of the host. *J Endocrinol, 218*(3), R37-47. doi:10.1530/JOE-13-0131

Falony, G., Vieira-Silva, S., & Raes, J. (2015). Microbiology Meets Big Data: The Case of Gut Microbiota-Derived Trimethylamine. *Annu Rev Microbiol, 69*, 305-321. doi:10.1146/annurev-micro-091014-104422

Falconi, C. A., Junho, C., Fogaca-Ruiz, F., Vernier, I. C. S., da Cunha, R. S., Stinghen, A. E. M.et al. (2021). Uremic Toxins: An Alarming Danger Concerning the Cardiovascular System. *Front Physiol, 12*, 686249. doi:10.3389/fphys.2021.686249

Fenwick, E. M., Marty, A., & Neher, E. (1982). Sodium and calcium channels in bovine chromaffin cells. *J Physiol, 331*, 599-635. doi:10.1113/jphysiol.1982.sp014394

Ferdinandy, P., Danial, H., Ambrus, I., Rothery, R. A., & Schulz, R. (2000). Peroxynitrite is a major contributor to cytokine-induced myocardial contractile failure. *Circ Res, 87*(3), 241-247. doi:10.1161/01.res.87.3.241

Ferreri-Jacobia, M., Mak, D. O., & Foskett, J. K. (2005). Translational mobility of the type 3 inositol 1,4,5-trisphosphate receptor Ca2+ release channel in endoplasmic reticulum membrane. *J Biol Chem, 280*(5), 3824-3831. doi:10.1074/jbc.M409462200

Ferrick, D. A., Neilson, A., & Beeson, C. (2008). Advances in measuring cellular bioenergetics using extracellular flux. *Drug Discov Today, 13*(5-6), 268-274. doi:10.1016/j.drudis.2007.12.008

Fiehn, O. (2002). Metabolomics--the link between genotypes and phenotypes. *Plant Mol Biol, 48*(1-2), 155-171. Retrieved from https://www.ncbi.nlm.nih.gov/pubmed/11860207

Flanagan, J. L., Simmons, P. A., Vehige, J., Willcox, M. D., & Garrett, Q. (2010). Role of carnitine in disease. *Nutr Metab (Lond), 7*, 30. doi:10.1186/1743-7075-7-30

Flint, H. J., Scott, K. P., Louis, P., & Duncan, S. H. (2012). The role of the gut microbiota in nutrition and health. *Nat Rev Gastroenterol Hepatol, 9*(10), 577-589. doi:10.1038/nrgastro.2012.156

Fodor, A. (2014). Utilizing "omics" tools to study the complex gut ecosystem. *Adv Exp Med Biol, 817*, 25-38. doi:10.1007/978-1-4939-0897-4_2

Foster, J. A., & McVey Neufeld, K. A. (2013). Gut-brain axis: how the microbiome influences anxiety and depression. *Trends Neurosci, 36*(5), 305-312. doi:10.1016/j.tins.2013.01.005

Foster, M. N., & Coetzee, W. A. (2016). KATP Channels in the Cardiovascular System. *Physiol Rev, 96*(1), 177-252. doi:10.1152/physrev.00003.2015

Freeland, K. R., & Wolever, T. M. (2010). Acute effects of intravenous and rectal acetate on glucagon-like peptide-1, peptide YY, ghrelin, adiponectin and tumour necrosis factor-alpha. *Br J Nutr, 103*(3), 460-466. doi:10.1017/S0007114509991863

Friedrich, T., & Bottcher, B. (2004). The gross structure of the respiratory complex I: a Lego System. *Biochim Biophys Acta, 1608*(1), 1-9. doi:10.1016/j.bbabio.2003.10.002

Fu, D. G. (2015). Cardiac Arrhythmias: Diagnosis, Symptoms, and Treatments. *Cell Biochem Biophys, 73*(2), 291-296. doi:10.1007/s12013-015-0626-4

Fu, Q., Zhao, M., Wang, D., Hu, H., Guo, C., Chen, W.et al. (2016). Coronary Plaque Characterization Assessed by Optical Coherence Tomography and Plasma Trimethylamine-N-oxide Levels in Patients With Coronary Artery Disease. *Am J Cardiol, 118*(9), 1311-1315. doi:10.1016/j.amjcard.2016.07.071

Fujino, M., Ishihara, M., Honda, S., Kawakami, S., Yamane, T., Nagai, T.et al. (2014). Impact of acute and chronic hyperglycemia on in-hospital outcomes of patients with acute myocardial infarction. *Am J Cardiol, 114*(12), 1789-1793. doi:10.1016/j.amjcard.2014.09.015

Furusawa, Y., Obata, Y., Fukuda, S., Endo, T. A., Nakato, G., Takahashi, D.et al. (2013). Commensal microbe-derived butyrate induces the differentiation of colonic regulatory T cells. *Nature, 504*(7480), 446-450. doi:10.1038/nature12721

Fuster, V., Ryden, L. E., Cannom, D. S., Crijns, H. J., Curtis, A. B., Ellenbogen, K. A.et al. (2006). ACC/AHA/ESC 2006 Guidelines for the Management of Patients with Atrial Fibrillation: a report of the American College of Cardiology/American Heart Association Task Force on Practice Guidelines and the European Society of Cardiology Committee for Practice Guidelines (Writing Committee to Revise the 2001 Guidelines for the Management of Patients With Atrial Fibrillation): developed in collaboration with the European Heart Rhythm Association and the Heart Rhythm Society. *Circulation, 114*(7), e257-354. doi:10.1161/CIRCULATIONAHA.106.177292

Gan, X. T., Ettinger, G., Huang, C. X., Burton, J. P., Haist, J. V., Rajapurohitam, V.et al. (2014). Probiotic administration attenuates myocardial hypertrophy and heart failure after myocardial infarction in the rat. *Circ Heart Fail, 7*(3), 491-499. doi:10.1161/CIRCHEARTFAILURE.113.000978

Gansevoort, R. T., Correa-Rotter, R., Hemmelgarn, B. R., Jafar, T. H., Heerspink, H. J., Mann, J. F.et al. (2013). Chronic kidney disease and cardiovascular risk: epidemiology, mechanisms, and prevention. *Lancet, 382*(9889), 339-352. doi:10.1016/S0140-6736(13)60595-4

Gardner, L. S., Nguyen-Pham, S., Greenslade, J. H., Parsonage, W., D'Emden, M., Than, M.et al. (2015). Admission glycaemia and its association with acute coronary syndrome in Emergency Department patients with chest pain. *Emerg Med J, 32*(8), 608-612. doi:10.1136/emermed-2014-204046

Gawrys-Kopczynska, M., Konop, M., Maksymiuk, K., Kraszewska, K., Derzsi, L., Sozanski, K.et al. (2020). TMAO, a seafood-derived molecule, produces diuresis and reduces mortality in heart failure rats. *Elife, 9*. doi:10.7554/eLife.57028

Gessner, A., di Giuseppe, R., Koch, M., Fromm, M. F., Lieb, W., & Maas, R. (2020). Trimethylamine-N-oxide (TMAO) determined by LC-MS/MS: distribution and correlates in the population-based PopGen cohort. *Clin Chem Lab Med, 58*(5), 733-740. doi:10.1515/cclm-2019-1146

Gho, B. C., Eskildsen-Helmond, Y. E., de Zeeuw, S., Lamers, J. M., & Verdouw, P. D. (1997). Does protein kinase C play a pivotal role in the mechanisms of ischemic preconditioning? *Cardiovasc Drugs Ther, 10*(6), 775-786. doi:10.1007/BF00053036

Gibson, G. R., & Roberfroid, M. B. (1995). Dietary modulation of the human colonic microbiota: introducing the concept of prebiotics. *J Nutr, 125*(6), 1401-1412. doi:10.1093/jn/125.6.1401

Gill, S. R., Pop, M., Deboy, R. T., Eckburg, P. B., Turnbaugh, P. J., Samuel, B. S.et al. (2006). Metagenomic analysis of the human distal gut microbiome. *Science, 312*(5778), 1355-1359. doi:10.1126/science.1124234

Gohil, V. M., Sheth, S. A., Nilsson, R., Wojtovich, A. P., Lee, J. H., Perocchi, F.et al. (2010). Nutrient-sensitized screening for drugs that shift energy metabolism from mitochondrial respiration to glycolysis. *Nat Biotechnol, 28*(3), 249-255. doi:10.1038/nbt.1606

Gomez, A. M., Guatimosim, S., Dilly, K. W., Vassort, G., & Lederer, W. J. (2001). Heart failure after myocardial infarction: altered excitation-contraction coupling. *Circulation, 104*(6), 688-693. doi:10.1161/hc3201.092285

Gomez-Guzman, M., Toral, M., Romero, M., Jimenez, R., Galindo, P., Sanchez, M.et al. (2015). Antihypertensive effects of probiotics Lactobacillus strains in spontaneously hypertensive rats. *Mol Nutr Food Res, 59*(11), 2326-2336. doi:10.1002/mnfr.201500290

Goodrich, J. K., Davenport, E. R., Beaumont, M., Jackson, M. A., Knight, R., Ober, C.et al. (2016). Genetic Determinants of the Gut Microbiome in UK Twins. *Cell Host Microbe, 19*(5), 731-743. doi:10.1016/j.chom.2016.04.017

Goodrich, J. K., Waters, J. L., Poole, A. C., Sutter, J. L., Koren, O., Blekhman, R.et al. (2014). Human genetics shape the gut microbiome. *Cell, 159*(4), 789-799. doi:10.1016/j.cell.2014.09.053

Goonasekera, S. A., Hammer, K., Auger-Messier, M., Bodi, I., Chen, X., Zhang, H.et al. (2012). Decreased cardiac L-type Ca(2)(+) channel activity induces hypertrophy and heart failure in mice. *J Clin Invest, 122*(1), 280-290. doi:10.1172/JCI58227

Granata, V., Palladino, P., Tizzano, B., Negro, A., Berisio, R., & Zagari, A. (2006). The effect of the osmolyte trimethylamine N-oxide on the stability of the prion protein at low pH. *Biopolymers, 82*(3), 234-240. doi:10.1002/bip.20481

Grehan, M. J., Borody, T. J., Leis, S. M., Campbell, J., Mitchell, H., & Wettstein, A. (2010). Durable alteration of the colonic microbiota by the administration of donor fecal flora. *J Clin Gastroenterol, 44*(8), 551-561. doi:10.1097/MCG.0b013e3181e5d06b

Gross, P., Massy, Z. A., Henaut, L., Boudot, C., Cagnard, J., March, C.et al. (2015). Para-cresyl sulfate acutely impairs vascular reactivity and induces vascular remodeling. *J Cell Physiol, 230*(12), 2927-2935. doi:10.1002/jcp.25018

Gryp, T., Vanholder, R., Vaneechoutte, M., & Glorieux, G. (2017). p-Cresyl Sulfate. *Toxins (Basel), 9*(2). doi:10.3390/toxins9020052

Gyorke, S., & Terentyev, D. (2008). Modulation of ryanodine receptor by luminal calcium and accessory proteins in health and cardiac disease. *Cardiovasc Res, 77*(2), 245255. doi:10.1093/cvr/cvm038

H.A., K. (1937). The citric acid cycle. *Science, Technology and Management, 5*.

Hai, X., Landeras, V., Dobre, M. A., DeOreo, P., Meyer, T. W., & Hostetter, T. H. (2015). Mechanism of Prominent Trimethylamine Oxide (TMAO) Accumulation in Hemodialysis Patients. *PLoS One, 10*(12), e0143731. doi:10.1371/journal.pone.0143731

Hall, A. B., Tolonen, A. C., & Xavier, R. J. (2017). Human genetic variation and the gut microbiome in disease. *Nat Rev Genet, 18*(11), 690-699. doi:10.1038/nrg.2017.63

Hansen, J., Gulati, A., & Sartor, R. B. (2010). The role of mucosal immunity and host genetics in defining intestinal commensal bacteria. *Curr Opin Gastroenterol, 26*(6), 564-571. doi:10.1097/MOG.0b013e32833f1195

Hartiala, J., Bennett, B. J., Tang, W. H., Wang, Z., Stewart, A. F., Roberts, R.et al. (2014). Comparative genome-wide association studies in mice and humans for trimethylamine N-oxide, a proatherogenic metabolite of choline and L-carnitine. *Arterioscler Thromb Vasc Biol, 34*(6), 1307-1313. doi:10.1161/ATVBAHA.114.303252

Heaney, L. M. (2020). Applying mass spectrometry-based assays to explore gut microbial metabolism and associations with disease. *Clin Chem Lab Med, 58*(5), 719-732. doi:10.1515/cclm-2019-0974

Heijman, J., Voigt, N., Nattel, S., & Dobrev, D. (2014). Cellular and molecular electrophysiology of atrial fibrillation initiation, maintenance, and progression. *Circ Res, 114*(9), 1483-1499. doi:10.1161/CIRCRESAHA.114.302226

Heinken, A., Khan, M. T., Paglia, G., Rodionov, D. A., Harmsen, H. J., & Thiele, I. (2014). Functional metabolic map of Faecalibacterium prausnitzii, a beneficial human gut microbe. *J Bacteriol, 196*(18), 3289-3302. doi:10.1128/JB.01780-14

Herlaar, E., & Brown, Z. (1999). p38 MAPK signalling cascades in inflammatory disease. *Mol Med Today, 5*(10), 439-447. doi:10.1016/s1357-4310(99)01544-0

Hibino, H., Inanobe, A., Furutani, K., Murakami, S., Findlay, I., & Kurachi, Y. (2010). Inwardly rectifying potassium channels: their structure, function, and physiological roles. *Physiol Rev, 90*(1), 291-366. doi:10.1152/physrev.00021.2009

Hill, M. J. (1997). Intestinal flora and endogenous vitamin synthesis. *Eur J Cancer Prev, 6 Suppl 1*, S43-45. Retrieved from http://www.ncbi.nlm.nih.gov/pubmed/9167138

Hiraoka, M., Kawano, S., Hirano, Y., & Furukawa, T. (1998). Role of cardiac chloride currents in changes in action potential characteristics and arrhythmias. *Cardiovasc Res, 40*(1), 23-33. doi:10.1016/s0008-6363(98)00173-4

Hirst, J. (2009). Towards the molecular mechanism of respiratory complex I. *Biochem J, 425*(2), 327-339. doi:10.1042/BJ20091382

Holmes, E., Li, J. V., Athanasiou, T., Ashrafian, H., & Nicholson, J. K. (2011). Understanding the role of gut microbiome-host metabolic signal disruption in health and disease. *Trends Microbiol, 19*(7), 349-359. doi:10.1016/j.tim.2011.05.006

Hong, T., & Shaw, R. M. (2017). Cardiac T-Tubule Microanatomy and Function. *Physiol Rev, 97*(1), 227-252. doi:10.1152/physrev.00037.2015

Honour, J. (1982). The possible involvement of intestinal bacteria in steroidal hypertension. *Endocrinology, 110*(1), 285-287. doi:10.1210/endo-110-1-285

Hreiche, R., Plante, I., David, L. P., Simard, C., Turgeon, J., & Drolet, B. (2009). Impact of glucose concentration on cardiac ventricular repolarization under I Kr/I Ks blocking agents. *J Mol Cell Cardiol, 47*(2), 210-220. doi:10.1016/j.yjmcc.2009.02.004

Hu, J., Lin, S., Zheng, B., & Cheung, P. C. K. (2018). Short-chain fatty acids in control of energy metabolism. *Crit Rev Food Sci Nutr, 58*(8), 1243-1249. doi:10.1080/10408398.2016.1245650

Huc, T., Drapala, A., Gawrys, M., Konop, M., Bielinska, K., Zaorska, E.et al. (2018). Chronic, low-dose TMAO treatment reduces diastolic dysfunction and heart fibrosis in hypertensive rats. *Am J Physiol Heart Circ Physiol, 315*(6), H1805H1820. doi:10.1152/ajpheart.00536.2018

Hughes, R., Cross, A. J., Pollock, J. R., & Bingham, S. (2001). Dose-dependent effect of dietary meat on endogenous colonic N-nitrosation. *Carcinogenesis, 22*(1), 199202. doi:10.1093/carcin/22.1.199

Human Microbiome Project, C. (2012a). A framework for human microbiome research. *Nature, 486*(7402), 215-221. doi:10.1038/nature11209

Human Microbiome Project, C. (2012b). Structure, function and diversity of the healthy human microbiome. *Nature, 486*(7402), 207-214. doi:10.1038/nature11234

Huse, S. M., Ye, Y., Zhou, Y., & Fodor, A. A. (2012). A core human microbiome as viewed through 16S rRNA sequence clusters. *PLoS One, 7*(6), e34242. doi:10.1371/journal.pone.0034242

Huttemann, M., Lee, I., Samavati, L., Yu, H., & Doan, J. W. (2007). Regulation of mitochondrial oxidative phosphorylation through cell signaling. *Biochim Biophys Acta, 1773*(12), 1701-1720. doi:10.1016/j.bbamcr.2007.10.001

Ikeda, Y., Shirakabe, A., Brady, C., Zablocki, D., Ohishi, M., & Sadoshima, J. (2015). Molecular mechanisms mediating mitochondrial dynamics and mitophagy and

their functional roles in the cardiovascular system. *J Mol Cell Cardiol, 78*, 116-122. doi:10.1016/j.yjmcc.2014.09.019

Isidoro Tavares, N., Philip-Couderc, P., Papageorgiou, I., Baertschi, A. J., Lerch, R., & Montessuit, C. (2007). Expression and function of ATP-dependent potassium channels in late post-infarction remodeling. *J Mol Cell Cardiol, 42*(6), 1016-1025. doi:10.1016/j.yjmcc.2007.04.008

Jalife, J. (2011). Deja vu in the theories of atrial fibrillation dynamics. *Cardiovasc Res, 89*(4), 766-775. doi:10.1093/cvr/cvq364

Janeiro, M. H., Ramirez, M. J., Milagro, F. I., Martinez, J. A., & Solas, M. (2018). Implication of Trimethylamine N-Oxide (TMAO) in Disease: Potential Biomarker or New Therapeutic Target. *Nutrients, 10*(10). doi:10.3390/nu10101398

Jansson, J., Willing, B., Lucio, M., Fekete, A., Dicksved, J., Halfvarson, J.et al. (2009). Metabolomics reveals metabolic biomarkers of Crohn's disease. *PLoS One, 4*(7), e6386. doi:10.1371/journal.pone.0006386

Jawien, J., Nastalek, P., & Korbut, R. (2004). Mouse models of experimental atherosclerosis. *J Physiol Pharmacol, 55*(3), 503-517. Retrieved from https://www.ncbi.nlm.nih.gov/pubmed/15381823

Jaworska, K., Hering, D., Mosieniak, G., Bielak-Zmijewska, A., Pilz, M., Konwerski, M.et al. (2019). TMA, A Forgotten Uremic Toxin, but Not TMAO, Is Involved in Cardiovascular Pathology. *Toxins (Basel), 11*(9). doi:10.3390/toxins11090490

Jeevaratnam, K., Chadda, K. R., Huang, C. L., & Camm, A. J. (2018). Cardiac Potassium Channels: Physiological Insights for Targeted Therapy. *J Cardiovasc Pharmacol Ther, 23*(2), 119-129. doi:10.1177/1074248417729880

Ji, Y., Yin, Y., Li, Z., & Zhang, W. (2019). Gut Microbiota-Derived Components and Metabolites in the Progression of Non-Alcoholic Fatty Liver Disease (NAFLD). *Nutrients, 11*(8). doi:10.3390/nu11081712

Jiang, C., Xie, C., Li, F., Zhang, L., Nichols, R. G., Krausz, K. W.et al. (2015). Intestinal farnesoid X receptor signaling promotes nonalcoholic fatty liver disease. *J Clin Invest, 125*(1), 386-402. doi:10.1172/JCI76738

Jonckheere, A. I., Smeitink, J. A., & Rodenburg, R. J. (2012). Mitochondrial ATP synthase: architecture, function and pathology. *J Inherit Metab Dis, 35*(2), 211-225. doi:10.1007/s10545-011-9382-9

Kalogeris, T., Baines, C. P., Krenz, M., & Korthuis, R. J. (2012). Cell biology of ischemia/reperfusion injury. *Int Rev Cell Mol Biol, 298*, 229-317. doi:10.1016/B978-0-12-394309-5.00006-7

Kalogeris, T., Bao, Y., & Korthuis, R. J. (2014). Mitochondrial reactive oxygen species: a double edged sword in ischemia/reperfusion vs preconditioning. *Redox Biol, 2*, 702-714. doi:10.1016/j.redox.2014.05.006

Kamalian, L., Chadwick, A. E., Bayliss, M., French, N. S., Monshouwer, M., Snoeys, J.et al. (2015). The utility of HepG2 cells to identify direct mitochondrial dysfunction in the absence of cell death. *Toxicol In Vitro, 29*(4), 732-740. doi:10.1016/j.tiv.2015.02.011

Kamalian, L., Douglas, O., Jolly, C. E., Snoeys, J., Simic, D., Monshouwer, M.et al. (2018). The utility of HepaRG cells for bioenergetic investigation and detection of drug-

induced mitochondrial toxicity. *Toxicol In Vitro, 53*, 136-147. doi:10.1016/j.tiv.2018.08.001

Karbach, S. H., Schonfelder, T., Brandao, I., Wilms, E., Hormann, N., Jackel, S.et al. (2016). Gut Microbiota Promote Angiotensin II-Induced Arterial Hypertension and Vascular Dysfunction. *J Am Heart Assoc, 5*(9). doi:10.1161/JAHA.116.003698

Karlsson, F. H., Tremaroli, V., Nookaew, I., Bergstrom, G., Behre, C. J., Fagerberg, B.et al. (2013). Gut metagenome in European women with normal, impaired and diabetic glucose control. *Nature, 498*(7452), 99-103. doi:10.1038/nature12198

Karwi, Q. G., Uddin, G. M., Ho, K. L., & Lopaschuk, G. D. (2018). Loss of Metabolic Flexibility in the Failing Heart. *Front Cardiovasc Med, 5*, 68. doi:10.3389/fcvm.2018.00068

Kawase, M., Hashimoto, H., Hosoda, M., Morita, H., & Hosono, A. (2000). Effect of administration of fermented milk containing whey protein concentrate to rats and healthy men on serum lipids and blood pressure. *J Dairy Sci, 83*(2), 255-263. doi:10.3168/jds.S0022-0302(00)74872-7

Kaysen, G. A., Johansen, K. L., Chertow, G. M., Dalrymple, L. S., Kornak, J., Grimes, B.et al. (2015). Associations of Trimethylamine N-Oxide With Nutritional and Inflammatory Biomarkers and Cardiovascular Outcomes in Patients New to Dialysis. *J Ren Nutr, 25*(4), 351-356. doi:10.1053/j.jrn.2015.02.006

Ke, Y., Li, D., Zhao, M., Liu, C., Liu, J., Zeng, A.et al. (2018). Gut flora-dependent metabolite Trimethylamine-N-oxide accelerates endothelial cell senescence and vascular aging through oxidative stress. *Free Radic Biol Med, 116*, 88-100. doi:10.1016/j.freeradbiomed.2018.01.007

Kelly, R. H., & Yancey, P. H. (1999). High contents of trimethylamine oxide correlating with depth in deep-sea teleost fishes, skates, and decapod crustaceans. *Biol Bull, 196*(1), 18-25. doi:10.2307/1543162

Khalesi, S., Sun, J., Buys, N., & Jayasinghe, R. (2014). Effect of probiotics on blood pressure: a systematic review and meta-analysis of randomized, controlled trials. *Hypertension, 64*(4), 897-903. doi:10.1161/HYPERTENSIONAHA.114.03469

Khosravi, A., Yanez, A., Price, J. G., Chow, A., Merad, M., Goodridge, H. S.et al. (2014). Gut microbiota promote hematopoiesis to control bacterial infection. *Cell Host Microbe, 15*(3), 374-381. doi:10.1016/j.chom.2014.02.006

Kim, C. H. (2018). Microbiota or short-chain fatty acids: which regulates diabetes? *Cell Mol Immunol, 15*(2), 88-91. doi:10.1038/cmi.2017.57

Kim, J. B. (2014). Channelopathies. *Korean J Pediatr, 57*(1), 1-18. doi:10.3345/kjp.2014.57.1.1

Kim, H. Y., Yoo, T. H., Cho, J. Y., Kim, H. C., & Lee, W. W. (2019). Indoxyl sulfate-induced TNF-alpha is regulated by crosstalk between the aryl hydrocarbon receptor, NF-kappaB, and SOCS2 in human macrophages. *FASEB J, 33*(10), 10844-10858. doi:10.1096/fj.201900730R

Kleiner, M. (2019). Metaproteomics: Much More than Measuring Gene Expression in Microbial Communities. *mSystems, 4*(3). doi:10.1128/mSystems.00115-19

Klupczynska, A., Derezinski, P., & Kokot, Z. J. (2015). Metabolomics in Medical Sciences--Trends, Challenges and Perspectives. *Acta Pol Pharm, 72*(4), 629-641. Retrieved from https://www.ncbi.nlm.nih.gov/pubmed/26647618

Koeth, R. A., Levison, B. S., Culley, M. K., Buffa, J. A., Wang, Z., Gregory, J. C.et al. (2014). gamma-Butyrobetaine is a proatherogenic intermediate in gut microbial metabolism of L-carnitine to TMAO. *Cell Metab, 20*(5), 799-812. doi:10.1016/j.cmet.2014.10.006

Koeth, R. A., Wang, Z., Levison, B. S., Buffa, J. A., Org, E., Sheehy, B. T.et al. (2013). Intestinal microbiota metabolism of L-carnitine, a nutrient in red meat, promotes atherosclerosis. *Nat Med, 19*(5), 576-585. doi:10.1038/nm.3145

Koloski, N. A., Jones, M., Kalantar, J., Weltman, M., Zaguirre, J., & Talley, N. J. (2012). The brain--gut pathway in functional gastrointestinal disorders is bidirectional: a 12-year prospective population-based study. *Gut, 61*(9), 1284-1290. doi:10.1136/gutjnl-2011-300474

Kolwicz, S. C., Jr., Olson, D. P., Marney, L. C., Garcia-Menendez, L., Synovec, R. E., & Tian, R. (2012). Cardiac-specific deletion of acetyl CoA carboxylase 2 prevents metabolic remodeling during pressure-overload hypertrophy. *Circ Res, 111*(6), 728-738. doi:10.1161/CIRCRESAHA.112.268128

Koopman, M., Michels, H., Dancy, B. M., Kamble, R., Mouchiroud, L., Auwerx, J.et al. (2016). A screening-based platform for the assessment of cellular respiration in Caenorhabditis elegans. *Nat Protoc, 11*(10), 1798-1816. doi:10.1038/nprot.2016.106

Krumsiek, J., Mittelstrass, K., Do, K. T., Stuckler, F., Ried, J., Adamski, J.et al. (2015). Gender-specific pathway differences in the human serum metabolome. *Metabolomics, 11*(6), 1815-1833. doi:10.1007/s11306-015-0829-0

Kuhn, T., Rohrmann, S., Sookthai, D., Johnson, T., Katzke, V., Kaaks, R.et al. (2017). Intraindividual variation of plasma trimethylamine-N-oxide (TMAO), betaine and choline over 1 year. *Clin Chem Lab Med, 55*(2), 261-268. doi:10.1515/cclm-20160374

Kumar, S., Kain, V., & Sitasawad, S. L. (2012). High glucose-induced Ca2+ overload and oxidative stress contribute to apoptosis of cardiac cells through mitochondrial dependent and independent pathways. *Biochim Biophys Acta, 1820*(7), 907-920. doi:10.1016/j.bbagen.2012.02.010

Kummen, M., Vesterhus, M., Troseid, M., Moum, B., Svardal, A., Boberg, K. M.et al. (2017). Elevated trimethylamine-N-oxide (TMAO) is associated with poor prognosis in primary sclerosing cholangitis patients with normal liver function. *United European Gastroenterol J, 5*(4), 532-541. doi:10.1177/2050640616663453

Kuntz, T. M., & Gilbert, J. A. (2017). Introducing the Microbiome into Precision Medicine. *Trends Pharmacol Sci, 38*(1), 81-91. doi:10.1016/j.tips.2016.10.001

Kushnir, A., & Marks, A. R. (2010). The ryanodine receptor in cardiac physiology and disease. *Adv Pharmacol, 59*, 1-30. doi:10.1016/S1054-3589(10)59001-X

Labbe, G., Pessayre, D., & Fromenty, B. (2008). Drug-induced liver injury through mitochondrial dysfunction: mechanisms and detection during preclinical safety studies. *Fundam Clin Pharmacol, 22*(4), 335-353. doi:10.1111/j.14728206.2008.00608.x

Lam, V., Su, J., Hsu, A., Gross, G. J., Salzman, N. H., & Baker, J. E. (2016). Intestinal Microbial Metabolites Are Linked to Severity of Myocardial Infarction in Rats. *PLoS One, 11*(8), e0160840. doi:10.1371/journal.pone.0160840

Lam, V., Su, J., Koprowski, S., Hsu, A., Tweddell, J. S., Rafiee, P.et al. (2012). Intestinal microbiota determine severity of myocardial infarction in rats. *FASEB J, 26*(4), 1727-1735. doi:10.1096/fj.11-197921

Landstrom, A. P., Dobrev, D., & Wehrens, X. H. T. (2017). Calcium Signaling and Cardiac Arrhythmias. *Circ Res, 120*(12), 1969-1993. doi:10.1161/CIRCRESAHA.117.310083

Lanner, J. T., Georgiou, D. K., Joshi, A. D., & Hamilton, S. L. (2010). Ryanodine receptors: structure, expression, molecular details, and function in calcium release. *Cold Spring Harb Perspect Biol, 2*(11), a003996. doi:10.1101/cshperspect.a003996

Lau, K., Srivatsav, V., Rizwan, A., Nashed, A., Liu, R., Shen, R.et al. (2017). Bridging the Gap between Gut Microbial Dysbiosis and Cardiovascular Diseases. *Nutrients, 9*(8). doi:10.3390/nu9080859

Lavelle, A., & Sokol, H. (2020). Gut microbiota-derived metabolites as key actors in inflammatory bowel disease. *Nat Rev Gastroenterol Hepatol, 17*(4), 223-237. doi:10.1038/s41575-019-0258-z

Lawrence, K. M., Chanalaris, A., Scarabelli, T., Hubank, M., Pasini, E., Townsend, P. A.et al. (2002). K(ATP) channel gene expression is induced by urocortin and mediates

its cardioprotective effect. *Circulation, 106*(12), 1556-1562. doi:10.1161/01.cir.0000028424.02525.ae

Le Chatelier, E., Nielsen, T., Qin, J., Prifti, E., Hildebrand, F., Falony, G.et al. (2013). Richness of human gut microbiome correlates with metabolic markers. *Nature, 500*(7464), 541-546. doi:10.1038/nature12506

Lederer, W. J., Berlin, J. R., Cohen, N. M., Hadley, R. W., Bers, D. M., & Cannell, M. B. (1990). Excitation-contraction coupling in heart cells. Roles of the sodiumcalcium exchange, the calcium current, and the sarcoplasmic reticulum. *Ann N Y Acad Sci, 588*, 190-206. doi:10.1111/j.1749-6632.1990.tb13210.x

Lederer, W. J., & Nichols, C. G. (1989). Nucleotide modulation of the activity of rat heart ATP-sensitive K+ channels in isolated membrane patches. *J Physiol, 419*, 193-211. doi:10.1113/jphysiol.1989.sp017869

Lee, D., Albenberg, L., Compher, C., Baldassano, R., Piccoli, D., Lewis, J. D.et al. (2015). Diet in the pathogenesis and treatment of inflammatory bowel diseases. *Gastroenterology, 148*(6), 1087-1106. doi:10.1053/j.gastro.2015.01.007

Lefebvre, P., Cariou, B., Lien, F., Kuipers, F., & Staels, B. (2009). Role of bile acids and bile acid receptors in metabolic regulation. *Physiol Rev, 89*(1), 147-191. doi:10.1152/physrev.00010.2008

Lehninger, A. L., Rossi, C. S., & Greenawalt, J. W. (1963). Respiration-dependent accumulation of inorganic phosphate and Ca ions by rat liver mitochondria. *Biochem Biophys Res Commun, 10*, 444-448. doi:10.1016/0006-291x(63)903772

Lemos, B. S., Medina-Vera, I., Malysheva, O. V., Caudill, M. A., & Fernandez, M. L. (2018). Effects of Egg Consumption and Choline Supplementation on Plasma Choline and Trimethylamine-N-Oxide in a Young Population. *J Am Coll Nutr, 37*(8), 716-723. doi:10.1080/07315724.2018.1466213

Lengyel, C., Iost, N., Virag, L., Varro, A., Lathrop, D. A., & Papp, J. G. (2001). Pharmacological block of the slow component of the outward delayed rectifier current (I(Ks)) fails to lengthen rabbit ventricular muscle QT(c) and action potential duration. *Br J Pharmacol, 132*(1), 101-110. doi:10.1038/sj.bjp.0703777

Lever, M., George, P. M., Slow, S., Bellamy, D., Young, J. M., Ho, M.et al. (2014). Betaine and Trimethylamine-N-Oxide as Predictors of Cardiovascular Outcomes Show Different Patterns in Diabetes Mellitus: An Observational Study. *PLoS One, 9*(12), e114969. doi:10.1371/journal.pone.0114969

Levy, M., Thaiss, C. A., & Elinav, E. (2016). Metabolites: messengers between the microbiota and the immune system. *Genes Dev, 30*(14), 1589-1597. doi:10.1101/gad.284091.116

Ley, R. E., Backhed, F., Turnbaugh, P., Lozupone, C. A., Knight, R. D., & Gordon, J. I. (2005). Obesity alters gut microbial ecology. *Proc Natl Acad Sci U S A, 102*(31), 11070-11075. doi:10.1073/pnas.0504978102

Ley, R. E., Hamady, M., Lozupone, C., Turnbaugh, P. J., Ramey, R. R., Bircher, J. S.et al. (2008). Evolution of mammals and their gut microbes. *Science, 320*(5883), 16471651. doi:10.1126/science.1155725

Ley, R. E., Turnbaugh, P. J., Klein, S., & Gordon, J. I. (2006). Microbial ecology: human gut microbes associated with obesity. *Nature, 444*(7122), 1022-1023. doi:10.1038/4441022a

Li, J., Jia, H., Cai, X., Zhong, H., Feng, Q., Sunagawa, S.et al. (2014). An integrated catalog of reference genes in the human gut microbiome. *Nat Biotechnol, 32*(8), 834841. doi:10.1038/nbt.2942

Li, M., Wang, B., Zhang, M., Rantalainen, M., Wang, S., Zhou, H.et al. (2008). Symbiotic gut microbes modulate human metabolic phenotypes. *Proc Natl Acad Sci U S A, 105*(6), 2117-2122. doi:10.1073/pnas.0712038105

Li, N., Wu, J. X., Ding, D., Cheng, J., Gao, N., & Chen, L. (2017). Structure of a Pancreatic ATP-Sensitive Potassium Channel. *Cell, 168*(1-2), 101-110 e110. doi:10.1016/j.cell.2016.12.028

Li, T., Chen, Y., Gua, C., & Li, X. (2017). Elevated Circulating Trimethylamine N-Oxide Levels Contribute to Endothelial Dysfunction in Aged Rats through Vascular Inflammation and Oxidative Stress. *Front Physiol, 8*, 350. doi:10.3389/fphys.2017.00350

Li, X. S., Obeid, S., Klingenberg, R., Gencer, B., Mach, F., Raber, L.et al. (2017). Gut microbiota-dependent trimethylamine N-oxide in acute coronary syndromes: a prognostic marker for incident cardiovascular events beyond traditional risk factors. *Eur Heart J, 38*(11), 814-824. doi:10.1093/eurheartj/ehw582

Lin, S. L., Zarrine-Afsar, A., & Davidson, A. R. (2009). The osmolyte trimethylamine-Noxide stabilizes the Fyn SH3 domain without altering the structure of its folding transition state. *Protein Sci, 18*(3), 526-536. doi:10.1002/pro.52

Lindskog Jonsson, A., Caesar, R., Akrami, R., Reinhardt, C., Fak Hallenius, F., Boren, J.et al. (2018). Impact of Gut Microbiota and Diet on the Development of Atherosclerosis in Apoe(-/-) Mice. *Arterioscler Thromb Vasc Biol, 38*(10), 2318-2326. doi:10.1161/ATVBAHA.118.311233

Lopez, A. D., Mathers, C. D., Ezzati, M., Jamison, D. T., & Murray, C. J. (2006). Global and regional burden of disease and risk factors, 2001: systematic analysis of population health data. *Lancet, 367*(9524), 1747-1757. doi:10.1016/S01406736(06)68770-9

Mackay, R. J., McEntyre, C. J., Henderson, C., Lever, M., & George, P. M. (2011). Trimethylaminuria: causes and diagnosis of a socially distressing condition. *Clin Biochem Rev, 32*(1), 33-43. Retrieved from https://www.ncbi.nlm.nih.gov/pubmed/21451776

Mafune, A., Iwamoto, T., Tsutsumi, Y., Nakashima, A., Yamamoto, I., Yokoyama, K.et al. (2016). Associations among serum trimethylamine-N-oxide (TMAO) levels, kidney function and infarcted coronary artery number in patients undergoing cardiovascular surgery: a cross-sectional study. *Clin Exp Nephrol, 20*(5), 731-739. doi:10.1007/s10157-015-1207-y

Magnusdottir, S., Heinken, A., Kutt, L., Ravcheev, D. A., Bauer, E., Noronha, A.et al. (2017). Generation of genome-scale metabolic reconstructions for 773 members of the human gut microbiota. *Nat Biotechnol, 35*(1), 81-89. doi:10.1038/nbt.3703

Makki, K., Deehan, E. C., Walter, J., & Backhed, F. (2018). The Impact of Dietary Fiber on Gut Microbiota in Host Health and Disease. *Cell Host Microbe, 23*(6), 705-715. doi:10.1016/j.chom.2018.05.012

Makrecka-Kuka, M., Volska, K., Antone, U., Vilskersts, R., Grinberga, S., Bandere, D.et al. (2017). Trimethylamine N-oxide impairs pyruvate and fatty acid oxidation in cardiac mitochondria. *Toxicol Lett, 267*, 32-38. doi:10.1016/j.toxlet.2016.12.017

Malik, A., Brito, D., & Chhabra, L. (2020). Congestive Heart Failure (CHF). In *StatPearls*. Treasure Island (FL).

Manor, O., Levy, R., & Borenstein, E. (2014). Mapping the inner workings of the microbiome: genomic- and metagenomic-based study of metabolism and metabolic interactions in the human microbiome. *Cell Metab, 20*(5), 742-752. doi:10.1016/j.cmet.2014.07.021

Maranduba, C. M., De Castro, S. B., de Souza, G. T., Rossato, C., da Guia, F. C., Valente, M. A.et al. (2015). Intestinal microbiota as modulators of the immune system and neuroimmune system: impact on the host health and homeostasis. *J Immunol Res, 2015*, 931574. doi:10.1155/2015/931574

Marks, A. R. (2013). Calcium cycling proteins and heart failure: mechanisms and therapeutics. *J Clin Invest, 123*(1), 46-52. doi:10.1172/JCI62834

Marroquin, L. D., Hynes, J., Dykens, J. A., Jamieson, J. D., & Will, Y. (2007). Circumventing the Crabtree effect: replacing media glucose with galactose increases susceptibility of HepG2 cells to mitochondrial toxicants. *Toxicol Sci, 97*(2), 539547. doi:10.1093/toxsci/kfm052

Martin, J. C., Canlet, C., Delplanque, B., Agnani, G., Lairon, D., Gottardi, G.et al. (2009). 1H NMR metabonomics can differentiate the early atherogenic effect of dairy

products in hyperlipidemic hamsters. *Atherosclerosis, 206*(1), 127-133. doi:10.1016/j.atherosclerosis.2009.01.040

Maslowski, K. M., Vieira, A. T., Ng, A., Kranich, J., Sierro, F., Yu, D.et al. (2009). Regulation of inflammatory responses by gut microbiota and chemoattractant receptor GPR43. *Nature, 461*(7268), 1282-1286. doi:10.1038/nature08530

Mayer, E. A., Padua, D., & Tillisch, K. (2014). Altered brain-gut axis in autism: comorbidity or causative mechanisms? *Bioessays, 36*(10), 933-939. doi:10.1002/bies.201400075

McCarville, J. L., Caminero, A., & Verdu, E. F. (2016). Novel perspectives on therapeutic modulation of the gut microbiota. *Therap Adv Gastroenterol, 9*(4), 580-593. doi:10.1177/1756283X16637819

McPherson, C. D., Pierce, G. N., & Cole, W. C. (1993). Ischemic cardioprotection by ATPsensitive K+ channels involves high-energy phosphate preservation. *Am J Physiol, 265*(5 Pt 2), H1809-1818. doi:10.1152/ajpheart.1993.265.5.H1809

Meyer, K. A., Benton, T. Z., Bennett, B. J., Jacobs, D. R., Jr., Lloyd-Jones, D. M., Gross, M. D.et al. (2016). Microbiota-Dependent Metabolite Trimethylamine N-Oxide and Coronary Artery Calcium in the Coronary Artery Risk Development in Young Adults Study (CARDIA). *J Am Heart Assoc, 5*(10). doi:10.1161/JAHA.116.003970

Meyer, T. W., & Hostetter, T. H. (2012). Uremic solutes from colon microbes. *Kidney Int, 81*(10), 949-954. doi:10.1038/ki.2011.504

Miller, A. L., Elam, W. A., Johnson, B. H., Khan, S. H., Kumar, R., & Thompson, E. B. (2017). Restored mutant receptor:Corticoid binding in chaperone complexes by trimethylamine N-oxide. *PLoS One, 12*(3), e0174183. doi:10.1371/journal.pone.0174183

Miller, C. A., Corbin, K. D., da Costa, K. A., Zhang, S., Zhao, X., Galanko, J. A.et al. (2014). Effect of egg ingestion on trimethylamine-N-oxide production in humans: a randomized, controlled, dose-response study. *Am J Clin Nutr, 100*(3), 778-786. doi:10.3945/ajcn.114.087692

Mimaki, M., Wang, X., McKenzie, M., Thorburn, D. R., & Ryan, M. T. (2012). Understanding mitochondrial complex I assembly in health and disease. *Biochim Biophys Acta, 1817*(6), 851-862. doi:10.1016/j.bbabio.2011.08.010

Mingatto, F. E., Rodrigues, T., Pigoso, A. A., Uyemura, S. A., Curti, C., & Santos, A. C. (2002). The critical role of mitochondrial energetic impairment in the toxicity of nimesulide to hepatocytes. *J Pharmacol Exp Ther, 303*(2), 601-607. doi:10.1124/jpet.102.038620

Missailidis, C., Hallqvist, J., Qureshi, A. R., Barany, P., Heimburger, O., Lindholm, B.et al. (2016). Serum Trimethylamine-N-Oxide Is Strongly Related to Renal Function

and Predicts Outcome in Chronic Kidney Disease. *PLoS One, 11*(1), e0141738. doi:10.1371/journal.pone.0141738

Mitra, S., Forster-Fromme, K., Damms-Machado, A., Scheurenbrand, T., Biskup, S., Huson, D. H.et al. (2013). Analysis of the intestinal microbiota using SOLiD 16S rRNA gene sequencing and SOLiD shotgun sequencing. *BMC Genomics, 14 Suppl 5*, S16. doi:10.1186/1471-2164-14-S5-S16

Miura, S. I., Shiga, Y., Ike, A., & Iwata, A. (2019). Atherosclerotic Coronary Artery Disease in Patients With Cardiometabolic Syndrome. *Cardiol Res, 10*(2), 69-73. doi:10.14740/cr857

Mohammad, S., & Thiemermann, C. (2020). Role of Metabolic Endotoxemia in Systemic Inflammation and Potential Interventions. *Front Immunol, 11*, 594150. doi:10.3389/fimmu.2020.594150

Montaigne, D., Marechal, X., Lacroix, D., & Staels, B. (2015). From cardiac mitochondrial dysfunction to clinical arrhythmias. *Int J Cardiol, 184*, 597-599. doi:10.1016/j.ijcard.2015.03.012

Moreno-Indias, I., Cardona, F., Tinahones, F. J., & Queipo-Ortuno, M. I. (2014). Impact of the gut microbiota on the development of obesity and type 2 diabetes mellitus. *Front Microbiol, 5*, 190. doi:10.3389/fmicb.2014.00190

Morgan, M. Y. (1991). The treatment of chronic hepatic encephalopathy. *Hepatogastroenterology, 38*(5), 377-387. Retrieved from https://www.ncbi.nlm.nih.gov/pubmed/1662661

Morrison, D. J., & Preston, T. (2016). Formation of short chain fatty acids by the gut microbiota and their impact on human metabolism. *Gut Microbes, 7*(3), 189-200. doi:10.1080/19490976.2015.1134082

Morrissey, A., Parachuru, L., Leung, M., Lopez, G., Nakamura, T. Y., Tong, X.et al. (2005). Expression of ATP-sensitive K+ channel subunits during perinatal maturation in the mouse heart. *Pediatr Res, 58*(2), 185-192. doi:10.1203/01.PDR.0000169967.83576.CB

Mosterd, A., & Hoes, A. W. (2007). Clinical epidemiology of heart failure. *Heart, 93*(9), 1137-1146. doi:10.1136/hrt.2003.025270

Movsesian, M. A., Karimi, M., Green, K., & Jones, L. R. (1994). Ca(2+)-transporting ATPase, phospholamban, and calsequestrin levels in nonfailing and failing human myocardium. *Circulation, 90*(2), 653-657. doi:10.1161/01.cir.90.2.653

Murphy, E., & Steenbergen, C. (2008). Mechanisms underlying acute protection from cardiac ischemia-reperfusion injury. *Physiol Rev, 88*(2), 581-609. doi:10.1152/physrev.00024.200

Murphy, M. P. (2009). How mitochondria produce reactive oxygen species. *Biochem J, 417*(1), 1-13. doi:10.1042/BJ20081386

Murry, C. E., Jennings, R. B., & Reimer, K. A. (1986). Preconditioning with ischemia: a delay of lethal cell injury in ischemic myocardium. *Circulation, 74*(5), 1124-1136. doi:10.1161/01.cir.74.5.1124

Nagoshi, T., Yoshimura, M., Rosano, G. M., Lopaschuk, G. D., & Mochizuki, S. (2011). Optimization of cardiac metabolism in heart failure. *Curr Pharm Des, 17*(35), 3846-3853. doi:10.2174/138161211798357773

Naseribafrouei, A., Hestad, K., Avershina, E., Sekelja, M., Linlokken, A., Wilson, R.et al. (2014). Correlation between the human fecal microbiota and depression. *Neurogastroenterol Motil, 26*(8), 1155-1162. doi:10.1111/nmo.12378

Nattel, S. (2002). New ideas about atrial fibrillation 50 years on. *Nature, 415*(6868), 219226. doi:10.1038/415219a

Neish, A. S. (2009). Microbes in gastrointestinal health and disease. *Gastroenterology, 136*(1), 65-80. doi:10.1053/j.gastro.2008.10.080

Nerbonne, J. M., & Kass, R. S. (2005). Molecular physiology of cardiac repolarization. *Physiol Rev, 85*(4), 1205-1253. doi:10.1152/physrev.00002.2005

Nesci, S. (2018). A Lethal Channel between the ATP Synthase Monomers. *Trends Biochem Sci, 43*(5), 311-313. doi:10.1016/j.tibs.2018.02.013

Nichols, C. G. (2016). Adenosine Triphosphate-Sensitive Potassium Currents in Heart Disease and Cardioprotection. *Card Electrophysiol Clin, 8*(2), 323-335. doi:10.1016/j.ccep.2016.01.005

Nicholson, J. K., Holmes, E., & Wilson, I. D. (2005). Gut microorganisms, mammalian metabolism and personalized health care. *Nat Rev Microbiol, 3*(5), 431-438. doi:10.1038/nrmicro1152

Nigam, S. K., & Bush, K. T. (2019). Uraemic syndrome of chronic kidney disease: altered remote sensing and signalling. *Nat Rev Nephrol, 15*(5), 301-316. doi:10.1038/s41581-019-0111-1

Noecker, C., Eng, A., Srinivasan, S., Theriot, C. M., Young, V. B., Jansson, J. K.et al. (2016). Metabolic Model-Based Integration of Microbiome Taxonomic and Metabolomic Profiles Elucidates Mechanistic Links between Ecological and Metabolic Variation. *mSystems, 1*(1). doi:10.1128/mSystems.00013-15

Nojiri, H., Shimizu, T., Funakoshi, M., Yamaguchi, O., Zhou, H., Kawakami, S.et al. (2006). Oxidative stress causes heart failure with impaired mitochondrial respiration. *J Biol Chem, 281*(44), 33789-33801. doi:10.1074/jbc.M602118200

Nowinski, A., & Ufnal, M. (2018). Trimethylamine N-oxide: A harmful, protective or diagnostic marker in lifestyle diseases? *Nutrition, 46*, 7-12. doi:10.1016/j.nut.2017.08.001

O'Connell, T. D., Jensen, B. C., Baker, A. J., & Simpson, P. C. (2014). Cardiac alpha1adrenergic receptors: novel aspects of expression, signaling mechanisms, physiologic function, and clinical importance. *Pharmacol Rev, 66*(1), 308-333. doi:10.1124/pr.112.007203

O'Hara, A. M., & Shanahan, F. (2006). The gut flora as a forgotten organ. *EMBO Rep, 7*(7), 688-693. doi:10.1038/sj.embor.7400731

Obeid, R., Awwad, H. M., Rabagny, Y., Graeber, S., Herrmann, W., & Geisel, J. (2016). Plasma trimethylamine N-oxide concentration is associated with choline, phospholipids, and methyl metabolism. *Am J Clin Nutr, 103*(3), 703-711. doi:10.3945/ajcn.115.121269

Ogden, D. C., & Colquhoun, D. (1983). The efficacy of agonists at the frog neuromuscular junction studied with single channel recording. *Pflugers Arch, 399*(3), 246-248. doi:10.1007/BF00656725

Oka, T., Hikoso, S., Yamaguchi, O., Taneike, M., Takeda, T., Tamai, T.et al. (2012). Mitochondrial DNA that escapes from autophagy causes inflammation and heart failure. *Nature, 485*(7397), 251-255. doi:10.1038/nature10992

Organ, C. L., Otsuka, H., Bhushan, S., Wang, Z., Bradley, J., Trivedi, R.et al. (2016). Choline Diet and Its Gut Microbe-Derived Metabolite, Trimethylamine N-Oxide, Exacerbate Pressure Overload-Induced Heart Failure. *Circ Heart Fail, 9*(1), e002314. doi:10.1161/CIRCHEARTFAILURE.115.002314

Ortiz, D., Gossack, L., Quast, U., & Bryan, J. (2013). Reinterpreting the action of ATP analogs on K(ATP) channels. *J Biol Chem, 288*(26), 18894-18902. doi:10.1074/jbc.M113.476887

Ouzounian, M., Lee, D. S., & Liu, P. P. (2008). Diastolic heart failure: mechanisms and controversies. *Nat Clin Pract Cardiovasc Med, 5*(7), 375-386. doi:10.1038/ncpcardio1245

Ovize, M., Baxter, G. F., Di Lisa, F., Ferdinandy, P., Garcia-Dorado, D., Hausenloy, D. J.et al. (2010). Postconditioning and protection from reperfusion injury: where do we stand? Position paper from the Working Group of Cellular Biology of the Heart of the European Society of Cardiology. *Cardiovasc Res, 87*(3), 406-423. doi:10.1093/cvr/cvq129

Palsson, J., Ricksten, S. E., Delle, M., & Lundin, S. (1988). Changes in renal sympathetic nerve activity during experimental septic and endotoxin shock in conscious rats. *Circ Shock, 24*(2), 133-141. Retrieved from https://www.ncbi.nlm.nih.gov/pubmed/3286033

Papandreou, C., More, M., & Bellamine, A. (2020). Trimethylamine N-Oxide in Relation to Cardiometabolic Health-Cause or Effect? *Nutrients, 12*(5). doi:10.3390/nu12051330

Pappo, I., Bercovier, H., Berry, E. M., Haviv, Y., Gallily, R., & Freund, H. R. (1992). Polymyxin B reduces total parenteral nutrition-associated hepatic steatosis by its antibacterial activity and by blocking deleterious effects of lipopolysaccharide. *JPEN J Parenter Enteral Nutr, 16*(6), 529-532. doi:10.1177/0148607192016006529

Park, J. E., Miller, M., Rhyne, J., Wang, Z., & Hazen, S. L. (2019). Differential effect of short-term popular diets on TMAO and other cardio-metabolic risk markers. *Nutr Metab Cardiovasc Dis, 29*(5), 513-517. doi:10.1016/j.numecd.2019.02.003

Patel, M. S., & Korotchkina, L. G. (2006). Regulation of the pyruvate dehydrogenase complex. *Biochem Soc Trans, 34*(Pt 2), 217-222. doi:10.1042/BST20060217

Paul, B., Barnes, S., Demark-Wahnefried, W., Morrow, C., Salvador, C., Skibola, C.et al. (2015). Influences of diet and the gut microbiome on epigenetic modulation in cancer and other diseases. *Clin Epigenetics, 7*, 112. doi:10.1186/s13148-0150144-7

Penna, C., Mancardi, D., Rastaldo, R., & Pagliaro, P. (2009). Cardioprotection: a radical view Free radicals in pre and postconditioning. *Biochim Biophys Acta, 1787*(7), 781-793. doi:10.1016/j.bbabio.2009.02.008

Perez-Riera, A. R., Barbosa-Barros, R., Daminello Raimundo, R., da Costa de Rezende Barbosa, M. P., Esposito Sorpreso, I. C., & de Abreu, L. C. (2018). The congenital long QT syndrome Type 3: An update. *Indian Pacing Electrophysiol J, 18*(1), 2535. doi:10.1016/j.ipej.2017.10.011

Perry, S. W., Norman, J. P., Barbieri, J., Brown, E. B., & Gelbard, H. A. (2011). Mitochondrial membrane potential probes and the proton gradient: a practical usage guide. *Biotechniques, 50*(2), 98-115. doi:10.2144/000113610

Petersen, C. C. H. (2017). Whole-Cell Recording of Neuronal Membrane Potential during Behavior. *Neuron, 95*(6), 1266-1281. doi:10.1016/j.neuron.2017.06.049

Pluznick, J. L., Protzko, R. J., Gevorgyan, H., Peterlin, Z., Sipos, A., Han, J.et al. (2013). Olfactory receptor responding to gut microbiota-derived signals plays a role in renin secretion and blood pressure regulation. *Proc Natl Acad Sci U S A, 110*(11), 4410-4415. doi:10.1073/pnas.1215927110

Popkov, V. A., Zharikova, A. A., Demchenko, E. A., Andrianova, N. V., Zorov, D. B., & Plotnikov, E. Y. (2022). Gut Microbiota as a Source of Uremic Toxins. *Int J Mol Sci, 23*(1). doi:10.3390/ijms23010483

Postma, A. V., Denjoy, I., Kamblock, J., Alders, M., Lupoglazoff, J. M., Vaksmann, G.et al. (2005). Catecholaminergic polymorphic ventricular tachycardia: RYR2 mutations, bradycardia, and follow up of the patients. *J Med Genet, 42*(11), 863870. doi:10.1136/jmg.2004.028993

Priyadarshini, M., Kotlo, K. U., Dudeja, P. K., & Layden, B. T. (2018). Role of Short Chain Fatty Acid Receptors in Intestinal Physiology and Pathophysiology. *Compr Physiol, 8*(3), 1091-1115. doi:10.1002/cphy.c170050

Qi, X., Yeh, Y. H., Chartier, D., Xiao, L., Tsuji, Y., Brundel, B. J.et al. (2009). The calcium/calmodulin/kinase system and arrhythmogenic afterdepolarizations in bradycardia-related acquired long-QT syndrome. *Circ Arrhythm Electrophysiol, 2*(3), 295-304. doi:10.1161/CIRCEP.108.815654

Qi, Y., Aranda, J. M., Rodriguez, V., Raizada, M. K., & Pepine, C. J. (2015). Impact of antibiotics on arterial blood pressure in a patient with resistant hypertension - A case report. *Int J Cardiol, 201*, 157-158. doi:10.1016/j.ijcard.2015.07.078

Qin, J., Li, R., Raes, J., Arumugam, M., Burgdorf, K. S., Manichanh, C.et al. (2010). A human gut microbial gene catalogue established by metagenomic sequencing. *Nature, 464*(7285), 59-65. doi:10.1038/nature08821

Qin, J., Li, Y., Cai, Z., Li, S., Zhu, J., Zhang, F.et al. (2012). A metagenome-wide association study of gut microbiota in type 2 diabetes. *Nature, 490*(7418), 55-60. doi:10.1038/nature11450

Querio, G., Antoniotti, S., Levi, R., & Gallo, M. P. (2019). Trimethylamine N-Oxide Does Not Impact Viability, ROS Production, and Mitochondrial Membrane Potential of Adult Rat Cardiomyocytes. *Int J Mol Sci, 20*(12). doi:10.3390/ijms20123045

Rakoff-Nahoum, S., Paglino, J., Eslami-Varzaneh, F., Edberg, S., & Medzhitov, R. (2004). Recognition of commensal microflora by toll-like receptors is required for intestinal homeostasis. *Cell, 118*(2), 229-241. doi:10.1016/j.cell.2004.07.002

Rana, A., Goyal, N., Ahlawat, A., Jamwal, S., Reddy, B. V., & Sharma, S. (2015). Mechanisms involved in attenuated cardio-protective role of ischemic preconditioning in metabolic disorders. *Perfusion, 30*(2), 94-105. doi:10.1177/0267659114536760

Rana, P., Nadanaciva, S., & Will, Y. (2011). Mitochondrial membrane potential measurement of H9c2 cells grown in high-glucose and galactose-containing media does not provide additional predictivity towards mitochondrial assessment. *Toxicol In Vitro, 25*(2), 580-587. doi:10.1016/j.tiv.2010.11.016

Rasmussen, L. G., Winning, H., Savorani, F., Toft, H., Larsen, T. M., Dragsted, L. O.et al. (2012). Assessment of the effect of high or low protein diet on the human urine metabolome as measured by NMR. *Nutrients, 4*(2), 112-131. doi:10.3390/nu4020112

Ratajczak, W., Ryl, A., Mizerski, A., Walczakiewicz, K., Sipak, O., & Laszczynska, M. (2019). Immunomodulatory potential of gut microbiome-derived short-chain fatty acids (SCFAs). *Acta Biochim Pol, 66*(1), 1-12. doi:10.18388/abp.2018_2648

Ravens, U. (2015). Pathophysiology and progression of atrial fibrillation: Do we have a comprehensive model? *Trends Cardiovasc Med, 25*(6), 485-486. doi:10.1016/j.tcm.2015.01.003

Ravens, U., & Cerbai, E. (2008). Role of potassium currents in cardiac arrhythmias. *Europace, 10*(10), 1133-1137. doi:10.1093/europace/eun193

Reitzer, L. J., Wice, B. M., & Kennell, D. (1979). Evidence that glutamine, not sugar, is the major energy source for cultured HeLa cells. *J Biol Chem, 254*(8), 2669-2676. Retrieved from https://www.ncbi.nlm.nih.gov/pubmed/429309

Rexidamu, M., Li, H., Jin, H., & Huang, J. (2019). Serum levels of Trimethylamine-N-oxide in patients with ischemic stroke. *Biosci Rep, 39*(6). doi:10.1042/BSR20190515

Rhee, E. P., Clish, C. B., Ghorbani, A., Larson, M. G., Elmariah, S., McCabe, E.et al. (2013). A combined epidemiologic and metabolomic approach improves CKD prediction. *J Am Soc Nephrol, 24*(8), 1330-1338. doi:10.1681/ASN.2012101006

Rhee, S. H., Pothoulakis, C., & Mayer, E. A. (2009). Principles and clinical implications of the brain-gut-enteric microbiota axis. *Nat Rev Gastroenterol Hepatol, 6*(5), 306314. doi:10.1038/nrgastro.2009.35

Rijkers, G. T., de Vos, W. M., Brummer, R. J., Morelli, L., Corthier, G., & Marteau, P. (2011). Health benefits and health claims of probiotics: bridging science and marketing. *Br J Nutr, 106*(9), 1291-1296. doi:10.1017/S000711451100287X

Rios, E. (2018). Calcium-induced release of calcium in muscle: 50 years of work and the emerging consensus. *J Gen Physiol, 150*(4), 521-537. doi:10.1085/jgp.201711959

Rizzuto, R., De Stefani, D., Raffaello, A., & Mammucari, C. (2012). Mitochondria as sensors and regulators of calcium signalling. *Nat Rev Mol Cell Biol, 13*(9), 566578. doi:10.1038/nrm3412

Robinson, B. H., Petrova-Benedict, R., Buncic, J. R., & Wallace, D. C. (1992). Nonviability of cells with oxidative defects in galactose medium: a screening test for affected patient fibroblasts. *Biochem Med Metab Biol, 48*(2), 122-126. doi:10.1016/08854505(92)90056-5

Roden, D. M. (2016). Pharmacogenetics of Potassium Channel Blockers. *Card Electrophysiol Clin, 8*(2), 385-393. doi:10.1016/j.ccep.2016.02.003

Rodriguez, J. M., Murphy, K., Stanton, C., Ross, R. P., Kober, O. I., Juge, N.et al. (2015). The composition of the gut microbiota throughout life, with an emphasis on early life. *Microb Ecol Health Dis, 26*, 26050. doi:10.3402/mehd.v26.26050

Rodriguez-Enriquez, S., Juarez, O., Rodriguez-Zavala, J. S., & Moreno-Sanchez, R. (2001). Multisite control of the Crabtree effect in ascites hepatoma cells. *Eur J Biochem, 268*(8), 2512-2519. doi:10.1046/j.1432-1327.2001.02140.x

Roh, S., Choi, S., & Lim, I. (2007). Involvement of protein kinase A in nitric oxide stimulating effect on a BK(Ca) channel of human dermal fibroblasts. *J Invest Dermatol, 127*(11), 2533-2538. doi:10.1038/sj.jid.5700907

Romano, K. A., Vivas, E. I., Amador-Noguez, D., & Rey, F. E. (2015). Intestinal microbiota composition modulates choline bioavailability from diet and accumulation of the proatherogenic metabolite trimethylamine-N-oxide. *mBio, 6*(2), e02481. doi:10.1128/mBio.02481-14

Ronco, C., Haapio, M., House, A. A., Anavekar, N., & Bellomo, R. (2008). Cardiorenal syndrome. *J Am Coll Cardiol, 52*(19), 1527-1539. doi:10.1016/j.jacc.2008.07.051

Sabbah, H. N. (2016). Targeting mitochondrial dysfunction in the treatment of heart failure. *Expert Rev Cardiovasc Ther, 14*(12), 1305-1313. doi:10.1080/14779072.2016.1249466

Salzman, N. H., Underwood, M. A., & Bevins, C. L. (2007). Paneth cells, defensins, and the commensal microbiota: a hypothesis on intimate interplay at the intestinal mucosa. *Semin Immunol, 19*(2), 70-83. doi:10.1016/j.smim.2007.04.002

Samuel, B. S., Shaito, A., Motoike, T., Rey, F. E., Backhed, F., Manchester, J. K.et al. (2008). Effects of the gut microbiota on host adiposity are modulated by the short-chain fatty-acid binding G protein-coupled receptor, Gpr41. *Proc Natl Acad Sci U S A, 105*(43), 16767-16772. doi:10.1073/pnas.0808567105

Santisteban, M. M., Qi, Y., Zubcevic, J., Kim, S., Yang, T., Shenoy, V.et al. (2017). Hypertension-Linked Pathophysiological Alterations in the Gut. *Circ Res, 120*(2), 312-323. doi:10.1161/CIRCRESAHA.116.309006

Santulli, G., Lewis, D., des Georges, A., Marks, A. R., & Frank, J. (2018). Ryanodine Receptor Structure and Function in Health and Disease. *Subcell Biochem, 87*, 329-352. doi:10.1007/978-981-10-7757-9_11

Santulli, G., Lewis, D. R., & Marks, A. R. (2017). Physiology and pathophysiology of excitation-contraction coupling: the functional role of ryanodine receptor. *J Muscle Res Cell Motil, 38*(1), 37-45. doi:10.1007/s10974-017-9470-z

Santulli, G., Nakashima, R., Yuan, Q., & Marks, A. R. (2017). Intracellular calcium release channels: an update. *J Physiol, 595*(10), 3041-3051. doi:10.1113/JP272781

Saraswati, S., & Sitaraman, R. (2014). Aging and the human gut microbiota-from correlation to causality. *Front Microbiol, 5*, 764. doi:10.3389/fmicb.2014.00764

Savi, M., Bocchi, L., Bresciani, L., Falco, A., Quaini, F., Mena, P.et al. (2018). Trimethylamine-N-Oxide (TMAO)-Induced Impairment of Cardiomyocyte Function and the Protective Role of Urolithin B-Glucuronide. *Molecules, 23*(3). doi:10.3390/molecules23030549

Schaper, J., Meiser, E., & Stammler, G. (1985). Ultrastructural morphometric analysis of myocardium from dogs, rats, hamsters, mice, and from human hearts. *Circ Res, 56*(3), 377-391. Retrieved from http://www.ncbi.nlm.nih.gov/pubmed/3882260

Schnabel, R., & Blankenberg, S. (2007). Oxidative stress in cardiovascular disease: successful translation from bench to bedside? *Circulation, 116*(12), 1338-1340. doi:10.1161/CIRCULATIONAHA.107.728394

Schneck, E., Horinek, D., & Netz, R. R. (2013). Insight into the molecular mechanisms of protein stabilizing osmolytes from global force-field variations. *J Phys Chem B, 117*(28), 8310-8321. doi:10.1021/jp400790f

Schuett, K., Kleber, M. E., Scharnagl, H., Lorkowski, S., Marz, W., Niessner, A.et al. (2017). Trimethylamine-N-oxide and Heart Failure With Reduced Versus Preserved Ejection Fraction. *J Am Coll Cardiol, 70*(25), 3202-3204. doi:10.1016/j.jacc.2017.10.064

Schultz, B. E., & Chan, S. I. (2001). Structures and proton-pumping strategies of mitochondrial respiratory enzymes. *Annu Rev Biophys Biomol Struct, 30*, 23-65. doi:10.1146/annurev.biophys.30.1.23

Seldin, M. M., Meng, Y., Qi, H., Zhu, W., Wang, Z., Hazen, S. L.et al. (2016). Trimethylamine N-Oxide Promotes Vascular Inflammation Through Signaling of Mitogen-Activated Protein Kinase and Nuclear Factor-kappaB. *J Am Heart Assoc, 5*(2). doi:10.1161/JAHA.115.002767

Sender, R., Fuchs, S., & Milo, R. (2016). Revised Estimates for the Number of Human and Bacteria Cells in the Body. *PLoS Biol, 14*(8), e1002533. doi:10.1371/journal.pbio.1002533

Senthong, V., Li, X. S., Hudec, T., Coughlin, J., Wu, Y., Levison, B.et al. (2016). Plasma Trimethylamine N-Oxide, a Gut Microbe-Generated Phosphatidylcholine Metabolite, Is Associated With Atherosclerotic Burden. *J Am Coll Cardiol, 67*(22), 2620-2628. doi:10.1016/j.jacc.2016.03.546

Senthong, V., Wang, Z., Fan, Y., Wu, Y., Hazen, S. L., & Tang, W. H. (2016). Trimethylamine N-Oxide and Mortality Risk in Patients With Peripheral Artery Disease. *J Am Heart Assoc, 5*(10). doi:10.1161/JAHA.116.004237

Shaw, R. M., & Colecraft, H. M. (2013). L-type calcium channel targeting and local signalling in cardiac myocytes. *Cardiovasc Res, 98*(2), 177-186. doi:10.1093/cvr/cvt021

Shi, K., Wang, F., Jiang, H., Liu, H., Wei, M., Wang, Z.et al. (2014). Gut bacterial translocation may aggravate microinflammation in hemodialysis patients. *Dig Dis Sci, 59*(9), 2109-2117. doi:10.1007/s10620-014-3202-7

Shoaie, S., Ghaffari, P., Kovatcheva-Datchary, P., Mardinoglu, A., Sen, P., Pujos-Guillot, E.et al. (2015). Quantifying Diet-Induced Metabolic Changes of the Human Gut Microbiome. *Cell Metab, 22*(2), 320-331. doi:10.1016/j.cmet.2015.07.001

Simren, M., Barbara, G., Flint, H. J., Spiegel, B. M., Spiller, R. C., Vanner, S.et al. (2013). Intestinal microbiota in functional bowel disorders: a Rome foundation report. *Gut, 62*(1), 159-176. doi:10.1136/gutjnl-2012-302167

Sims, M. W., Winter, J., Brennan, S., Norman, R. I., Ng, G. A., Squire, I. B.et al. (2014). PKC-mediated toxicity of elevated glucose concentration on cardiomyocyte function. *Am J Physiol Heart Circ Physiol, 307*(4), H587-597. doi:10.1152/ajpheart.00894.2013

Singh, H., Hudman, D., Lawrence, C. L., Rainbow, R. D., Lodwick, D., & Norman, R. I. (2003). Distribution of Kir6.0 and SUR2 ATP-sensitive potassium channel subunits in isolated ventricular myocytes. *J Mol Cell Cardiol, 35*(5), 445-459. doi:10.1016/s0022-2828(03)00041-5

Sirangelo, T. M. (2018). Human Gut Microbiome Analysis and Multi-omics Approach. *International Journal of Pharma Medicine and Biological Sciences, 7*(3), 52-57.

Skibsbye, L., & Ravens, U. (2016). Mechanism of Proarrhythmic Effects of Potassium Channel Blockers. *Card Electrophysiol Clin, 8*(2), 395-410. doi:10.1016/j.ccep.2016.02.004

Smith, K., McCoy, K. D., & Macpherson, A. J. (2007). Use of axenic animals in studying the adaptation of mammals to their commensal intestinal microbiota. *Semin Immunol, 19*(2), 59-69. doi:10.1016/j.smim.2006.10.002

Smith, P. K., Krohn, R. I., Hermanson, G. T., Mallia, A. K., Gartner, F. H., Provenzano, M. D.et al. (1985). Measurement of protein using bicinchoninic acid. *Anal Biochem, 150*(1), 76-85. doi:10.1016/0003-2697(85)90442-7

Smits, J. P., Veldkamp, M. W., & Wilde, A. A. (2005). Mechanisms of inherited cardiac conduction disease. *Europace, 7*(2), 122-137. doi:10.1016/j.eupc.2004.11.004

Solenkova, N. V., Solodushko, V., Cohen, M. V., & Downey, J. M. (2006). Endogenous adenosine protects preconditioned heart during early minutes of reperfusion by activating Akt. *Am J Physiol Heart Circ Physiol, 290*(1), H441-449. doi:10.1152/ajpheart.00589.2005

Sollini, M., Frieden, M., & Beny, J. L. (2002). Charybdotoxin-sensitive small conductance K(Ca) channel activated by bradykinin and substance P in endothelial cells. *Br J Pharmacol, 136*(8), 1201-1209. doi:10.1038/sj.bjp.0704819

Solmaz, S. R., & Hunte, C. (2008). Structure of complex III with bound cytochrome c in reduced state and definition of a minimal core interface for electron transfer. *J Biol Chem, 283*(25), 17542-17549. doi:10.1074/jbc.M710126200

Sommer, C. J. (2017). Ischemic stroke: experimental models and reality. *Acta Neuropathol, 133*(2), 245-261. doi:10.1007/s00401-017-1667-0

Squire, I. B., Nelson, C. P., Ng, L. L., Jones, D. R., Woods, K. L., & Lambert, P. C. (2010). Prognostic value of admission blood glucose concentration and diabetes diagnosis on survival after acute myocardial infarction: results from 4702 index cases in routine practice. *Clin Sci (Lond), 118*(8), 527-535. doi:10.1042/CS20090322

Steinberg, S. F. (2013). Oxidative stress and sarcomeric proteins. *Circ Res, 112*(2), 393405. doi:10.1161/CIRCRESAHA.111.300496

Stinson, L. F., Payne, M. S., & Keelan, J. A. (2017). Planting the seed: Origins, composition, and postnatal health significance of the fetal gastrointestinal microbiota. *Crit Rev Microbiol, 43*(3), 352-369. doi:10.1080/1040841X.2016.1211088

Stubbs, J. R., House, J. A., Ocque, A. J., Zhang, S., Johnson, C., Kimber, C.et al. (2016). Serum Trimethylamine-N-Oxide is Elevated in CKD and Correlates with Coronary Atherosclerosis Burden. *J Am Soc Nephrol, 27*(1), 305-313. doi:10.1681/ASN.2014111063

Su, H., Ji, L., Xing, W., Zhang, W., Zhou, H., Qian, X.et al. (2013). Acute hyperglycaemia enhances oxidative stress and aggravates myocardial ischaemia/reperfusion injury: role of thioredoxin-interacting protein. *J Cell Mol Med, 17*(1), 181-191. doi:10.1111/j.1582-4934.2012.01661.x

Sun, H. S., & Feng, Z. P. (2013). Neuroprotective role of ATP-sensitive potassium channels in cerebral ischemia. *Acta Pharmacol Sin, 34*(1), 24-32. doi:10.1038/aps.2012.138

Sun, M., Wu, W., Liu, Z., & Cong, Y. (2017). Microbiota metabolite short chain fatty acids, GPCR, and inflammatory bowel diseases. *J Gastroenterol, 52*(1), 1-8. doi:10.1007/s00535-016-1242-9

Sun, X., Jiao, X., Ma, Y., Liu, Y., Zhang, L., He, Y.et al. (2016). Trimethylamine N-oxide induces inflammation and endothelial dysfunction in human umbilical vein endothelial cells via activating ROS-TXNIP-NLRP3 inflammasome. *Biochem Biophys Res Commun, 481*(1-2), 63-70. doi:10.1016/j.bbrc.2016.11.017

Sung, J., Kim, S., Cabatbat, J. J. T., Jang, S., Jin, Y. S., Jung, G. Y.et al. (2017). Global metabolic interaction network of the human gut microbiota for context-specific community-scale analysis. *Nat Commun, 8*, 15393. doi:10.1038/ncomms15393

Suzuki, M., Sasaki, N., Miki, T., Sakamoto, N., Ohmoto-Sekine, Y., Tamagawa, M.et al. (2002). Role of sarcolemmal K(ATP) channels in cardioprotection against ischemia/reperfusion injury in mice. *J Clin Invest, 109*(4), 509-516. doi:10.1172/JCI14270

Swulius, M. T., & Waxham, M. N. (2008). Ca(2+)/calmodulin-dependent protein kinases. *Cell Mol Life Sci, 65*(17), 2637-2657. doi:10.1007/s00018-008-8086-2

Szeto, C. C., Kwan, B. C., Chow, K. M., Lai, K. B., Chung, K. Y., Leung, C. B.et al. (2008). Endotoxemia is related to systemic inflammation and atherosclerosis in peritoneal dialysis patients. *Clin J Am Soc Nephrol, 3*(2), 431-436. doi:10.2215/CJN.03600807

Takimoto, E., & Kass, D. A. (2007). Role of oxidative stress in cardiac hypertrophy and remodeling. *Hypertension, 49*(2), 241-248. doi:10.1161/01.HYP.0000254415.31362.a7

Tanai, E., & Frantz, S. (2015). Pathophysiology of Heart Failure. *Compr Physiol, 6*(1), 187214. doi:10.1002/cphy.c140055

Tanca, A., Palomba, A., Pisanu, S., Addis, M. F., & Uzzau, S. (2015). Enrichment or depletion? The impact of stool pretreatment on metaproteomic characterization of the human gut microbiota. *Proteomics, 15*(20), 3474-3485. doi:10.1002/pmic.201400573

Tang, W. H., & Hazen, S. L. (2014). The contributory role of gut microbiota in cardiovascular disease. *J Clin Invest, 124*(10), 4204-4211. doi:10.1172/JCI72331

Tang, W. H., Kitai, T., & Hazen, S. L. (2017). Gut Microbiota in Cardiovascular Health and Disease. *Circ Res, 120*(7), 1183-1196. doi:10.1161/CIRCRESAHA.117.309715

Tang, W. H., Wang, Z., Fan, Y., Levison, B., Hazen, J. E., Donahue, L. M.et al. (2014). Prognostic value of elevated levels of intestinal microbe-generated metabolite trimethylamine-N-oxide in patients with heart failure: refining the gut hypothesis. *J Am Coll Cardiol, 64*(18), 1908-1914. doi:10.1016/j.jacc.2014.02.617

Tang, W. H., Wang, Z., Kennedy, D. J., Wu, Y., Buffa, J. A., Agatisa-Boyle, B.et al. (2015). Gut microbiota-dependent trimethylamine N-oxide (TMAO) pathway contributes to both development of renal insufficiency and mortality risk in chronic kidney disease. *Circ Res, 116*(3), 448-455. doi:10.1161/CIRCRESAHA.116.305360

Tang, W. H., Wang, Z., Levison, B. S., Koeth, R. A., Britt, E. B., Fu, X.et al. (2013). Intestinal microbial metabolism of phosphatidylcholine and cardiovascular risk. *N Engl J Med, 368*(17), 1575-1584. doi:10.1056/NEJMoa1109400

Tannock, G. W. (2001). Molecular assessment of intestinal microflora. *Am J Clin Nutr, 73*(2 Suppl), 410S-414S. doi:10.1093/ajcn/73.2.410s

Tannock, G. W., Munro, K., Harmsen, H. J., Welling, G. W., Smart, J., & Gopal, P. K. (2000). Analysis of the fecal microflora of human subjects consuming a probiotic product containing Lactobacillus rhamnosus DR20. *Appl Environ Microbiol, 66*(6), 2578-2588. doi:10.1128/aem.66.6.2578-2588.2000

Terentyev, D., Kubalova, Z., Valle, G., Nori, A., Vedamoorthyrao, S., Terentyeva, R.et al. (2008). Modulation of SR Ca release by luminal Ca and calsequestrin in cardiac myocytes: effects of CASQ2 mutations linked to sudden cardiac death. *Biophys J, 95*(4), 2037-2048. doi:10.1529/biophysj.107.128249

Thaiss, C. A., Levy, M., Suez, J., & Elinav, E. (2014). The interplay between the innate immune system and the microbiota. *Curr Opin Immunol, 26*, 41-48. doi:10.1016/j.coi.2013.10.016

Thibodeaux, C. J., & van der Donk, W. A. (2012). Converging on a mechanism for choline degradation. *Proc Natl Acad Sci U S A, 109*(52), 21184-21185. doi:10.1073/pnas.1219534110

Thomas, C., Pellicciari, R., Pruzanski, M., Auwerx, J., & Schoonjans, K. (2008). Targeting bile-acid signalling for metabolic diseases. *Nat Rev Drug Discov, 7*(8), 678-693. doi:10.1038/nrd2619

Thompson, E., Eldstrom, J., Westhoff, M., McAfee, D., Balse, E., & Fedida, D. (2017). cAMP-dependent regulation of IKs single-channel kinetics. *J Gen Physiol, 149*(8), 781-798. doi:10.1085/jgp.201611734

Thorburn, A. N., Macia, L., & Mackay, C. R. (2014). Diet, metabolites, and "western-lifestyle" inflammatory diseases. *Immunity, 40*(6), 833-842. doi:10.1016/j.immuni.2014.05.014

Thorburn, A. N., McKenzie, C. I., Shen, S., Stanley, D., Macia, L., Mason, L. J.et al. (2015). Evidence that asthma is a developmental origin disease influenced by maternal diet and bacterial metabolites. *Nat Commun, 6*, 7320. doi:10.1038/ncomms8320

Thygesen, K., Alpert, J. S., Jaffe, A. S., Chaitman, B. R., Bax, J. J., Morrow, D. A.et al. (2018). Fourth Universal Definition of Myocardial Infarction (2018). *Circulation, 138*(20), e618-e651. doi:10.1161/CIR.0000000000000617

Tian, M., Yuan, Y. C., Li, J. Y., Gionfriddo, M. R., & Huang, R. C. (2015). Tumor necrosis factor-alpha and its role as a mediator in myocardial infarction: A brief review. *Chronic Dis Transl Med, 1*(1), 18-26. doi:10.1016/j.cdtm.2015.02.002

Tolhurst, G., Heffron, H., Lam, Y. S., Parker, H. E., Habib, A. M., Diakogiannaki, E.et al. (2012). Short-chain fatty acids stimulate glucagon-like peptide-1 secretion via the G-protein-coupled receptor FFAR2. *Diabetes, 61*(2), 364-371. doi:10.2337/db11-1019

Tornroth-Horsefield, S., & Neutze, R. (2008). Opening and closing the metabolite gate.

Proc Natl Acad Sci U S A, 105(50), 19565-19566. doi:10.1073/pnas.0810654106

Trompette, A., Gollwitzer, E. S., Yadava, K., Sichelstiel, A. K., Sprenger, N., Ngom-Bru, C.et al. (2014). Gut microbiota metabolism of dietary fiber influences allergic airway disease and hematopoiesis. *Nat Med, 20*(2), 159-166. doi:10.1038/nm.3444

Troseid, M., Ueland, T., Hov, J. R., Svardal, A., Gregersen, I., Dahl, C. P.et al. (2015). Microbiota-dependent metabolite trimethylamine-N-oxide is associated with disease severity and survival of patients with chronic heart failure. *J Intern Med, 277*(6), 717-726. doi:10.1111/joim.12328

Turnbaugh, P. J., Hamady, M., Yatsunenko, T., Cantarel, B. L., Duncan, A., Ley, R. E.et al. (2009). A core gut microbiome in obese and lean twins. *Nature, 457*(7228), 480484. doi:10.1038/nature07540

Turrens, J. F. (2003). Mitochondrial formation of reactive oxygen species. *J Physiol, 552*(Pt 2), 335-344. doi:10.1113/jphysiol.2003.049478

Ufnal, M., Jazwiec, R., Dadlez, M., Drapala, A., Sikora, M., & Skrzypecki, J. (2014). Trimethylamine-N-oxide: a carnitine-derived metabolite that prolongs the hypertensive effect of angiotensin II in rats. *Can J Cardiol, 30*(12), 1700-1705. doi:10.1016/j.cjca.2014.09.010

van der Werf, C., & Wilde, A. A. (2013). Catecholaminergic polymorphic ventricular tachycardia: from bench to bedside. *Heart, 99*(7), 497-504. doi:10.1136/heartjnl-2012-302033

van Empel, V. P., & De Windt, L. J. (2004). Myocyte hypertrophy and apoptosis: a balancing act. *Cardiovasc Res, 63*(3), 487-499. doi:10.1016/j.cardiores.2004.02.013

Vasington, F. D., & Murphy, J. V. (1962). Ca ion uptake by rat kidney mitochondria and its dependence on respiration and phosphorylation. *J Biol Chem, 237*, 26702677. Retrieved from https://www.ncbi.nlm.nih.gov/pubmed/13925019

Vaziri, N. D., Wong, J., Pahl, M., Piceno, Y. M., Yuan, J., DeSantis, T. Z.et al. (2013). Chronic kidney disease alters intestinal microbial flora. *Kidney Int, 83*(2), 308-315. doi:10.1038/ki.2012.345

Velasquez, M. T., Ramezani, A., Manal, A., & Raj, D. S. (2016). Trimethylamine N-Oxide: The Good, the Bad and the Unknown. *Toxins (Basel), 8*(11). doi:10.3390/toxins8110326

Venetucci, L. A., Trafford, A. W., O'Neill, S. C., & Eisner, D. A. (2008). The sarcoplasmic reticulum and arrhythmogenic calcium release. *Cardiovasc Res, 77*(2), 285-292. doi:10.1093/cvr/cvm009

Ventura-Clapier, R., Garnier, A., & Veksler, V. (2004). Energy metabolism in heart failure. *J Physiol, 555*(Pt 1), 1-13. doi:10.1113/jphysiol.2003.055095

Vernocchi, P., Del Chierico, F., & Putignani, L. (2016). Gut Microbiota Profiling: Metabolomics Based Approach to Unravel Compounds Affecting Human Health. *Front Microbiol, 7*, 1144. doi:10.3389/fmicb.2016.01144

Videja, M., Vilskersts, R., Korzh, S., Cirule, H., Sevostjanovs, E., Dambrova, M.et al. (2020). Microbiota-Derived Metabolite Trimethylamine N-Oxide Protects Mitochondrial Energy Metabolism and Cardiac Functionality in a Rat Model of Right Ventricle Heart Failure. *Front Cell Dev Biol, 8*, 622741. doi:10.3389/fcell.2020.622741

Vrieze, A., Van Nood, E., Holleman, F., Salojarvi, J., Kootte, R. S., Bartelsman, J. F.et al. (2012). Transfer of intestinal microbiota from lean donors increases insulin sensitivity in individuals with metabolic syndrome. *Gastroenterology, 143*(4), 913-916 e917. doi:10.1053/j.gastro.2012.06.031

Wagner, A., Marc, A., Engasser, J. M., & Einsele, A. (1991). Growth and metabolism of human tumor kidney cells on galactose and glucose. *Cytotechnology, 7*(1), 7-13. doi:10.1007/BF00135633

Wallace, K. B., & Starkov, A. A. (2000). Mitochondrial targets of drug toxicity. *Annu Rev Pharmacol Toxicol, 40*, 353-388. doi:10.1146/annurev.pharmtox.40.1.353

Wang, M., Wang, F., Wang, Y., Ma, X., Zhao, M., & Zhao, C. (2013). Metabonomics study of the therapeutic mechanism of Gynostemma pentaphyllum and atorvastatin for hyperlipidemia in rats. *PLoS One, 8*(11), e78731. doi:10.1371/journal.pone.0078731

Wang, Y., & Hill, J. A. (2010). Electrophysiological remodeling in heart failure. *J Mol Cell Cardiol, 48*(4), 619-632. doi:10.1016/j.yjmcc.2010.01.009

Wang, Y., Tandan, S., & Hill, J. A. (2014). Calcineurin-dependent ion channel regulation in heart. *Trends Cardiovasc Med, 24*(1), 14-22. doi:10.1016/j.tcm.2013.05.004

Wang, Z., Bergeron, N., Levison, B. S., Li, X. S., Chiu, S., Jia, X.et al. (2019). Impact of chronic dietary red meat, white meat, or non-meat protein on trimethylamine N-oxide metabolism and renal excretion in healthy men and women. *Eur Heart J, 40*(7), 583-594. doi:10.1093/eurheartj/ehy799

Wang, Z., Klipfell, E., Bennett, B. J., Koeth, R., Levison, B. S., Dugar, B.et al. (2011). Gut flora metabolism of phosphatidylcholine promotes cardiovascular disease. *Nature, 472*(7341), 57-63. doi:10.1038/nature09922

Wang, Z., Levison, B. S., Hazen, J. E., Donahue, L., Li, X. M., & Hazen, S. L. (2014). Measurement of trimethylamine-N-oxide by stable isotope dilution liquid

chromatography tandem mass spectrometry. *Anal Biochem, 455*, 35-40. doi:10.1016/j.ab.2014.03.016

Wang, Z., Tang, W. H., Buffa, J. A., Fu, X., Britt, E. B., Koeth, R. A.et al. (2014). Prognostic value of choline and betaine depends on intestinal microbiota-generated metabolite trimethylamine-N-oxide. *Eur Heart J, 35*(14), 904-910. doi:10.1093/eurheartj/ehu002

Wang, W. L., Xu, S. Y., Ren, Z. G., Tao, L., Jiang, J. W., & Zheng, S. S. (2015). Application of metagenomics in the human gut microbiome. *World J Gastroenterol, 21*(3), 803-814. doi:10.3748/wjg.v21.i3.803

Wang, Z., & Zhao, Y. (2018). Gut microbiota derived metabolites in cardiovascular health and disease. *Protein Cell, 9*(5), 416-431. doi:10.1007/s13238-018-0549-0

Warburg, O. (1956). On the origin of cancer cells. *Science, 123*(3191), 309-314. doi:10.1126/science.123.3191.309

Weinstock, G. M. (2012). Genomic approaches to studying the human microbiota. *Nature, 489*(7415), 250-256. doi:10.1038/nature11553

Weiss, J. N., Garfinkel, A., Karagueuzian, H. S., Chen, P. S., & Qu, Z. (2010). Early afterdepolarizations and cardiac arrhythmias. *Heart Rhythm, 7*(12), 1891-1899. doi:10.1016/j.hrthm.2010.09.017

Weisser-Thomas, J., Kubo, H., Hefner, C. A., Gaughan, J. P., McGowan, B. S., Ross, R.et al. (2005). The Na+/Ca2+ exchanger/SR Ca2+ ATPase transport capacity regulates the contractility of normal and hypertrophied feline ventricular myocytes. *J Card Fail, 11*(5), 380-387. doi:10.1016/j.cardfail.2005.01.004

Widmer, R. J., Flammer, A. J., Lerman, L. O., & Lerman, A. (2015). The Mediterranean diet, its components, and cardiovascular disease. *Am J Med, 128*(3), 229-238. doi:10.1016/j.amjmed.2014.10.014

Wilde, A. A., & Brugada, R. (2011). Phenotypical manifestations of mutations in the genes encoding subunits of the cardiac sodium channel. *Circ Res, 108*(7), 884-897. doi:10.1161/CIRCRESAHA.110.238469

Wojtczak, L., & Zablocki, K. (2008). [Mitochondria in cell life, death and disease]. *Postepy Biochem, 54*(2), 129-141. Retrieved from https://www.ncbi.nlm.nih.gov/pubmed/18807924

Wolvers, D., Antoine, J. M., Myllyluoma, E., Schrezenmeir, J., Szajewska, H., & Rijkers, G. T. (2010). Guidance for substantiating the evidence for beneficial effects of probiotics: prevention and management of infections by probiotics. *J Nutr, 140*(3), 698S-712S. doi:10.3945/jn.109.113753

Wong, J., Piceno, Y. M., DeSantis, T. Z., Pahl, M., Andersen, G. L., & Vaziri, N. D. (2014). Expansion of urease- and uricase-containing, indole- and p-cresol-forming and contraction of short-chain fatty acid-producing intestinal microbiota in ESRD. *Am J Nephrol, 39*(3), 230-237. doi:10.1159/000360010

Wu, G. D., Chen, J., Hoffmann, C., Bittinger, K., Chen, Y. Y., Keilbaugh, S. A.et al. (2011). Linking long-term dietary patterns with gut microbial enterotypes. *Science, 334*(6052), 105-108. doi:10.1126/science.1208344

Wu, G. D., Compher, C., Chen, E. Z., Smith, S. A., Shah, R. D., Bittinger, K.et al. (2016). Comparative metabolomics in vegans and omnivores reveal constraints on dietdependent gut microbiota metabolite production. *Gut, 65*(1), 63-72. doi:10.1136/gutjnl-2014-308209

Wu, H., Esteve, E., Tremaroli, V., Khan, M. T., Caesar, R., Manneras-Holm, L.et al. (2017). Metformin alters the gut microbiome of individuals with treatment-naive type 2 diabetes, contributing to the therapeutic effects of the drug. *Nat Med, 23*(7), 850-858. doi:10.1038/nm.4345

Wu, J., Ding, W. G., & Horie, M. (2016). Molecular pathogenesis of long QT syndrome type 1. *J Arrhythm, 32*(5), 381-388. doi:10.1016/j.joa.2015.12.006

Xu, J., Bjursell, M. K., Himrod, J., Deng, S., Carmichael, L. K., Chiang, H. C.et al. (2003). A genomic view of the human-Bacteroides thetaiotaomicron symbiosis. *Science, 299*(5615), 2074-2076. doi:10.1126/science.1080029

Xu, J., Mahowald, M. A., Ley, R. E., Lozupone, C. A., Hamady, M., Martens, E. C.et al. (2007). Evolution of symbiotic bacteria in the distal human intestine. *PLoS Biol, 5*(7), e156. doi:10.1371/journal.pbio.0050156

Yancey, P. H., Gerringer, M. E., Drazen, J. C., Rowden, A. A., & Jamieson, A. (2014). Marine fish may be biochemically constrained from inhabiting the deepest ocean depths. *Proc Natl Acad Sci U S A, 111*(12), 4461-4465. doi:10.1073/pnas.1322003111

Yancey, P. H., Rhea, M. D., Kemp, K. M., & Bailey, D. M. (2004). Trimethylamine oxide, betaine and other osmolytes in deep-sea animals: depth trends and effects on enzymes under hydrostatic pressure. *Cell Mol Biol (Noisy-le-grand), 50*(4), 371-376. Retrieved from https://www.ncbi.nlm.nih.gov/pubmed/15529747

Yancey, P. H., & Siebenaller, J. F. (1999). Trimethylamine oxide stabilizes teleost and mammalian lactate dehydrogenases against inactivation by hydrostatic pressure and trypsinolysis. *J Exp Biol, 202*(Pt 24), 3597-3603. Retrieved from https://www.ncbi.nlm.nih.gov/pubmed/10574736

Yang, T., Santisteban, M. M., Rodriguez, V., Li, E., Ahmari, N., Carvajal, J. M.et al. (2015). Gut dysbiosis is linked to hypertension. *Hypertension, 65*(6), 1331-1340. doi:10.1161/HYPERTENSIONAHA.115.05315

Yang, Y., Yang, Y., Liang, B., Liu, J., Li, J., Grunnet, M.et al. (2010). Identification of a Kir3.4 mutation in congenital long QT syndrome. *Am J Hum Genet, 86*(6), 872880. doi:10.1016/j.ajhg.2010.04.017

Yassour, M., Vatanen, T., Siljander, H., Hamalainen, A. M., Harkonen, T., Ryhanen, S. J.et al. (2016). Natural history of the infant gut microbiome and impact of antibiotic treatment on bacterial strain diversity and stability. *Sci Transl Med, 8*(343), 343ra381. doi:10.1126/scitranslmed.aad0917

Yatsunenko, T., Rey, F. E., Manary, M. J., Trehan, I., Dominguez-Bello, M. G., Contreras, M.et al. (2012). Human gut microbiome viewed across age and geography. *Nature, 486*(7402), 222-227. doi:10.1038/nature11053

Yuan, X., Jing, S., Wu, L., Chen, L., & Fang, J. (2014). Pharmacological postconditioning with tanshinone IIA attenuates myocardial ischemia-reperfusion injury in rats by activating the phosphatidylinositol 3-kinase pathway. *Exp Ther Med, 8*(3), 973977. doi:10.3892/etm.2014.1820

Zeisel, S. H., Mar, M. H., Howe, J. C., & Holden, J. M. (2003). Concentrations of cholinecontaining compounds and betaine in common foods. *J Nutr, 133*(5), 1302-1307. doi:10.1093/jn/133.5.1302

Zeisel, S. H., & Warrier, M. (2017). Trimethylamine N-Oxide, the Microbiome, and Heart and Kidney Disease. *Annu Rev Nutr, 37*, 157-181. doi:10.1146/annurev-nutr071816-064732

Zeisel, S. H., Wishnok, J. S., & Blusztajn, J. K. (1983). Formation of methylamines from ingested choline and lecithin. *J Pharmacol Exp Ther, 225*(2), 320-324. Retrieved from https://www.ncbi.nlm.nih.gov/pubmed/6842395

Zhang, A. Q., Mitchell, S., & Smith, R. (1995). Fish odour syndrome: verification of carrier detection test. *J Inherit Metab Dis, 18*(6), 669-674. doi:10.1007/BF02436755

Zhang, A. Q., Mitchell, S. C., & Smith, R. L. (1999). Dietary precursors of trimethylamine in man: a pilot study. *Food Chem Toxicol, 37*(5), 515-520. doi:10.1016/s02786915(99)00028-9

Zhang, C., Yin, A., Li, H., Wang, R., Wu, G., Shen, J.et al. (2015). Dietary Modulation of Gut Microbiota Contributes to Alleviation of Both Genetic and Simple Obesity in Children. *EBioMedicine, 2*(8), 968-984. doi:10.1016/j.ebiom.2015.07.007

Zhang, D. Q., & McMahon, D. G. (2000). Direct gating by retinoic acid of retinal electrical synapses. *Proc Natl Acad Sci U S A, 97*(26), 14754-14759. doi:10.1073/pnas.010325897

Zhang, X., Li, L., Butcher, J., Stintzi, A., & Figeys, D. (2019). Advancing functional and translational microbiome research using meta-omics approaches. *Microbiome, 7*(1), 154. doi:10.1186/s40168-019-0767-6

Zhang, X., Ning, Z., Mayne, J., Moore, J. I., Li, J., Butcher, J.et al. (2016). MetaPro-IQ: a universal metaproteomic approach to studying human and mouse gut microbiota. *Microbiome, 4*(1), 31. doi:10.1186/s40168-016-0176-z

Zhang, X., Zhao, Y., Xu, J., Xue, Z., Zhang, M., Pang, X.et al. (2015). Modulation of gut microbiota by berberine and metformin during the treatment of high-fat dietinduced obesity in rats. *Sci Rep, 5*, 14405. doi:10.1038/srep14405

Zhao, Z. H., Xin, F. Z., Zhou, D., Xue, Y. Q., Liu, X. L., Yang, R. X.et al. (2019). Trimethylamine N-oxide attenuates high-fat high-cholesterol diet-induced steatohepatitis by reducing hepatic cholesterol overload in rats. *World J Gastroenterol, 25*(20), 2450-2462. doi:10.3748/wjg.v25.i20.2450

Zhu, W., Gregory, J. C., Org, E., Buffa, J. A., Gupta, N., Wang, Z.et al. (2016). Gut Microbial Metabolite TMAO Enhances Platelet Hyperreactivity and Thrombosis Risk. *Cell, 165*(1), 111-124. doi:10.1016/j.cell.2016.02.011

Zhu, W., Wang, Z., Tang, W. H. W., & Hazen, S. L. (2017). Gut Microbe-Generated Trimethylamine N-Oxide From Dietary Choline Is Prothrombotic in Subjects. *Circulation, 135*(17), 1671-1673. doi:10.1161/CIRCULATIONAHA.116.025338

Zhu, Y., Jameson, E., Crosatti, M., Schafer, H., Rajakumar, K., Bugg, T. D.et al. (2014). Carnitine metabolism to trimethylamine by an unusual Rieske-type oxygenase from human microbiota. *Proc Natl Acad Sci U S A, 111*(11), 4268-4273. doi:10.1073/pnas.1316569111

Zoni-Berisso, M., Lercari, F., Carazza, T., & Domenicucci, S. (2014). Epidemiology of atrial fibrillation: European perspective. *Clin Epidemiol, 6*, 213-220. doi:10.2147/CLEP.S47385

Zorov, D. B., Juhaszova, M., & Sollott, S. J. (2014). Mitochondrial reactive oxygen species (ROS) and ROS-induced ROS release. *Physiol Rev, 94*(3), 909-950. doi:10.1152/physrev.00026.2013